INFORMATION TO USERS

This manuscript has been reproduced from the microfilm master. UMI films the text directly from the original or copy submitted. Thus, some thesis and dissertation copies are in typewriter face, while others may be from any type of computer printer.

The quality of this reproduction is dependent upon the quality of the copy submitted. Broken or indistinct print, colored or poor quality illustrations and photographs, print bleedthrough, substandard margins, and improper alignment can adversely affect reproduction.

In the unlikely event that the author did not send UMI a complete manuscript and there are missing pages, these will be noted. Also, if unauthorized copyright material had to be removed, a note will indicate the deletion.

Oversize materials (e.g., maps, drawings, charts) are reproduced by sectioning the original, beginning at the upper left-hand corner and continuing from left to right in equal sections with small overlaps.

ProQuest Information and Learning
300 North Zeeb Road, Ann Arbor, MI 48106-1346 USA
800-521-0600

ROLE OF CHOLINERGIC BASAL FOREBRAIN NEURONS IN THE MODULATION OF CORTICAL ACTIVITY ACROSS THE SLEEP-WAKING CYCLE: A PHARMACOLOGICAL STUDY

Edmund G. Cape

Department of Neurology and Neurosurgery

McGill University

A Thesis submitted to the Faculty of Graduate Studies and Research
in partial fulfillment of the requirements of the degree
Doctor of Philosophy

THESIS PREFACE

Candidates have the option of including, as part of the thesis, the text of one or more papers submitted or to be submitted for publication, or the clear-duplicated text of one or more published papers. These texts must be bound as an integral part of the thesis.

If the option is chosen, **connecting texts that provide logical bridges between the different papers are mandatory**. The thesis must be written in such a way that it is more than a mere collection of manuscripts; in other words, results of a series of papers must be integrated.

The thesis must still conform to all other requirements of the "Guidelines for Thesis Preparation". **The thesis must include**: A table of contents, an abstract in English and French, an introduction which clearly states the rationale and objectives of the study, a review of the literature, a final conclusion and summary, and a thorough bibliography or reference list.

Additional material must be provided where appropriate (e.g. in appendices) and in sufficient detail to allow a clear and precise judgment to be made of the importance and originality of the research reported in the thesis.

In the case of manuscripts co-authored by the candidate and others, **the candidate is required to make an explicit statement in the thesis as to who contributed to such work and to what extent**. Supervisors must attest to the accuracy of such statements at the doctoral oral defense. Since the task of the examiners is made more difficult in these cases, it is in the candidates interest to make perfectly clear the responsibilities of all the authors of the co-authored papers.

ABSTRACT

Serving as the extra-thalamic relay from the ascending reticular activating system to the cerebral cortex, basal forebrain neurons and particularly the cholinergic neurons therein, are believed to play an important role in cortical activation that occurs during waking and paradoxical sleep (PS). However, basal forebrain neurons are also thought to be involved in slow wave sleep (SWS), and thus accordingly influence cortical activity in different ways across the sleep-waking cycle. The present research aimed to elucidate the way the basal forebrain modulates cortical activity and sleep-wake states in response to the different neurotransmitters contained in its brainstem afferents. Microinjections of chemicals into the basal forebrain of rats were performed using a remotely controlled apparatus that allowed study of electroencephalographic (EEG) and behavioral changes without disturbing the rat's normal sleep-waking cycle. In a first study using spectral analysis of the EEG, it was established that high frequency gamma (30-60 Hz) activity reflects cortical activation and behavioral arousal during waking and PS and that gamma varies reciprocally with delta (1-4 Hz) and positively with theta (4-8 Hz) across these states. Noradrenaline, which excites cholinergic neurons to discharge in a tonic mode and has differential effects on non-cholinergic neurons, increased gamma and decreased delta EEG activities while eliciting waking. The glutamate agonist, AMPA, produced similar effects, and NMDA, which is known to induce a bursting discharge in cholinergic neurons, additionally increased theta activity in association with an active waking state. Moreover, neurotensin, which acts selectively to excite cholinergic cells to discharge in a bursting mode, evoked gamma and theta while enhancing both waking and PS in the provoked absence of SWS. In contrast, serotonin, which inhibits cholinergic neurons and has minimal effects on non-cholinergic neurons, decreased gamma and theta, while permitting SWS and preventing PS. These results demonstrate that through differential modulation by the neurotransmitters contained in their afferents, basal forebrain neurons have a potent capacity to influence cortical activity and sleep-wake state. By different modes of discharge and concerted participation of particular neuronal cohorts, cholinergic basal forebrain neurons can promote gamma and theta activity with either active waking or PS states.

RÉSUMÉ

Servant de relais extrathalamique entre le système d'activation réticulaire ascendant et le cortex cérébral, les neurones du cerveau antérieur basal, et plus particulièrement les neurones cholinergiques de cette structure, jouent probablement un rôle important dans l'activation corticale qui a lieu pendant l'état de veille et le sommeil paradoxal (SP). Toutefois, on pense que les neurones du cerveau antérieur basal jouent également un rôle dans le sommeil à ondes lentes (SOL), et donc influencent l'activité corticale de différentes manières au cours du cycle sommeil-veille. Notre projet de recherche visait à élucider les modalités selon lesquelles le cerveau antérieur basal module l'activité corticale et les états de sommeil-veille en réponse aux différents neurotransmetteurs présents dans les voies afférentes du tronc cérébral. Des micro-injections de substances chimiques ont été effectuées dans le cerveau antérieur basal de rats au moyen d'un dispositif télécommandé qui permettait l'étude des modifications électro-encéphalographiques (EEG) et comportementales sans interférer avec le cycle sommeil-veille normal des animaux. Au cours d'une première étude d'analyse spectrale de l'EEG, il a été établi qu'une activité gamma de haute fréquence (30 à 60 Hz) reflète l'activation corticale et la stimulation comportementale au cours de l'état de veille et du SP et que l'activité gamma varie de manière inversement proportionnelle avec l'activité delta (1 à 4 Hz) et de manière proportionnelle avec l'activité thêta (4 à 8 Hz) au cours de ces états. La noradrénaline, qui entraîne une décharge tonique des neurones cholinergiques et qui exerce des effets différentiels sur les neurones non cholinergiques, a augmenté l'activité EEG gamma et a diminué l'activité EEG delta tout en déclenchant l'éveil. L'AMPA, agoniste du glutamate, a produit des effets similaires et le NMDA, qui est connu pour induire des décharges en salve des neurones cholinergiques, a produit une augmentation supplémentaire de l'activité thêta en association avec un état de veille active. De plus, la neurotensine, qui excite sélectivement les cellules cholinergiques à produire des décharger en salves, a induit une activité gamma et thêta tout en stimulant l'état de veille et le SP en l'absence provoquée de SOL. Par contre, la sérotonine, qui inhibe les neurones cholinergiques et exerce des effets minimes sur les neurones non cholinergiques, a diminué l'activité gamma et thêta, tout en permettant le SOL et en prévenant le SP. Ces résultats démontrent que, en exerçant une modulation différentielle par les neurotransmetteurs présents dans leurs voies afférentes, les

neurones du cerveau antérieur basal ont la capacité considérable de modifier l'activité corticale et l'état sommeil-veille. Par divers modes de décharge et la participation concertée de cohortes neuronales sélectionnées, les neurones du cerveau antérieur basal peuvent promouvoir une activité thêta et gamma de haute fréquence dans les états de veille active et les états de SP.

CLAIM OF ORIGINALITY AND CONTRIBUTION OF CO-AUTHORS

This work is part of an ongoing research program concerning the role of the basal forebrain in sleep-wakes in the laboratory of Dr. Barbara E. Jones. The success of these series of experiments was due to the central participation of Dr. Jones in her careful supervision of this work. The thesis is comprised of four chapters based on four major manuscripts that have either been published or have been prepared for submission for publication. Many of the results have also been presented orally or in poster form at the 1994,1996,1997,1998 and 1999 Society for Neuroscience meetings in addition to the 1999 World Sleep Federation sleep meeting in Dresden, Germany.

The first chapter (published in Neuroscience) was the result of a collaboration by myself and Dr. Jones with Karen Maloney and Dr. Jean Gotman. The collaboration divided the responsibilities as follows: The surgery and execution of the experiments was done by me and the bulk of the analysis and parsing of the data was performed by Karen Maloney. The manuscript was primarily composed by Karen Maloney and Dr. Jones. I played a role in editing and revising the final manuscript. Dr. Jean Gotman provided key insight into the EEG spectral analysis.

The subsequent chapters describe my original contributions to the study of the role of the basal forebrain in the modulation of cortical activation across the sleep-waking cycle. The results are the product of a unique procedure and apparatus that I developed to ensure the reliable microinjection of drugs into the basal forebrain while not disturbing the normal sleep cycle of the animal. This apparatus represented a new approach that was subsequently studied by the McGill University technology transfer group. Based on the fact that I was the first in this lab to perform such experiments with rats, I was responsible for the design and execution of every logistical aspect of these experiments.

Processing of all the data generated by these experiments was performed by myself. This included analyzing and compiling the raw EEG data. This process was ultimately facilitated by a computer program I developed using Java software programming language. I subsequently worked with Systat software in the multivariate statistical analysis of the data.

I performed some of the immunohistochemistry during the pilot phase, whereas Lynda Mainville performed the vast amount of immunohistostaining for the c-Fos studies (Chapter 3) using procedures developed by Dr. Jones. Lynda and I performed the immunohistochemistry for the neurotensin internalization studies (Chapter 4). I performed the required image analysis using a computer based atlas previously developed by Drs. Jones and Ivana Gritti for plotting the distribution of cells in the basal forebrain using Biocom image analysis system.

The last chapter represents a collaboration by myself and Dr. Jones with Ian Manns and Drs. Alain Beaudet and Angel Alonso. Dr. Alain Beaudet played a key role in the study of the internalization of Neurotensin in association with examination of its electrophysiological effects. Ian Manns, a graduate student working with Dr. Barbara Jones and Angel Alonso, played a central role in extending our *in vivo* work to include the study of unit activity in response to NT. He used a novel procedure that enables the juxtacellular labeling of the recorded cell, that allows for the subsequent immunohistochemical analysis for identification of the neurotransmitter type. This technique combined with my expertise with microinjections represents a concerted effort that yielded data that is at the forefront of our research field.

Manuscripts were composed by myself before being co-edited by Dr. Jones and myself in a condensed manner suitable for publication. Sections of chapter four, which is in preparation for submission, have also been reviewed by Drs. Alain Beaudet, Angel

Alonso and Ian Manns. Production of the figures was done by myself. This included developing an appropriate format for the presentation, layout of the data and producing and editing the photomicrographs. Lastly, to complement these publications, a demonstration of the procedures developed during my work was presented online and includes an interactive Java multimedia presentation.

Finally, this body of work represents a unique contribution to the field of sleep research and study of the mechanisms of vigilance. The findings here document for the first time the relationship between gamma, theta and delta EEG activities as they vary in the freely moving, naturally sleeping-waking rat. The work then provides novel insight into how the monoamines, previously found to fire in parallel maximally during wake, slower during SWS and off during PS, in fact have differential effects on cortical activation and the sleeping-waking cycle through the basal forebrain in a manner consistent with how these neurotransmitters were previously found to differently modulate cholinergic basal forebrain neurons. The next series of experiments with glutamatergic agonists, in addition to corroborating findings with noradrenaline that excitation of basal forebrain cholinergic neurons enhances gamma activity, extend the work by showing that NMDA, which has the capacity to induce rhythmic bursting in the cholinergic cells, stimulates theta activity on the cerebral cortex in association with a behaviorally active waking state.. The last chapter goes further in demonstrating that the selective activation of cholinergic basal forebrain neurons by the peptide, neurotensin, is sufficient to induce cortical activation in association with the states of wake and PS. The study also documents important corroborating evidence for both the selective nature of the activation, and the fact that NT potentiates bursting activity in association with rhythmic EEG activity. The latter study moreover demonstrates for the first time the potential for the basal forebrain to play an important role in promoting paradoxical sleep. These studies show that the basal forebrain may serve to modulate cortical activity in a

rhythmic manner within a theta frequency and accordingly advance the new concept that such rhythmic modulation in the basalo-cortical system may parallel that in the septo-hippocampal system, and thus share an important role in synchronizing coherent discharge across distributed regions of the cortex, as is important for coordinated activity. Altogether, these studies establish in a unique and unequivocal manner, the potent capacity and importance of the basal forebrain for modulating cortical activity and sleep-wake state.

ACKNOWLEDGMENTS

I would first like to thank Dr. Jones for providing me with such a fantastic opportunity. Through Dr. Jones I have had the fortune to be engaged in research in this most stimulating field of sleep research while working with and meeting wonderful people from around the world. Your contributions to the sleep field are clear - it has been an absolute pleasure working with you. Your patience, generosity, and kind nature were certainly appreciated. You are a great mentor. I would also like to thank Drs. Bendena, Hay and Thorne each from Queen's University, for each having taught me well and ultimately vouching for me in my application to McGill. I would like to thank my friends and family for their support. First and foremost my father: While many paths seemed possible to me, continuing with my research has most certainly provided a wealth of experience and opportunity. Thank you for providing the guidance and support that made this volume of work possible. These past six years in Montreal have been filled with first rate experiences, the best of them were spent with you. To my Mum: It is clear to me that because of your clear vision during my junior and high school years, I got off to a great start. What I learned then I am still applying now on a regular basis. To all my brothers and sisters – including all of my nephews and nieces, through your example, I am continually reminded of what first class people are made. Thank you for providing the love and support that I have felt on a continual basis. To Martine, your support and participation was greatly appreciated. Our poster presentations have never looked so good! Thank you very much for taking the time and effort in such a selfless way. To Lynda, you set the stage and mood at the lab. Your professional and kind approach was greatly appreciated. To everyone on the eighth floor of the south wing at the Neuro, Karen, Ian, Clayton and Mark (you were on the eighth floor often enough) – you made the day to day an absolute pleasure. Which brings me to Alain Beaudet:

Thank you very much for being a great friend. Not only have I appreciated the people that you brought to your lab over the years (eg. Helene, Thomas, Mau etc.) whom have all been fun people to work along with, I have greatly appreciated working and kidding with you. You are a great example of a basic researcher. I would like to thank Ed and Brian at Neuroelectronics. With their capacity to perform first rate work building our microinjection apparatus, and continually rebuilding our electrode cables, our job was made much easier. Lastly, this work was funded mostly by funds provided by the FRSQ.

TABLE OF CONTENTS

CHAPTER 1

CHAPTER 2

CHAPTER 3

CHAPTER 4

CHAPTER 5

INTRODUCTION TO THE THESIS

INTRODUCTION

Cortical activation occurs during wake (W) and paradoxical sleep (PS) states and is manifest on the EEG as low voltage, fast activity. Across the sleep-waking cycle, the periods of maximal cortical activation are associated with maximal release of acetylcholine (ACh) in the cerebral cortex (Celesia and Jasper, 1966; Jasper and Tessier, 1971). ACh appears to facilitate cortical activation through an excitatory action upon cortical neurons (see for review, (McCormick, 1992a)). The primary source of cholinergic innervation to the cortex is the nucleus basalis of Meynert in the basal forebrain (Lehmann and Saper, 1985; Shute and Lewis, 1967). Lesions of basal forebrain cholinergic cells decrease cortical ACh release with a parallel decrease in cortical activation (Buzsaki *et al.*, 1988; Lo Conte *et al.*, 1982; Stewart *et al.*, 1984), while electrical stimulation of the cholinergic basalis neurons leads to an increase in cortical ACh release and cortical activation (Casamenti *et al.*, 1986). Accordingly, they are believed to play an important role in the generation and transmission of activating input from the brainstem to the cortex during waking and Paradoxical Sleep. Despite the clear significance of this system in cortical activation, the precise role of the cholinergic neurons and their modulation in cortical activity and sleep-wake states remains to be tested and elucidated.

As a potential mechanism to regulate cortical activation across the sleep-waking cycle, electrophysiological studies have revealed an intrinsic capacity of the cholinergic basal forebrain neurons to fire in two distinct modes: a tonic mode when activated from a relatively depolarized level and a slow rhythmic bursting mode (1.7 - 5 Hz) when activated from a relatively hyperpolarized level (Khateb *et al.*, 1992b). Accordingly, they share certain electrophysiological properties with thalamocortical cells which endow them with the capacity to fire in different modes in association with different states. It

has been suggested that the slow bursting rate of the basalis neurons could correspond to a delta (1 - 4 Hz) or theta (4 - 10 Hz) range of activity in cortical rhythms (Alonso *et al.*, 1996; Khateb *et al.*, 1992b). Thus by different activity patterns and/or different amounts of ACh release, the cholinergic neurons may modulate cortical activity across states.

Modulation of the basalis neurons by chemical neurotransmitters contained in their afferents may be crucial in producing the EEG associated with each state. Cholinergic basalis neurons lie in the path of the major ascending fiber system from the brainstem reticular activating system and thus serve as the ventral extrathalamic relay to the cortex (Moruzzi and Magoun, 1949; Starzl *et al.*, 1951). The chemical identity of the major neuronal substrates responsible for transmitting the ascending activating input from the brainstem to the cortex has been revealed over the past 30 years. After the ascending reticular activation system (A.R.A.S.) was first described by Moruzzi and Magoun (1949), the substrate for this system was presumed to be cholinergic based on the results of initial histochemical studies identifying cells that contained acetylcholine esterase (AChE), the catabolic enzyme for ACh, in the pontomesencephalic tegmentum (Shute and Lewis, 1963). These neurons gave rise to ascending projections into the forebrain, including a significant contingent to the basal forebrain, where other AChE-stained neurons were localized and found to project in turn to the cortex. This system would be referred to as the "ascending cholinergic activating system" (Shute and Lewis, 1963).

Subsequent studies utilizing immunohistochemical reaction of choline acetyl transferase (ChAT), demonstrated that the AChE stained cells projecting to the cortex were indeed cholinergic (Mesulam *et al.*, 1983; Rye *et al.*, 1984). On the other hand, only a small minority of the brainstem afferents were found to be cholinergic (see for review (Jones, 1993)). Thus a very small number of cholinergic neurons in the laterodorsal and pedunculopontine tegmental nuclei of the projected to the basal

forebrain but only represented a small minority (<1%) of the total afferent population to the basalis region in the brainstem (Jones and Cuello, 1989).

In addition to the small cholinergic afferent input, monoaminergic input to the basal forebrain from brainstem cell groups was identified as originally primarily in the dorsal raphe nucleus and locus coeruleus (Jones and Cuello, 1989). For many years, monoaminergic influence on the sleep-waking cycle had been recognized (see (Jouvet, 1972)). An important role of serotonin in the sleep-waking cycle was originally demonstrated by the effect of lesions of the dorsal raphe which produced a state of insomnia. Despite the initial indication of a significant role of serotonin during sleep, subsequent studies indicated that serotonin was not necessary for the appearance of slow wave sleep, even though it could normally facilitate the onset of sleep (see for review (Jacobs and Fornal, 1991; Jacobs and Jones, 1978; Jones, 1994)). Furthermore, unit recording studies revealed that dorsal raphe neurons fire at their highest rates during waking and decrease their rate of firing during slow wave sleep to eventually shut off during paradoxical sleep (McGinty and Harper, 1976; Trulson and Jacobs, 1979) (see for review (Jacobs and Fornal, 1991)). It has accordingly been thought that the serotonergic neurons may be important for the onset of slow wave sleep but not for the generation of the state and would play a permissive role in paradoxical sleep. Given the serotonergic innervation in the basal forebrain, serotonin's role in the sleep-waking cycle, may at least in part be effected through its innervation of the cholinergic basal forebrain neurons.

Similarly, an important role of noradrenergic locus coeruleus neurons in the facilitation of cortical activation and waking has been recognized for many years (see (Jones *et al.*, 1973; Jouvet, 1972)). Even though lesion studies have shown that these neurons are not essential for the maintenance of these activities (see (Jones, 1991; Jones *et al.*, 1977)), multiple pharmacological and physiological studies have

demonstrated that they normally have the capacity to facilitate and prolong cortical activation and waking (see (Jacobs and Jones, 1978)). Although the locus coeruleus neurons project directly to the thalamus and cerebral cortex (Jones and Yang, 1985), they also appear to send collaterals to the basal forebrain in addition to other subcortical relay stations (Fort *et al.*, 1995; Jones and Yang, 1985), and could thereby influence cortical activity by acting upon the cortically projecting cholinergic basalis neurons. Pharmacological depletion of catecholamines produces hypersomnia, an increase in both SWS and PS, while drugs that enhance their release (eg. amphetamine), also enhance W while consequently suppressing sleep (Jacobs and Jones, 1978). Electrophysiological studies indicate that noradrenergic LC neurons (like serotonergic raphe neurons) decrease their rate of firing during SWS to eventually cease firing during PS, suggesting that noradrenergic LC neurons (and serotonergic raphe neurons) act during W and would play a permissive role in PS (Hobson *et al.*, 1975).

The cholinergic basal forebrain neurons are modulated by serotonin and noradrenaline. By intracellular recording and labelling *in vitro*, identified cholinergic basalis neurons were shown to be directly innervated by serotonergic and noradrenergic fibres and to be modulated in different ways by these two neurotransmitters (Fort *et al.*, 1995; Khateb *et al.*, 1993; Khateb *et al.*, 1992a). Serotonin was found to hyperpolarize and inhibit the cholinergic neurons, whereas noradrenaline was found to depolarize and excite them.

In addition to the smaller but significant monoaminergic neuronal input from the noradrenergic locus coeruleus neurons and serotonergic midbrain raphe neurons (Jones, 1989), the brainstem neurons projecting to the basal forebrain are comprised predominantly of glutamatergic neurons of the reticular formation (see for review (Jones, 1995). In addition, glutamatergic afferent input to the basal forebrain originates in the cerebral cortex (Davies *et al.*, 1984). Based on previous descriptions of

glutamatergic projections from the hippocampus and a glutamatergic feedback from the cortex to the basal forebrain, quantitative autoradiographic study revealed L-glutamate binding sites in the basal forebrain region (Zilles *et al.*, 1991). The findings show a substantial number of L-glutamate binding sites, being higher in number than the muscarinic, or monoaminergic receptor populations.

Glutamate is well known as an excitatory neurotransmitter of cell populations in the CNS, and has been used as a chemical means to stimulate cells as an alternative to electrical stimulation (Goodchild *et al.*, 1982). However, the potential role that the glutamate receptors in transmitting at least in part, the ascending input from the brainstem has only recently been suggested (Rasmusson *et al.*, 1994). In urethane-anesthetized rats, increases in cortical ACh release induced by electrically stimulating the pontomesencephalic tegmentum, were significantly reduced in the presence of glutamate antagonists injected in the basal forebrain. On the other hand, muscarinic and nicotinic cholinergic blockers injected in the basalis region did not block the effect of brainstem stimulation. Conclusions from this study suggest that excitatory afferent input from the brainstem reticular formation, that has been historically so significant in modulating and maintaining cortical activation (Moruzzi and Magoun, 1949), may occur predominantly via glutamatergic and not cholinergic synapses as had been originally postulated by Shute and Lewis (1963). These results and conclusions are supported by the chemo-neuroanatomical studies (above) showing a minor contribution from cholinergic neurons and a major contribution from putative glutamatergic neurons of the pontomesencephalic tegmentum.

Intracellular recordings performed within the basal forebrain of guinea-pig brain slices showed that cholinergic neurons are differentially modulated by different glutamate receptor agonists (Khateb *et al.*, 1995). While they all depolarize and excite the cholinergic neurons, the results also show that activation of NMDA (N-methyl-D-

aspartate) receptor may maintain these cells in a rhythmic bursting mode if they are simultaneously held at a hyperpolarized level. Assuming the presence of contingent hyperpolarizing afferent input, these data suggest that brainstem and cortical afferents that release glutamate could stimulate rhythmic bursting via NMDA receptors in the cholinergic cells *in vivo*. Such rhythmic oscillations in the basalis neurons would provide a rhythmic modulation to target neurons within the cerebral cortex and thereby potentially promote slow oscillations within a delta or theta frequency range in cortical activity across the sleep-waking cycle (Khateb *et al.*, 1995).

Cortical ACh release from the basal forebrain has recently been shown to be sensitive to neurotensin (NT) (Lapchak *et al.*, 1990), a neuropeptide distributed throughout the CNS (Nemeroff *et al.*, 1980). A selective association of high-affinity NT binding sites was also demonstrated on cholinergic basalis neurons (Szigethy *et al.*, 1990). *In vivo* intracerebroventricular (ICV) administration of NT produced an increase in theta activity in the EEG (Castel *et al.*, 1989). Intracellular recordings in guinea pig brain slices revealed the capacity of NT to produce a slow depolarization in cholinergic basalis cells (Alonso *et al.*, 1994). Prolonged exposure produced a very prominent slow rhythmic bursting pattern that could shape into complex spindle-like sequences that were intrinsically generated by the cholinergic cells. Identification of the cholinergic neurons as direct NT targets was further provided by confocal laser scanning microscopic demonstration of internalization of fluoresceinylated derivative of NT (fluo-NT). Despite very little current understanding of the significance of neurotensin in cortical activation across the sleep-wake cycle, an important role for neurotensin in the modulation of cholinergic cell activity and in particular in the generation of forebrain network oscillations is strongly suggested (Alonso *et al.*, 1994).

Although a major contingent of cells within the basal forebrain are magnocellular cholinergic neurons that serve as a primary source of cortical acetylcholine (Rye *et al.*,

1984), the region consists of a heterogeneous population of neurons. In particular, the basal forebrain contain GABAergic neurons which project to the cortical mantle equally number with the cholinergic cells (Gritti *et al.*, 1993). Although each cell population has its own distinct electrophysiological properties, these non-cholinergic projections show, like the cholinergic cortical projecting neurons, a capacity to fire in a rhythmic manner (Alonso *et al.*, 1996). The overlapping distribution, projection targets, and firing properties, suggest that these two cell populations could fire in a coordinated manner at low frequencies *in vivo*. There is evidence to show that they are selectively and differentially modulated by the neurotransmitters contained in the brainstem afferents (Fort *et al.*, 1992).

AIM

The precise role of the basalis cholinergic neurons and their modulation by brainstem afferents in cortical activity and sleep-wake states remains to be tested. Thus the aim of the proposed experiments is to reveal the potential capacity of the basal forebrain by means of their cortical projections, to regulate the cortical EEG and the state of a naturally sleeping-waking animal. The results of these studies should elucidate the importance and role of cholinergic basal forebrain neurons and their modulation in cortical activation, which underlies consciousness and cognitive processes of the states of wakefulness and paradoxical sleep.

EXPERIMENTAL APPROACH

With our current knowledge of the intrinsic properties and chemo-modulation of identified cholinergic neurons from *in vitro* electrophysiological studies, it has become possible to test the effect of this established modulation of cholinergic basal forebrain neurons *in vivo* by microinjections of the chemical neurotransmitters contained in the afferent systems. The benefits of chemical modulation of specific neuronal targets by chemical microinjection were first explored by Goodchild *et al.*, (1982). The immediate advantage of chemical versus artificial electrical stimulation was that only the cells present in the vicinity, and not the axons passing through the region, would in fact be stimulated. Furthermore, modulation of neuronal activity with chemical neurotransmitters can act selectively and/or differentially on specific cell populations according to their specific receptors.

Although chemical microinjection experiments performed up to the present have been useful in identifying potential drug effects throughout the CNS, they have been limited in their ability to study the immediate effects of drugs in a naturally sleeping-

waking animal. Microinjections in anaesthetised (Rasmusson *et al.*, 1994) or brainstem transected animals (Casamenti *et al.*, 1986) are difficult to interpret because the experimental procedures alter the normal states and associated ACh release (Celesia and Jasper, 1966) and consequently do not allow assessment of effects upon natural sleep-wake states.

A source of this shortcoming lies in the current procedures for delivering the microinjection that invariably awaken a naturally sleep-waking animal. Most studies have required that the animal's head be restrained during the injection procedure (Nishino *et al.*, 1995), creating an artificial state of agitated wake with associated changes in ACh release (see (Sarter and Bruno, 1994)). During a period of the day when the animals are normally found asleep, significant changes in EEG and behavior are bound to occur as a result of the injections of ringer or saline when compared to a naturally sleeping-waking animal. Thus, subtle effects upon EEG activity and state could be missed. Although microdialysis can be used to certain advantage for continuous, remote chemical delivery (Quan and Blatteis, 1989), it has the disadvantage of necessitating a large area of exposure for the probe and a long period of perfusion to attain the pharmacological levels of the drugs in the brain tissue.

To maximize the resolution of the data that can be acquired from the microinjection technique, in the present study we developed an apparatus and procedure which allowed delivery of the drugs while the animal was in a normal sleep-waking cycle. Although placement of the filled cannulae on the animal's head does require temporarily interrupting the sleep cycle of the rat, the cannulae are only lowered to their ultimate target by remote control after a natural sleep cycle is observed. Accordingly, the animal is allowed to recover from the handling procedure prior to any exposure of the tissue to the chemical. In fact, the experimental procedure was successful in delivering a ringer injection that had no significant change in sleep-wake

state when compared to the baseline data from the naturally sleeping-waking rat. Discreet, remote delivery of a known amount of chemical into the brains of naturally sleeping-waking rats during continuous EEG recording and behavioral observation is thus accomplished.

To measure changes in cortical activation as a result of manipulating the neuronal activity of the basal forebrain, high frequency activity in the EEG will be measured. In particular, gamma activity (30 - 60 Hz) will be described as a reliable indicator of cortical and behavioral arousal in the rat (Chapter 2) (Maloney *et al.*, 1997). As a reflection of state, gamma activity was highest during wake and paradoxical sleep with a reciprocal decrease in delta (Maloney *et al.*, 1997). In fact, the degree of gamma amplitude (in contrast to high beta: 20 - 30 Hz) and its reciprocal relationship with delta (1 - 4 Hz) discerned different degrees of cortical activation between various waking behaviors. Within the state of wake, peaks in gamma were found during attentive, moving and eating behaviors (Maloney *et al.*, 1997). These findings are especially significant for our studies in light of the fact that the basal forebrain neurons increase their rate of activity during these types of active behaviors (Rolls, 1979; Buzsaki *et al.*, 1988), when there is also an increase in cortical ACh release and turnover (Day *et al.*, 1991; Inglis *et al.*, 1994). Thus based on these previous findings, it would seem possible to suggest the effects of the microinjections on the activity of the basalis cholinergic cells by measuring the changes in cortical gamma activity.

EXPERIMENTAL DESIGN

During a period of the day when the rats are normally found asleep the majority of the time, the effects of chemical microinjections in the basal forebrain will be assessed upon EEG and state in freely moving rats. Microinjections will be delivered with chronically indwelling guide cannulae. EEG will be recorded from electrodes placed directly on the dura (Fig. 1). The EEG will be analysed by spectral analysis to determine changes in high frequency, gamma activity (30 - 60 Hz), which we have shown to be a specific indicator of both behavioral and cortical arousal in the rat (Maloney *et al.*, 1997). The concurrent effects on theta (4.5 - 8.0 Hz) measured as Th/De and delta (1 - 4 Hz) will also be analysed, as well as EMG.

Changes in sleep-wake state will also be measured. The rat's state will be assessed using the behavioral annotations (monitored using video), in addition to the EEG and EMG records. Particularly during the experimental (drug injected) condition, the annotations will identify any dissociations between behavior and the EEG patterns normally associated with the different states.

Bilateral microinjections of drugs will be carried out with an apparatus that permits delivery of the injections while not interrupting the natural sleep-waking cycle in freely moving rats. Inner cannulae, loaded with a drug, are inserted into indwelling outer cannulae at the beginning of the experiment but not lowered into the brain in order to avoid premature leakage of the drug (Fig. 1). After the animal has recovered from the handling procedure to resume a normal sleeping cycle, the inner drug-filled cannulae are lowered into position by a remote mechanism, when soon after, the microinjection is begun using a micro syringe pump. All drugs are injected bilaterally in volumes of 0.5 µl over 5 min.

Thus these experiments will explore the role of the basal forebrain in the modulation of the sleep-wake cycle. The results of this work will allow us to further understand the importance and role of the basal forebrain neuronal population and their neuromodulation in cortical activation and SWS. Most interestingly, they may indicate what the significance of rhythmic firing by the cholinergic neurons is in modulating cortical activity and sleep-wake states.

LITERATURE CITED

Alonso A, Faure M-P, Beaudet A (1994) Neurotensin promotes oscillatory bursting behavior and is internalized in basal forebrain cholinergic neurons. *J. Neurosci.*, **14,** 5778-5792.

Alonso A, Khateb A, Fort P, Jones BE, Muhlethaler M (1996) Differential oscillatory properties of cholinergic and non-cholinergic nucleus Basalis neurons in guinea pig brain slice. *Eur. J. Neurosci.*, **8,** 169-182.

Buzsaki G, Bickford RG, Ponomareff G, Thal LJ, Mandel R, Gage FH (1988) Nucleus basalis and thalamic control of neocortical activity in the freely moving rat. *J. Neurosci.*, **8,** 4007-4026.

Casamenti F, Deffenu G, Abbamondi AL, Pepeu G (1986) Changes in cortical acetylcholine output induced by modulation of the nucleus basalis. *Brain Res. Bull.*, **16,** 689-695.

Celesia GG, Jasper HH (1966) Acetylcholine released from cerebral cortex in relation to state of activation. *Neurology*, **16,** 1053-1064.

Davies SW, McBean GJ, Roberts PJ (1984) A glutamatergic innervation of the nucleus basalis/substantia innominata. *Neurosci. Lett.*, **45,** 105-110.

Day J, Damsma G, Fibiger HC (1991) Cholinergic activity in the rat hippocampus, cortex and striatum correlates with locomotor activity: an in vivo microdialysis study. *Pharmacol. Biochem. Behav.*, **38,** 723-729.

Fort P, Khateb A, Alonso A, Jones BE, Muhlethaler M (1992) Pharmacological heterogeneity of basal forebrain neurones. *Soc. Neurosci. Abst.*, **18,** 881.

Fort P, Khateb A, Pegna A, Muhlethaler M, Jones BE (1995) Noradrenergic modulation of cholinergic nucleus basalis neurons demonstrated by *in vitro* pharmacological and immunohistochemical evidence in the guinea pig brain. *Eur. J. Neurosci.*, **7,** 1502-1511.

Goodchild AK, Dampney RAL, Bandler R (1982) A method for evoking physiological responses by stimulation of cell bodies, but not axons of passage, within localized regions of the central nervous system. *J. Neurosci. Meth.*, **6,** 351-363.

Gritti I, Mainville L, Jones BE (1993) Codistribution of GABA- with acetylcholine-synthesizing neurons in the basal forebrain of the rat. *J. Comp. Neurol.*, **329,** 438-457.

Hobson JA, McCarley RW, Wyzinski PW (1975) Sleep cycle oscillation: reciprocal discharge by two brainstem neuronal groups. *Science*, **189,** 55-58.

Inglis FM, Day JC, Fibiger HC (1994) Enhanced acetylcholine release in hippocampus and cortex during the anticipation and consumption of a palatable meal. *Neuroscience*, **62,** 1049-1056.

Jacobs BL, Fornal CA (1991) Activity of brain serotonergic neurons in the behaving animal. *Pharmacol. Rev.*, **43,** 563-578.

Jacobs BL, Jones BE (1978) The role of central monoamine and acetylcholine systems in sleep-wakefulness states: mediation or modulation. In: *Cholinergic-Monoaminergic Interactions in the Brain.* Edited by L. L. Butcher. New York: Academic Press, pp. 271-290.

Jasper HH, Tessier J (1971) Acetylcholine liberation from cerebral cortex during paradoxical (REM) sleep. *Science*, **172,** 601-602.

Jones BE (1989) The relationship among acetylcholine, noradrenaline and GABA neurons within the pons of the rat. *Anat. Rec.*, **223,** 57A.

Jones BE (1991) Noradrenergic locus coeruleus neurons: their distant connections and their relationship to neighboring--including cholinergic and GABAergic--neurons of the central gray and reticular formation. In: *Neurobiology of the Locus Coeruleus. Progress in Brain Research, Vol. 85*, Volume 85. Edited by C. Barnes and O. Pompeiano. Amsterdam: Elsevier, pp. 15-30.

Jones BE (1993) The organization of central cholinergic systems and their functional importance in sleep-waking states. In: *Cholinergic Function and Dysfunction, Progress in Brain Research, Vol. 98*, Volume 98. Edited by A. C. Cuello. Amsterdam: Elsevier, pp. 61-71.

Jones BE (1994) Basic mechanisms of sleep-wake states. In: *Principles and Practice of Sleep Medicine, 2nd Edition.* Edited by M. H. Kryger, T. Roth and W. C. Dement. Philadelphia: Saunders, pp. 145-162.

Jones BE (1995) Reticular formation. Cytoarchitecture, transmitters and projections. In: *The Rat Nervous System.* Edited by G. Paxinos. New South Wales: Academic Press Australia, pp. 155-171.

Jones BE, Bobillier P, Pin C, Jouvet M (1973) The effect of lesions of catecholamine-containing neurons upon monoamine content of the brain and EEG and behavioral waking in the cat. *Brain Res.*, **58,** 157-177.

Jones BE, Cuello AC (1989) Afferents to the basal forebrain cholinergic cell area from pontomesencephalic--catecholamine, serotonin, and acetylcholine--neurons. *Neuroscience*, **31,** 37-61.

Jones BE, Harper ST, Halaris AE (1977) Effects of locus coeruleus lesions upon cerebral monoamine content, sleep-wakefulness states and the response to amphetamine. *Brain Res.*, **124,** 473-496.

Jones BE, Yang T-Z (1985) The efferent projections from the reticular formation and the locus coeruleus studied by anterograde and retrograde axonal transport in the rat. *J. Comp. Neurol.*, **242,** 56-92.

Jouvet M (1972) The role of monoamines and acetylcholine-containing neurons in the regulation of the sleep-waking cycle. *Ergeb. Physiol.*, **64,** 165-307.

Khateb A, Fort P, Alonso A, Jones BE, Muhlethaler M (1993) Pharmacological and immunohistochemical evidence for a serotonergic input to cholinergic nucleus basalis neurons. *Eur. J. Neurosci.*, **5,** 541-547.

Khateb A, Fort P, Serafin M, Jones BE, Muhlethaler M (1995) Rhythmical bursts induced by NMDA in cholinergic nucleus basalis neurones *in vitro*. *J. Physiol. (Lond.)*, **487.3,** 623-638.

Khateb A, Muhlethaler M, Alonso A, Jones BE (1992a) Oscillatory bursts in basal forebrain cholinergic neurons induced by NMDA. *Soc. Neurosci. Abst.*, **18,** 881.

Khateb A, Muhlethaler M, Alonso A, Serafin M, Mainville L, Jones BE (1992b) Cholinergic nucleus basalis neurons display the capacity for rhythmic bursting activity mediated by low threshold calcium spikes. *Neuroscience*, **51,** 489-494.

Lapchak PA. Araujo DM. Quirion R. Beaudet A. (1990) Neurotensin regulation of endogenous acetylcholine release from rat cerebral cortex: effect of quinolinic acid lesions of the basal forebrain. *J. of Neurochem.* **55**(4):1397-403.

Lehmann W, Saper CB (1985) Evidence for a cortical projection to the magnocellular basal nucleus in the rat: an electron microscopic axonal transport study. *Brain Res.*, **334,** 339-343.

Lo Conte G, Casamenti F, Bigi V, Milaneschi E, Pepeu G (1982) Effect of magnocellular forebrain nuclei lesions on acetylcholine output from the cerebral cortex, electrocorticogram and behaviour. *Arch. ital Biol.*, **120,** 176-188.

Maloney KJ, Cape EG, Gotman J, Jones BE (1997) High frequency gamma electroencephalogram activity in association with sleep-wake states and spontaneous behaviors in the rat. *Neuroscience*, **76,** 541-555.

McCormick DA (1992a) Cellular mechanisms underlying cholinergic and noradrenergic modulation of neuronal firing mode in the cat and guinea pig dorsal lateral geniculate nucleus. *J. Neurosci.*, **12,** 278-289.

McCormick DA (1992b) Neurotransmitter actions in the thalamus and cerebral cortex and their role in neuromodulation of thalamocortical activity. *Progr. Neurobiol.*, **39,** 337-388.

McGinty D, Harper RM (1976) Dorsal raphe neurons: depression of firing during sleep in cats. *Brain Res.*, **101,** 569-575.

Moruzzi G, Magoun HW (1949) Brain stem reticular formation and activation of the EEG. *Electroenceph. clin. Neurophysiol.*, **1,** 455-473.

Nemeroff CB. Bissette G. Manberg PJ. Osbahr AJ 3d. Breese GR. Prange AJ Jr. (1980) Neurotensin-induced hypothermia: evidence for an interaction with dopaminergic systems and the hypothalamic--pituitary--thyroid axis. *Brain Research* **195**(1), 69-84.

Nishino S, Tafti M, Reid MS, Shelton J, Siegel JM, Dement WC *et al.* (1995) Muscle atonia is triggered by cholinergic stimulation of the basal forebrain: implication for the pathophysiology of canine narcolepsy. *J. Neurosci.*, **15,** 4806-4814.

Quan N, Blatteis CM (1989) Microdialysis: a system for localized drug delivery into the brain. *Brain Res. Bull.*, **22,** 621-625.

Rasmusson DD, Clow K, Szerb JC (1994) Modification of neocortical acetylcholine release and electroencephalogram desynchronization due to brainstem stimulation by drugs applied to the basal forebrain. *Neuroscience*, **60,** 665-677.

Rye DB, Wainer BH, Mesulam M-M, Mufson EJ, Saper CB (1984) Cortical projections arising from the basal forebrain: a study of cholinergic and noncholinergic components employing combined retrograde tracing and immunohistochemical localization of choline acetyltransferase. *Neuroscience*, **13,** 627-643.

Sarter MF, Bruno JP (1994) Cognitive functions of cortical ACh: lessons from studies on trans-synaptic modulation of activated efflux. *Trends Neurosci.*, **17,** 217-221.

Shute CCD, Lewis PR (1963) Cholinesterase-containing systems of the brain of the rat. *Nature*, **199,** 1160-1164.

Shute CCD, Lewis PR (1967) The ascending cholinergic reticular system: neocortical, olfactory and subcortical projections. *Brain*, **90,** 497-520.

Starzl TE, Taylor CW, Magoun HW (1951) Ascending conduction in reticular activating system, with special reference to the diencephalon. *J. Neurophysiol.*, **14,** 461-477.

Stewart DJ, Macfabe DF, Vanderwolf CH (1984) Cholinergic activation of the electrocorticogram: Role of the substantia innominata and effects of atropine and quinuclidinyl benzilate. *Brain Res.*, **322,** 219-232.

Szigethy E. Leonard K. Beaudet A. (1990) Ultrastructural localization of [125I]neurotensin binding sites to cholinergic neurons of the rat nucleus basalis magnocellularis. *Neuroscience* **36**(2), 377-91.

Trulson ME, Jacobs BL (1979) Raphe unit activity in freely moving cats: correlation with level of behavioral arousal. *Brain Res.*, **163,** 135-150.

Zilles K, Werner L, Qu M, Schleicher A, Gross G (1991) Quantitative autoradiography of 11 different transmitter binding sites in the basal forebrain region of the rat--evidence of heterogeneity in distribution patterns. *Neuroscience*, **42,** 473-481.

Figure 1. Top view of the rat skull indicating the placement of the EEG and chronically implanted cannulae (A) and the 2 step process for inserting the drug loaded cannulae (B). The EEG electrodes (A, black) were placed bilaterally by reference to Bregma over frontal (2.7-3.0 mm anterior, 0.6 mm lateral), retrosplenial (3.5 mm posterior, 0.6 mm lateral), parietal (0.5 mm posterior, 5.0 mm lateral) and occipital (7.5 mm posterior, 5.0 mm lateral) cortical regions. A reference electrode was cemented in bone rostral to the frontal cortex and caudal to the olfactory bulbs (5.5 mm anterior, 0.6 mm lateral). Field potential recordings were also performed in some animals within the hippocampus (-4.0 mm AP, 2.2 mm L, -3.5 mm V relative to bregma) and entorhinal cortex (-7.6 mm AP, 5.2 mm L, -7.2 mm V relative to bregma) using tripolar tungsten wire electrodes (A, green). EMG (not shown) was recorded by means of 2 stainless steel wires inserted in the neck musculature. A ground electrode was implanted over the cerebellum (approximately 1 mm posterior to lambda and 2 mm from the midline). For microinjections, stainless-steel cannulae were placed bilaterally (A, blue) such that when the internal cannulae were lowered 2.0 mm below the tip of the guides, they reached the target site in the basal forebrain (using Anterior-Posterior (AP), Lateral (L) and Vertical (V) coordinates with reference to ear bar zero: AP +7.7 mm, L 2.5 mm, V +1.5 mm). Drugs were delivered in a 2 step process allowing the injection to take place during a natural sleep cycle (B). Drug loaded cannulae were first inserted on the animals head such that the tip of the cannulae remained inside the guide cannulae. With a remote controlled, movable inner cannulae, once the animal had resumed a regular sleep cycle, the second step of lowering the drug loaded cannulae into the basal forebrain target was executed. The guide cannulae and electrodes were fixed to the skull with dental cement.

A

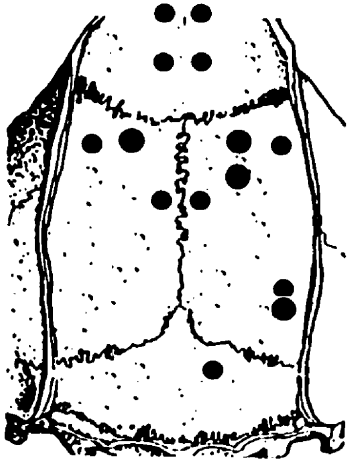

screws placed on dura ●

implanted deep electrodes ●

inserted guide cannulae ●

B

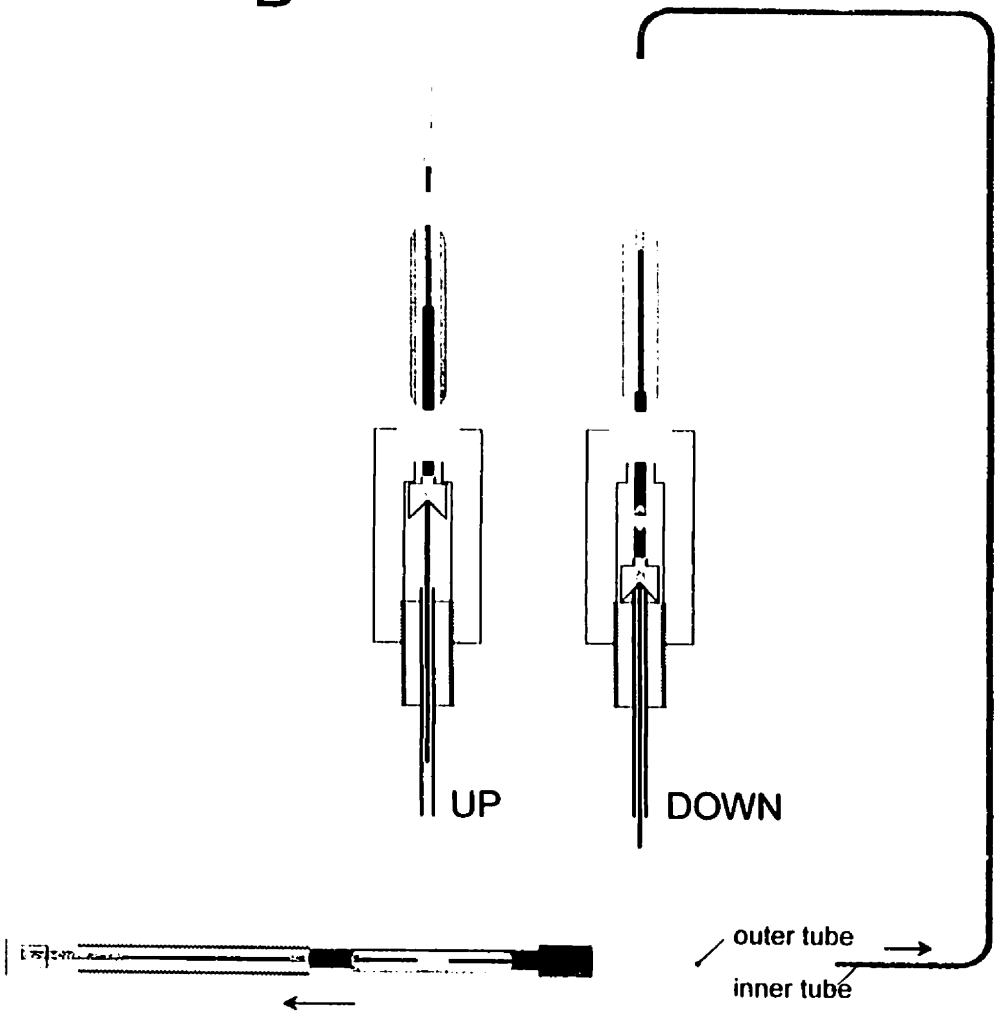

HIGH FREQUENCY GAMMA EEG ACTIVITY IN ASSOCIATION WITH SLEEP-WAKE STATES AND SPONTANEOUS BEHAVIORS IN THE RAT

Karen J. Maloney, Edmund G. Cape, Jean Gotman and Barbara E. Jones

Published, Neuroscience, 76(2) pp. 541-555, 1997

PREFACE

To quantify changes in cortical activation, experiments were initially performed to study the specific trends in the electroencephalogram (EEG) in freely moving rats in association with specific behaviors during the normal sleep-wake cycle. This study would identify high frequency gamma EEG activity along with theta that would distinguish active wake from quiet wake and slow wave sleep (SWS). These activities would serve as reliable indicators of behavioral and cortical arousal across the sleep-waking cycle and independent of changes in muscle tone, since they varied with paradoxical sleep (PS) in a manner parallel to that during active waking behavior.

ABSTRACT

The occurrence of high frequency gamma activity (30-60 Hz) and its relationship to other frequency band activities were examined by spectral analysis of the EEG in association with sleep-wake states and spontaneous behaviors in the rat. In the EEG, gamma wave activity was evident in unfiltered and high frequency filtered recordings, in which it was prominent during attentive or active Wake episodes and during Paradoxical Sleep, when theta-like activity was also apparent. In amplitude spectra from these episodes, multiple peaks were evident within the gamma frequency band, indicating broad band high frequency activity, in association with a single low frequency peak in the theta band. Gamma peaks were attenuated during Waking quiet, in association with a low frequency peak between theta and delta, and during Slow Wave Sleep, in association with a low frequency peak in the delta band. In coherence spectra from ipsilateral cortical leads, peaks were also present within the gamma range and were significantly higher in Waking moving and Paradoxical Sleep than in Waking quiet and Slow Wave Sleep. In measures of frequency band amplitude, activity in the gamma frequency band (30.5-58.0 Hz) varied significantly across the sleep-waking cycle, being greatest during Wake and Paradoxical Sleep and lowest during Slow Wave Sleep. Across these states, gamma was negatively correlated with delta (1.5-4.0 Hz). In contrast, high beta activity (19.0-30.0 Hz) was significantly lower in Wake than in Slow Wave Sleep and was positively correlated with delta activity. Gamma differed significantly across specific behaviors, being highest in Paradoxical Sleep with *twitches* and during Waking

eating and *moving* behaviors, slightly lower in Waking *attentive,* lower in Waking *grooming* and as low in Waking *quiet* as during Slow Wave Sleep in a *curled* posture.

These results indicate that the reciprocal variation of high frequency gamma activity (and not beta) with low frequency, delta activity best reflects the sleep-waking cycle of the rat. Moreover, gamma activity reflects the degree of behavioral arousal, since it is high during active Waking, when the EMG is high, and low during *quiet* Waking, when the EMG is low. It also reflects cortical arousal, independent of motor activity, since it attains high levels in association with *attentive* immobility and maximal levels only during particular Waking behaviors (*eating* and *moving* and not *grooming*), and it also attains maximal levels during Paradoxical Sleep, when the nuchal EMG is minimal, but small *twitches* evidence dreaming. The covariation of gamma and a slow oscillation in the theta band across states and behaviors suggests that a common system may modulate these fast and slow EEG rhythms, and that such modulation, potentially emanating from the basal forebrain, could predominate during particular behaviors or states, notably Paradoxical Sleep.

INTRODUCTION

Over many years, sleep-wake states in mammals have been distinguished by the association of particular behaviors or postures with predominant patterns on the electroencephalographic (EEG) record. In association with various waking behaviors in animals, the EEG of the Wake (W) state has been characterized by low voltage, fast activity. During behaviorally 'quiet sleep', the EEG has been distinguished by high voltage, slow activity, and the state thus referred to as 'Slow Wave Sleep' (SWS). During sleep accompanied by rapid eye movements, muscular twitches and an ostensibly paradoxical loss of postural muscle tone, the EEG in animals has been characterized as similar to that during the Wake state, this sleep state being referred to as 'REM', 'active' or 'Paradoxical Sleep' (PS). Whereas the EEG during 'quiet' sleep has been referred to as 'synchronized', that during waking and 'active' sleep has been described as 'desynchronized'. With the development of quantitative techniques for the analysis of the EEG, including spectral analysis, the predominant frequencies of the different EEG patterns have been analyzed. This analysis primarily concerned frequencies up to 32 Hz, and accordingly Wake and Paradoxical Sleep were characterized by a predominance of the frequencies in the beta range (~ 15-30 Hz) and Slow Wave Sleep by the presence of slow waves in the delta range (1-4 Hz) (Trachsel *et al.*, 1988; Uchida *et al.*, 1992). More recently, attentive and responsive states have been with a higher frequency activity (30-60 Hz), called 'gamma' activity (Bressler, 1990; Freeman, 1991). As that originally discovered in the olfactory bulb, gamma activity is often found in the olfactory

and neocortex at a frequency near 40 Hz (see for review (Freeman and Skarda, 1985; Gray, 1994; Singer, 1993)). Reports from animal and human studies have indicated that cortical gamma activity is associated with attentiveness (Bouyer *et al.*, 1981; Rougeul-Buser *et al.*, 1975), focused arousal (Sheer, 1989), sensory perception (Gray *et al.*, 1989), movement (Murthy and Fetz, 1992; Pfurtscheller and Neuper, 1992) and perceptuomotor behavior (Bressler *et al.*, 1993). In addition, unlike olfactory bulb gamma waves which are present during waking but not during sleep (Hernandez-Peon *et al.*, 1960), cortical gamma waves have been reported to be present during PS-REM sleep in animals and humans (Franken *et al.*, 1994; Itil, 1970; Llinas and Ribary, 1993; Mann *et al.*, 1993; Parmeggiani and Zanocco, 1963). It has been proposed that synchronization at this high frequency across functionally related cortical areas provides the 'binding' necessary for unified cognitive experience in waking and dreaming (Joliot *et al.*, 1994; Llinas and Ribary, 1993). Results in animals and humans thus suggest that active waking and 'active sleep' (PS) may be characterized by the presence of synchronized gamma activity in the cerebral cortex.

The present study was undertaken to investigate the presence and characteristics of gamma EEG activity in the rat across sleep-wake states and in association with common spontaneous behaviors or postures of these states. The relationship of the gamma frequency band (30.5-60 Hz) to the other high frequency beta bands (beta2: 19-30 Hz and beta1: 14.5-18.5 Hz) and to the low frequency bands (sigma: 9.0-14 Hz, theta: 4.5-8.5 Hz, and delta: 1-4 Hz) was also examined. As part of a larger study, aimed at

determining the modulation of cortical gamma activity by subcortical systems, some of these results were reported in abstract form (Cape and Jones, 1994).

METHODS

Animals and surgery

Five male Wistar rats, weighing approximately 225 grams, were operated under barbiturate anesthesia (Somnotol, 67 mg/kg, i.p.) for the implantation of chronically indwelling electrodes. For the EEG, stainless steel jeweller's screws were threaded into holes drilled in the skull to be in contact with the dura. They were placed with reference to bregma and the midline sutures over: 1) the left and right anterior medial frontal cortex (LF and RF: 2.75 mm anterior and 0.6 mm lateral), 2) the left and right retrosplenial cortex (LRS and RRS: 3.5 mm posterior and 0.6 mm lateral), 3) the left and right parietal cortex (LP and RP: 0.5 mm posterior and 5.0 mm lateral), and 4) the left and right occipital cortex (LO and RO: 7.5 mm posterior and 5.0 mm lateral) (Paxinos and Watson, 1986). For the reference, screws were placed in the frontal bone rostral to the frontal cortex and caudal to the olfactory bulb, ($\sim$5.5 mm anterior to bregma and 0.8 mm lateral to the midline). A ground screw was placed over the cerebellum (2.0 mm posterior to lambda and $\sim$2 mm from the midline). For the EMG, two stainless steel loops were inserted into the muscles of the neck. All leads were connected to a miniature (12 lead) plug which was cemented to the skull. Animals were allowed a minimum of two days to recover from surgery.

EEG recording and behavioral notation

For EEG recording, each animal was housed in a plexiglass box within a large electrically shielded recording chamber and allowed a minimum of two days habituation prior to recording. The rat was connected to a cable attached to a commutator and suspended with a balanced boom to allow free

movement. As was the case in the animal rooms, a 12 hour light/dark cycle was maintained in the recording rooms (with lights on from 7:00 a.m. to 7:00 p.m.). Recording and behavioral observations were performed in the afternoon (~12:00 - 3:00 p.m.). The EEG and EMG signals were recorded with a Grass Model 78D Polygraph. The EEG signals were recorded with the same gain on each channel and filtered between 1.0 to 100 Hz. The amplifier output was sent to a computer (ALR 386SX) for analog to digital conversion (ADC), filtering and storage on hard disk with the aid of Stellate Systems (Montreal) computer software for EEG recording, spectral analysis and sleep-wake state scoring. The signals were digitized on-line at a rate of 512 samples per second and filtered with a Finite Impulse Response (FIR) filter having a cut-off frequency at 64 Hz to insure elimination of activity above that frequency. Data were subsequently sampled and stored for analysis at 256 samples per second.

The behavior of the rats was monitored by video camera and marked by on-line annotation on the EEG computer records. Nine annotations for behavior were established according to the common sequence of behaviors that occurred during the sleep-waking cycle of the rat during the day-time recording sessions and which allowed behavioral scoring of this cycle. 1) 'Waking *attentive*' (W*attentive*, W*a*) was scored when the rat was awake and immobile yet attentive, seemingly stopping to attend to a noise or other stimulus, and marked by an alert, standing posture with eyes wide open. If three clear periods of spontaneous attentive behavior were not observed during the recording session, this behavior was elicited by tapping on the cage. 2)

'Waking *moving*' (W*moving*, W*m*) was scored when the rat walked around or moved from one place to another in the cage. 3) 'Waking *eating*' (W*eating*, W*e*), was elicited by placing a piece of food on the floor of the cage (which the rats would always eat in lieu of working for the food available ad lib in metal holders). 4) 'Waking *grooming*' (W*grooming*, W*g*) usually followed eating. 5) 'Waking *quiet*' (W*quiet*, W*q*), often followed grooming and preceded sleep and was scored when the rat was reclined on the cage floor with eyes open. 6) 'Sleep *uncurled*' (S*uncurled*, S*u*) usually typified the onset of sleep and was scored when the rat lay immobile on its side with its body and limbs partly outstretched and its eyes closed. 7) 'Sleep *curled*' (S*curled*, S*c*) usually occurred as sleep progressed and was scored when the rat was immobile with its head, body and limbs curled into a crescent or ball and with its eyes closed. 8) 'Sleep moving' (S*moving*, S*m*) usually occurred after a certain period of sleep and was scored when the rat made a slight movement or changed position while maintaining its eyes closed. It could be followed by continued sleep or awakening. 9) 'Sleep *twitch*' (S*twitch*, S*t*) usually occurred after a certain period of sleep and often following a slight movement and was scored when distinct, repetitive, small movements of the vibrissae, nose, or ears were evident during sleep.

Data Analysis and Statistics

The EEG was examined by off-line analysis on computer screen and scored by visual assessment according to sleep-wake states in 20 sec epochs using Eclipse software (Stellate Systems). By referring to EEG and EMG, epochs were scored as one of the three major states (W, SWS or PS) or

transitional (*t*) stages between states: 1) Wake (W) by the presence of low voltage fast activity associated with EMG tonus, 2) transition from Wake into Slow Wave Sleep (*t*SWS) characterized by mixed or moderate amplitude slow activity, 3) continuous Slow Wave Sleep (SWS) with high amplitude slow activity, 4) transition from Slow Wave Sleep into Paradoxical Sleep marked by a decrease in high amplitude slow activity and the appearance of spindles and theta waves (*t*PS), or 5) Paradoxical Sleep (PS) marked by a prominence of theta waves with low EMG activity. The average percent time spent in each of these was relatively similar for the five rats across the 3 hour recording periods (mean ± s.e.m.: W: 31.6 ± 5.5%; *t*SWS: 21.4 ± 0.7%; SWS: 25.9 ± 2.5%; *t*PS: 10.9 ± 2.8%; PS 10.3 ± 1.8%). For each rat, sleep-wake hypnograms were displayed in association with EEG frequency band activities (below) for 20 sec epochs over the full 3 hour recording session using the Eclipse software.

Spectral analysis was performed using Rhythm software (Stellate Systems) for 4 sec epochs scored according to behavior in addition to state. Three sample epochs per behavior per animal were selected. Each epoch was chosen in association with a behavioral notation and for continuity of behavior and uniformity of EEG activity during the 4 sec sample in order to maximally approach stationarity of the EEG signal for spectral analysis. As intended, each behavioral notation was commonly associated with one sleep-wake EEG state. In order to streamline the analysis of behaviors and states, the samples of each behavior were always selected from the same, most commonly associated EEG state within the sleep-waking cycle. Thus, '*Wattentive*',

'W*moving*', 'W*eating*' and 'W*grooming*' epochs were all selected from Wake scored EEG sections and were, in fact, exclusively associated with the Wake state. 'W*quiet*' epochs were selected from Wake scored EEG sections, although W*quiet* notations were occasionally found in sections scored as *t*SWS. 'S*uncurled*' epochs were selected from *t*SWS scored sections, with which these notations were usually associated, although they were also found less frequently in sections scored as SWS. 'S*curled*' epochs were selected from SWS scored sections, with which these notations were usually associated, although they were also less frequently found in sections scored as *t*SWS. 'S*moving*' epochs were selected from *t*PS scored sections, with which they were frequently though by no means exclusively associated, occurring also in *t*SWS or during shifts to W. 'S*twitch*' epochs were selected from EEG sections scored as PS and were usually associated with this state.

For both the 20 sec state epoch data and 4 sec state-behavior epoch data, Fast Fourier Transform (FFT) was performed to determine power spectra and frequency band activities using Eclipse and Rhythm software (Stellate Systems). The FFT was computed on 512 points corresponding to 2 sec epochs with a resolution of 0.5 Hz. A 7-point smoothing window was applied allowing a minimum frequency of 1.5 Hz and a maximum frequency of 63.5 Hz in the spectrum computation. The spectra and band activity were displayed and reported using amplitude units (square root of power), since the dynamic range of amplitude is lower than that for power and allows visualization on the same scale of both low (eg. delta) and high (eg. gamma) frequency activities in the same manner and proportions that they are seen in the EEG record. The

average gain was calibrated as ~1500 AD units per mV on the EEG channels. In preliminary spectral analyses, frequency band ranges were established by conformity with traditional settings but also by maximization, as much as possible, of the separation between predominant peak frequencies in the rat EEG. Non-overlapping bands were accordingly set for the duration of the study at the following ranges; delta: 1.5-4.0 Hz, theta: 4.5-8.5 Hz, sigma: 9.0-14.0 Hz, beta1: 14.5-18.5 Hz, beta2: 19.0-30.0 Hz, and gamma: 30.5-58.0 Hz (eliminating frequencies around 60 Hz to avoid any possible contamination from AC noise). Activities in each band were reported as AD units. Relative amplitudes of each band were also reported and correspond to the % of the total spectrum up to 58.0 Hz. The ratio of theta/delta was also calculated and reported (as explained in Results). EMG amplitude was computed for the total spectrum up to 58.0 Hz.

Analyses of EEG, amplitude spectra, coherence spectra and frequency band activities were carried out in each of the individual rats on right cortical leads with particular focus on the retrosplenial lead. Statistical analyses of frequency band activities were performed on 20 sec epoch data from one full recording session (~500 epochs) in individual rats, first, using Pearson pairwise correlations between band activities (with Bonferroni probabilities) to determine their covariation across the sleep-waking cycle and second, using one way ANOVAs per frequency band across the (5) sleep-wake states with Bonferroni post hoc paired comparisons between states to determine significant differences in band activities in the respective states. Differences in the mean values of each frequency band per state per animal were also tested

across rats by a repeated measures ANOVA with post hoc comparisons performed using a C matrix. Analyses were also performed on 4 sec epoch data that were scored for state and behavior. Variations in EEG frequency band activities (and also low peak frequency and EMG) across state-behavior epochs were examined for the five rats by employing a repeated measures ANOVA for each band (or peak frequency or EMG) with two factors (9 behaviors and 3 samples per behavior per rat). Post hoc comparisons were made for repeated measures by employing a C matrix. All statistics were performed using Systat for Windows (Evanston, Illinois).

RESULTS

The EEG of the rat manifests specific changes across the sleep-waking cycle and in association with specific behaviors of the Wake (W) state, as assessed first qualitatively and illustrated in Fig. 1. In the unfiltered EEG record (top panel, Fig. 1), activity in a low frequency range is most prominent. As particularly apparent in the right retrosplenial cortex (RRS) and right occipital cortex (RO), this activity was in a theta range (4.5-8.5 Hz) during Waking *attentive* (immobile) or Waking *moving* and slowed progressively during Waking *quiet* (immobile) to be within a delta range (0-4.0 Hz) during Slow Wave Sleep (SWS), and then return to a theta range during Paradoxical Sleep (PS). Riding upon the slow waves in the unfiltered EEG record, low amplitude fast oscillations could also be detected, particularly in association with the theta range slow activity in W and PS. During these states, the frequency of the fast oscillations could be visually ascertained as being greater than 30 Hz and less than 50 Hz, corresponding to a gamma range of frequencies.

In EEG digitally filtered for higher frequencies, a clear distinction across states and behaviors was evident when the filtering was performed for frequencies in the gamma range (30.5-58.0 Hz) (Fig. 1, bottom panel). Such a distinction was not apparent when filtering was performed for frequencies in the beta range (19.0-30.0 Hz). Moreover, in the gamma filtered EEG, the waves matched the predominant fast activity evident in the unfiltered record (Fig. 2). Gamma activity was evident across the sleep-waking cycle but varied in amplitude in association with different states and behaviors or postures, appearing high during W*attentive* and more so during W*moving* and low during W*quiet* behavior and SWS (Fig. 1). During PS when *twitches* were apparent, gamma activity appeared as high as during active W episodes.

Differences in EEG spectra across states and behaviors

The EEG spectra differ across sleep-wake states and spontaneous behaviors in a systematic manner, as illustrated in a representative case from the right retrosplenial cortex in Fig. 3. Associated with each state-behavior, there was a major peak of varying frequency, sharpness and amplitude in the low frequency range. This low frequency peak varied significantly across behaviors (assessed by repeated measures ANOVA with post hoc comparisons, $n = 5$, $p < .05$). During W*attentive* and active behaviors, the peak frequency was in the theta range, and though not differing significantly between these behaviors, was highest during W*moving* (mean ± s.e.m. for 5 animals, = 6.67 ± 0.27 Hz). In W*quiet*, the peak frequency slowed to one intermediate between theta and delta ranges (4.37 ± 0.60 Hz), which was significantly lower than that during all other Waking behaviors ($p < .05$). During *t*SWS in an uncurled position and during SWS in a curled position, the peak frequency was clearly within a delta range (*t*SWS-S*uncurled* = 3.47 ± 0.39 Hz; SWS-S*curled* = 2.42 ± 0.11 Hz) and significantly lower than during Waking *attentive* or active behaviors. The delta peak was quite broad, and its base extended into the theta range contributing amplitude to the theta band in absence of any regular theta activity in the EEG. A secondary peak was often present within the sigma band (between 10.0-14.0 Hz), indicative of spindles in SWS and *t*PS. During *t*PS (-S*moving)* and during PS (-S*twitch*), a sharp peak in the theta range became apparent (*t*PS-S*moving* = 5.67 ± 0.42 Hz; PS-S*twitch* = 7.57 ± 0.20 Hz). The peak low frequency varied significantly as a function of state-behavior on all cortical leads (one way ANOVA with repeated measures

per cortical lead, $p < .05$) and was consistently significantly higher during PS (-*Stwitch*) and *Weating* than during SWS (-*Scurled*) (post hoc for repeated measures, $p < .05$). Although the absolute values of peak frequency differed across leads (tested with repeated measures ANOVA for four cortical areas, $p < .05$), the low frequency peak was in the theta range in association with PS-*Stwitch* and *Weating* on all cortical leads.

Within the high frequency range, multiple peaks were present in beta2 and gamma bands as evident for the right retrospleniai cortex (Fig. 3). No single peak or predominant peak could be systematically identified in either of these bands in association with particular behaviors or states. However, in all animals, peaks and/or total activity in the gamma range appeared consistently higher in Waking *attentive* or active behaviors (*Wmoving*, *Weating*, *Wgrooming*) and in PS-*Stwitch* than in Waking *quiet* and than in *t*SWS (-*Suncurled*) and SWS (-*Scurled*). Peaks in the beta2 band appeared greatest in association with *Weating* or PS (-*Stwitch*) state-behaviors.

Similar patterns in the high frequency range of the amplitude spectra were evident on all cortical leads. During epochs of *Wmoving* and PS(-*Stwitch*), a peak in the region of 40 Hz (35-45 Hz) in the right retrosplenial cortex was often associated with a similar peak in other cortical leads, but particularly in the right occipital cortex, where a more prominent peak at the same frequency was often apparent. In coherence spectra from ipsilateral cortical leads, peaks were present in the same range and associated with positive or negative phase shifts which varied for different cortical leads. Coherence was systematically investigated between RRS and RO, for which

the autospectra appeared to be the most similar and the coherence peaks, the highest, across certain state-behaviors (10 samples of 4 sec epochs with maximal uniformity of activity in W*moving*, W*quiet*, SWS-S*curled* and PS-S*twitch* being selected from rat BE10). Peaks in the coherence spectra located near 40 Hz (the highest peak between 35-45 Hz, mean ± s.e.m. = 40.7 ± 0.3 Hz, n = 40) varied significantly in percent as a function of state and behavior (based upon one way ANOVA for state-behavior, $p < .05$). The gamma coherence peaks were significantly higher in W*moving* (69.5 ± 3.3 %) and PS-S*twitch* (74.6 ± 1.8%) than in W*quiet* (62.1 ± 3.5 %) and/or SWS-S*curled* (58.8 ± 2.5%) (based upon post-hoc comparisons, $p < .05$). Coherence peaks, which were consistently associated with phase shifts, were also present in the low frequency range, being in the theta band for W*moving* and PS-S*twitch* (mean ± s.e.m. = 7.1 ± 0.1 Hz, n = 20) in which they were particularly high (W*moving* = 83.8 ± 2.3%; PS-S*twitch* = 88.3 ± 1.9%). Both theta and gamma coherence peaks in W*moving* and PS-S*twitch* were significantly higher than delta coherence peaks in SWS-S*curled* (at 1.7 ± 0.1 Hz, 65.1 ± 2.3%; $p < .05$).

Variations in EEG frequency band activities across the sleep-waking cycle

The activities of the frequency bands varied differentially across the sleep-waking cycle, as seen in the activities from the right retrosplenial cortex in association with the hypnogram in Fig. 4 (from rat BE10). Gamma activity was relatively high during periods of W, however it varied considerably during this state in association with different behaviors (Fig. 4, see next section below). It was low during the transitional stage, *t*SWS, passing from W to

SWS and remained low during deep SWS. In the transitional stage (*t*PS) from SWS to PS and during PS, gamma activity increased and appeared to attain levels that were approximately equal to the highest levels that occurred during W (Fig. 4). Across the sleep-waking cycle, gamma appeared to vary inversely with delta. In contrast, beta2 activity appeared to increase in association with slow wave sleep, although the amplitude changes were minimal and difficult to assess visually. Beta1 appeared to covary with sigma, which in turn largely covaried with delta. Theta appeared to covary partly with delta, which was explained by the overlap of the high amplitude delta activity into the theta band seen in the spectra (above). But theta was high when gamma was high; and when plotted as the ratio of theta to delta (Th/De), it clearly covaried with gamma, being uniquely high during Wake and PS periods (and also reflecting the regular theta waves evident in the EEG record). Similar patterns and relationships of frequency band activities (and Th/De ratio) were evident from all cortical leads.

Correlations across frequency bands were examined for the right retrosplenial cortex in individual rats. Across sleep-wake states, gamma was significantly negatively correlated with delta in all rats ($r = -.481$, $p < .001$ in rat BE10, $n = 528$ 20 sec epochs; average $r = -.436$ for 5 rats, and was not significantly correlated with sigma). In contrast, beta2 was significantly positively correlated with delta in all rats ($r = .554$, $p < .001$ in rat BE10; average $r = .470$ for 5 rats, and most highly positively correlated with sigma, average $r = .818$). Across the sleep cycle, excluding the W state, gamma was similarly negatively correlated with delta ($r = -.553$, $p < .001$, average $r =$ -

.524, and not significantly correlated with sigma), and beta2 was positively correlated with delta, although with a lower correlation coefficient ($r = .206$, $p < .05$; average $r = .331$, and highly positively correlated with sigma, average $r = .758$). Beta1 was positively correlated with delta ($r = .724$, $p < .001$; average $r = .647$) like sigma ($r = .799$, $p < .001$; average $r = .689$) across the sleep-waking cycle. Gamma was not consistently significantly correlated with theta but was consistently significantly positively correlated with Th/De ($r = .748$, $p < .001$; average $r = .626$ for 5 rats). Across the sleep-waking cycle, there was a positive correlation between gamma and EMG, a correlation which was particularly high and significant when examined for W, *t*SWS and SWS ($r = .747$, $p < .001$, $n = 493$ epochs for rat BE10; average $r = .705$ for 5 rats), with the exclusion of *t*PS and PS when gamma was high and EMG low in association with the neck muscle atonia of that state.

In comparisons of frequency band activities across states within individual animals, gamma was significantly higher in W, *t*PS and PS than in the *t*SWS and SWS (based upon one way ANOVAs for state with post hoc paired comparisons in each rat, $n = 528$, 20 sec epochs in rat BE10, $p < .001$; and upon repeated measures ANOVA of mean values for 5 rats with $p < .05$, Table 1 for RRS). In contrast, beta2 was significantly lower in W than in SWS (in 4/5 rats and across rats, Table 1) and not significantly different between PS and SWS. Beta1 and sigma were significantly lower during W and PS than during SWS. Like gamma, Th/De, reflecting theta activity, was significantly higher in W and PS than in *t*SWS and SWS, and also higher in PS than in W. Although gamma was on average higher in PS than in W, this difference was

not significant in every animal or across animals, because gamma varied greatly during the W state, since it depended upon the behavior of the animal, as was systematically investigated (below).

Variation in frequency band activities with state-behaviors

All frequency bands varied in activity significantly as a function of state-associated-behaviors (according to one way repeated measures ANOVA, $p<.05$), as illustrated for the right retrosplenial cortex in Fig. 5. However, the manner and degree to which the absolute amplitude reflected state-behaviors differed markedly according to the different bands (as assessed with post hoc tests for repeated measures in 5 rats with significance set at $p<.05$, Fig. 5, left panel). Thus, absolute gamma activity was significantly greater in immobile attentive (W*attentive*) and active Waking behaviors (W*moving*, W*eating* and W*grooming*) and in *t*PS-S*moving* and PS-S*twitch* than in SWS-S*curled*. In contrast, beta2 was not significantly different in any Waking behavior or PS-S*twitch* as compared to SWS-S*curled*. Beta1, like sigma, was significantly lower in most Waking behaviors as compared to SWS-S*curled*, but was not significantly different in PS as compared to SWS-S*curled*. As to be expected, delta was significantly higher in SWS-S*curled* than in every other state-behavior. Theta band activity was not significantly different in Waking behaviors from SWS-S*curled*, but the ratio of Th/De revealed a clear variation in association with state-behaviors, being significantly higher in Waking behaviors and *t*PS-S*moving* and PS-S*twitch* than in SWS-S*curled*. Total amplitude predominantly reflected the slow wave activities, particularly delta but also theta. The relative amplitude, as percent of the total, thus reflected

the variations in delta and theta as much as, if not more than (in the case of beta2), the variation of the higher frequencies (Fig. 5, right panel). As percent of total, both gamma and beta2 were significantly greater in all Waking behaviors and *t*PS-S*moving* and PS-S*twitch* than in SWS-S*curled*. The variations in absolute and relative amplitudes of the frequency bands (and Th/De ratio) were similar for all cortical leads.

Gamma activity differed between the various Waking behaviors, as evident for the right retrosplenial cortex (Fig. 5). Compared across animals (with post hoc tests for repeated measures in 5 rats, Table 2), gamma was highest in W*eating*, followed by W*moving* from which it did not differ significantly. Gamma was significantly higher in W*eating* than in W*attentive* and was higher in W*eating*, W*moving* and W*attentive* than in W*grooming*. Gamma was higher in all the latter behaviors than in W*quiet*. Gamma was not significantly different in PS-S*twitch* than during the most active Waking behaviors (W*eating* and W*moving*). It was significantly greater in PS-S*twitch* than in W*attentive*, W*grooming* and W*quiet*. Beta2 was higher in PS-S*twitch* than in most Waking behaviors, except W*eating*. PS-S*twitch* differed from all Waking behaviors by significantly higher theta and Th/De (Fig. 5) (which was the case on all cortical leads).

Gamma varied as a function of state-behavior and in a reciprocal manner to delta across sleep-wake states on all cortical leads (Fig. 6). It was highest in association with the same behaviors (W*eating* and W*moving*) on all cortical leads and significantly higher in attentive and active Waking behaviors and PS-S*twitch*

than in W*quiet* on all cortical leads. Gamma did not differ significantly between W*quiet* and SWS-S*curled* on any cortical lead.

DISCUSSION

The results of the present study show that high frequency waves in the gamma range are present in the EEG and vary in amplitude as a function of both state and behavior in the rat. Across sleep-wake states, gamma, and not beta, varies inversely with delta. Gamma activity is high in association with attentive and active Waking and paradoxical or 'active sleep', and low in association with quiet waking and 'quiet sleep'. It thus reflects the degree of behavioral and cortical arousal in the rat.

Gamma waves in the EEG and spectra

High frequency components were evident in the unfiltered record of the rat EEG during attentive and active Wake and Paradoxical Sleep state-behaviors in the present study. Such high frequency activity had previously been seen in the unfiltered EEG of the cat and human during Paradoxical Sleep (Itil, 1970; Parmeggiani and Zanocco, 1963; Rougeul-Buser *et al.*, 1975). As could be appreciated by comparing the unfiltered to the gamma filtered EEG signal here in the rat, the predominant high frequency component of the 'low voltage fast' EEG, characterizing these states, appeared to be in the gamma range (>30 Hz). In human magnetoencephalographic (MEG) studies, 40 Hz activity had been identified in records filtered for gamma activity in a narrow range (35-45 Hz) (Llinas and Ribary, 1993). Here in the rat, there was no evidence in the EEG record or spectra for a single frequency or peak frequency at 40 Hz, indicating that the gamma oscillations occur in a relatively broad band of frequencies during spontaneous behaviors and states.

As evident in autospectra and coherence spectra, both amplitude and coherence in the gamma band varied as a function of state and behavior. The degree of coherence between distant cortical leads on the same side was significantly higher during active Waking and Paradoxical Sleep than during quiet Waking and Slow Wave Sleep. Coherent high frequency activity has been described in cats, monkeys and humans in both narrow and broad high frequency ranges in association with perceptuomotor behaviors during Waking (Bressler *et al.*, 1993; Gray, 1994; Joliot *et al.*, 1994; Murthy and Fetz, 1992; Ribary *et al.*, 1992) and during REM sleep (Llinas and Ribary, 1993). Here in the rat, the higher coherence in gamma during active Waking and Paradoxical Sleep, as compared to that in both gamma and delta activity in Slow Wave Sleep, indicates that the term 'desynchronized' has been inappropriately applied to the EEG of the active Waking and 'active' sleeping brain, as compared to the 'synchronized' EEG of the 'quiet' sleeping brain. Clearly, the EEG of active Waking and 'active' sleep is characterized by prominent, synchronized high frequency gamma activity that underlies cortical activation.

Gamma band activity across the sleep-waking cycle

The present study demonstrated that activity in the gamma frequency band is on average significantly higher during Wake and Paradoxical Sleep states than during Slow Wave Sleep. These results substantiate other recent reports in rats (Franken *et al.*, 1994) and humans (Llinas and Ribary, 1993; Mann *et al.*, 1993). Furthermore, the present study showed that gamma varies reciprocally with delta across the sleep-waking cycle, whereas activity in the high beta frequency band (~ 20-30 Hz) varies positively with delta and

sigma, and is lower in Wake and PS than in Slow Wave Sleep. These results may be compared to those of early human EEG studies which reported that beta activity was actually enhanced during Stage 1 and 2 sleep, as well as sedation, as compared to the Wake state (see for review, (Kozelka and Pedley, 1990)). On the other hand, beta was reported to be greater in REM than in non-REM sleep (SWS) and to vary reciprocally with delta across the sleep cycle in rats and humans (Campbell and Feinberg, 1993; Mann *et al.*, 1993; Uchida *et al.*, 1992). Only when viewed as relative amplitude was that the case in the present study. More recently in the rat (Franken *et al.*, 1994) however, it was found by analyzing transitions between sleep stages, that frequencies between 20-30 Hz increased during the transition to Paradoxical Sleep to subsequently decrease during Paradoxical Sleep, results which conform to those reported here showing parallel variation of hi and lo beta with sigma (spindle) activity which is high in the transition into Paradoxical Sleep. The results of the present study indicate that the reciprocal variation of gamma, and not beta, with delta clearly reflects the sleep-waking cycle in the rat.

Gamma band activity as a function of specific state-behaviors

This study presents quantitative results that demonstrate significantly greater gamma activity in association with spontaneous attentive and active Waking behaviors than with quiet Waking and 'quiet sleep' behaviors. They also show that gamma is as high during 'active sleep' as during the most active Waking behaviors. These results clearly demonstrate that gamma is a sensitive indicator of behavioral and cortical arousal in the rat.

Gamma was positively correlated with EMG across Wake and Slow Wave Sleep and was highest in association with movement during locomotion-*moving* and *eating* on all cortical leads. These results substantiate those in the monkey and human in which increases in gamma were reported over sensorimotor cortex in association with various movements (Murthy and Fetz, 1992; Nashmi *et al.*, 1994; Pfurtscheller *et al.*, 1994). They also show that movement alone, which is equivalent during *eating* and *grooming* activities, does not account for the degree of gamma, which is significantly higher during *eating* than during *grooming*. The results accordingly suggest that gamma is a reflection of the arousal level associated with particular behaviors, stimuli or situations. In the monkey, gamma was also found to be high not only in association with actual movement and activities, but also with the planning of a movement or general attention when performing a specific task associated with a consummatory reward (Murthy and Fetz, 1992; Sanes and Donoghue, 1993). Studies in the cat originally described bursts of high frequency activity (35-45 Hz) in fronto-parietal cortex when an animal "exploring an unknown environment" or perceiving "a strange sound or noise" would "undergo phases of immobility" (Bouyer *et al.*, 1981; Rougeul-Buser *et al.*, 1975). Here in the rat during similarly defined *attentive* immobility, gamma was lower than during Waking *moving* or, more particularly, *eating* on all cortical leads. Gamma was nonetheless higher in *attentive* immobility, when the rat stands with head and body erect seemingly attending to a stimulus, than during *quiet* immobility, when the rat is recumbent and relaxed yet with eyes open, indicating once

again that gamma is a reflection of global attention and cortical arousal during the Waking state.

Gamma was also high in association with Sleep *twitch* behavior in Paradoxical Sleep, during which the nuchal EMG was minimal. It was in fact as high as the highest levels that occur during Waking with *moving* or *eating*, indicating that gamma reflects the degree of cortical arousal in addition to behavioral arousal, as has also been suggested from human studies in which dreaming was associated with high gamma activity (Llinas and Ribary, 1993). These results indicate that in high frequency EEG activity, Paradoxical Sleep is not different from the most aroused Waking state.

Association of gamma with theta

Gamma waves were prominent in association with rhythmic slow waves of theta frequency in the unfiltered EEG record during Paradoxical Sleep and during certain periods of active Waking here in the rat. The simultaneous presence of high frequency activity with slow, theta-like activity had also been noted previously in the EEG of cat (Parmeggiani and Zanocco, 1963) and human during REM sleep (Itil, 1970; Jouvet *et al.*, 1960). This same association was evident here in amplitude spectra, in which higher amplitude in the gamma range was associated with a distinct peak in the theta range, indicative of regular theta activity in the EEG. First recorded in the hippocampus, in which fast (40-50 Hz) waves were riding on slower (4-7 Hz) theta waves (Buzsaki *et al.*, 1983; Stumpf, 1965), an association of gamma and theta waves has also been documented in medial, limbic cortex (entorhinal (Boeijinga and Lopes da Silva, 1988) and cingulate (Leung and Borst, 1987)),

where theta waves have been shown to be generated as well (Borst *et al.*, 1987; Holsheimer, 1982; Leung and Borst, 1987). Although evidence is lacking for generation of theta in lateral, isocortex and its presence there and from the medial, limbic cortex of the rat may be explained by volume conduction from the dorsal hippocampus (Gerbrandt *et al.*, 1978), the present results, together with earlier results in other species (above), suggest that theta oscillations may occur in these areas during particular behavior-states. First, volume conduction is not always considered to play a prominent role in local EEG signals (Petsche and Rappelsberger, 1992), particularly when (as is the case here with the frontal and parietal leads) both active and referential electrodes are located at a significant distance from (and rostral to) the possible subcortical source. Second, although peaks were present in the theta band on all cortical leads, the peak frequencies differed across these leads. Third, the change in peak frequency was progressive across the state-behavioral changes going from a high theta frequency in active Waking and Paradoxical Sleep to a delta frequency in Slow Wave Sleep, and the amplitude of the theta peaks was within a similar range as the delta peaks (which are presumed to originate from cerebral cortex). A rhythmic slow rhythm in the theta range could be transmitted through pathways to isocortical regions from other cortical or subcortical limbic structures during particular behaviors and states, such as Paradoxical Sleep. The association of a slow theta-like oscillation with a fast gamma oscillation might suggest that the two rhythms are modulated by a common system.

Theta rhythm in the cingulate cortex is modulated by cholinergic input from the diagonal band, parallel with but independent from theta rhythm in the hippocampus, which is modulated by cholinergic input from the medial septum (Borst *et al.*, 1987; Leung and Borst, 1987). It is possible that cholinergic afferents to both medial and lateral cortex could carry a slow rhythmic input, particularly given recent evidence for rhythmic oscillatory properties in the low frequency range of identified cholinergic basalis neurons (Khateb *et al.*, 1992). In addition, cholinergic input from the basal forebrain has been shown to stimulate high frequency gamma activity in the cerebral cortex (Cape and Jones, 1994; Metherate *et al.*, 1992). Moreover, recent electrophysiological studies have also revealed coupled slow and fast oscillatory properties of fast spiking, non-cholinergic neurons, in addition to the slow oscillatory properties of cholinergic neurons, in the basal forebrain that could provide the basis for coordinated parallel modulation of slow and fast cortical rhythms (Alonso *et al.*, 1996). Assuming that slow rhythmic activity in the theta range reflects an input from the basal forebrain, its association with gamma during certain active Waking behaviors and most particularly during 'active' sleep, suggests that a prominent influence from the basal forebrain may simultaneously enhance rhythmic slow theta-like and fast, gamma activities during these state-behaviors.

Reciprocal variation of gamma and delta and mechanisms of gamma modulation

The reciprocal variation of gamma and delta clearly reflects the sleep-waking cycle in the rat. Whereas gamma activity indicates the degree of behavioral

and cortical arousal of Waking and 'active sleep', delta appears to reflect the degree of behavioral and cortical 'quiet sleep', since it increases progressively in the behavioral and EEG transition into deep Slow Wave Sleep. These activities are the manifestation of different modes of tonic versus burst firing by populations of cortical neurons (Steriade *et al.*, 1996), which are in turn modulated by subcortical systems (see for review, (Steriade *et al.*, 1994)). Multiple lines of evidence indicate that the thalamus may modulate gamma and delta activity by different modes of fast tonic versus slow burst firing by the thalamo-cortical neurons and networks in activated versus Slow Wave Sleep states (Llinas and Ribary, 1993; Ribary *et al.*, 1992; Steriade *et al.*, 1994; Steriade *et al.*, 1991a; Steriade *et al.*, 1991b). These different modes of firing depend upon the membrane potential of the thalamic and cortical neurons, which is in turn modulated by brainstem afferents and their neurotransmitters (McCormick, 1992). Thalamo-cortical neurons show fast oscillations in the gamma range, and stimulation of the brainstem can evoke cortical gamma activity transmitted via the thalamus (Canu *et al.*, 1994; Steriade *et al.*, 1991b). It has been proposed from human MEG studies that 40 Hz resonance in thalamo-cortical loops could impose a coherent rostro-caudal sweep with a particular phase shift that would allow scanning of broad cortical expanses to permit global binding in the cortex (Llinas and Ribary, 1993). Activation is also transmitted from the brainstem reticular activating system to the cerebral cortex through the basal forebrain, comprising the ventral extra-thalamic relay (see for review, (Jones, 1995; Stewart *et al.*, 1984)), and gamma activity can be evoked in the cortex by electrical stimulation or microinjections into the basal forebrain of the neurotransmitters contained within the brainstem afferents (Cape and Jones, 1994; Cape and Jones, 1998; Metherate *et al.*, 1992). Rostro-caudal propagation and

coordination of gamma activity could well be imposed by basal forebrain afferent fibers which course tangentially from rostral to caudal in the deep cortical white matter (Luiten *et al.*, 1987; Saper, 1984). Amplitude and coherence in cortical gamma activity could be enhanced by coordinated participation of both thalamo-cortical and basalo-cortical systems but also potentially modulated by differential dominance of these subcortical systems in association with different behaviors and states.

CONCLUSIONS

By reciprocal variation with delta activity, high frequency gamma (30-60), and not beta (20-30), EEG activity reflects the sleep-waking cycle in the rat. Moreover, gamma, and not beta, is a sensitive indicator of behavioral and cortical arousal of the animal across sleep-wake states, being high in association with attentive and active Waking behaviors and 'active', Paradoxical Sleep and being low during quiet Waking and 'quiet', Slow Wave Sleep.

ACKNOWLEDGEMENTS

We thank Lynda Mainville for her technical assistance in this work. We would also like to thank Angel Alonso for invaluable discussion. The research was supported by a grant to BEJ from the Medical Research Council of Canada. Karen Maloney was supported by a Studentship from the Faculty of Medicine, McGill University and Edmund Cape by a Studentship from the Fonds de Recherche pour la Santé au Québec.

ABBREVIATIONS

De	Delta
EEG	electroencephalogram
EMG	electromyogram
Ga	Gamma
PS	Paradoxical Sleep
RF	Right Frontal cortex
RO	Right Occipital cortex
RP	Right Parietal cortex
RRS	Right Retrosplenial cortex
Sc	Sleep *curled*
Sm	Sleep *moving*
St	Sleep *twitch*
Su	Sleep *uncurled*
SWS	Slow Wave Sleep
*T*PS	transition into Paradoxical Sleep
*T*SWS	transition into Slow Wave Sleep
Th	theta
W	Wake
Wa	Waking *attentive*
We	Waking *eating*
Wg	Waking *grooming*
Wm	Waking *moving*
Wq	Waking *quiet*

LITERATURE CITED

Alonso A, Faure M-P, Beaudet A (1994) Neurotensin promotes oscillatory bursting behavior and is internalized in basal forebrain cholinergic neurons. *J. Neurosci.*, **14,** 5778-5792.

Alonso A, Khateb A, Fort P, Jones BE, Muhlethaler M (1996) Differential oscillatory properties of cholinergic and non-cholinergic nucleus Basalis neurons in guinea pig brain slice. *Eur. J. Neurosci.*, **8,** 169-182.

Boeijinga PH, Lopes da Silva FH (1988) Differential distribution of β and θ EEG activity in the entorhinal cortex of the cat. *Brain Res.*, **448,** 272-286.

Borst JGG, Leung L-WS, MacFabe DF (1987) Electrical activity of the cingulate cortex. II. Cholinergic modulation. *Brain Res.*, **407,** 81-93.

Bouyer JJ, Montaron MF, Rougeul A (1981) Fast fronto-parietal rhythms during combined focused attentive behaviour and immobility in cat: cortical and thalamic localizations. *Electroenceph. clin. Neurophysiol.*, **51,** 244-252.

Bressler SL (1990) The gamma wave: a cortical information carrier. *Trends Neurosci.*, **13,** 161-162.

Bressler SL, Coppola R, Nakamura R (1993) Episodic multiregional cortical coherence at multiple frequencies during visual task performance. *Nature*, **366,** 153-155.

Buzsaki G, Bickford RG, Ponomareff G, Thal LJ, Mandel R, Gage FH (1988) Nucleus basalis and thalamic control of neocortical activity in the freely moving rat. *J. Neurosci.*, **8,** 4007-4026.

Buzsaki G, Leung L-WS, Vanderwolf CH (1983) Cellular bases of hippocampal EEG in the behaving rat. *Brain Res. Rev.*, **6,** 139-171.

Campbell IB, Feinberg I (1993) A cortical EEG frequency with a REM-specific increase in amplitude. *J. Neurophysiol.*, **69,** 1368-1371.

Canu M-H, Buser P, Rougeul A (1994) Relationship between posterior thalamic nucleus unit activity and parietal cortial rhythms (beta) in the waking cat. *Neurosci.*, **60,** 679-688.

Cape E, Jones BE (1994) Modulation of sleep-wake state and cortical activity following injection of agonists into the region of cholinergic basal forebrain neurons. *Soc. Neurosci. Abst.*, **20,** 156.

Cape EG, Jones BE (1998) Differential modulation of high frequency gamma electroencephalogram activity and sleep-wake state by noradrenaline and serotonin microinjections into the region of cholinergic basalis neurons. *J. Neurosci.*, **18,** 2653-2666.

Casamenti F, Deffenu G, Abbamondi AL, Pepeu G (1986) Changes in cortical acetylcholine output induced by modulation of the nucleus basalis. *Brain Res. Bull.*, **16,** 689-695.

Celesia GG, Jasper HH (1966) Acetylcholine released from cerebral cortex in relation to state of activation. *Neurology*, **16,** 1053-1064.

Davies SW, McBean GJ, Roberts PJ (1984) A glutamatergic innervation of the nucleus basalis/substantia innominata. *Neurosci. Lett.*, **45,** 105-110.

Fort P, Khateb A, Alonso A, Jones BE, Muhlethaler M (1992) Pharmacological heterogeneity of basal forebrain neurones. *Soc. Neurosci. Abst.*, **18,** 881.

Fort P, Khateb A, Pegna A, Muhlethaler M, Jones BE (1995) Noradrenergic modulation of cholinergic nucleus basalis neurons demonstrated by *in vitro* pharmacological and immunohistochemical evidence in the guinea pig brain. *Eur. J. Neurosci.*, **7,** 1502-1511.

Franken P, Dijk D-J, Tobler I, Borbely AA (1994) High-frequency components of the rat electrocorticogram are modulated by the vigilance states. *Neurosci. Lett.*, **167,** 89-92.

Freeman WJ (1991) The physiology of perception. *Sci. Amer.*, **264,** 78-85.

Freeman WJ, Skarda CA (1985) Spatial EEG patterns, non-linear dynamics and perception: the neo-Sherringtonian view. *Brain Res. Rev.*, **10,** 147-175.

Gerbrandt LK, Lawrence JC, Eckardt MJ, Lloyd RL (1978) Origin of the neocortically monitored theta rhythm in the curarized rat. *Electroenceph. clin Neurophysiol.*, **45,** 454-467.

Goodchild AK, Dampney RAL, Bandler R (1982) A method for evoking physiological responses by stimulation of cell bodies, but not axons of passage, within localized regions of the central nervous system. *J. Neurosci. Meth.*, **6,** 351-363.

Gray C (1994) Synchronous oscillations in neuronal systems: mechanisms and functions. *J. Computational Neurosci.*, **1,** 11-38.

Gray CM, Konig P, Engel AK, Singer W (1989) Oscillatory responses in cat visual cortex exhibit inter-columnar synchronization which reflects global stimulus properties. *Nature*, **338,** 334-337.

Gritti I, Mainville L, Jones BE (1993) Codistribution of GABA- with acetylcholine-synthesizing neurons in the basal forebrain of the rat. *J. Comp. Neurol.*, **329,** 438-457.

Hernandez-Peon R, Lavin A, Alcocer-Cuaron C, Marcelin JP (1960) Electrical activity of the olfactory bulb during wakefulness and sleep. *Electroenceph. clin. Neurophysiol.*, **12,** 41-58.

Hobson JA, McCarley RW, Wyzinski PW (1975) Sleep cycle oscillation: reciprocal discharge by two brainstem neuronal groups. *Science*, **189,** 55-58.

Holsheimer J (1982) Generation of theta activity (RSA) in the cingulate cortex of the rat. *Exp. Brain Res.*, **47,** 309-312.

Itil TM (1970) Digital computer analysis of the electroencephalogram during rapid eye movement sleep state in man. *J. Nerv. Ment. Dis.*, **150,** 201-208.

Jacobs BL, Fornal CA (1991) Activity of brain serotonergic neurons in the behaving animal. *Pharmacol. Rev.*, **43,** 563-578.

Jacobs BL, Jones BE (1978) The role of central monoamine and acetylcholine systems in sleep-wakefulness states: mediation or modulation. In: *Cholinergic-Monoaminergic Interactions in the Brain*. Edited by L. L. Butcher. New York: Academic Press, pp. 271-290.

Jasper HH, Tessier J (1971) Acetylcholine liberation from cerebral cortex during paradoxical (REM) sleep. *Science*, **172,** 601-602.

Joliot M, Ribary U, Llinas R (1994) Human oscillatory brain activity near 40 Hz coexists with cognitive temporal binding. *Proc. Natl. Acad. Sci. USA*, **91,** 11748-11751.

Jones BE (1989) The relationship among acetylcholine, noradrenaline and GABA neurons within the pons of the rat. *Anat. Rec.*, **223,** 57A.

Jones BE (1991) Noradrenergic locus coeruleus neurons: their distant connections and their relationship to neighboring--including cholinergic and GABAergic--neurons of the central gray and reticular formation. In: *Neurobiology of the Locus Coeruleus. Progress in Brain Research, Vol. 85*, Volume 85. Edited by C. Barnes and O. Pompeiano. Amsterdam: Elsevier, pp. 15-30.

Jones BE (1993) The organization of central cholinergic systems and their functional importance in sleep-waking states. In: *Cholinergic Function and Dysfunction, Progress in Brain Research, Vol. 98*, Volume 98. Edited by A. C. Cuello. Amsterdam: Elsevier, pp. 61-71.

Jones BE (1994) Basic mechanisms of sleep-wake states. In: *Principles and Practice of Sleep Medicine, 2nd Edition*. Edited by M. H. Kryger, T. Roth and W. C. Dement. Philadelphia: Saunders, pp. 145-162.

Jones BE (1995) Reticular formation. Cytoarchitecture, transmitters and projections. In: *The Rat Nervous System*. Edited by G. Paxinos. New South Wales: Academic Press Australia, pp. 155-171.

Jones BE, Bobillier P, Pin C, Jouvet M (1973) The effect of lesions of catecholamine-containing neurons upon monoamine content of the brain and EEG and behavioral waking in the cat. *Brain Res.*, **58,** 157-177.

Jones BE, Cuello AC (1989) Afferents to the basal forebrain cholinergic cell area from pontomesencephalic--catecholamine, serotonin, and acetylcholine--neurons. *Neuroscience*, **31,** 37-61.

Jones BE, Harper ST, Halaris AE (1977) Effects of locus coeruleus lesions upon cerebral monoamine content, sleep-wakefulness states and the response to amphetamine. *Brain Res.*, **124,** 473-496.

Jones BE, Yang T-Z (1985) The efferent projections from the reticular formation and the locus coeruleus studied by anterograde and retrograde axonal transport in the rat. *J. Comp. Neurol.*, **242,** 56-92.

Jouvet M (1972) The role of monoamines and acetylcholine-containing neurons in the regulation of the sleep-waking cycle. *Ergeb. Physiol.*, **64,** 165-307.

Jouvet M, Michel F, Mounier D (1960) Analyse electroencephalographique comparee du sommeil physiologique chez le chat et chez l'homme. *Rev. Neurol. (Paris)*, **103,** 189-205.

Khateb A, Fort P, Alonso A, Jones BE, Muhlethaler M (1993) Pharmacological and immunohistochemical evidence for a serotonergic input to cholinergic nucleus basalis neurons. *Eur. J. Neurosci.*, **5,** 541-547.

Khateb A, Fort P, Serafin M, Jones BE, Muhlethaler M (1995) Rhythmical bursts induced by NMDA in cholinergic nucleus basalis neurones *in vitro*. *J. Physiol. (Lond.)*, **487.3,** 623-638.

Khateb A, Muhlethaler M, Alonso A, Jones BE (1992a) Oscillatory bursts in basal forebrain cholinergic neurons induced by NMDA. *Soc. Neurosci. Abst.*, **18,** 881.

Khateb A, Muhlethaler M, Alonso A, Serafin M, Mainville L, Jones BE (1992b) Cholinergic nucleus basalis neurons display the capacity for rhythmic bursting activity mediated by low threshold calcium spikes. *Neuroscience*, **51,** 489-494.

Kozelka JW, Pedley TA (1990) Beta and mu rhythms. *J. Clin. Neurophysiol.*, **7,** 191-207.

Lehmann W, Saper CB (1985) Evidence for a cortical projection to the magnocellular basal nucleus in the rat: an electron microscopic axonal transport study. *Brain Res.*, **334,** 339-343.

Leung L-WS, Borst JGG (1987) Electrical activity of the cingulate cortex. I. Generating mechanisms and relations to behavior. *Brain Res.*, **407,** 68-80.

Llinas R, Ribary U (1993) Coherent 40-Hz oscillation characterizes dream state in humans. *Proc. Natl. Acad. Sci. USA*, **90,** 2078-2081.

Lo Conte G, Casamenti F, Bigi V, Milaneschi E, Pepeu G (1982) Effect of magnocellular forebrain nuclei lesions on acetylcholine output from the cerebral cortex, electrocorticogram and behaviour. *Arch. ital Biol.*, **120,** 176-188.

Luiten PGM, Gaykema RPA, Traber J, Spencer DG (1987) Cortical projection patterns of magnocellular basal nucleus subdivisions as revealed by anterogradely transported Phaseolus vulgaris leucoagglutinin. *Brain Res.*, **413,** 229-250.

Mann K, Backer P, Roschke J (1993) Dynamical properties of the sleep EEG in different frequency bands. *Intern. J. Neurosci.*, **73,** 161-169.

McCormick DA (1992a) Cellular mechanisms underlying cholinergic and noradrenergic modulation of neuronal firing mode in the cat and guinea pig dorsal lateral geniculate nucleus. *J. Neurosci.*, **12,** 278-289.

McCormick DA (1992b) Neurotransmitter actions in the thalamus and cerebral cortex and their role in neuromodulation of thalamocortical activity. *Progr. Neurobiol.*, **39,** 337-388.

McGinty D, Harper RM (1976) Dorsal raphe neurons: depression of firing during sleep in cats. *Brain Res.*, **101,** 569-575.

Metherate R, Cox CL, Ashe JH (1992) Cellular bases of neocortical activation: modulation of neural oscillations by the nucleus basalis and endogenous acetylcholine. *J. Neurosci.*, **12,** 4701-4711.

Moruzzi G, Magoun HW (1949) Brain stem reticular formation and activation of the EEG. *Electroenceph. clin. Neurophysiol.*, **1,** 455-473.

Murthy VN, Fetz EE (1992) Coherent 25- to 35-Hz oscillations in the sensorimotor cortex of awake behaving monkeys. *Proc. Natl. Acad. Sci. USA*, **89,** 5670-5674.

Nashmi R, Mendonca AJ, MacKay WA (1994) EEG rhythms of the sensorimotor region during hand movements. *Electroenceph. clin. Neurophysiol.*, **91,** 456-467.

Parmeggiani PL, Zanocco G (1963) A study of the bioelectrical rhythms of cortical and subcortical structures during activated sleep. *Arch. Ital. Biol.*, **101,** 385-412.

Paxinos G, Watson C (1986) *The Rat Brain in Stereotaxic Coordinates.* Sydney: Academic Press.

Petsche H, Rappelsberger P (1992) Is there any message hidden in the human EEG? In: *Induced Rhythms in the Brain.* Edited by E. Basar and T. H. Bullock. Boston: Birkhauser, pp. 103-116.

Pfurtscheller G, Flotzinger D, Neuper C (1994) Differentiation between finger, toe and tongue movement in man based on 40 Hz EEG. *Electroenceph. clin. Neurophysiol.*, **90,** 456-460.

Pfurtscheller G, Neuper C (1992) Simultaneous EEG 10 Hz desynchronization and 40 Hz synchronization during finger movements. *NeuroReport*, **3,** 1057-1060.

Rasmusson DD, Clow K, Szerb JC (1994) Modification of neocortical acetylcholine release and electroencephalogram desynchronization due to brainstem stimulation by drugs applied to the basal forebrain. *Neuroscience*, **60,** 665-677.

Ribary U, Ioannides AA, Singh KD, Hasson R, Bolton JPR, Lado F *et al.* (1992) Magnetic field tomography of coherent thalamocortical 40-Hz oscillations in humans. *Proc. Natl. Acad. Sci. USA*, **89,** 11037-11041.

Rougeul-Buser A, Bouyer JJ, Buser P (1975) From attentiveness to sleep. A topographical analysis of localized 'synchronized' activities on the cortex of normal cat and monkey. *Acta Neurobiol. Exp.*, **35,** 805-819.

Rye DB, Wainer BH, Mesulam M-M, Mufson EJ, Saper CB (1984) Cortical projections arising from the basal forebrain: a study of cholinergic and noncholinergic components employing combined retrograde tracing and immunohistochemical localization of choline acetyltransferase. *Neuroscience*, **13,** 627-643.

Sanes JN, Donoghue JP (1993) Oscillations in local field potentials of the primate motor cortex during voluntary movement. *Proc. Natl. Acad. Sci. USA*, **90,** 4470-4474.

Saper CB (1984) Organization of cerebral cortical afferent systems in the rat. I. Magnocellular basal nucleus. *J. Comp. Neurol.*, **222,** 313-342.

Sheer DE (1989) Sensory and cognitive 40-Hz event-related potentials: behavioral correlates, brain function and clinical application. In: *Brain Dynamics*. Edited by E. Basar and T. H. Bullock. Berlin: Springer-Verlag, pp. 339-374.

Shute CCD, Lewis PR (1963) Cholinesterase-containing systems of the brain of the rat. *Nature*, **199,** 1160-1164.

Shute CCD, Lewis PR (1967) The ascending cholinergic reticular system: neocortical, olfactory and subcortical projections. *Brain*, **90,** 497-520.

Singer W (1993) Synchronization of cortical activity and its putative role in information processing and learning. *Ann. Rev. Physiol.*, **55,** 349-374.

Starzl TE, Taylor CW, Magoun HW (1951) Ascending conduction in reticular activating system, with special reference to the diencephalon. *J. Neurophysiol.*, **14,** 461-477.

Steriade M, Amzica F, Contreras D (1996) Synchronization of fast (30-40 Hz) spontaneous cortical rhythms during brain activation. *J. Neurosci.*, **16,** 392-417.

Steriade M, Contreras D, Amzica F (1994) Synchronized sleep oscillations and their paroxysmal developments. *Trends Neurosci.*, **17,** 199-208.

Steriade M, Curro Dossi R, Nunez A (1991a) Network modulation of a slow intrinsic oscillation of cat thalamocortical neurons implicated in sleep delta waves, cortically induced synchronization and brainstem cholinergic suppression. *J. Neurosci.*, **11,** 3200-3217.

Steriade M, Curro Dossi R, Pare D, Oakson G (1991b) Fast oscillations (20-40Hz) in thalamocortical systems and their potentiation by mesopontine cholinergic nuclei in the cat. *Proc. Natl. Acad. Sci. USA*, **88,** 4396-4400.

Stewart DJ, Macfabe DF, Vanderwolf CH (1984) Cholinergic activation of the electrocorticogram: Role of the substantia innominata and effects of atropine and quinuclidinyl benzilate. *Brain Res.*, **322,** 219-232.

Stumpf C (1965) The fast component in the electrical activity of rabbit's hippocampus. *Electroenceph. clin. Neurophysiol.*, **18,** 477-486.

Trachsel L, Tobler I, Borbely AA (1988) Electroencephalogram analysis of non-rapid eye movement sleep in rats. *Am. J. Physiol.*, **255,** R27-R37.

Trulson ME, Jacobs BL (1979) Raphe unit activity in freely moving cats: correlation with level of behavioral arousal. *Brain Res.*, **163,** 135-150.

Uchida S, Maloney T, Feinberg I (1992) Beta (20-28 Hz) and Delta (0.3-3 Hz) EEGs oscillate reciprocally across NREM and REM sleep. *Sleep*, **15,** 352-358.

Zilles K, Werner L, Qu M, Schleicher A, Gross G (1991) Quantitative autoradiography of 11 different transmitter binding sites in the basal forebrain region of the rat--evidence of heterogeneity in distribution patterns. *Neuroscience*, **42,** 473-481.

Figure 1. Unfiltered and high frequency filtered (for gamma: 30.5-58.0 Hz) EEG associated with different behaviors and states. During Waking *attentive* (immobile) and more so during Waking *moving* behaviors of the WAKE state, relatively high amplitude gamma wave activity is evident in both filtered and unfiltered EEG, where it is seen in association with theta activity. Gamma waves are reduced in Waking *quiet* (relaxed with eyes open) and more so in sleep to be lowest in association with a Sleep *curled* posture during SWS. During Sleep *twitch* which corresponds to PS, gamma wave activity is similar in amplitude to that during *attentive* or *moving* Waking behaviors. The EEG was recorded (by reference to an electrode in the rostral frontal bone) from the right frontal (RF), right retrosplenial (RRS), right parietal (RP) and right occipital (RO) cortices. Voltage scales are the same for all cortical leads and are shown at the right of the top traces of the unfiltered and gamma filtered EEG respectively.

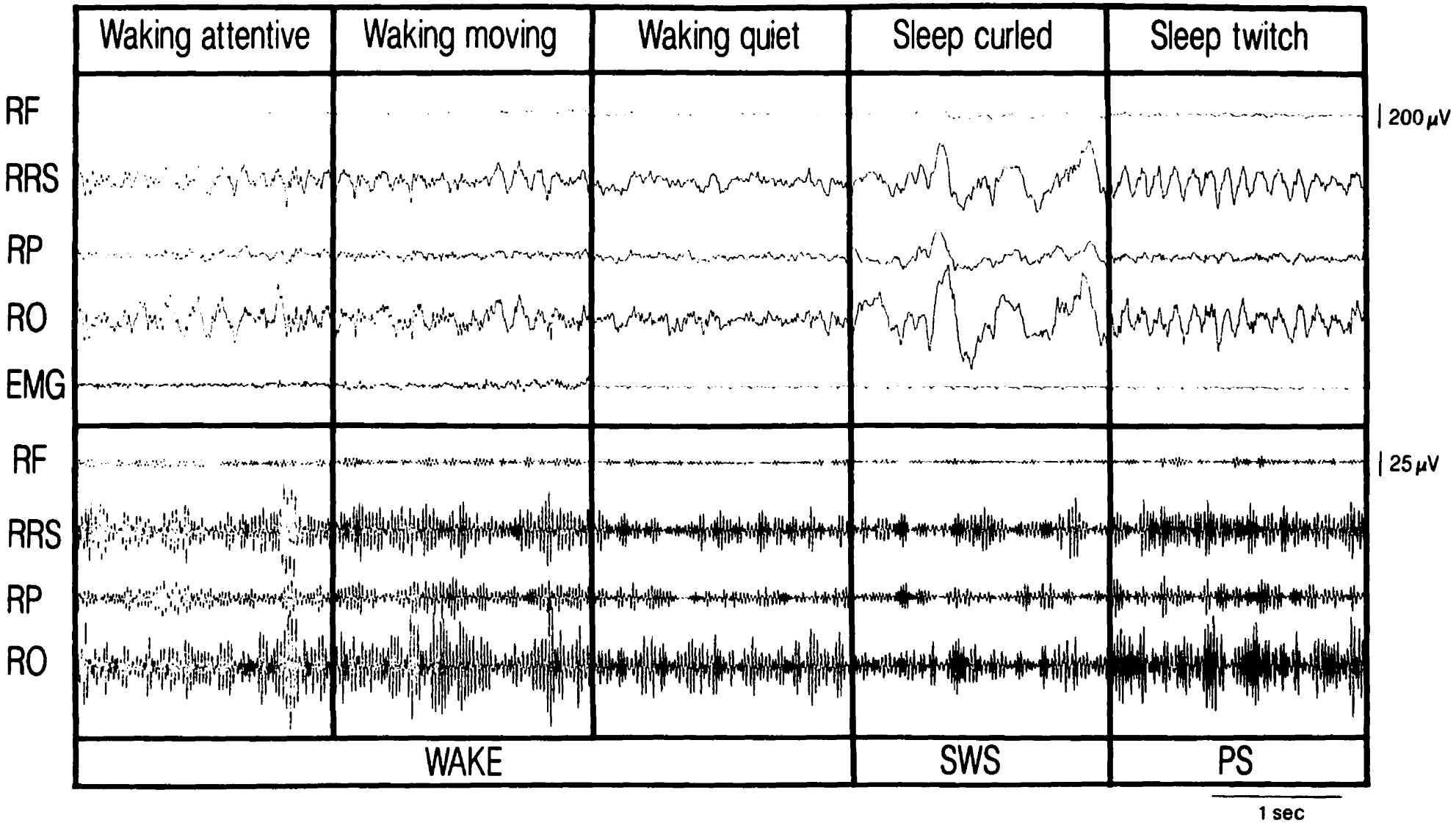
Waking attentive
Waking moving
Waking quiet
Sleep curled
Sleep twitch
RF
RRS
RP
RO
EMG
200 μV
RF
RRS
RP
RO
25 μV
WAKE
SWS
PS
1 sec

Figure 2. Unfiltered (a, black trace) and high frequency filtered (for gamma: 30.5-58.0 Hz) (b, gray trace) EEG during Waking *moving* (1 sec segment expanded from Fig. 1). The gamma filtered signal appears to correspond closely to the high frequency component of the unfiltered EEG.

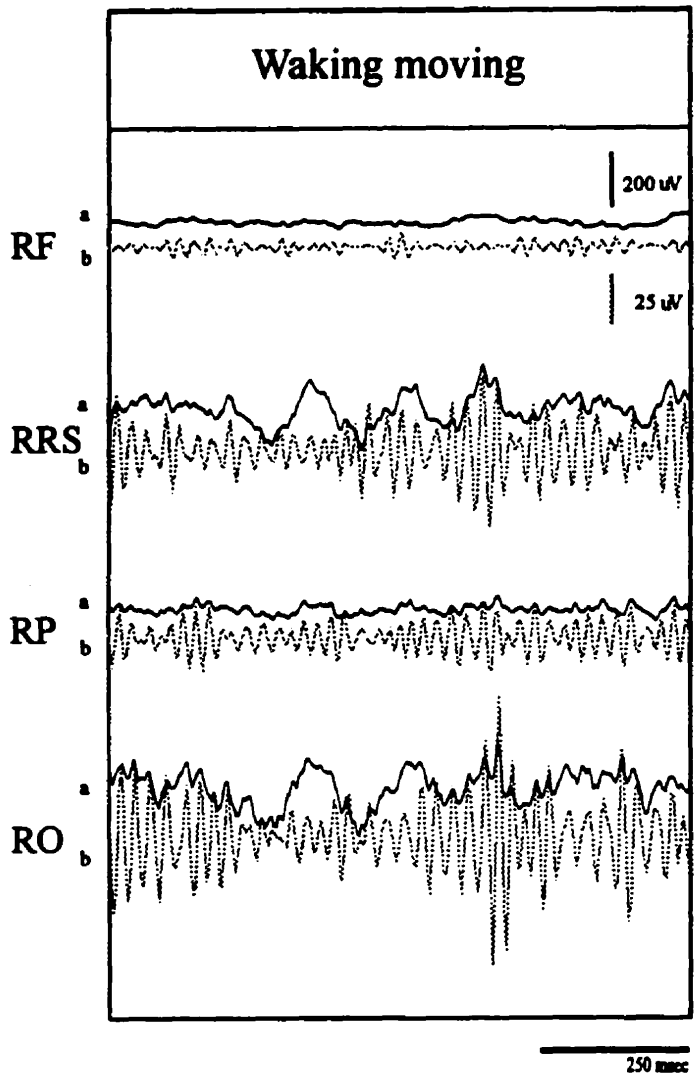
Waking moving
200 uV
25 uV
RF
a
b
RRS
a
b
RP
a
b
RO
a
b
250 msec

Figure 3. Spectra of (4 sec) EEG segments (from RRS cortex) associated with different states and behaviors or postures. A single peak is always prominent in the low frequency range (1.5-18.5 Hz), whereas multiple peaks are present in the high frequency range (19.0-58.0 Hz, shown at a higher gain, see lower right plot). A prominent peak is evident in the theta band during immobile Waking *attentive* (W*attentive*, 7.0 Hz peak frequency) or active Waking behaviors (W*moving*, 7.0 Hz; W*eating*, 7.5 Hz; and W*grooming*, 6.0 Hz) and during sleep with movement (S*moving*, 6.0 Hz) or twitches (S*twitch*, 7.5 Hz), which correspond to *t*PS and PS respectively. Multiple and irregular peaks are present in the high frequency gamma band during these same behaviors. A dull peak in the low theta to delta (4.0 Hz) range occurs in association with Waking *quiet* (W*quiet*), when the amplitude and peaks in the high frequency gamma band are attenuated. A prominent peak is present in the delta band (and secondary peak often in the sigma band) during *t*SWS, when the animal is frequently in a recumbent, though uncurled position (S*uncurled*) and during SWS, when the animal is most frequently in a curled position (S*curled*). The presence of a peak in the delta range during sleep is associated with a decrease in the amplitude as well as sharpness of the multiple peaks in the high frequency gamma band. Spectra taken from the same rat as in Figs. 1 and 2 (BE10). Frequency bands are indicated in lower right graph, along with the different display gains which were employed for the low frequency range (3x with the full scale = 60 AD, ★ 47 μV, for <18.5 Hz) and high frequency range (10x with full scale = 18 AD units, ~ 14 μV, for >19 Hz) in order to best illustrate peaks in each range. Abbreviations for States: W, Wake; *t*SWS,

transition into SWS; SWS, Slow Wave Sleep; *t*PS, transition into PS; PS, Paradoxical Sleep. Abbreviations for bands: De, Delta; Th, theta; Si, sigma; B1 and B2, Beta1 and 2; Ga, gamma.

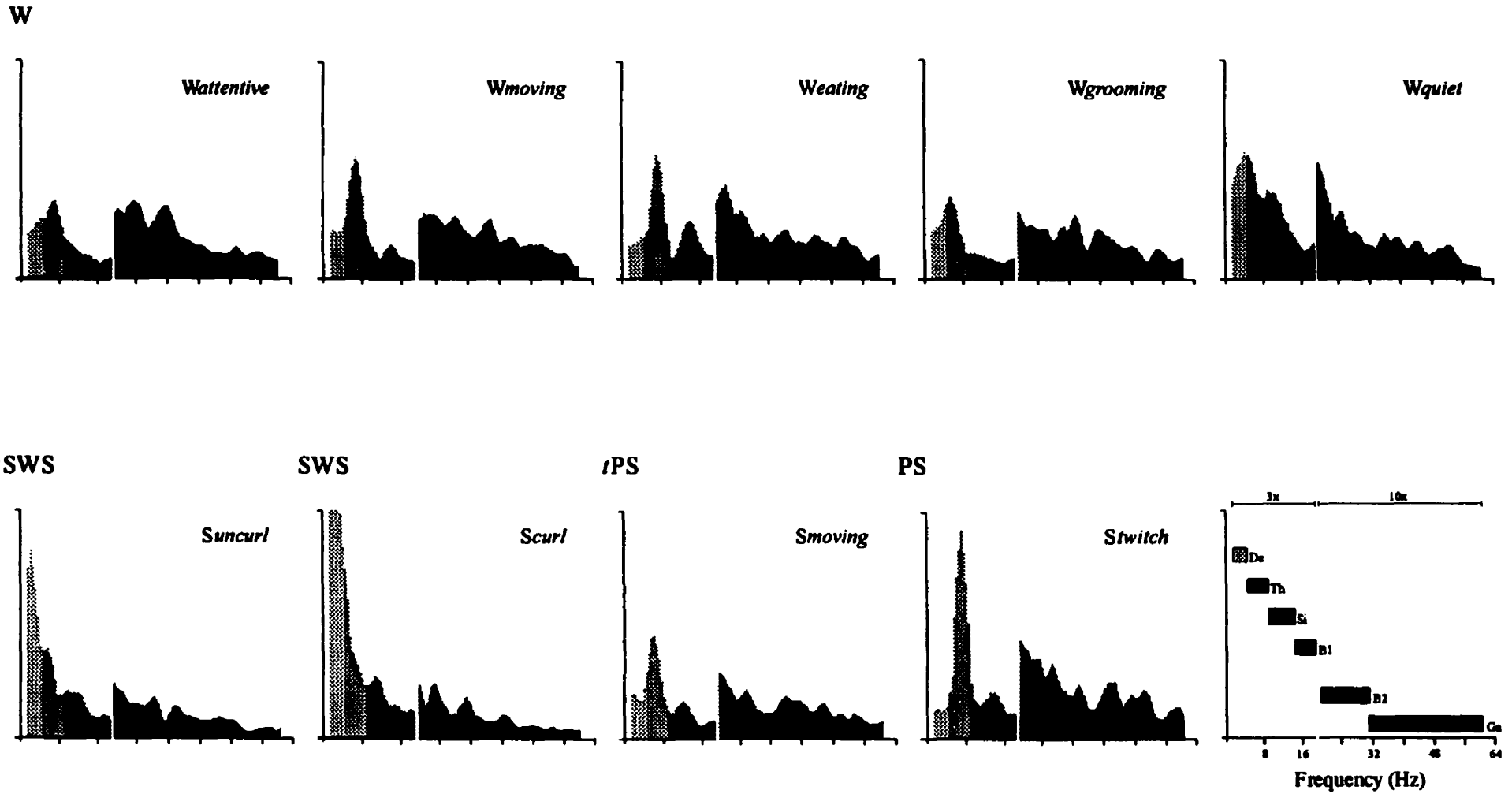
W
Wattentive
Wmoving
Weating
Wgrooming
Wquiet
tSWS
SWS
tPS
PS
Suncurl
Scurl
Smoving
Stwitch
3s
10s
De
Th
Si
B1
B2
Ga
8
16
32
48
64
Frequency (Hz)

Figure 4. Activity in EEG frequency bands (per 20 sec epochs for 1¾ hrs from RRS) across the sleep-waking cycle scored for sleep-wake states in hypnogram (top). During Wake (W), gamma is on average higher than during the transition into SWS (*t*SWS) and during deep SWS, when it reaches the lowest levels. It also varies, however, during W as a function of behavior (as annotated in specific epochs marked by dotted lines). From SWS, it increases slightly in the brief transition into PS (*t*PS) and markedly during PS. In contrast, beta2 does not appear to be greater in amplitude during W or PS than during SWS. The amplitudes of sigma (reflecting sleep spindles) and more markedly delta increase from W in *t*SWS and during SWS and subsequently decrease in PS. Theta activity (evident by the ratio of Th/De) varies in a similar state-dependent manner as gamma activity. Both gamma and Th/De covary with EMG amplitude across the sleep-waking cycle, except in association with PS, when they both increase in amplitude, while the EMG remains low. Data taken from the same rat as in Figs. 1-3 (BE10). Amplitude scale (left, expressed in AD amplitude units) is the same for all EEG frequency bands (300 AD units, ~ 237 μV). Abbreviations for behaviors W*a*, Waking *attentive*; W*m*, Waking *moving*; W*e*, Waking *eating*; W*g*, Waking *grooming*; W*q*, Waking *quiet*; S*u*, Sleep *uncurled*; S*c*, Sleep *curled*; S*m*, Sleep *moving*; and S*t*, Sleep *twitch*. See Fig. 3 for abbreviations.

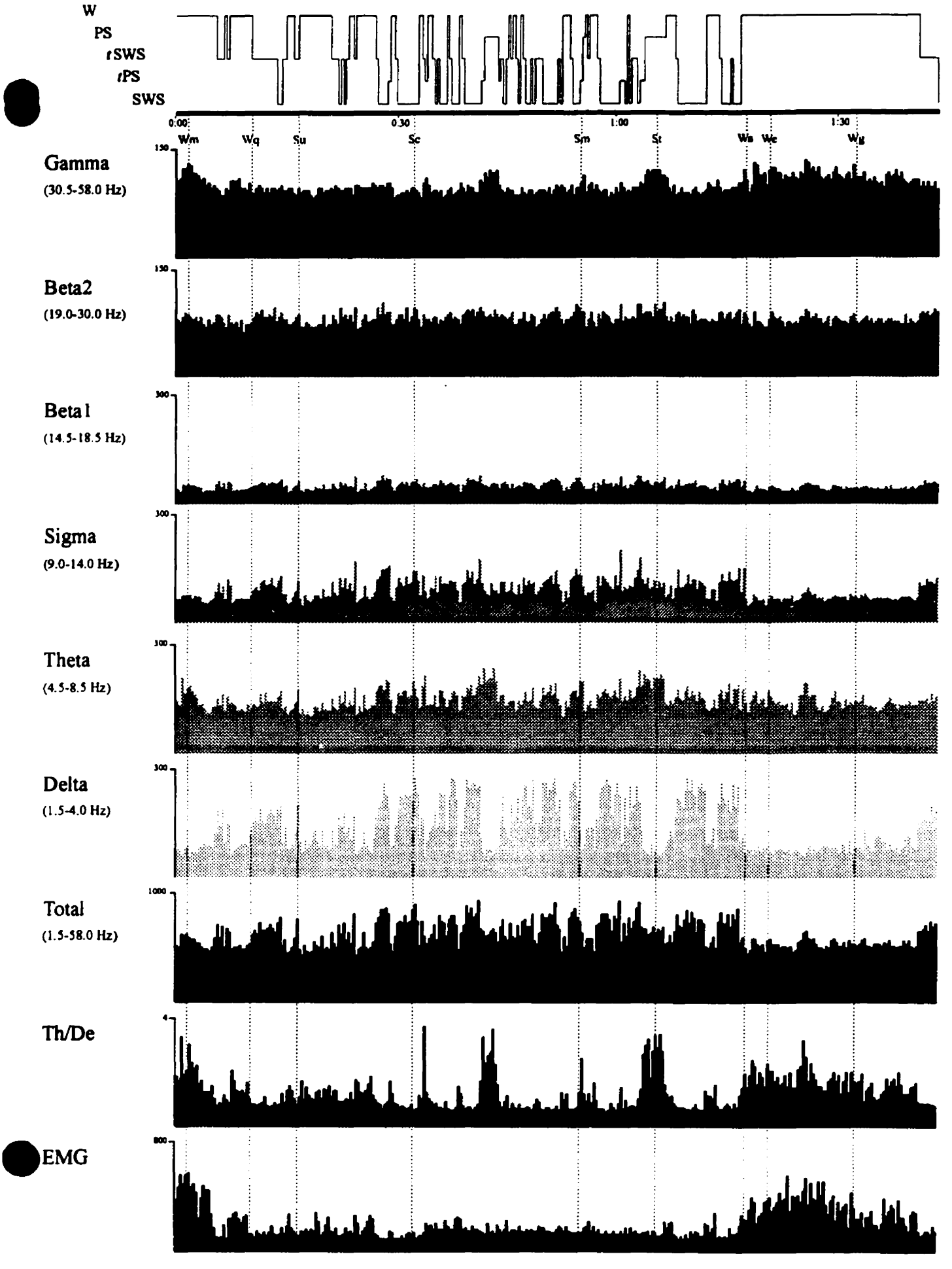
W
PS
tSWS
tPS
SWS
0:00
0:30
1:00
1:30
Wm
Wq
Su
Sc
Sm
St
We
Wg
Gamma
(30.5-58.0 Hz)
Beta2
(19.0-30.0 Hz)
Beta1
(14.5-18.5 Hz)
Sigma
(9.0-14.0 Hz)
Theta
(4.5-8.5 Hz)
Delta
(1.5-4.0 Hz)
Total
(1.5-58.0 Hz)
Th/De
EMG

Figure 5. Activities in EEG frequency bands (per 4 sec epochs from RRS) across different states and behaviors (mean + s.e.m. in 5 rats). Whereas the absolute amplitude (integrated AD amplitude units) of all frequency bands varies significantly as a function of behavior (* indicates an F statistic with a $p<0.05$ for 8 d.f., in a 2 way repeated measures ANOVA for 3 observations per 9 behaviors per rat), only the absolute amplitude of the gamma band is significantly greater during Waking and PS behaviors and states than in association with SWS-Sc (+ indicates greater according to a post hoc comparison with a $p<0.05$ for 1 d.f.). Conversely the absolute amplitude of the delta band is significantly lower in all Waking and PS behaviors than in SWS (- indicates lower according to a post hoc comparison with a $p<0.05$ for 1 d.f.). The relative amplitude (expressed as the % of total amplitude) of gamma and beta2, as well as the ratio of Th/De, are significantly greater in association with Waking and PS behaviors than in association with SWS. See text and Table 2 for other comparisons. (For EEG frequency bands, 100 AD units ~ 79 μV.) See Figs. 3 & 4 for abbreviations.

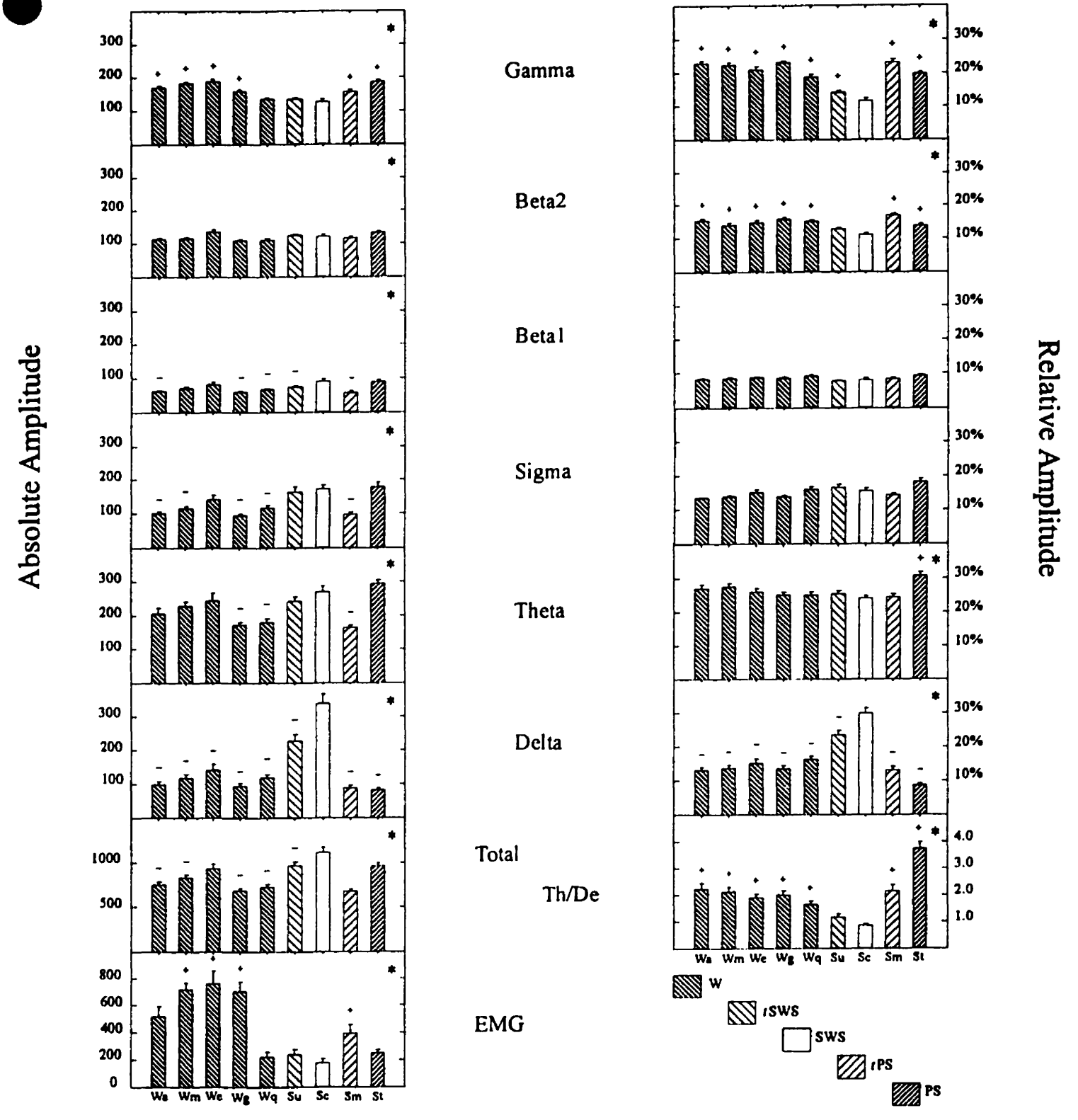
Absolute Amplitude
Relative Amplitude
Gamma
Beta2
Beta1
Sigma
Theta
Delta
Total
Th/De
EMG
Wa Wm We Wg Wq Su Sc Sm St
W
rSWS
SWS
rPS
PS

Figure 6 Activities in gamma and delta frequency bands from different cortical regions across different states and behaviors (as in Fig. 5, mean + s.e.m. AD units for 5 rats). The reciprocal variation of gamma and delta frequency bands across the sleep-wake states and the variation of gamma as a function of behavior is similar on all cortical leads. (100 AD units ~ 79 μV.) See Figs. 3 & 4 for abbreviations.

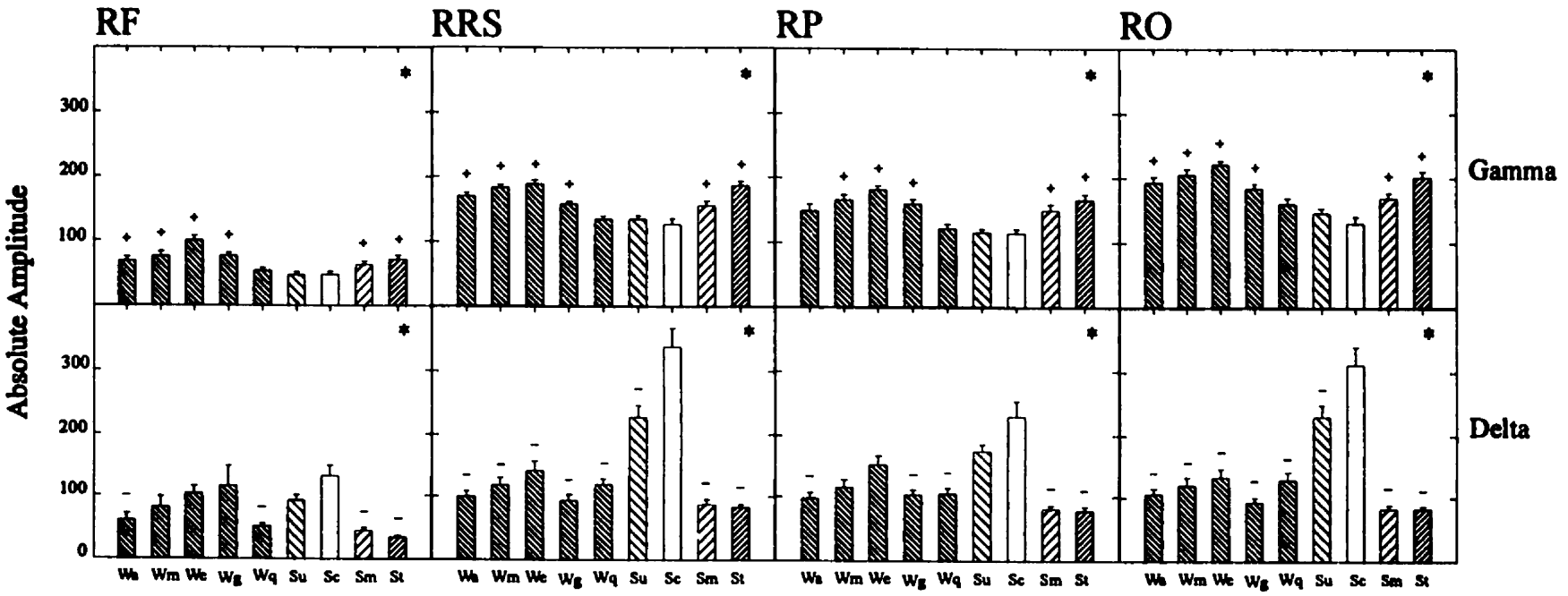
RF
RRS
RP
RO
Absolute Amplitude
300
200
100
0
Gamma
Delta
Wa Wm We Wg Wq Su Sc Sm St

Table 1. Mean frequency band activities across sleep-wake states and differences with respect to SWS[1].

Band \ State	W	*t*SWS	SWS	*t*PS	PS
Gamma ***	+ 134.09±9.88*	+ 118.11±5.93*	117.19±6.11	+ 125.96±7.17*	+ 142.39±7.77***
Beta2 **	− 102.87±7.70**	− 105.93±5.95**	113.13±6.72	116.99±8.82	108.49±4.46
Beta1 ***	− 61.91±6.09**	− 73.85±5.05*	84.99±6.14	89.02±8.23	− 67.74±2.71*
Sigma***	− 111.42±12.95***	159.34±12.54	172.46±13.22	189.76±19.59	− 126.84±7.45**
Delta ***	− 127.57±10.72***	− 180.70±16.47***	256.26±19.92	− 186.62±16.22*	− 87.18±5.25***
Th/De***	+ 1.54±0.04***	+ 1.14±0.07***	0.90±0.05	+ 1.37±0.07*	+ 2.87±0.14***

[1]Differences in frequency band activities (on RRS) for each state (from mean values per state per animal from ~500 20 sec epochs in 5 animals) as compared to SWS, with + or - reflecting a significant difference (tested by post-hoc C-Matrix following a repeated measures ANOVA for 5 rats). Each band varied significantly as a function of state (for overall F-statistic and individual cell differences: *, $p<.05$; **, $p<.01$; ***, $p<.001$). Mean and s.e.m. are presented for each cell and represent amplitude in AD units (100 AD units ~ 79 μV).

Table 2. Matrix comparing gamma activity across the different state-behaviors[1].

	Wattentive	*Wmoving*	*Weating*	*Wgrooming*	*Wquiet*	*Suncurl*	*Scurl*	*Smoving*	*Stwitch*
Wattentive									
Wmoving	2.94								
Weating	+ 8.47°	0.46							
Wgrooming	− 14.94°	− 10.61°	− 11.72°						
Wquiet	− 14.26°	− 42.90°°	− 17.51°	− 11.71°					
Suncurl	− 25.81°°	− 63.12°°°	− 30.47°°	− 20.48°	0.02				
Scurl	− 27.65°°	− 230.57°°°	− 38.99°°	− 14.52°	0.69	0.94			
Smoving	− 7.69°	− 26.89°°	− 34.57°°	0.13	6.41	+ 10.90°	+ 16.13°		
Stwitch	+ 7.76°	0.46	0.04	+ 33.83°°	+ 76.31°°°	+ 74.98°°°	+ 99.27°°°	+ 40.69°°	

[1]Comparisons based upon post-hoc tests (by C Matrix) of data presented in Fig. 5 for gamma absolute amplitude across state-behaviors (one way repeated measures ANOVA, df=8, F=21.64, p=.000). Plus or minus sign indicates that gamma of the row behavior is significantly greater or lesser than that of the column behavior. F-statistics and probabilities for simple comparisons are provided in lower corner of each block. (*, p<.05; **, p<.01; ***, p<.001)

DIFFERENTIAL MODULATION OF HIGH FREQUENCY GAMMA EEG ACTIVITY AND SLEEP-WAKE STATE BY MICROINJECTIONS OF NORADRENALINE AND SEROTONIN INTO THE REGION OF CHOLINERGIC BASALIS NEURONES

Edmund G. Cape and Barbara E. Jones

Published, Journal of Neuroscience, Vol. 18(7), pp. 2653-2666, 1998

PREFACE

The next series of experiments were aimed at studying the role of the basal forebrain in the modulation of cortical activation across the sleep-waking cycle. For this purpose, changes in gamma and theta EEG activity were examined following pharmacological manipulation of the basal forebrain neurons. To study these effects in a freely moving naturally sleeping-waking animal required the development of a microinjection procedure that would provide reliable delivery of drugs first at volumes below 1 μl, second, in such a way to allow reliable measure of effects from the moment that the drugs come into contact with the tissue and third, without disturbing the natural sleep cycle of the animal. This technique was refined to a point where the experiments could take place over the course of up to five weeks per animal while allowing the direct comparison of doses given over that time frame.

The first series of experiments using this technique explores the *in vivo* significance of the *in vitro* established differential modulation of cholinergic basalis neurons by noradrenaline versus serotonin. The neurotransmitters were injected into the region of the basalis neurons by remote control in freely moving, naturally sleeping-waking rats during the day when the rats are normally asleep the majority of the time. Effects were observed on behavior and EEG activity, including high-frequency gamma activity, which has been demonstrated to reflect behavioral and cortical arousal in the rat.

ABSTRACT

Several lines of evidence indicate that cholinergic basalis neurons play an important role in cortical activation. The present study was undertaken to determine the effect of noradrenergic and serotonergic modulation of the cholinergic neurons upon cortical EEG activity and sleep-wake states. The neurotransmitters were injected into the region of the basalis neurons by remote control in freely moving, naturally sleeping-waking rats during the day when the rats are normally asleep the majority of the time. Effects were observed upon behavior and EEG activity, including high frequency, gamma activity (30-60 Hz), which has been demonstrated to reflect behavioral and cortical arousal in the rat. Noradrenaline, which has been shown in previous *in vitro* studies to depolarize and excite the cholinergic cells, produced a dose-dependent increase in gamma EEG activity, decrease in delta activity and increase in waking. Serotonin, which has been found in previous *in vitro* studies to hyperpolarize the cholinergic neurons, produced a dose-dependent decrease in gamma EEG activity with no significant change in amounts of wake or slow wave sleep. Both chemicals resulted in a dose-dependent decrease in paradoxical sleep.

These results demonstrate that noradrenaline and serotonin exert differential modulatory effects upon EEG activity through the basal forebrain, the one facilitating gamma activity and eliciting waking, the other diminishing gamma activity and not significantly affecting slow wave sleep. The results also confirm that the cholinergic basalis neurons play an important role in cortical activation and particularly in the high frequency gamma activity that underlies cortical and behavioral arousal of the wake state.

INTRODUCTION

Early studies, which investigated the effects of pharmacological manipulation of cholinergic transmission or examined the release of acetylcholine (ACh) from the cerebral cortex across sleep-wake states, clearly indicated that cholinergic neurons play an important role in cortical activation that occurs during the states of wake and paradoxical sleep (Celesia and Jasper, 1966; Longo, 1966; Jasper and Tessier, 1971) (see for review (Jones, 1993)). The neurons which provide the major cholinergic innervation to the cerebral cortex are located in the nucleus basalis of Meynert (Shute and Lewis, 1967; Lehmann *et al.*, 1980; Rye *et al.*, 1984). Lesions of the basal forebrain cholinergic cells are associated with a decrease in cortical ACh release and parallel decrease in cortical activation (Lo Conte *et al.*, 1982; Stewart *et al.*, 1984; Buzsaki *et al.*, 1988). Reciprocally, electrical or chemical stimulation of the cholinergic basalis neurons in anesthetized or brainstem transected animals, leads to a parallel increase in cortical ACh release and cortical activation (Casamenti *et al.*, 1986; Rasmusson *et al.*, 1994). In the present study, we examined the effects of chemical stimulation in naturally sleeping-waking rats upon sleep-wake state and EEG activity, focussing upon high frequency gamma activity (30-60 Hz), which we have shown to be indicative of behavioral and cortical arousal in the rat (Maloney *et al.*, 1997).

Cholinergic basal forebrain neurons lie in the path of the major ascending fiber system from the brainstem reticular activating system and thus serve as the ventral extrathalamic relay to the cerebral cortex (Moruzzi and Magoun, 1949; Starzl *et al.*, 1951). The brainstem neurons projecting into the region of the cholinergic basalis neurons are comprised of monoaminergic neurons, in addition to putative glutamatergic neurons of the reticular formation (see for review (Jones,

1995)). Thus, noradrenergic locus coeruleus and serotonergic raphe neurons project into the basal forebrain, in addition to projecting directly to the cerebral cortex (Semba *et al.*, 1988; Jones and Cuello, 1989; Jones, 1995). More recently, by intracellular recording and labelling *in vitro*, identified cholinergic basalis neurons were shown to be innervated by noradrenergic and serotonergic fibers and to be modulated in different ways by these two neurotransmitters (Khateb *et al.*, 1992; Khateb *et al.*, 1993; Fort *et al.*, 1995). Noradrenaline was found to depolarize and excite, whereas serotonin (5-hydroxytryptamine, 5-HT) was found to hyperpolarize and inhibit the cholinergic cells. The significance or role of this modulation *in vivo*, however, remains to be determined. The aim of the present study was thus to examine the effects of microinjections of noradrenaline and serotonin into the region of the cholinergic basalis neurons upon cortical EEG activity and sleep-wake state in freely moving, naturally sleeping-waking animals. This was accomplished by development of a microinjection procedure allowing remote control for the lowering of the filled cannulae and injection of the chemicals. The results show different effects of noradrenaline and serotonin upon gamma EEG activity and sleep-wake states. Preliminary results of this study were previously reported (Cape and Jones, 1994).

METHODS

Animals and surgery

A total of 24 male Wistar rats (Charles River Canada, Montreal) weighing between 200 - 250 g at the time of surgery, were employed in this study. Nine animals were used for pilot studies and 15 for experimental studies. For implantation of electrodes and cannulae, animals were anesthetized with barbiturate anesthesia (Somnotol, 67 mg/kg i.p.) and placed in the stereotaxic instrument with the tooth bar set at -0.33 mm. For EEG recording, jeweller's screws (1 mm diameter at exposed tip and 3 mm in length) were threaded into burr holes in the skull to come into minimal contact with the dura. They were placed bilaterally by reference to Bregma over frontal (2.7-3.0 mm anterior, 0.6 mm lateral), retrosplenial (3.5 mm posterior, 0.6 mm lateral), parietal (0.5 mm posterior, 5.0 mm lateral) and occipital (7.5 mm posterior, 5.0 mm lateral) cortical regions. A reference electrode was cemented in bone rostral to the frontal cortex and caudal to the olfactory bulbs (5.5 mm anterior, 0.6 mm lateral). EMG was recorded by means of 2 stainless steel wires inserted in the neck musculature. A ground electrode was implanted over the cerebellum (approximately 1 mm posterior to lambda and 2 mm from the midline). The electrodes were joined to a small female connector.

For microinjections, stainless-steel cannulae (Plastics One, Roanoke, Virginia) were employed and included guide cannulae (26 gauge, 0.46 mm o.d.) with fitted dummy stylets and internal cannulae (33 gauge, 0.20 mm o.d.). The guide cannulae were placed bilaterally such that when the internal cannulae were lowered 2.0 mm below the tip of the guides, they reached the target site in the basal forebrain (using Anterior-Posterior (AP), Lateral (L) and Vertical (V)

coordinates with reference to ear bar zero: AP +7.7 mm, L 2.5 mm, V +1.5 mm) (Fig. 1). The guide cannulae were implanted and maintained with dummy stylets that extended beyond the guides by 0.5 mm. The guide cannulae and electrodes were fixed to the skull with dental cement.

After a minimum of two days recovery following surgery, each rat was individually housed in a plexiglass box inside a large electrically shielded recording chamber in which they were maintained on a 12:12 light-dark cycle (lights on: 700-1900 h). They had free access to rat chow and water. For the duration of the experiment, the connector on the rat's head was attached to a cable connected to a commutator which was suspended with a balanced boom to allow free movement of the animal in the chamber. Baseline recording was initiated after a minimum of 2 days habituation to the chamber and cable.

At the end of the experiments, the animals were sacrificed under barbiturate anesthesia (Somnotol, ~120 mg/kg). Most (20/24) were perfused through the heart with a fixative solution (3.0% paraformaldehyde, as published previously (Gritti *et al.*, 1993)). The brains were frozen and subsequently processed for histology and choline acetyltransferase immunohistochemistry (Gritti *et al.*, 1993) to examine the placement of the cannulae.

EEG recording and behavioral observations

The EEG and EMG signals were recorded with a Grass Model 78D Polygraph. All signals were filtered between 1.0 to 100 Hz. The EEG signals were recorded with a gain that was adjusted to be the same on each channel and to remain the same for the duration of the study. The amplifier output was sent to an IBM compatible computer running Stellate Systems software (Montreal, Quebec) for on-line analogue to digital (AD) conversion and off-line analysis of EEG. The

signals were sampled at a rate of 512 Hz and filtered with a Finite Impulse Response (FIR) filter with a cut-off frequency at 128 Hz. The data were stored at a sampling rate of 256 Hz.

The rat's behavior was observed with the aid of a video monitor and marked on-line by annotations on the computer record. Behavioral annotations included the following in the order in which they frequently occur during a normal sleep-wake cycle in association with a Waking (W) or Sleep (S) posture: W*attentive* (when the animal was immobile and seemingly attending to a stimulus), W*moving* (including walking), W*eating*, W*grooming*, W*quiet* (when the animal was lying down but with eyes open), S*uncurled* (outstretched with eyes closed), S*curled* (curled up with eyes closed), S*moving* (adjusting posture with eyes closed), and S*twitch* (showing rapid movements of eyes, ears or whiskers while asleep with eyes closed) (Maloney *et al.*, 1997).

Recording was performed beginning in the late morning and usually ending by 1500 h in the afternoon. The EEG computer file consisted of a morning recording period (~1100-1130, taken prior to handling) and an afternoon recording period (~1230-1500, taken following handling and the placement of the inner cannulae for microinjections). The afternoon recording was not begun until the animal had recovered from the handling as evidenced behaviorally by the resumption of sleep. For baseline recording which was performed prior to any injections, the animal was picked up and handled during the time that the injection cannulae would be inserted.

Injection procedure

Ringer and chemical injections proceeded in several stages (see Fig. 1A). Following the 30 min morning recording (defined as the pre-injection period), the

animal was picked up for removal of the stylets and manual placement of the filled internal cannulae. The filled cannulae were inserted into the guide cannulae and held there in a position approximately ~2 mm above the tissue (i.e. ~4 mm dorsal to their eventual target, Fig. 1A) in order to avoid premature contact of the chemical solution with the brain. Following recovery from the handling procedure, evidenced behaviorally by the apparent resumption of sleep, the afternoon recording session was begun. After the appearance of a full sleep cycle, evidenced on the EEG by the passage through SWS into transition into PS (*t*PS) or PS (usually over a ~30 min period), the filled inner cannulae were lowered into the brain. This was accomplished without disturbing the rat by use of a remotely controlled mechanism consisting of inner tubing connected to the inner cannula and sliding within outer tubing connected to the outer cannula's cap on the rat's head. From outside the cage, the inner tubing was slid forward to a point determined by the fitting of the hub of the inner cannulae into the cap of the outer cannula, which corresponds to the point of full descent of the inner cannula into the brain. The left and right cannulae were lowered in sequence. The injections were subsequently begun ~2 min after the cannulae came into contact with the brain tissue. They were made bilaterally with a syringe pump (Sage Instruments, Cambridge, Mass.) which simultaneously advanced both syringe plungers over a period of ~5 min. The post-injection condition was defined for statistical analysis as the 30 min period immediately following the injection and was based upon the period during which the chemicals would diffuse maximally within the restricted radius of the injection site (Martin, 1991). Recording was nonetheless continued for at least 60 min following the injection, after which the inner cannulae and tubes were removed from the brain and head of the animal.

Chemical microinjections

Chemicals were delivered using two 1 µl Hamilton syringes (Reno, Nevada) simultaneously driven by a syringe pump (model 341 A, Sage Instruments, Orion Research Inc., Cambridge, Massachusetts). Connected to the syringes, polyethylene tubing (~50 cm) was filled with paraffin oil up to the last ~1 cm (or ~1.5 µl) of each inner cannula, which was filled with the chemical solution. The chemicals were dissolved in buffered ringer (156.14 mM NaCl, 3.35 mM KCl, 2.70 mM $CaCl_2$, and 2.38 mM $NaHCO_3$).

All solutions were injected in volumes of 0.5 µl (at a rate of ~0.1 µl per min), which based upon previous injections of neuroanatomical tracers into the basal forebrain (Jones and Yang, 1985; Jones and Beaudet, 1987), was estimated to diffuse from the tip of the cannula in a radius of up to 1 mm around the tip and greater than 1 mm along the shaft of the cannulae (Fig. 1). Initial doses and/or concentrations of noradrenaline and serotonin were based upon those utilized in published studies and aimed at reaching adequate concentrations at neurotransmitter receptors over a wide area (Myers, 1974; Wenk, 1984). In pilot studies, noradrenaline (L-arterenol bitartrate; Sigma) was injected at doses of 600, 250, 75, 50 and 25 nmol, which all produced an awakening and arousal of differing intensities and durations. A dose of 75 nmol noradrenaline (15 µg in 0.5 µl total dose per side, corresponding to a concentration of 150 mM) was selected for a consistent, robust effect and administered to 8 rats. Serotonin (5-hydroxytryptamine creatine sulfate, 5-HT; Sigma Chemical Co., St. Louis, Missouri) was injected at doses of 1000, 500, 250, 125 and 62.5 nmol, none of which produced an awakening but instead all appeared to produce a change in EEG activity that was apparent during diurnal sleep at the higher doses. A dose of 250

nmol serotonin (53.2 µg in 0.5 µl total dose per side, corresponding to a concentration of 500 mM) was selected for a consistent, robust effect and administered to 11 animals. In 8 animals receiving both 5-HT and noradrenaline, the two drugs were administered in random order, with at least 48 hours between drug administrations.

Another series of experiments were subsequently conducted in 5 rats to establish if the effects observed were dose-dependent. In addition to ringer, four doses of each drug were administered, using the dose employed in the main study as the maximum dose. For noradrenaline, the low dose was established as that producing a lesser but apparent effect, and the range represented doses at 100%, 67%, 50%, and 33% of the dose employed in the main study. For serotonin, the drug was administered at doses representing 100%, 50%, 25% and 12.5% of the dose employed in the main study, in order to include doses overlapping with those of noradrenaline. In these animals, the order in which noradrenaline and serotonin were administered was varied across rats and the interval separating the two drug administrations was at least 48 hours.

Data analysis

The EEG was examined using off-line analysis on a computer screen and scored by visual assessment according to sleep-wake states in 20 sec epochs. State was classified as one of 5 states: 1) Wake (W), 2) transition into Slow Wave Sleep (*t*SWS), 3) Slow Wave Sleep (SWS), 4) transition into Paradoxical Sleep (*t*PS) and 5) Paradoxical Sleep (PS) (Maloney *et al.*, 1997). Particularly during the post-injection condition, the state of the rat was also assessed by consideration of the behavioral annotations, in addition to the EEG and EMG activities. Consequently, the annotations were used to identify any dissociations between

behavior and the normal associated EEG patterns of the different states (Maloney *et al.*, 1997). Each state was reported for the post-injection recording period as % of total recording time.

Spectra were computed using Stellate Systems software by Fast Fourier Transform (FFT) based on 512 points corresponding to 2 sec epochs with a resolution of 0.5 Hz. A 7-point smoothing window is applied by this program thus allowing a minimum of 1.5 Hz and a maximum 63.5 Hz in the spectral computation. Frequency bands were set at the following ranges: delta: 1.5 - 4.0 Hz, theta: 4.5 - 8.5 Hz, sigma: 9.0 - 14.0 Hz, beta1: 14.5 - 18.5 Hz, beta2: 19.0 - 30.0 Hz, and gamma: 30.5 - 58.0 Hz (eliminating frequencies around 60 Hz to avoid any possible contamination from AC noise) (Maloney *et al.*, 1997). Total activity within each band was automatically calculated for 20 sec recording epochs that were scored for sleep-wake state. Based upon the scored records, sleep-wake hypnograms were displayed in association with EEG frequency band activities from the right retrosplenial lead for 20 sec epochs over the recording sessions using Eclipse software (Stellate Systems). Spectral analysis was also performed using Rhythm software (Stellate Systems) on 4 sec epoch samples (n = 5 per rat) which were selected for uniformity, as well as representativeness, of EEG activity at one minute intervals ~2 - 8 min post-injection. Spectrum and frequency band activities were displayed and reported in AD amplitude units for which the average gain was calibrated as ~1500 AD units per mV on the EEG channels. Relative amplitudes of each band were also reported and correspond to the % of total activity (1.5 - 58.0 Hz). The ratio of theta/delta (Th/De) was calculated and reported as a reflection of regular theta activity in the EEG (Maloney *et al.*, 1997). EMG amplitude was computed for the total spectrum up to 58.0 Hz.

EEG records and hypnograms displaying sleep-wake state and frequency band activity were examined following recording to establish first, a normal EEG and second, an effective microinjection. Data were excluded from analysis if any signs of abnormal EEG activity were evident as indicative of seizure-like activity common to rodents (Vergnes *et al.*, 1982). Of 15 rats, 3 had to be eliminated for this reason, and data points were eliminated in 2 other rats due to the presence of abnormal activity following noradrenaline. One rat was eliminated due to an apparent failure of the drugs to be consistently delivered and interpreted as due to clogging of the cannulae.

Statistical comparisons were performed for average % sleep-wake state and for EEG and EMG activity. For EEG activity, statistics are presented from the right retrosplenial cortical lead for gamma and delta activity and Th/De ratio, which were previously shown to maximally reflect behavioral and state changes in the rat (Maloney *et al.*, 1997). Comparisons were made first between post-ringer and baseline conditions (in 8 rats using paired *t*-tests) to determine if the ringer microinjections were associated with any significant changes in EEG, behavior or sleep-wake states. Comparisons were subsequently made between post-noradrenaline (in 5 rats) or post-serotonin (in 8 rats, of which 5 also received noradrenaline) and post-ringer conditions by paired comparisons (using Student *t*-tests) for individual animals involving one trial per condition per animal. For analysis of the dose-response relationships, an analysis of covariance was employed (ANCOVA), with dose as the main factor (df = 4) and subject as a covariate (df = 1) involving 4 rats for noradrenaline and 3 overlapping rats for serotonin (with a total of 31 data points). All statistics were performed using Systat software (Evanston, Illinois).

RESULTS

In histology, tracks of the injection cannulae were evident passing through the caudate-putamen and globus pallidus into the substantia innominata (at the border between the anterior (SIa) and posterior (SIp) sectors) and above the magnocellular preoptic nucleus, where the cholinergic cell bodies are located (Fig. 1B). They were bilaterally symmetric in all animals.

Baseline

During baseline recording periods, rats manifested brief waking episodes with alternating more prolonged periods of sleep. During the 30 min recording period of the afternoon (generally occurring between ~1300 and 1400 h), they all passed through at least one complete sleep cycle, as marked by the appearance of *t*PS and PS following *t*SWS and SWS (n = 8, Fig. 2). The alternation of waking and sleeping and the full cycle passing from Wake through *t*SWS-SWS into *t*PS-PS were associated with differential changes in EEG frequency bands (Fig. 2). As shown previously (Maloney *et al.*, 1997), gamma activity was high during attentive and active periods of Wake, often marked by increases in EMG activity, and during PS periods, which were characterized by low EMG activity. Delta increased in the transition into SWS (*t*SWS) and was high during SWS. The ratio of Th/De, which reflects EEG rhythmic slow activity in the theta range (Maloney *et al.*, 1997), appeared to vary in parallel with gamma.

During the 30 min afternoon recording period in the baseline condition, which would correspond approximately to the post-injection period in the experimental condition, the rats were asleep on average the majority of the time (>70%, Fig. 3). They spent ~55% of the time in *t*SWS & SWS and >15% in *t*PS & PS. Gamma varied significantly as a function of state and was higher during Wake

and *t*PS & PS than during *t*SWS & SWS, and delta varied significantly in a reciprocal manner to gamma across these states (as examined by repeated measures ANOVA, df = 4, 24; $p \leq .05$). Th/De also varied significantly as a function of state and like gamma, was highest in Wake and PS, though much higher on average in PS than in Wake.

Microinjections

Whereas microinjections of ringer solution did not appear to alter the sleep-wake states or EEG activities of the rats (Fig. 4), microinjections of noradrenaline (Fig. 5) and serotonin (Fig. 6) appeared to alter these in different ways (Figs. 7 - 10).

Ringer

Most animals were briefly awakened when the injection cannulae were lowered into the basal forebrain, but all resumed sleeping prior to or during injections with ringer solution (n = 8, Fig. 4). After the injection was stopped, all rats experienced some epochs of SWS within the first 5 min. In the 30 min post-injection period, all animals showed an alternation of Wake and SWS and a progression through SWS to *t*PS-PS or *t*PS. During these state changes, the EEG frequency band activities varied in association with state and behavior in a manner that was not distinguishable from that in the pre-injection period or that in the baseline post-injection recording period.

As compared to the baseline afternoon recording period, there were no significant changes in the average relative amounts of sleep-wake states following ringer injections (as examined in 8 rats with paired comparison *t*-tests). The rats were still asleep the majority of the time (>80%) and spent >65% of time in *t*SWS &

SWS and ~15% in *t*PS & PS (Fig. 7), even though the %PS was insignificantly lower than that in baseline. Similarly, the average gamma and delta activities were not different following ringer (Fig. 8) compared to baseline over the 30 min afternoon or post-injection period or in any of the sleep-wake states during that period. There was a significant change in Th/De ratio, being lower during the post-injection period following ringer.

Noradrenaline

Upon lowering of the filled cannulae, all rats woke up and remained awake prior to and during the injection of noradrenaline (75 nmol per side, n = 5, Fig. 5). In the 30 min post-injection period, all rats remained awake except for some brief episodes of *t*SWS or SWS in some rats (2/5). EEG frequency band activities showed variable but generally moderately high gamma activity during the post-injection period, which reached levels present during active waking or PS during the pre-injection recording period in all rats. Delta remained low during the post-injection recording period in all rats. The animals manifested normal Waking behaviors, which included W*attentive* (standing motionless with body and head erect) or W*moving* (moving or walking about the cage) but also occasionally W*quiet* (recumbent with eyes open).

Across animals, the Wake state was significantly increased (to an average of more than 95% of recording time), *t*SWS & SWS were significantly decreased and PS & *t*PS were absent during the post-injection recording period following noradrenaline (Fig. 7). There was a significant increase in average gamma activity and a significant decrease in average delta activity as compared to that following ringer during this period (Fig. 8). The average EMG activity was higher than that following ringer, though not significantly so ($p = 0.08$).

The EEG during the post-injection period following noradrenaline was characterized by a low voltage, fast pattern (Fig. 9), which is normally characteristic of the Wake state. In the high frequency filtered record, relatively high amplitude gamma activity was apparent. In average spectra of epochs during the post-injection period, a small peak was evident in the theta band, which is normally the case during waking attentive or active behaviors in the rat (Maloney *et al.*, 1997). Although no distinct peak was present in the high frequency portion of the spectra, the amplitude in the gamma band was relatively high, as has also been found to be the case during attentive or active waking behaviors (Maloney *et al.*, 1997). The Wake state after noradrenaline compared to that after ringer had significantly higher relative gamma activity (Table 1). The EMG was also higher during Wake after noradrenaline, though not significantly so (Table 1, $p = 0.07$).

Serotonin

As was the case for ringer, all animals resumed sleeping after the filled cannulae were lowered or the injection was started with serotonin (250 nmol per side, $n = 8$, Fig. 6). SWS occurred in all rats in the 30 min post-injection period. PS occurred in only one rat (out of 8) during this same time period. In EEG activity, serotonin microinjections were associated with an apparent decrease in gamma activity (8/8 rats) through most of the post-injection period (Fig. 6). Delta activity could be relatively high during this period, reaching levels apparently equal to or higher than those present during SWS in the pre-injection recording period. Th/De ratio remained low. During these episodes of high delta, two behavioral states were observed: sleeping or quiet waking. During sleeping behavior (marked by eyes closed), high delta activity was usually associated with a normal sleep posture and behavior (S*curled* or more often S*uncurled*), though in one rat, it was associated

with an abnormal outstretched posture. All these epochs were scored as SWS or *t*SWS. During waking behavior (marked by eyes open), the delta activity, which appeared to be of lower amplitude than that during sleeping behavior, was associated with quiet behavior (usually recumbent, noted as W*quiet*, though also occasionally moving during positional shifts, noted as W*moving*). This apparent dissociation between EEG delta activity and waking behavior was seen in half the rats. These epochs were scored as the Wake state, according to the behavioral notation and despite the presence of EEG delta activity. During both the SWS and Wake episodes in many rats, the EMG activity appeared relatively high as compared to the pre-injection levels.

During the post-injection recording period following serotonin, the average percent of the Wake state did not differ significantly from that following ringer, although it did appear to be higher (Fig. 7). Similarly, the average amount of slow wave sleep (*t*SWS & SWS) was not significantly changed (representing >55%). On the other hand, average *t*PS & PS were significantly decreased (to <3%). Across animals, the EEG was altered during the post-injection period by significantly lower average gamma activity as compared to ringer (Fig. 8). The ratio of Th/De was also significantly lower than that with ringer (which in turn was significantly lower than that in baseline, above). EMG amplitude was significantly higher following serotonin than following ringer.

The EEG during the post-injection period following serotonin was often characterized by high voltage slow waves with relatively low amplitude gamma activity (Fig. 9), thereby resembling that of SWS. The average spectra for epochs sampled during this period revealed a large peak in the delta band (Fig. 10), which is typical of natural SWS. The EEG of SWS epochs compared with those of ringer

had significantly higher relative delta activity and lower Th/De ratio (Table 1). The EMG activity was also higher than that in normal SWS epochs, although not significantly so. The post-serotonin Wake epochs, which include the anomalous Wake episodes (above), also differed from those following ringer by significantly lower relative gamma, higher relative delta, lower Th/De and higher EMG activities (Table 1).

Dose-response relationships

The differential effects of noradrenaline and serotonin on gamma EEG activity were found to be dose-dependent (Fig. 11). Whereas increasing doses of noradrenaline were associated with increases in average gamma during the post-injection period, increasing doses of serotonin were associated with decreases in average gamma, each reaching a plateau at the maximum dose employed in the main study. Noradrenaline was also associated with a dose-dependent decrease in delta activity. With regard to state, the increase in Wake and decrease in SWS produced by noradrenaline were significantly dependent on dose (with ANCOVA, df = 4, 1; $p \leq 0.05$, not shown). Serotonin had no significant dose-dependent effect on delta activity or on Wake or SWS states. On the other hand, the decreases in PS following noradrenaline and serotonin were both significantly dose-dependent (with ANCOVA, df = 4, 1; $p \leq 0.05$, not shown).

DISCUSSION

The results of the present study demonstrate that noradrenaline and serotonin, which have been shown *in vitro* to exert respective depolarizing versus hyperpolarizing influences upon cholinergic basalis neurons (Khateb *et al.*, 1993; Fort *et al.*, 1995), produce differential effects upon EEG activity and sleep-wake state when microinjected *in vivo* into the region of the cholinergic basalis neurons. Whereas noradrenaline facilitated gamma activity and elicited waking, serotonin diminished high frequency gamma activity and did not significantly affect slow wave sleep in the naturally sleeping/waking rat during the day when the animals are normally asleep the majority of the time. On the other hand, both neurotransmitters eliminated paradoxical sleep.

Noradrenaline facilitates gamma EEG activity and elicits waking

Noradrenaline microinjections into the basal forebrain produced a significant and dose-dependent increase in gamma activity and reciprocal decrease in delta activity associated with an increase in the wake state. This effect upon EEG activity is interpreted as being due to the depolarization and excitation of the cholinergic basalis neurons by noradrenaline that have been demonstrated *in vitro* (Fort *et al.*, 1995). Driven into a tonic mode of firing, the cholinergic basalis neurons could be expected to exert a tonic facilitatory influence upon cortical neurons and activity that would be evident as a decrease in low frequency, burst firing and an increase in high frequency tonic firing by the cortical neurons (Krnjevic, 1967; McCormick, 1992; Metherate *et al.*, 1992). At the level of EEG activity, these changes would underlie a shift from delta to gamma activity during the period of the day when the animals are normally asleep. It must also be considered that noradrenaline may additionally exert its effects through the basal forebrain via non-cholinergic, putative

cortically projecting cells, the vast majority of which are also depolarized and excited by noradrenaline (Fort *et al.*, 1992; Fort *et al.*, In press). In the present study, the EEG changes were associated with the intrusion of the wake state into diurnal sleep and moreover the stimulation of a relatively aroused state of waking, marked by a higher relative amount of gamma activity, which is associated with attentive or active waking behaviors (Maloney *et al.*, 1997).

An important role of noradrenergic locus coeruleus neurons in the facilitation of cortical activation and waking has been recognized for many years (see (Jouvet, 1972; Jones *et al.*, 1973)). Even though studies have shown that these neurons are not essential for the maintenance of these activities (see (Jones *et al.*, 1977; Jones, 1991)), multiple pharmacological and physiological studies have demonstrated that the noradrenergic locus coeruleus neurons normally have the capacity to facilitate and prolong cortical activation and waking (see (Jacobs and Jones, 1978)). They discharge at the highest rate during active and attentive waking and decrease their rate of firing during quiet waking and slow wave sleep (Aston-Jones and Bloom, 1981a; Rasmussen *et al.*, 1986). They also increase their rate of firing transiently in association with responses to sensory stimuli, including orientation (Aston-Jones and Bloom, 1981b; Rasmussen *et al.*, 1986). Accordingly, they would be expected to exert a facilitatory influence on cholinergic basalis neurons in association with sensory stimulation and orientation which would in turn facilitate cortical activation (Metherate *et al.*, 1992). It has been found that stimulation of the locus coeruleus generates cortical activation with a shift from low-frequency to higher frequency EEG activity (Berridge and Foote, 1991) and that lesions of noradrenergic fibers are associated with a loss of high frequency EEG activity in response to sensory stimuli (Delagrange *et al.*, 1989). The present

results suggest that noradrenaline can facilitate high frequency gamma activity and waking by acting upon cholinergic basalis neurons, in addition to acting upon thalamic and cortical systems (McCormick, 1992).

The noradrenaline microinjections into the basal forebrain also resulted in a suppression of PS, which can be interpreted simply as due to the facilitation of waking, but possibly also to a general opposing role of noradrenaline in the generation of this state (Hobson *et al.*, 1975; Aston-Jones and Bloom, 1981a).

Serotonin diminishes gamma EEG activity and allows SWS

Serotonin produced a significant and dose-dependent decrease in high frequency gamma and did not significantly increase waking or decrease slow wave sleep during the daytime recording period when rats are naturally asleep the majority of the time. This EEG effect could be interpreted as being due to the hyperpolarization and inhibition of cholinergic basalis neurons by serotonin (Khateb *et al.*, 1993). It is additionally possible that the effect could be due to serotonin's action on non-cholinergic, putative cortically projecting basalis neurons, which are also hyperpolarized and inhibited by serotonin ((Fort *et al.*, 1992; Fort *et al.*, In press). It is presumed that by its action upon cortically projecting cells, serotonin diminishes cortical activation evidenced by decreased gamma activity and accordingly is associated with a quiet waking state or slow wave sleep during the day when the animal is naturally asleep.

The role of serotonin in sleep-wake states has been greatly debated over the past 25 years. The demonstration that lesions of the serotonergic raphe neurons could result in complete insomnia originally led Jouvet to propose that serotonergic neurons play a determining role in the generation of slow wave sleep (see for review (Jouvet, 1972)). In support of this theory, depletion of serotonin by

inhibition of tryptophan hydroxylase with para-chlorophenylalanine (PCPA) was also shown in the cat to produce insomnia, which could be reversed by subsequent peripheral or central administration of low doses of 5-hydroxytryptophan (5-HTP), the immediate precursor of serotonin ((Denoyer *et al.*, 1989); see for review (Jouvet, 1972)). However, subsequent studies, particularly in rats, indicated that serotonin was not necessary for the appearance of slow wave sleep, though it could facilitate the onset of sleep (see for review (Jacobs and Jones, 1978; Jacobs and Fornal, 1991; Jones, 1994)). Moreover, dorsal raphe neurons were found to discharge at their highest rates during waking and decrease their firing rate (by ~50%) during slow wave sleep, indicating that they did not likely generate slow wave sleep (McGinty and Harper, 1976; Trulson and Jacobs, 1979) (see for review (Jacobs and Fornal, 1991)). On the other hand, their higher discharge rate during waking could be specifically associated with suppression of particular waking behaviors and responses to inputs which can interfere with sleep onset (McGinty and Harper, 1976; Trulson and Jacobs, 1979). In fact, it has been found that upon presentation of sensory stimuli (Aghajanian *et al.*, 1978) and during orientation to stimuli (Jacobs and Fornal, 1991), many putative serotonergic raphe units cease firing (in contrast to the noradrenergic locus coeruleus neurons which increase firing). According to the *in vitro* results (Khateb *et al.*, 1993), this cessation of serotonergic neuronal discharge could be associated with a disinhibition of the cholinergic basalis neurons during the cortical activation that occurs with sensory stimulation and orientation. Conversely, discharge by the serotonergic neurons under other circumstances would hyperpolarize the cholinergic cells and prevent their tonic discharge, which could in turn be associated with a decrease in cortical activation, as that which we have measured here as a decrease in gamma EEG

activity following microinjections of serotonin. In accordance with this interpretation, the dorsal raphe neurons have been found to discharge at higher rates during grooming behavior (Fornal *et al.*, 1996), when cortical gamma activity is low (Maloney *et al.*, 1997), than during attentive behavior, when cortical gamma activity is high. A cortical 'deactivation' produced by the action of serotonin on cholinergic basalis neurons could thus be associated with relaxed or quiet waking or with slow wave sleep during the diurnal, maximal sleep period of the day.

Despite the continuity of slow wave sleep following serotonin microinjections, the resulting sleep and sleep cycle were not completely normal, but marked by higher EMG activity and the absence of paradoxical sleep, as well as diminished theta activity, which marks that state in cortical, as well hippocampal, EEG (Maloney *et al.*, 1997). The results of serotonin's effects in the basal forebrain concur with results showing a facilitatory role of serotonin through other areas of the central nervous system on muscle tonus and certain rhythmic motor behaviors and a suppressive role of serotonin in paradoxical sleep and theta activity (see for review, (Steriade and Hobson, 1976; Jacobs and Fornal, 1991; Holmes and Jones, 1994; Vertes *et al.*, 1994; Fornal *et al.*, 1996)). The partial dissociation between EEG activity and behavior seen in some rats following serotonin microinjections in the present study, is also well known to occur following systemic injections of atropine, which by blocking cholinergic, muscarinic receptors results in a pattern of slow wave EEG activity during a behaviorally awake state (Longo, 1966; Stewart *et al.*, 1984). Our results show that serotonin microinjections into the basal forebrain may similarly result in slow waves in the cerebral cortex, thought to be due in this case to the inhibition of cholinergic basalis neurons, but not necessarily in a decrease in muscle tone that normally occurs during slow wave sleep and precedes

paradoxical sleep. The results also suggest that serotonin may act on other non-cholinergic neurons in the area which through descending projections may be involved in movement and maintenance of muscle tone (Swanson *et al.*, 1984) that can persist during slow wave sleep but not paradoxical sleep.

CONCLUSIONS

When injected into the basal forebrain of a naturally sleeping/waking rat during the day, noradrenaline, which is known to depolarize cholinergic neurons, diminishes delta activity and slow wave sleep and stimulates high frequency gamma EEG activity and waking. In contrast, serotonin, which is known to hyperpolarize cholinergic basalis neurons, diminishes high frequency gamma EEG activity and has no decremental effect on delta activity or slow wave sleep. It is concluded that noradrenaline and serotonin may play differential roles in modulating cortical activity in part through their opposing actions upon cholinergic basalis neurons, which in turn have been shown to play an important role in facilitating high frequency gamma EEG activity and waking.

ACKNOWLEDGEMENTS

We would like to thank Lynda Mainville for her technical assistance and Jean Gotman, Angel Alonso and Michel Muhlethaler for their helpful consultation. The research was supported by a grant to BEJ from the Canadian Medical Research Council. EGC was supported as a graduate student by the Fonds de Recherche en Santé du Québec, Réseau de Santé Mentale, Axe Sommeil et Vigilance.

ABBREVIATIONS

AMPA	alpha-amino-3-hydroxy-5-methyl-4-isoxazole propionic acid
ACh	acetylcholine
ChAT	choline acetyltransferase
De	delta
EEG	electroencephalogram
EMG	electromyogram
Ga	gamma
GAD	glutamic acid decarboxylase
NMDA	N-methyl-D-aspartate
PS	paradoxical sleep
SWS	slow wave sleep
Th	theta
*t*PS	transition into paradoxical sleep
*t*SWS	transition into slow wave sleep
W	wake

LITERATURE CITED

Aghajanian GK, Wang RY, Barban J (1978) Serotonergic and non-serotonergic neurons of the dorsal raphe: reciprocal changes in firing induced by peripheral nerve stimulation. *Brain Res.*, **153,** 169-175.

Aston-Jones G, Bloom FE (1981a) Activity of norepinephrine-containing locus coeruleus neurons in behaving rats anticipates fluctuations in the sleep-waking cycle. *J. Neurosci.*, **1,** 876-886.

Aston-Jones G, Bloom FE (1981b) Norepinephrine-containing locus coeruleus neurons in behaving rats exhibit pronounced responses to non-noxious environmental stimuli. *J. Neurosci.*, **1,** 887-900.

Berridge CW, Foote SL (1991) Effects of locus coeruleus activation on electroencephalographic activity in neocortex and hippocampus. *J. Neurosci.*, **11,** 3135-3145.

Buzsaki G, Bickford RG, Ponomareff G, Thal LJ, Mandel R, Gage FH (1988) Nucleus basalis and thalamic control of neocortical activity in the freely moving rat. *J. Neurosci.*, **8,** 4007-4026.

Cape E, Jones BE (1994) Modulation of sleep-wake state and cortical activity following injection of agonists into the region of cholinergic basal forebrain neurons. *Soc. Neurosci. Abst.*, **20,** 156.

Casamenti F, Deffenu G, Abbamondi AL, Pepeu G (1986) Changes in cortical acetylcholine output induced by modulation of the nucleus basalis. *Brain Res. Bull.*, **16,** 689-695.

Celesia GG, Jasper HH (1966) Acetylcholine released from cerebral cortex in relation to state of activation. *Neurology*, **16,** 1053-1064.

Delagrange P, Tadjer D, Bouyer J-J, Rougeul A, Conrath M (1989) Effect of DSP4, a neurotoxic agent, on attentive behaviour and related electrocortical activity in cat. *Behav. Brain Res.*, **33,** 33-43.

Denoyer M, Sallanon M, Kitahama K, Aubert C, Jouvet M (1989) Reversibility of para-chlorophenylalanine-induced insomnia by intrahypothalamic microinjection of L-5-hydroxytryptophan. *Neuroscience*, **28,** 83-94.

Fornal CA, Metzler CW, Marrosu F, Ribiero-do-Valle LE, Jacobs BL (1996) A subgroup of dorsal raphe serotonergic neurons in the cat is strongly activated during oral-buccal movements. *Brain Res.*, **716,** 123-133.

Fort P, Khateb A, Alonso A, Jones BE, Muhlethaler M (1992) Pharmacological heterogeneity of basal forebrain neurones. *Soc. Neurosci. Abst.*, **18,** 881.

Fort P, Khateb A, Pegna A, Muhlethaler M, Jones BE (1995) Noradrenergic modulation of cholinergic nucleus basalis neurons demonstrated by *in vitro* pharmacological and immunohistochemical evidence in the guinea pig brain. *Eur. J. Neurosci.*, **7,** 1502-1511.

Fort P, Khateb A, Serafin M, Muhlethaler M, Jones BE (1998) Pharmacological characterization and differentiation of non-cholinergic nucleus basalis neurons *in vitro*. *NeuroReport*, **9,** 1-5.

Gritti I, Mainville L, Jones BE (1993) Codistribution of GABA- with acetylcholine-synthesizing neurons in the basal forebrain of the rat. *J. Comp. Neurol.*, **329,** 438-457.

Hobson JA, McCarley RW, Wyzinski PW (1975) Sleep cycle oscillation: reciprocal discharge by two brainstem neuronal groups. *Science*, **189,** 55-58.

Holmes CJ, Jones BE (1994) Importance of cholinergic, GABAergic, serotonergic and other neurons in the medullary reticular formation for sleep-wake states studied by cytotoxic lesions in the cat. *Neuroscience*, **62,** 1179-1200.

Jacobs BL, Fornal CA (1991) Activity of brain serotonergic neurons in the behaving animal. *Pharmacol. Rev.*, **43,** 563-578.

Jacobs BL, Jones BE (1978) The role of central monoamine and acetylcholine systems in sleep-wakefulness states: mediation or modulation. In: *Cholinergic-Monoaminergic Interactions in the Brain*. Edited by L. L. Butcher. New York: Academic Press, pp. 271-290.

Jasper HH, Tessier J (1971) Acetylcholine liberation from cerebral cortex during paradoxical (REM) sleep. *Science*, **172,** 601-602.

Jones BE (1991) The role of noradrenergic locus coeruleus neurons and neighboring cholinergic neurons of the pontomesencephalic tegmentum in sleep-wake states. In: *Neurobiology of the Locus Coeruleus. Progress in Brain Research, Vol. 85*, Volume 85. Edited by C. Barnes and O. Pompeiano. Amsterdam: Elsevier, pp. 532-543.

Jones BE (1993) The organization of central cholinergic systems and their functional importance in sleep-waking states. In: *Cholinergic Function and Dysfunction, Progress in Brain Research, Vol. 98*, Volume 98. Edited by A. C. Cuello. Amsterdam: Elsevier, pp. 61-71.

Jones BE (1994) Basic mechanisms of sleep-wake states. In: *Principles and Practice of Sleep Medicine, 2nd Edition*. Edited by M. H. Kryger, T. Roth and W. C. Dement. Philadelphia: Saunders, pp. 145-162.

Jones BE (1995) Reticular formation. Cytoarchitecture, transmitters and projections. In: *The Rat Nervous System*. Edited by G. Paxinos. New South Wales: Academic Press Australia, pp. 155-171.

Jones BE, Beaudet A (1987) Retrograde labeling of neurons in the brain stem following injections of [^{3}H]choline into the forebrain of the rat. *Exp. Brain Res.*, **65,** 437-448.

Jones BE, Bobillier P, Pin C, Jouvet M (1973) The effect of lesions of catecholamine-containing neurons upon monoamine content of the brain and EEG and behavioral waking in the cat. *Brain Res.*, **58,** 157-177.

Jones BE, Cuello AC (1989) Afferents to the basal forebrain cholinergic cell area from pontomesencephalic--catecholamine, serotonin, and acetylcholine--neurons. *Neuroscience*, **31,** 37-61.

Jones BE, Harper ST, Halaris AE (1977) Effects of locus coeruleus lesions upon cerebral monoamine content, sleep-wakefulness states and the response to amphetamine. *Brain Res.*, **124,** 473-496.

Jones BE, Yang T-Z (1985) The efferent projections from the reticular formation and the locus coeruleus studied by anterograde and retrograde axonal transport in the rat. *J. Comp. Neurol.*, **242,** 56-92.

Jouvet M (1972) The role of monoamines and acetylcholine-containing neurons in the regulation of the sleep-waking cycle. *Ergeb. Physiol.*, **64,** 165-307.

Khateb A, Fort P, Alonso A, Jones BE, Muhlethaler M (1993) Pharmacological and immunohistochemical evidence for a serotonergic input to cholinergic nucleus basalis neurons. *Eur. J. Neurosci.*, **5,** 541-547.

Khateb A, Muhlethaler M, Alonso A, Serafin M, Mainville L, Jones BE (1992) Cholinergic nucleus basalis neurons display the capacity for rhythmic bursting activity mediated by low threshold calcium spikes. *Neuroscience*, **51,** 489-494.

Krnjevic K (1967) Chemical transmission and cortical arousal. *Anesthesiology*, **28,** 100-104.

Lehmann J, Nagy JI, Atmadja S, Fibiger HC (1980) The nucleus basalis magnocellularis: the origin of a cholinergic projection to the neocortex of the rat. *Neuroscience*, **5,** 1161-1174.

Lo Conte G, Casamenti F, Bigi V, Milaneschi E, Pepeu G (1982) Effect of magnocellular forebrain nuclei lesions on acetylcholine output from the cerebral cortex, electrocorticogram and behaviour. *Arch. ital Biol.*, **120,** 176-188.

Longo VG (1966) Behavioral and electroencephalographic effects of atropine and related compounds. *Pharamacol. Rev.*, **18,** 965-996.

Maloney KJ, Cape EG, Gotman J, Jones BE (1997) High frequency gamma electroencephalogram activity in association with sleep-wake states and spontaneous behaviors in the rat. *Neuroscience*, **76,** 541-555.

Martin JH (1991) Autoradiographic estimation of the extent of reversible inactivation produced by microinjection of lidocaine and muscimol in the rat. *Neurosci. Lett.*, **127,** 160-164.

McCormick DA (1992) Neurotransmitter actions in the thalamus and cerebral cortex and their role in neuromodulation of thalamocortical activity. *Progr. Neurobiol.*, **39,** 337-388.

McGinty D, Harper RM (1976) Dorsal raphe neurons: depression of firing during sleep in cats. *Brain Res.*, **101,** 569-575.

Metherate R, Cox CL, Ashe JH (1992) Cellular bases of neocortical activation: modulation of neural oscillations by the nucleus basalis and endogenous acetylcholine. *J. Neurosci.*, **12,** 4701-4711.

Moruzzi G, Magoun HW (1949) Brain stem reticular formation and activation of the EEG. *Electroenceph. clin. Neurophysiol.*, **1,** 455-473.

Myers RD (1974) *Handbook of Drug and Chemical Stimulation of the Brain*. New York: Van Nostrand Reinhold Co.

Rasmussen K, Morilak DA, Jacobs BL (1986) Single unit activity of locus coeruleus neurons in the freely moving cat: I. During naturalistic behaviors and in response to simple and complex stimuli. *Brain Res.*, **371,** 324-334.

Rasmusson DD, Clow K, Szerb JC (1994) Modification of neocortical acetylcholine release and electroencephalogram desynchronization due to brainstem stimulation by drugs applied to the basal forebrain. *Neuroscience*, **60,** 665-677.

Rye DB, Wainer BH, Mesulam M-M, Mufson EJ, Saper CB (1984) Cortical projections arising from the basal forebrain: a study of cholinergic and noncholinergic components employing combined retrograde tracing and immunohistochemical localization of choline acetyltransferase. *Neuroscience*, **13,** 627-643.

Semba K, Reiner PB, McGeer EG, Fibiger HC (1988) Brainstem afferents to the magnocellular basal forebrain studied by axonal transport, immunohistochemistry and electrophysiology in the rat. *J. Comp. Neurol.*, **267,** 433-453.

Shute CCD, Lewis PR (1967) The ascending cholinergic reticular system: neocortical, olfactory and subcortical projections. *Brain*, **90,** 497-520.

Starzl TE, Taylor CW, Magoun HW (1951) Ascending conduction in reticular activating system, with special reference to the diencephalon. *J. Neurophysiol.*, **14,** 461-477.

Steriade M, Hobson JA (1976) Neuronal activity during the sleep-waking cycle. *Prog. Neurobiol.*, **6,** 155-376.

Stewart DJ, Macfabe DF, Vanderwolf CH (1984) Cholinergic activation of the electrocorticogram: Role of the substantia innominata and effects of atropine and quinuclidinyl benzilate. *Brain Res.*, **322,** 219-232.

Swanson LW, Mogenson GJ, Gerfen CR, Robinson P (1984) Evidence for a projection from the lateral preoptic area and substantia innominata to the 'Mesencephalic Locomotor Region' in the rat. *Brain Res.*, **295,** 161-178.

Trulson ME, Jacobs BL (1979) Raphe unit activity in freely moving cats: correlation with level of behavioral arousal. *Brain Res.*, **163,** 135-150.

Vergnes M, Marescaux C, Micheletti G, Reis J, Depaulis A, Rumbach L *et al.* (1982) Spontaneous paroxysmal electroclinical patterns in rat: a model of generalized non-convulsive epilepsy. *Neurosci. Lett.*, **33,** 97-101.

Vertes RP, Kinney GG, Kocsis B, Fortin WJ (1994) Pharmacological suppression of the median raphe nucleus with sertonin$_{1A}$ agonists, 8-OH-DPAT and buspirone, produces hippocampal theta rhythm in the rat. *Neuroscience*, **60,** 441-451.

Wenk GL (1984) Pharmacological manipulations of the substantia innominata-cortical cholinergic pathway. *Neurosci. Lett.*, **51,** 99-103.

Figure 1. A. Schematic drawing of the rat brain (in sagittal view) illustrating chemical microinjections into the region of cholinergic basalis neurons (open circles), which are known to project to the cerebral cortex (dashed lines) and to receive input from noradrenergic and serotonergic afferents (solid lines), respectively arriving from the dorsal raphe (DR) and locus coeruleus (LC) nuclei in the brainstem (adapted with permission from (Jones, 1995)). Bilateral microinjections of ringer, noradrenaline or serotonin were performed by insertion of inner injection cannulae into chronically indwelling guide cannulae. The cannulae are drawn according to the coordinates used for implantation and the histological verification of their position. At the time of the experiment, inner cannulae, which were filled with the chemical for injection, were first inserted within the guide cannulae (to within ~2 mm of tip, marked by arrow), where they were held until the time of injection. Immediately prior to injection, the inner cannulae on both sides were lowered by a remote driving mechanism (~4 mm) to pass out of the guide cannulae, through the globus pallidus (GP) into the substantia innominata (SI, to ~2 mm below guide cannulae, marked by lower arrow) and above the magnocellular preoptic nucleus (MCPO). The diffusion of the chemical solution is depicted according to estimates based upon previous injections of the same volume (0.5 µl) of neuroanatomical tracers into the basal forebrain ((Jones and Yang, 1985; Jones and Beaudet, 1987)). B. Drawing of coronal section through the middle of the injection site showing approximate placement of cannulae, based upon location of tracks, in relationship to ChAT-immunostained cells (mapped with the aid of an image analysis system). Abbreviations: ac, anterior commissure; AV, anteroventral thalamic nucleus; CL, centrolateral thalamic nucleus; CPu, caudate putamen; DpMe, deep mesencephalic reticular field; FF, fields of Forel; Gi, gigantocellular

reticular field; GiA, gigantocellular reticular field, alpha part; GiV, gigantocellular reticular field, ventral part; GP, globus pallidus; ic, internal capsule; LC, locus coeruleus; LD, laterodorsal thalamic nucleus; LH, lateral hypothalamic area; LP, lateral posterior thalamic nucleus; MCPO, magnocellular preoptic nucleus; oc, optic chiasm; opt, optic tract; OTuD, Olfactory Tubercle, Deep Layer; PC, paracentral thalamic nucleus; PF, parafascicular thalamic nucleus; PnC, pontine reticular field, caudal part; PnO, pontine reticular field, oral part; PnV, pontine reticular field, ventral part; PPTg, pedunculopontine tegmental nucleus; R, red nucleus; RRF, retrorubral field; Rt, reticular thalamic nucleus; SIA, Substantia Innnominata, anterior part; SIP, Substantia Innominata, posterior part; SN, substantia nigra; st, stria terminalis; VL, ventrolateral thalamic nucleus; VM, ventromedial thalamic nucleus; VTA, ventral tegmental area; ZI, zona incerta.

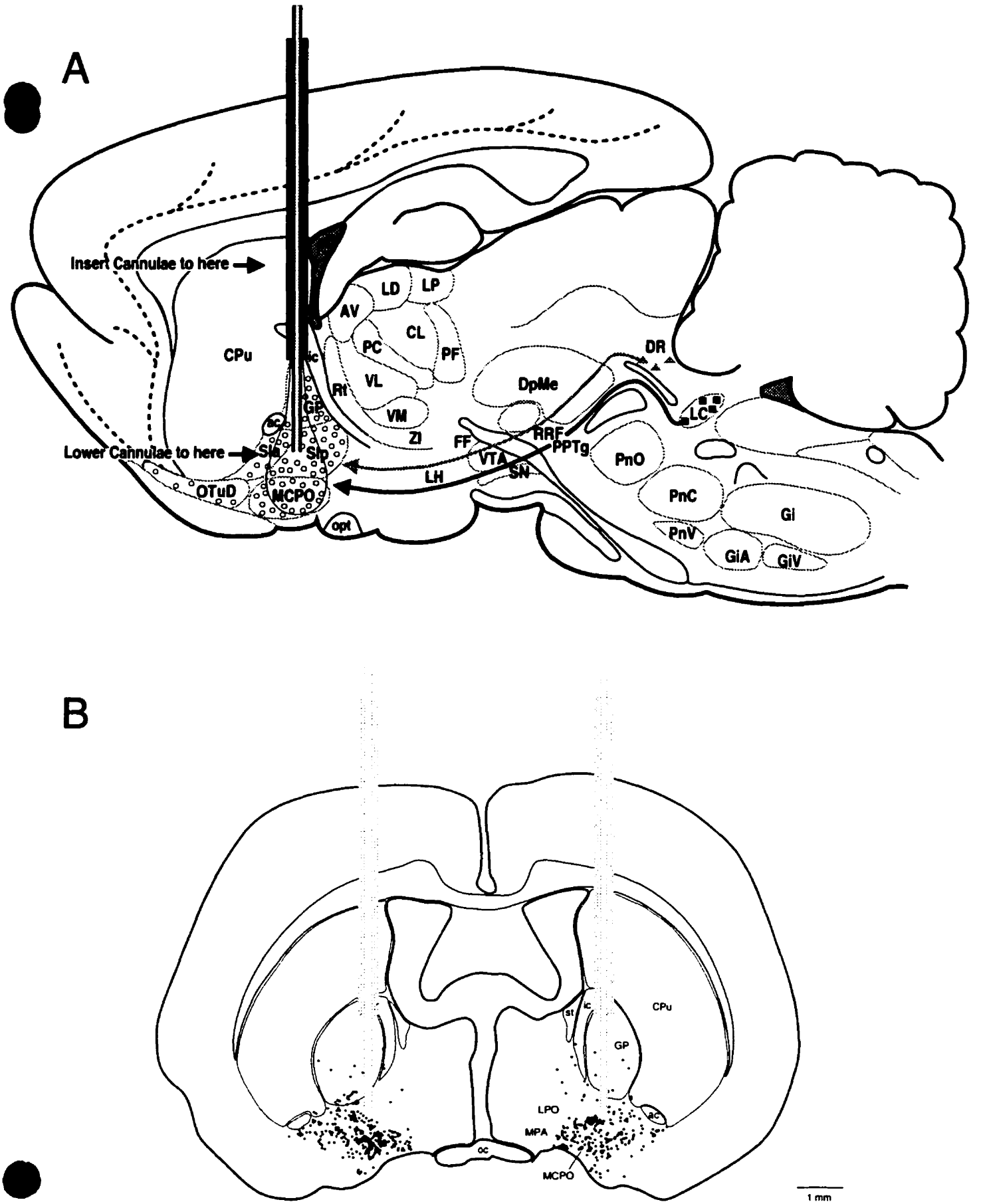
A
Insert Cannulae to here
Lower Cannulae to here
CPu
LD
LP
AV
CL
PC
PF
VL
Rt
VM
ZI
DpMe
DR
LC
RRF
PPTg
FF
VTA
SN
LH
PnO
PnC
Gi
PnV
GiA
GiV
ac
GP
Sib
Stp
OTuD
MCPO
opt
B
CPu
st
ic
GP
LPO
MPA
ac
oc
MCPO
1 mm

Fig. 1

Figure 2. Hypnogram (above) and EEG and EMG frequency band activities (below) per 20 sec epoch during morning (left) and afternoon (right) recording periods (rat B10). For EEG, gamma (Ga, 30.5-58.0 Hz) and delta (De, 1.5-4 Hz) absolute activities and theta/delta ratio (Th, 4.5-8.5 Hz/De, 1.5-4 Hz) from right retrosplenial cortex are displayed. Recording was begun in the morning (~1100 h = 0) and continued for ~30 min prior to handling the animal for mock insertion of injection cannulae (during break marked by dividing line). After relaxation and resumption of sleep (usually in ~30-45 min), recording was begun again for the afternoon. In this baseline record, 0 marks the approximate time at which an injection would have been performed and thus defines the 30 min baseline period with which the ringer post-injection period was compared (Fig. 4). In this undisturbed period during baseline recording, the rat is asleep the majority of the time. Gamma is highest in association with brief periods of active Wake (with high EMG activity) and with PS (with low EMG activity) and lowest in association with SWS. Delta varies in a reciprocal manner, high in association with SWS and low during both Wake and PS. Th/De ratio is high during brief periods of active Wake and highest during PS. Ga, De and EMG frequency band activities are displayed as amplitude units scaled to maximum activity. In this figure, the maximum amplitude for Ga is 157, for De is 417 and for EMG is 630 (AD units where 100 units $\approx$ 79 ΦV), and the maximum ratio of Th/De is 2.4. Time lines indicate the baseline periods corresponding to 30 min pre- and post-injection recording periods. Abbreviations: PS, Paradoxical Sleep; SWS, Slow Wave Sleep; *t*PS, transition into Paradoxical Sleep; *t*SWS, transition into Slow Wave Sleep.

Baseline

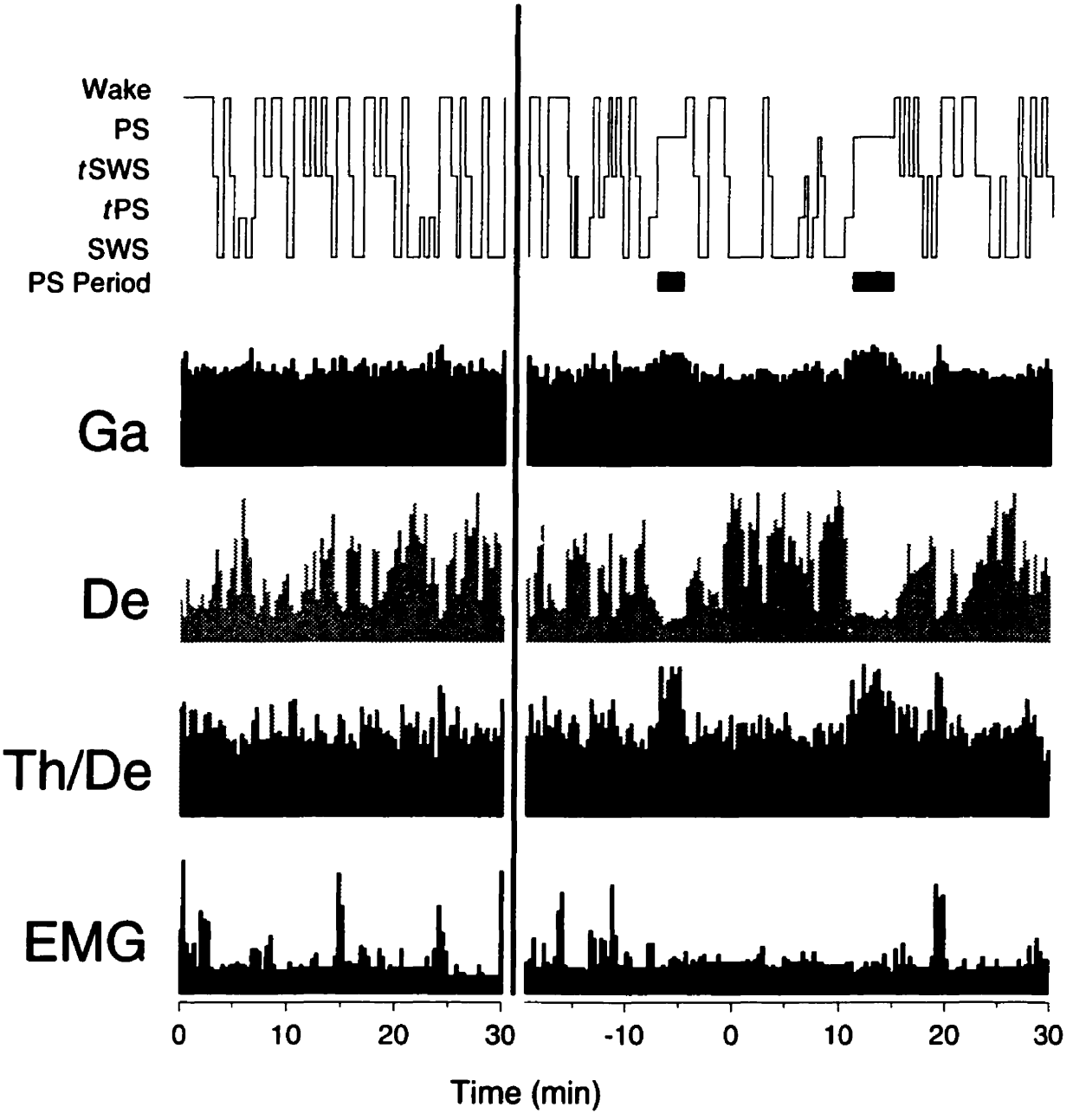

Fig. 2

Figure 3. Average % State and EEG and EMG activities from baseline recording during the 30 min afternoon (equivalent post-injection) recording period (Fig. 2), demonstrating the amounts of each state and the associated changes in EEG and EMG activities. The % State reflects the relative amounts of time spent in each state; Ga and De, frequency band activities, Th/De, the ratio of band activities and EMG, total spectral activity across sleep-wake states (EEG activities are taken from the right retrosplenial lead and reported together with EMG as amplitude, AD units, where 100 units $\approx$ 79μV, or as a ratio). Data presented as mean ± S.E.M. for 8 rats. Ga, De, Th/De and EMG all varied significantly as a function of state (repeated measures ANOVA with df = 4, 24, $p \leq .05$).

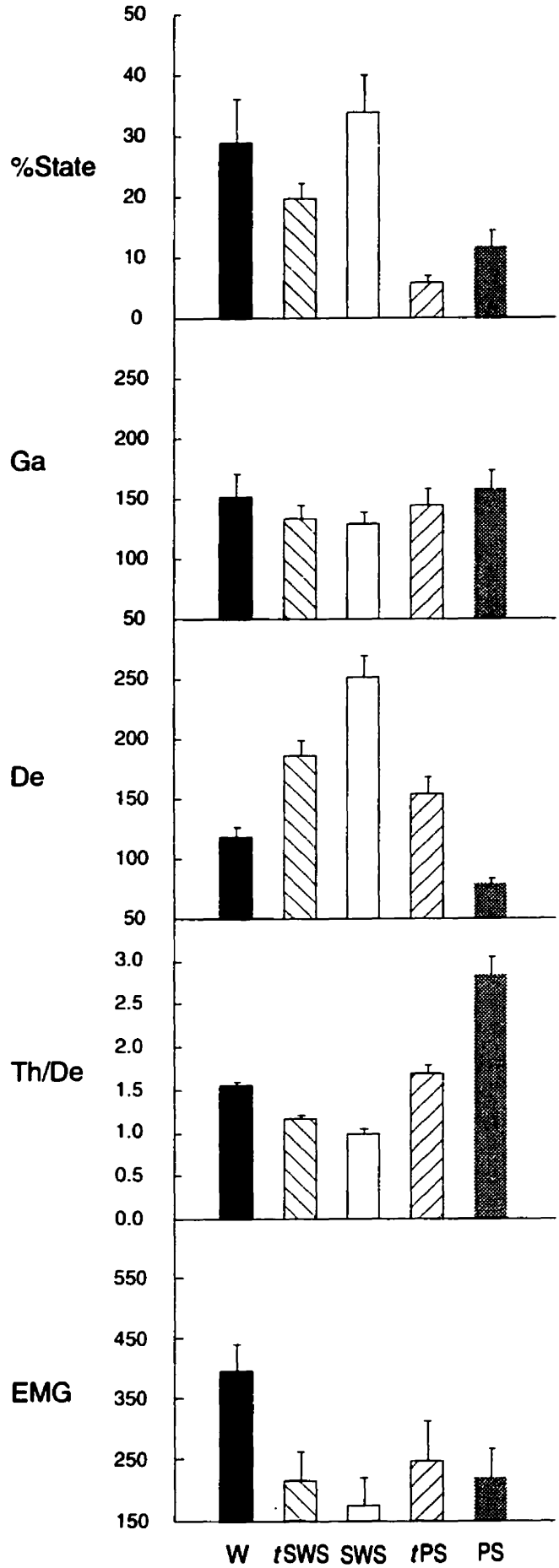
%State
50
40
30
20
10
0
Ga
250
200
150
100
50
De
250
200
150
100
50
Th/De
3.0
2.5
2.0
1.5
1.0
0.5
0.0
EMG
550
450
350
250
150
W
tSWS
SWS
tPS
PS

Fig. 3

Figure 4. Hypnogram and EEG and EMG activities (per 20 sec epoch) during ringer pre- and post-injection recording periods (rat B10). After the pre-injection recording period, the filled inner cannulae were inserted in the guide cannulae (Fig. 1), and the animal allowed to resume sleeping before recording was reinitiated. With the appearance of a normal sleep cycle, marked by SWS and *t*PS, leading to PS, the cannulae were lowered via remote control into the basal forebrain (Fig. 1); the bilateral injection was started ~2 min later and was performed over ~5 min. The post-injection recording period was defined as the 30 min period after the injection was stopped (Time 0-30 min at right). Note the minimal disturbance to the sleep-wake cycle caused by the injection procedure and the injection of ringer. EEG frequency band activity is from the right retrosplenial lead and together with EMG, is displayed as amplitude units or ratio scaled to maximum activity. In this figure, the maximum amplitude for Ga is 180, for De is 360 and for EMG is 475 (AD units where 100 units ≈ 79 ΦV), and the maximum Th/De ratio is 2.2.

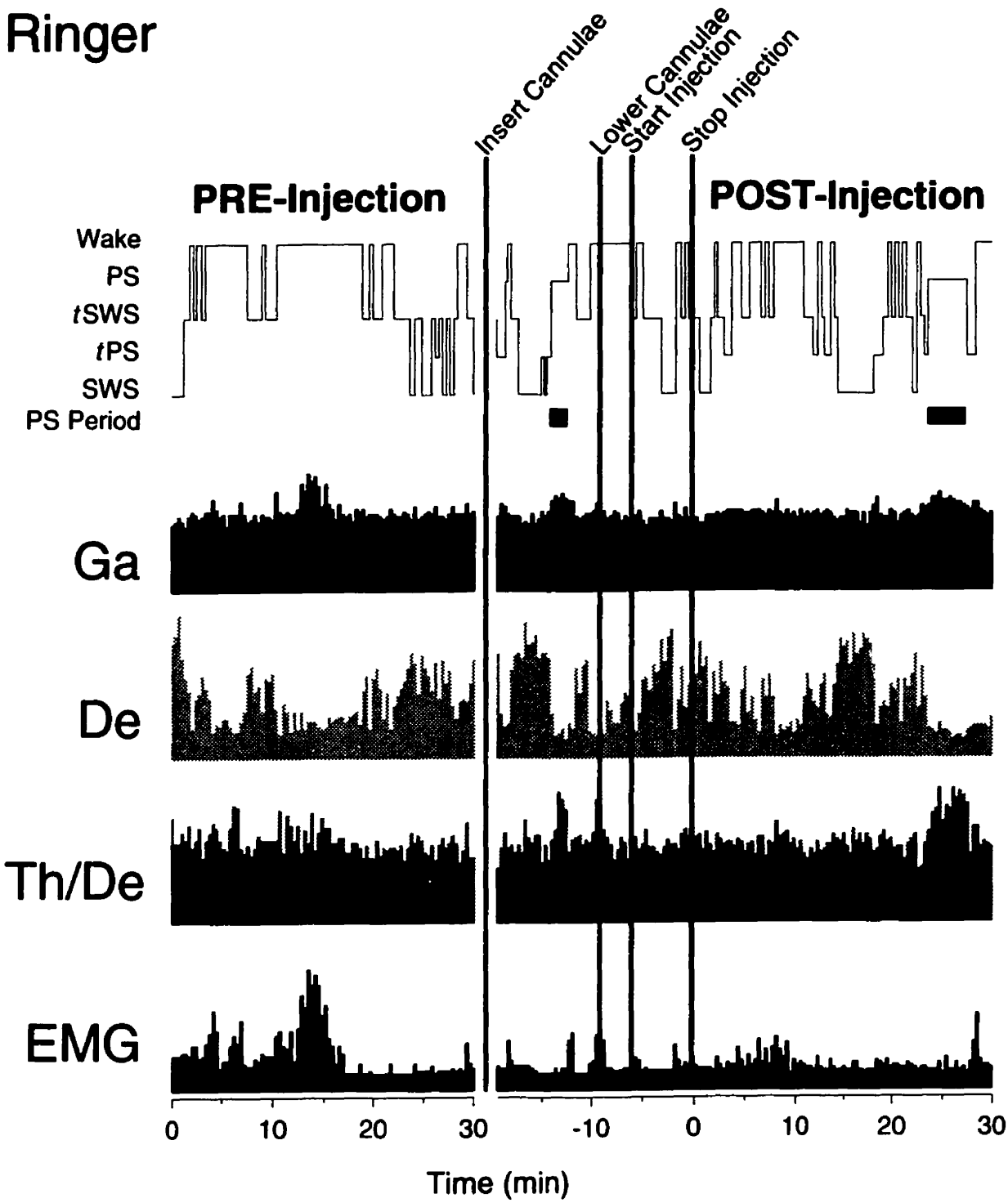
Ringer
Insert Cannulae
Lower Cannulae
Start Injection
Stop Injection
PRE-Injection
POST-Injection
Wake
PS
tSWS
tPS
SWS
PS Period
Ga
De
Th/De
EMG
0
10
20
30
-10
0
10
20
30
Time (min)

Fig. 4

Figure 5. Hypnogram and EEG and EMG activities (per 20 sec epoch) during noradrenaline pre- and post-injection recording periods (rat B10). Note the immediate occurrence of Wake once the filled cannulae are inserted and the maintenance of a Wake state in association with moderately high gamma EEG activity and low delta EEG activity during the entire post-injection period. Both Th/De and EMG remain relatively high. EEG frequency band activity is from the right retrosplenial lead and together with EMG, is displayed as amplitude units or ratio scaled to maximum activity. In this figure, the maximum amplitude for Ga is 155, for De is 395 and for EMG is 550 (AD units where 100 units $\approx$ 79 ΦV), and the maximum Th/De ratio is 2.3.

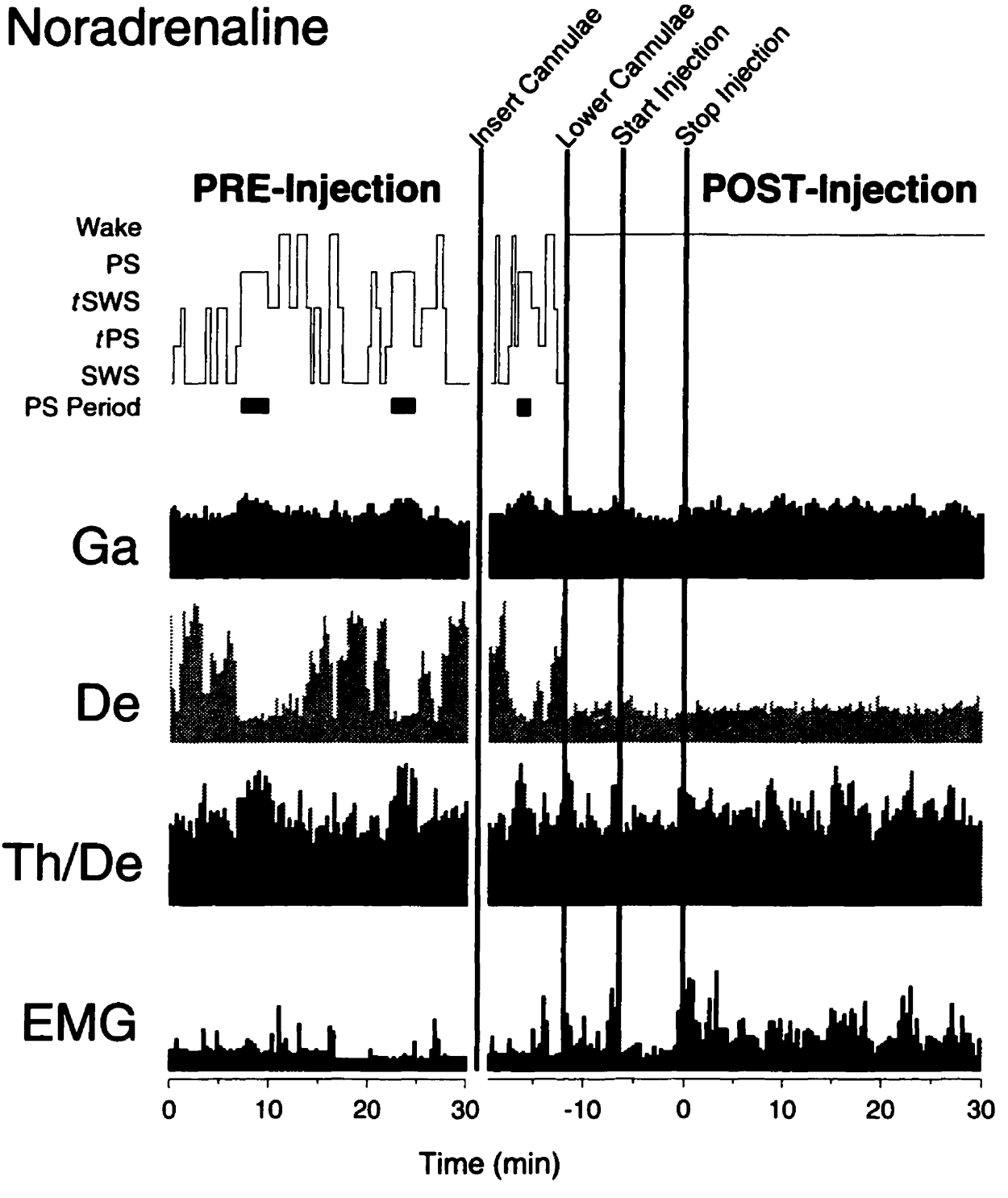
Noradrenaline
Insert Cannulae
Lower Cannulae
Start Injection
Stop Injection
PRE-Injection
POST-Injection
Wake
PS
tSWS
tPS
SWS
PS Period
Ga
De
Th/De
EMG
0
10
20
30
-10
0
10
20
30
Time (min)

Fig. 5

Figure 6. Hypnogram and EEG and EMG activities (per 20 sec epoch) during serotonin pre- and post-injection recording periods (rat B20). Note the continuity of SWS during and following the injection in association with a decrease in gamma activity and the persistence of delta activity. No PS occurs in the post-injection period and Th/De ratio remains low. Moderate EMG activity is present. EEG frequency band activity is from the right retrosplenial lead and together with EMG, is displayed as amplitude units or ratio scaled to maximum activity. In this figure, the maximum amplitude for Ga is 156, for De is 380 and for EMG is 800 (AD units where 100 units $\approx$ 79 ΦV), and the maximum Th/De ratio is 3.6.

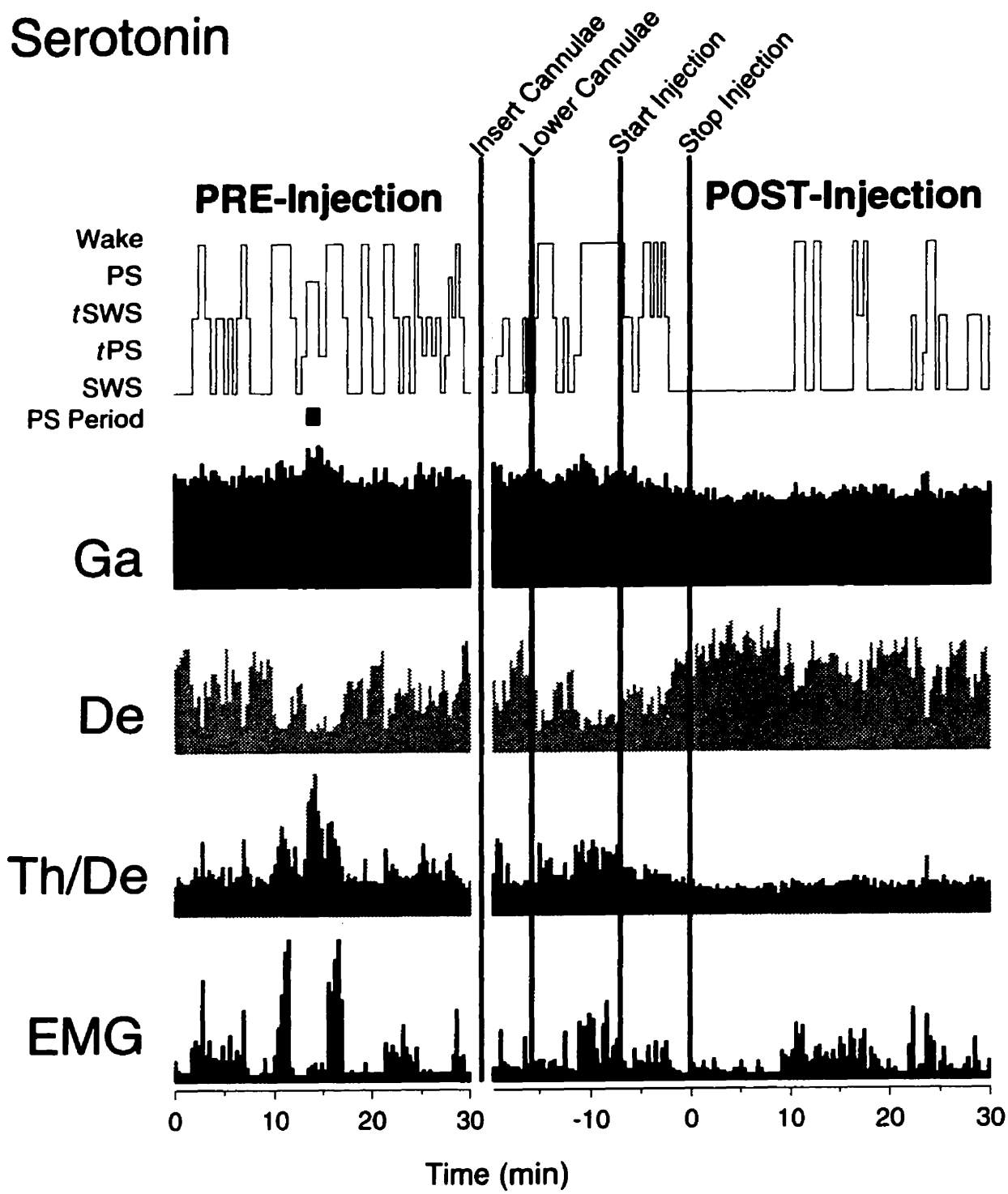
Serotonin
Insert Cannulae
Lower Cannulae
Start Injection
Stop Injection
PRE-Injection
POST-Injection
Wake
PS
tSWS
tPS
SWS
PS Period
Ga
De
Th/De
EMG
0
10
20
30
-10
0
10
20
30
Time (min)

Fig. 6

Figure 7. Percent time spent in sleep-wake states during ringer (R), noradrenaline (NA) and serotonin (5-HT) post-injection periods. Values are means ± S.E.M, for R, n = 8; for NA, n = 5; for 5-HT, n = 8. * indicates significantly different from ringer, according to paired comparison *t*-tests ($p \leq 0.05$).

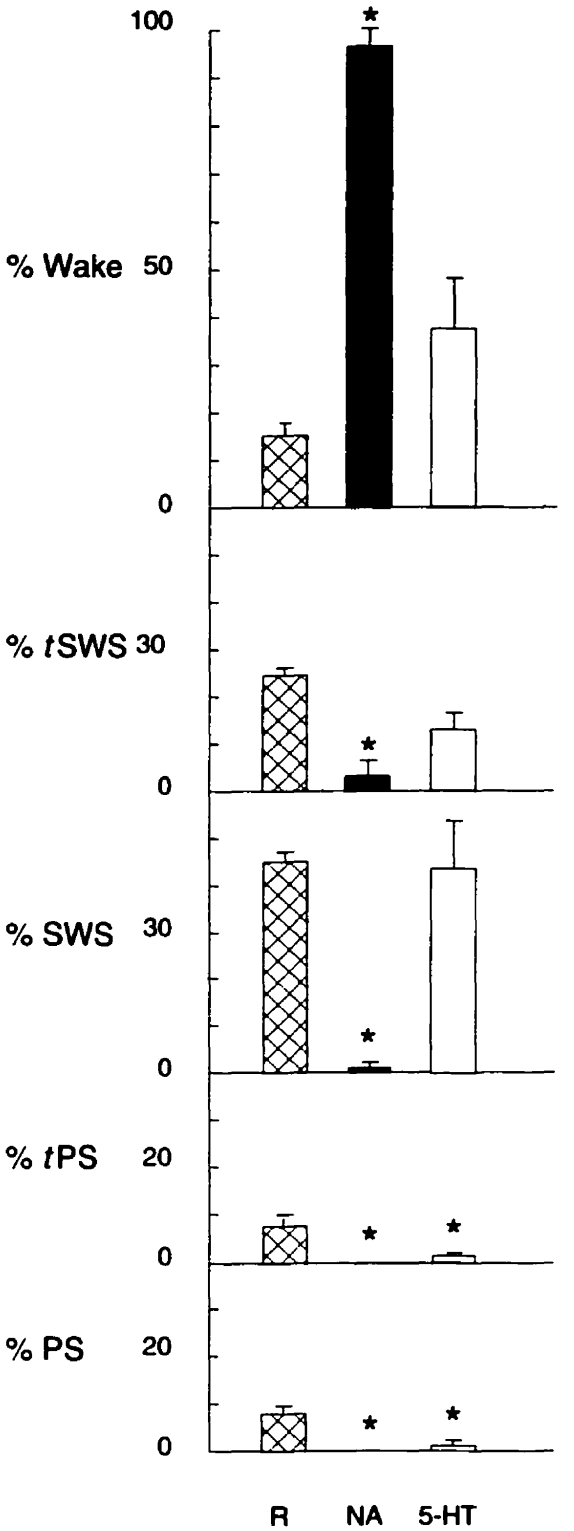

Fig. 7

Figure 8. Average EEG and EMG activities during post-injection recording periods after ringer (R), noradrenaline (NA) and serotonin (5-HT) microinjections. For EEG (from right retrosplenial lead), Ga and De are expressed as absolute activities in each frequency band (reported as amplitude in AD units where 100 units ≈ 79μV); Th/De, as the ratio of absolute activities in each band; and EMG also as absolute activity. Data are presented as mean ± S.E.M, for R, n = 8; for NA, n = 5; for 5-HT, n = 8;. * indicates significantly different from ringer, according to paired comparison *t*-tests ($p \leq 0.05$).

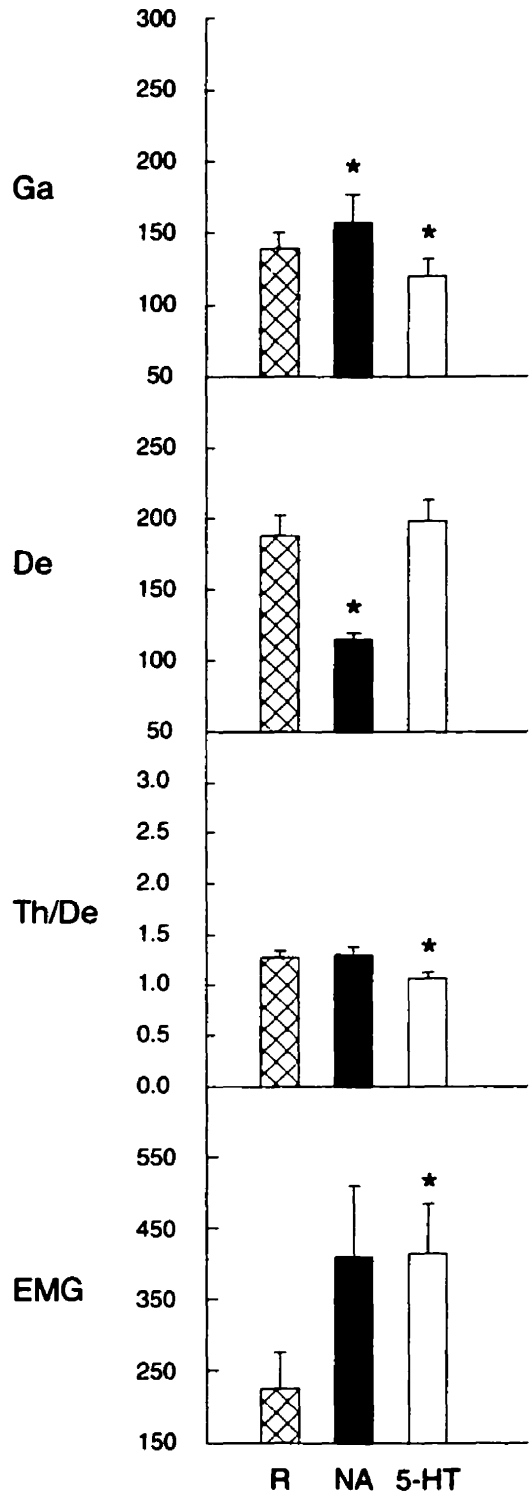
Ga
300
250
200
150
100
50
*
*
De
250
200
150
100
50
*
Th/De
3.0
2.5
2.0
1.5
1.0
0.5
0.0
*
EMG
550
450
350
250
150
*
R
NA
5-HT

Fig. 8

Figure 9. EEG samples from noradrenaline and serotonin post-injection recording periods. Unfiltered (above) and high frequency, gamma (30.5-58.0 Hz) filtered (below) EEG samples (2 sec each) illustrating EEG patterns that occurred during the respective post-injection recording periods. Noradrenaline produced a low voltage, fast EEG pattern (above), in association with relatively high gamma activity (below), similar to normal Wake (rat B10); whereas serotonin produced a high voltage, slow EEG pattern (above), in association with relatively low gamma activity (below), similar to normal SWS (rat B20). The samples were taken ~2-3 min after the injection was stopped. The EEG was recorded by reference to an electrode in the rostral frontal bone from the left and right frontal (LF & RF), retrosplenial (LRS & RRS), parietal (LP & RP) and occipital (LO & RO) cortical regions. Voltage scales are the same for all cortical leads.

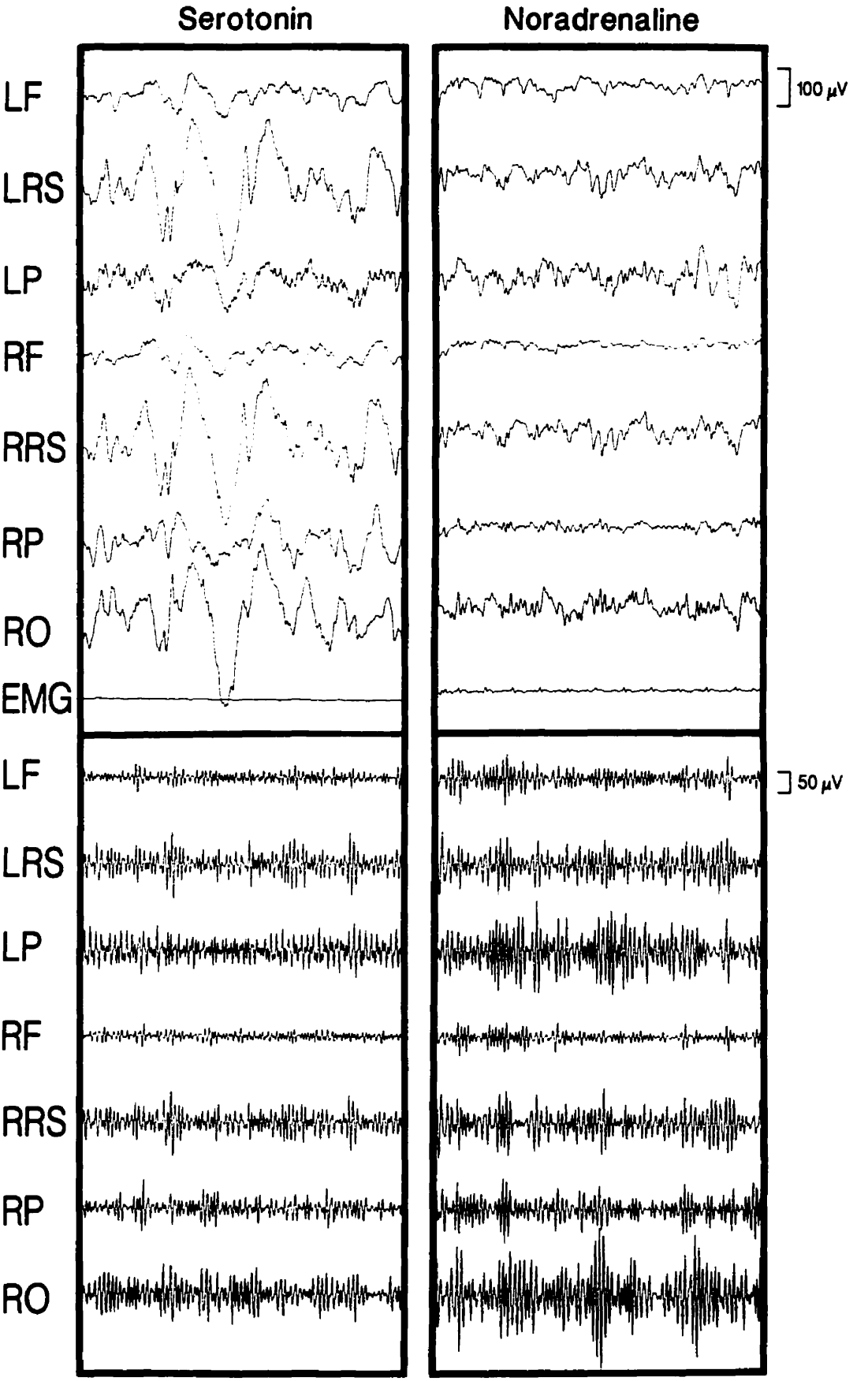
Serotonin
Noradrenaline
LF
LRS
LP
RF
RRS
RP
RO
EMG
100 µV
LF
LRS
LP
RF
RRS
RP
RO
50 µV

Figure 10. Average spectra from epochs following the injection of noradrenaline (rat B10) and serotonin (rat B20). Following noradrenaline, a small low frequency peak is in the theta range and the overall amplitude in the gamma range is relatively high. Following serotonin, a prominent peak is evident in the delta band and a relatively low overall amplitude in the gamma band. The spectra were computed from five, 4 sec EEG segments from the right retrosplenial lead that were each one minute apart and occurred within ~2 - 8 min after the injection. Spectra are displayed in amplitude (AD units, where 100 ≈ 79 μV) per 0.5 Hz shown at different scales for the low frequency range (1.5-18.5 Hz) and the high frequency range (19.0-58.0 Hz) in order to maximise the appearance of potential peaks in each range. Delta, theta and gamma frequency bands, which were used for calculation of total activity per band (Figs. 2-6, 8 and 11), are differentially shaded.

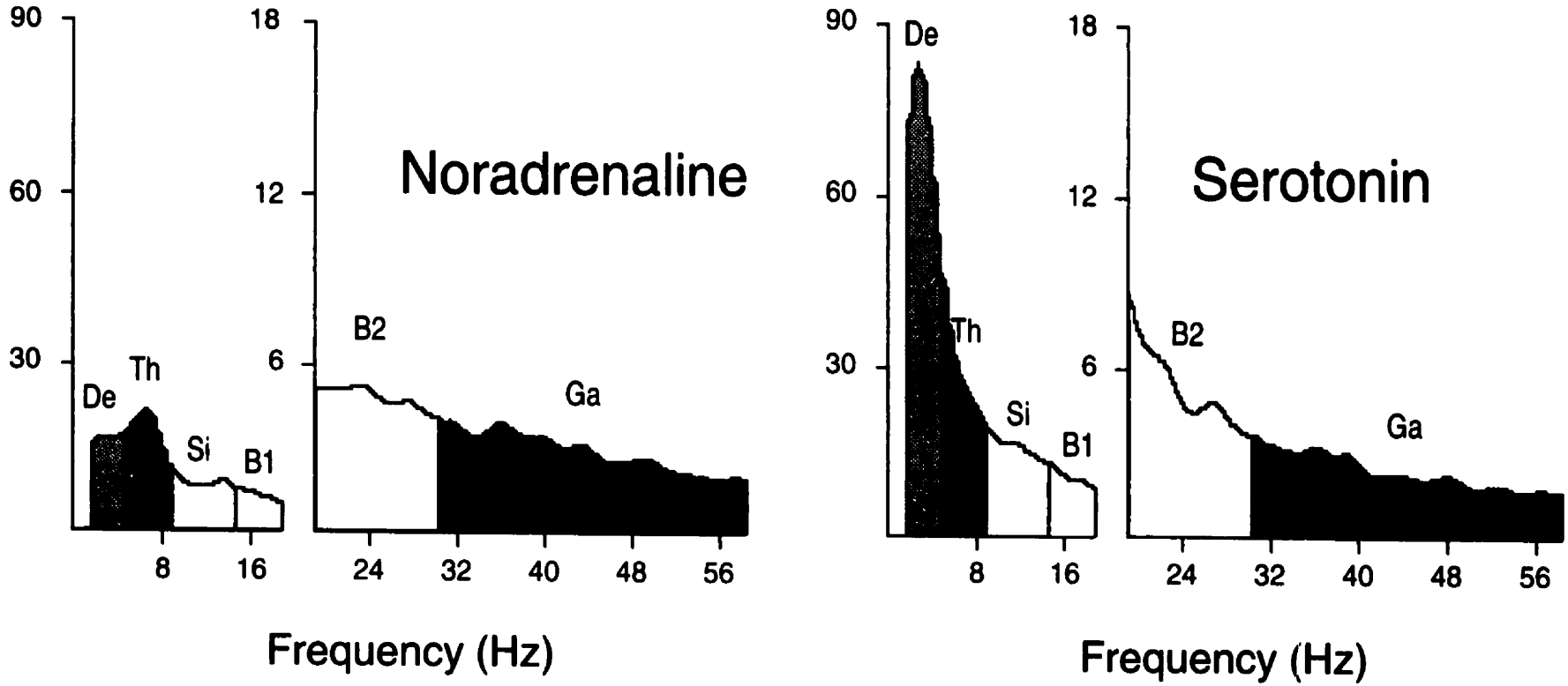
Noradrenaline
90
60
30
18
12
6
De
Th
Si
B1
B2
Ga
8
16
24
32
40
48
56
Frequency (Hz)
Serotonin
90
60
30
18
12
6
De
Th
Si
B1
B2
Ga
8
16
24
32
40
48
56
Frequency (Hz)

Fig. 10

Figure 11. Dose-response relationships showing the effect of increasing doses of noradrenaline and serotonin upon average EEG frequency band activity during the post-injection period (see Fig. 8). Least squares means plots are presented from the output of ANCOVAs (with dose as the main factor and rat as the covariate). EEG activities are taken from the right retrosplenial lead and reported as amplitude, AD units, where 100 units ≈ 79μV, or ratio. Dose indicates total nmol of drug injected on each side, and 0 corresponds to ringer. * indicates a significant main effect of dose for NA (n = 4) or 5-HT (n = 3) (ANCOVA, df = 4, 1; $p \leq 0.05$).

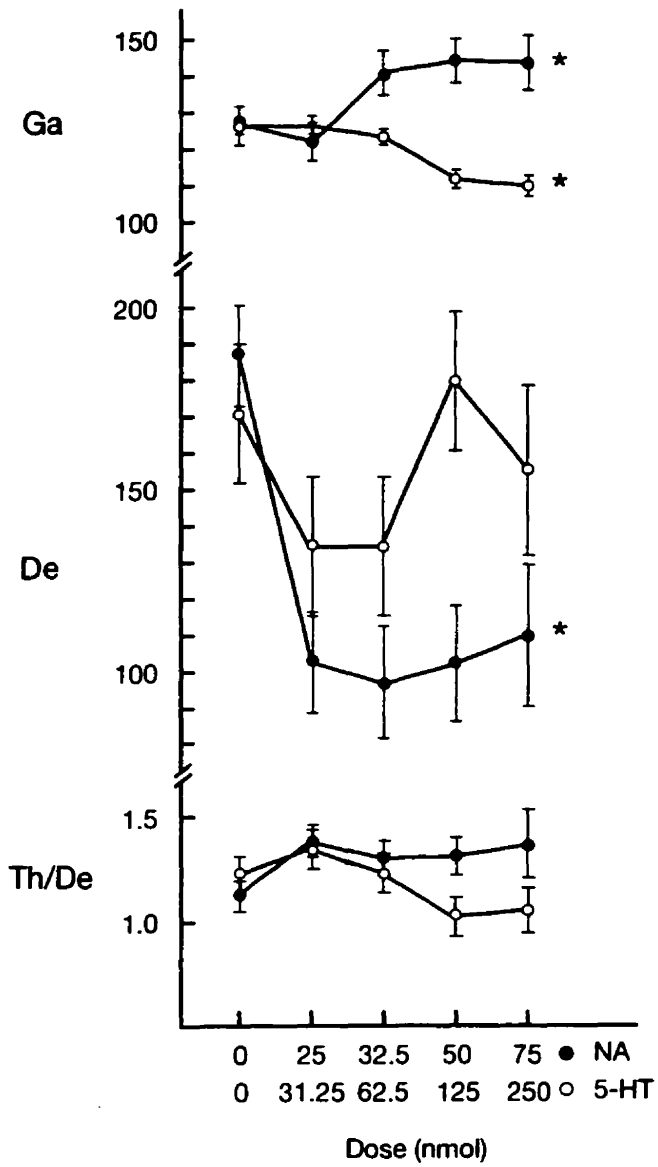
Ga
150
100
*
*
De
200
150
100
*
Th/De
1.5
1.0
0 25 32.5 50 75 ● NA
0 31.25 62.5 125 250 ○ 5-HT
Dose (nmol)

Fig. 11

Table 1. Relative gamma and delta activity, ratio of Th/De activities and EMG amplitude during the Post-Injection Total period or Wake and SWS states following Noradrenaline and Serotonin as compared to Ringer[1].

		Ringer	Noradrenaline	Serotonin
Total				
	Ga	15.51 ± 0.74	22.55 ± 1.59*	14.81 ± 0.57
	De	21.05 ± 1.06	17.44 ± 0.72*	23.94 ± 1.18*
	Th/De	1.28 ± 0.06	1.29 ± 0.03	1.08 ± 0.05*
	EMG	222.78 ± 52.95	357.03 ± 100.25*	335.42 ± 68.79*
Wake				
	Ga	20.09 ± 0.85	23.07 ± 1.51*	17.65 ± 0.60*
	De	16.80 ± 0.89	17.09 ± 0.68	20.93 ± 0.97*
	Th/De	1.44 ± 0.06	1.30 ± 0.03	1.21 ± 0.04*
	EMG	267.22 ± 53.21	360.65 ± 98.62	396.64 ± 68.28*
SWS				
	Ga	13.44 ± 0.59	-	12.42 ± 0.29
	De	24.07 ± 1.22	-	27.39 ± 0.73*
	Th/De	1.00 ± 0.06	-	0.88 ± 0.03
	EMG	209.33 ± 51.4	-	313.15 ± 75.5*

[1]Gamma and delta activities are presented as relative amplitude. Data are presented as mean ± S.E.M, for Ringer, n = 8; for Noradrenaline, n = 5 and for Serotonin, n = 8. * indicates significantly different from Ringer, according to paired comparison *t*-tests ($p \leq 0.05$).

CHAPTER FOUR

EFFECTS OF GLUTAMATE AGONIST VERSUS PROCAINE MICROINJECTIONS INTO THE BASAL FOREBRAIN CHOLINERGIC CELL AREA UPON GAMMA AND THETA EEG ACTIVITY AND SLEEP-WAKE STATE

Edmund G. Cape and Barbara E. Jones

Published, European Journal of Neuroscience Vol. 12, pp. 2166-2184, 2000

PREFACE

In the previous chapter, the monoamines, noradrenaline and serotonin, when injected into the basal forebrain each affected cortical activation in different ways. They are known to affect the cholinergic neurons differentially and as discussed, to have differential modulatory effects on cholinergic versus non-cholinergic neurons. This fact serves as an interesting contrast with the next series of experiments that explore changes in sleep-wake states during activation and inactivation of the entire basal forebrain region.

Glutamate is believed to be the primary neurotransmitter of the brainstem reticular activating system. The next set of experiments were undertaken to examine the effects upon EEG activity and sleep-wake state following activation of basal forebrain neurons with glutamate agonists or conversely their inactivation. Activation of the region was accomplished by microinjections of AMPA and NMDA. Inactivation was produced by microinjections of procaine into the basal forebrain. These experiments were also designed to study EEG effects of the contrasting modulation of AMPA and NMDA on cholinergic basalis neurons. NMDA has been documented *in vitro* to induce rhythmic bursting activity in the cholinergic neurons which was not true for AMPA.

ABSTRACT

Serving as the ventral, extrathalamic relay from the brainstem reticular activating system to the cerebral cortex, basal forebrain neurons, including importantly the cholinergic cells therein, are believed to play a significant role in eliciting and maintaining cortical activation during the states of waking and paradoxical sleep. The present study was undertaken in rats to examine the effects upon EEG activity and sleep-wake state of inactivating basal forebrain neurons with microinjections of procaine versus activating them with microinjections of agonists of glutamate, which is the primary neurotransmitter of the brainstem reticular activating system. Microinjections into the basal forebrain were performed using a remotely controlled device in freely moving, naturally sleeping/waking rats during the day when they are asleep the majority of the time. Procaine produced a decrease in gamma (30 - 60 Hz) and theta (4 - 8 Hz) EEG activities and an increase in delta (1 - 4 Hz) associated with a loss of paradoxical sleep, despite the persistence of slow wave sleep. AMPA and NMDA produced an increase in gamma and a decrease in delta, while eliciting waking. In addition, NMDA, which has been shown *in vitro* to induce rhythmic bursting in the cholinergic cells, significantly increased theta activity. Following the microinjections of NMDA, c-Fos protein, which has been shown to reflect neural activity, was found in numerous cholinergic, and also GABAergic and other non-cholinergic neurons, in the

substantia innominata and magnocellular preoptic nucleus near the microinjection cannulae. These results substantiate the role of cholinergic, possibly together with other, basal forebrain neurons in cortical activation, including elicitation of gamma and theta activities that underlie cortical arousal during waking and paradoxical sleep.

INTRODUCTION

As suggested in early studies to serve as the ventral extra-thalamic relay to the cerebral cortex from the brainstem reticular activating system (Moruzzi and Magoun, 1949; Starzl *et al.*, 1951; Shute and Lewis, 1967), the basal forebrain has long been implicated as playing an important role in cortical activation. This role has moreover been proposed to be fulfilled by the cholinergic neurons therein (Shute and Lewis, 1967), which provide the major cholinergic innervation to the cerebral cortex (Lehmann *et al.*, 1980). Lesions of the basal forebrain have resulted in a loss of cortical activation and parallel decrease in cortical ACh release (Lo Conte *et al.*, 1982; Stewart *et al.*, 1984; Buzsaki *et al.*, 1988). Stimulation of the basal forebrain, like that of the reticular formation, evoked cortical activation in association with enhanced cortical ACh release (Celesia and Jasper, 1966; Casamenti *et al.*, 1986). Moreover, the cortical activation and ACh release evoked by stimulation of the reticular formation could be attenuated by chemical inactivation of the basal forebrain (Rasmusson *et al.*, 1994). Finally, cortical ACh release has been shown to be higher during waking and paradoxical sleep (PS, also called rapid eye movement, REM), when cortical activation naturally occurs, than during slow wave sleep (SWS) (Jasper and Tessier, 1971; Marrosu *et al.*, 1995). The present research was aimed at further studying the way in which basal forebrain, including cholinergic, neurons modulate cortical activity and sleep-wake state by examining the effects of their inactivation with procaine microinjections and their activation with microinjections of agonists for glutamate, which is the primary neurotransmitter of the brainstem reticular activating system (Rasmusson *et al.*, 1994; Jones, 1995).

Recent *in vitro* studies characterizing the properties and modulation of immunohistochemically identified cholinergic, and also non-cholinergic, neurons

have revealed that basal forebrain cell populations are endowed with intrinsic properties that allow them to discharge rhythmically at low frequencies in addition to tonically at higher frequencies (Khateb *et al.*, 1992; Alonso *et al.*, 1996). Glutamate agonists, including those for AMPA and NMDA receptors, depolarize and excite cholinergic cells and tend to drive them into tonic discharge (Khateb *et al.*, 1995). NMDA, however, also induces rhythmic low threshold bursting in the cholinergic neurons, the significance of which remains to be established *in vivo* (Khateb *et al.*, 1995). In the present study, therefore, the agonists AMPA and NMDA were each administered by microinjections into the region of the cholinergic cells and the effects examined upon EEG activity and sleep-wake state.

Microinjections were placed in the region of the basal forebrain cholinergic cell area, which lies in the ventral path of the ascending fibers from the brainstem reticular formation, and were performed using remotely controlled injection cannulae in freely moving, naturally sleeping/waking animals (Fig. 1) (Cape and Jones, 1998). The effects of procaine versus AMPA and NMDA were examined upon cortical activity by spectral analysis of EEG activities, including importantly high frequency gamma activity (30 - 60 Hz) and theta activity (4 - 8 Hz), which are indicative of behavioral and cortical arousal in the rat (Maloney *et al.*, 1997). By examination of c-Fos protein, which was previously shown to be expressed in

cholinergic and non-cholinergic neurons following local injections of AMPA and NMDA into the basal forebrain (Page *et al.*, 1993), activation was assessed here of cholinergic and non-cholinergic, including GABAergic, basal forebrain neurons following the microinjections of NMDA. Preliminary results of this study have been reported (Cape and Jones, 1994).

METHODS

Animals and surgery

Twenty-one male Wistar rats (Charles River Canada, Montreal) weighing between 200-250g at the time of surgery, were used in this study. Nine animals were used for pilot studies and twelve for the experimental studies. Implantation of chronically indwelling EEG electrodes and cannulae was accomplished with a procedure previously reported and briefly described here (Cape and Jones, 1994). Animals were operated under barbiturate anesthesia (Somnotol, 67 mg/kg, i.p.). Small screws were threaded into the skull for epidural recording of EEG over the left and right frontal (2.75 mm Anterior, A, and 0.6 mm Lateral, L, to bregma), retrosplenial (3.5 mm posterior, P, and 0.6 mm L), parietal (0.5 mm P and 5.0 mm L) and occipital (7.5 mm P and 5.0 mm L) cortices. EEG recording was performed against a reference electrode cemented into the frontal bone anterior to the frontal cortex (5.5 mm A and 0.8 mm L). EMG was recorded with bipolar leads using 2 stainless steel wires inserted into the neck musculature. For the microinjections, stainless-steel guide cannulae were placed during surgery with a stereotaxic apparatus in the brain such that the inner cannulae would reach a position directly over the cholinergic cells (anterior 7.6 mm, lateral 2.5 mm, and vertical 1.5 mm relative to ear bar zero). After a minimum of two days recovery, the rats were individually housed in a plexiglas box inside a large electrically shielded recording chamber and maintained on a 12:12 light-dark cycle.

EEG recording and behavioral observations

Signals were recorded using a Grass polygraph and sent to an IBM compatible computer running Stellate Systems software (Montreal, Quebec) for

digitization, storage and subsequent analysis (Maloney *et al.*, 1997; Cape and Jones, 1998). The rats were also monitored behaviorally through a video camera. Nine categories of behavior were scored and annotated on the on-line EEG recording: attentive, moving, eating, grooming, and quiet waking behaviors plus uncurled, curled, moving (postural shifts), and twitch sleeping behaviors (Maloney *et al.*, 1997). Recording was performed beginning in the late morning and usually ending by 1500h. The EEG computer file consisted of a morning recording period (–1100-1130) taken prior to handling and injections (pre-injection) and an afternoon recording period (–1230-1500) taken following placement of the inner injection cannulae and the injection (post-injection). Prior to the microinjection experiments, baseline recordings were performed and similarly included a morning recording period taken prior to handling and an afternoon recording period taken following handling but did not involve placement of inner injection cannulae.

Injection procedure

The ringer and chemical microinjections proceeded in several stages (see Fig. 1), as previously described (Cape and Jones, 1998). Following the 30 min morning recording, the filled inner cannulae were inserted manually into the guide cannulae, while holding the rat. After recovery from the handling procedure (–30-60 min), evidenced by the resumption of sleep, recording was reinitiated for the afternoon. Once a full sleep cycle occurred, marked by the presence of SWS and PS or *t*PS, the inner cannulae were lowered by remote control into the basal forebrain. Approximately 2 min later, the injection was begun and performed over 5 min. The post-injection period was defined as the 30 min period immediately following the complete delivery of the injection.

Chemical microinjections

Bilateral microinjections were delivered using two 1 µl Hamilton syringes (Reno, Nevada) that were driven in parallel by a syringe pump (Sage Instruments, Cambridge, MA). The solutions were injected in a volume of 0.5 µl over 5 min. Doses of each drug were derived from published studies and tested in pilot studies. AMPA (alpha-amino-3-hydroxy-5-methyl-4-isoxazole propionic acid) was injected at a total dose of 0.75 nmol (20 ng in 0.5 Φl = 1.5 mM solution) and NMDA (N-methyl-D-aspartate) at a dose of 5 nmol (735 ng in 0.5 Φl = 10 mM solution), according to doses previously established to have excitatory effects without neurotoxic effects in the basal forebrain (Page *et al.*, 1993). These glutamate agonists were nonetheless associated with a certain incidence of seizure activity (detailed below). Procaine (p-aminobensoic acid diethylaminoethyl ester) was injected at a dose of 0.367 nmol (100 ng in 0.5 Φl = 20% solution), according to a dose previously shown to be effective in the septum (Lawson and Bland, 1993). All animals in the study received microinjections of ringer (n = 12). Of these, half also received AMPA and the other half NMDA. Among each of these subgroups, half also received procaine.

Data analysis

Based upon all EEG and the EMG leads, the polygraphic record was scored off-line by visual assessment of 20 sec epochs and labeled as either Wake (W), transition into Slow Wave Sleep (*t*SWS), Slow Wave Sleep (SWS), transition into Paradoxical Sleep (*t*PS) or Paradoxical Sleep (PS) (Maloney *et al.*, 1997). Behavioral annotations were considered together with the EEG and EMG activities for state scoring, particularly during the post-injection condition. Consequently, the annotations were used in order to identify any dissociations between behavior and

the normal associated EEG patterns of the different states. Each state was reported for the post-injection recording period as % of total recording time.

Spectra were computed using Stellate Systems software by Fast Fourier Transform (FFT) based on 512 points corresponding to 2 sec epochs with a resolution of 0.5 Hz. A 7-point smoothing window is applied by this program thus allowing a minimum of 1.5 Hz and a maximum 63.5 Hz in the spectral computation. Frequency bands were defined as delta (δ): 1.5 - 4.0 Hz, theta (θ): 4.5 - 8.5 Hz, sigma (σ): 9.0 - 14.0 Hz, beta1 ($\beta 1$): 14.5-18.5 Hz, beta2 ($\beta 2$): 19:0 - 30.0 Hz and gamma (γ): 30.5 - 58.0 Hz (eliminating frequencies of >58 Hz to avoid any possible contamination from AC noise) (Maloney *et al.*, 1997). EMG amplitude was computed for the total spectrum up to 58.0 Hz.

EEG frequency band activities were computed for the 20 sec epochs which had been scored for sleep-wake state over the full recording sessions (using Eclipse software, Stellate Systems). Frequency band activities were displayed and reported in AD (analog-to-digital converted) amplitude units for which the average gain was calibrated as 79 AD units per 100 μV (or $\cong$ 125 AD units per 100 μV) on the EEG channels. Relative amplitudes of each band were also reported and correspond to the % of total activity (1.5 - 58.0 Hz). For the measure of theta activity, the ratio of theta/delta was calculated and reported. This ratio was previously shown to best reflect amplitude in the theta band associated with a peak in the theta band as opposed to amplitude in that band associated with a peak in the delta band, which is found with high amplitude delta activity during slow wave sleep (Maloney *et al.*, 1997). In order to assess maximal gamma and theta activities, the retrosplenial cortical lead (on the right side) was used for computation of frequency band activities across the entire data set. It was previously shown that

the changes in gamma and delta on this lead parallel those on the other cortical leads with behavioral and state changes (Maloney *et al.*, 1997). With regard to theta, it was also found that a shift in peak frequency from a delta to a theta range occurred in the low frequencies in the transition from SWS to PS or active waking on all cortical leads and was reflected by significant increases in the theta/delta ratio (Maloney *et al.*, 1997). Based upon scored records, sleep-wake hypnograms were displayed in association with EEG frequency band activity from the retrosplenial cortex for all experiments.

In selected rats of each group, spectral analysis was also performed and examined for all leads (using Rhythm software, Stellate Systems) on 9, 4 sec epoch samples taken at one minute intervals in the period 5-13 minutes following ringer, procaine, AMPA and NMDA microinjections, when the effects were maximal and most uniform for the drugs. These samples were used for assessment of frequency peaks in the low and high frequency ranges in association with frequency band amplitude from the four cortical leads (below).

EEG records and hypnograms displaying sleep-wake state and frequency band activity were examined following recording to establish that the EEG appeared normal and that the microinjection appeared effective. Of 12 rats, 3 showed abnormal spontaneous seizure activity, which has been described previously in a similar proportion within this strain of rat (Vergnes *et al.*, 1982); all data from these animals were eliminated. Seizure-like activity was also elicited by the glutamate agonists, producing abnormal EEG for a significant proportion of the post-injection recording period in some rats such that the experiments from these rats had to be eliminated, representing those from 1 rat (out of 6) with AMPA and 1 rat (out of 6) with NMDA. In other cases (1/5 for AMPA and 3/5 for NMDA), the seizure activity

was intermittent and did not represent more than 10% of the post-injection recording period, in which case the seizure epochs were scored as artifact and eliminated from the quantitative analysis of post-injection data.

Baseline EEG data from the retrosplenial cortical lead were examined by analysis of covariance (ANCOVA with state as the independent variable and rat as covariate) to document that gamma, delta, and theta/delta activities, as well as EMG activity, varied significantly as a function of state in this data set, as had been previously established for all cortical leads (Maloney *et al.*, 1997). Ringer and baseline conditions (9 rats) were subsequently compared (for the same lead) using the paired Student t-test to determine if the ringer microinjections were associated with any significant changes in EEG or sleep-wake states. The 30 min post-drug conditions were then compared to the post-ringer condition in the same animals using paired t-test comparisons with 5 rats per drug condition in the final experimental series. Comparisons were made for average % sleep-wake state, relative gamma and delta activity, theta/delta ratio and EMG. Prior to performing the statistics, it was established that these relative measures of EEG amplitude were normally distributed across the data set, since the % of total amplitude and the ratio of theta/delta measures eliminate the variations in absolute EEG amplitude that occur across animals. A chi square statistic was also employed to determine if the incidence of PS was significantly different from ringer for each group during this period.

The 4 sec epoch spectral samples (from 5-13 minutes post-injection) were employed for quantitative study of spectral peaks and associated band amplitudes across four cortical leads on the right side and across drug conditions and thus different groups and animals. The frequency of the highest amplitude peak in the

high, gamma range (30-60 Hz) and that in the low, delta to theta range (1-10 Hz, excluding frequencies >10Hz) were recorded for each cortical area (4) for each condition (4) of each rat, having selected three rats from each drug condition (yielding a total of 9). The integrated amplitude of the delta, theta and gamma bands was also recorded, as well as the EMG for each epoch. In order to compare these measures across animals and conditions, the data were first normalized by taking the natural log (Ln) values of each measure. An analysis of covariance (ANCOVA) was subsequently performed for each measure, with the EEG measurement as the dependent variable, the drug condition (4) and area (4) as the independent variables and the spectral samples (9) and rat (9) as covariates. With significant main effects, post-hoc paired comparisons were performed using Fisher's least significant difference between drug conditions. With a significant interaction between drug and area, an ANCOVA was performed for each area and with a significant main effect of drug, post-hoc paired comparisons were performed between drug conditions. To further examine significant interactions between drug and area (for gamma activity), an ANCOVA was performed on relative amplitude data, in which the absolute amplitude differences between areas and animals are normalized. Mean and s.e.m. were calculated and reported from the raw values in Hz for frequency and AD units for amplitude or ratio of theta/delta. All statistics were performed using Systat software (Evanston, Illinois).

Immunohistochemical assessment of microinjections

At the end of all experiments, animals were anesthetized with a high dose of sodium pentobarbital (Somnotol, 120 mg/kg, i.p.) and perfused through the heart with a fixative solution (3.0% paraformaldehyde) for preservation of the brains, which were frozen and stored after being immersed in 30% sucrose overnight. All

brains were processed for ChAT immunohistochemistry in order to assess the placement of the cannulae in relation to the cholinergic neurons. To examine the presence of c-Fos in neurons after microinjections of NMDA, brains (n = 3) were also processed for dual-immunostaining of c-Fos with ChAT or GAD. For this purpose, the animals were anesthetized and perfused immediately following the 30 min post-injection recording period.

Coronal sections were cut at 25 Φm thickness on a freezing microtome. Series of adjacent sections were collected every 200 Φm for immunohistochemical processing. Immunohistochemistry was performed using the peroxidase-antiperoxidase (PAP) technique, according to previously published procedures (Gritti *et al.*, 1993; Maloney *et al.*, 1999). For immunostaining of neurotransmitter enzymes, rabbit anti-ChAT antiserum (1:3000, Chemicon International, Temecula, CA), and rabbit anti-GAD antiserum (1:3000, Chemicon International) were used. For the immunostaining of c-Fos protein, an anti-c-Fos antiserum from sheep (Cambridge Research Biochemicals, Cheshire, U.K.) was used at a dilution of 1:3000. Incubations with the primary antibodies were carried out overnight at room temperature using a Tris saline solution (0.1M) containing 1% normal donkey serum (NDS), following a pre-incubation with Tris saline containing 6% NDS. For the ChAT antibody, Triton (0.1%) was added to the incubation solution. Sections were placed in donkey anti-rabbit secondary antisera following either ChAT or GAD primary antisera, and into donkey anti-sheep secondary antisera following c-Fos antisera, then in the respective rabbit and sheep PAP antibodies (Jackson ImmunoResearch Laboratories, West Grove, PA). c-Fos was immunostained in combination with either ChAT or GAD using a sequential procedure staining c-Fos in the second position. The enzymes were immunostained and revealed in the first position with

3,3' diaminobenzidine (DAB), producing a brown floccular reaction product, and c-Fos was immunostained and revealed in the second position with benzidine dihydrochloride (BDHC), producing a blue granular reaction product. Controls in the absence of primary antibodies and in the presence of normal sera were routinely run with every immunostaining procedure to ensure the absence of nonspecific single or double immunostaining in the material.

Analysis of immunohistochemical data

Sections were viewed with a Leitz Orthoplan microscope equipped with a two dimensional movement-sensitive stage and CCD camera attached to a computer. Single-immunostained (ChAT-positive, + or c-Fos+) and dual-immunostained (ChAT+/c-Fos+ and GAD+/c-Fos+) cells were mapped using a computer-based image analysis system (Biocom, Paris) with a resident atlas of sections through the basal forebrain (Gritti *et al.*, 1993). Location of injection cannulae in the region of cholinergic cells was confirmed in all rats included in the study.

RESULTS

It was confirmed in all animals that the microinjection cannulae were placed in the basal forebrain within the region of the cholinergic cells (Fig. 1, see below for further details). It was also established in these animals that the natural pattern of sleep-wake states and associated EEG activity documented during baseline recordings (Figs. 2 and 3) was not significantly altered by microinjections of ringer (Fig. 4). It was subsequently determined by comparison to ringer, that procaine (Fig. 5), on the one hand, and AMPA or NMDA (Figs. 6 and 7) on the other, significantly and differentially altered both EEG and state of the animals (Figs. 8 - 12, Table 1), as detailed below.

Baseline

During the 30 min period corresponding approximately to the post-injection experimental period, rats passed through at least one complete sleep cycle, marked by the presence of SWS and PS in baseline conditions (Fig. 2). They were asleep the majority of the time (>70%), spending ~60% of the time in *t*SWS and SWS and ~15% in *t*PS and PS (Fig. 3). As measured from the retrosplenial cortical lead, relative gamma activity varied significantly as a function of state ($F = 20.92$, $df = 4$, $p < .001$) and was higher during Wake and *t*PS & PS than during *t*SWS & SWS (according to Fisher's post-hoc paired comparisons, $p < .05$, Fig. 3). Delta varied significantly in a reciprocal manner to gamma across these states ($F = 66.47$, $df = 4$, $p < .001$). Theta/delta, reflecting theta activity, also varied significantly as a function of state ($F = 44.11$, $df = 4$, $p < .001$) and, like gamma, was highest in Wake and PS (Fig. 2), though higher on average in PS than in Wake (according to Fisher's post-hoc paired comparisons, $p < .05$, Fig. 3). As previously established (Maloney *et al.*, 1997), these changes in relative EEG activities measured from the

retrosplenial cortical lead reflected changes in absolute EEG activities and were paralleled by changes in EEG activities measured from other cortical leads.

Ringer

The normal sleep-wake cycle and associated modulation of the EEG and EMG did not appear to be affected by microinjections of ringer (Fig. 4). During the 30 min post-injection period, most rats passed through a sleep cycle (Fig. 4) that included SWS and PS (8/9 rats) or *t*PS (9/9 rats). The incidence of PS was not significantly different in the ringer condition (n = 9) as compared to that in baseline (n = 9, according to a chi square statistic). The animals engaged in a full variety of behaviors including normal sleep and wake postures and behaviors, including moving, attentive, eating and grooming waking behaviors, as previously documented in baseline conditions (Maloney *et al.*, 1997). As in baseline, the rats were asleep on average the majority of the time (>80%), spending more than 65% of the time in *t*SWS & SWS and ~15% in *t*PS & PS (Fig. 8). For the total set of rats (n = 9), there was no statistically significant difference in percent state or relative amplitude of EEG activities from retrosplenial cortex between baseline and ringer conditions.

Procaine

Microinjection of procaine resulted in a reduction of gamma activity and enhancement of delta activity, that was evident from the moment the procaine came into contact with the brain tissue (Fig. 5). The theta/delta ratio remained low for a prolonged period post-injection. In most cases, these EEG changes measured on the retrosplenial cortex but also evident on other cortical leads were associated with a behavioral state of SWS with the animal reclined and

outstretched or curled up on the floor of the cage with its eyes closed. In other cases, EEG slow wave activity was associated with quiet waking behavior with the animal standing or lying quietly with eyes open. According to the corresponding behavioral annotations of quiet wake, these epochs were scored as wake. Despite the occurrence of SWS, PS was completely absent in 4 animals and occurred only toward the end of the post-injection period in 1 animal (Fig. 5). The incidence of PS after procaine ($n = 5$) was significantly different from that in the ringer group ($n = 9$, chi square = 6.644, $df = 1$, $p < .05$).

In the quantitative analysis of the state changes, it was apparent that the natural sleep cycle was affected by procaine during the 30 min post-injection period (Fig. 8). There was a decrease in PS (though not quite significant, $t = 2.44$, $df = 4$, $p = 0.07$) and *t*PS ($t = 3.40$, $df = 4$, $p < .05$, according to paired t test comparisons). There was no significant change in SWS (Fig. 8), but there was a significant decrease in *t*SWS ($t = 9.07$, $df = 4$, $p < .05$). The latter decrease was mirrored by an apparent, though insignificant, increase in wake, due to those episodes in which the EEG was characterized by slow wave activity and the behavior was scored as quiet wake. These changes in sleep-wake states were associated with average significant decreases in relative gamma and increases in relative delta activities on the retrosplenial cortex (Fig. 9). There was also a significant reduction in theta/delta ratio. The average EMG amplitude was not significantly changed. In the wake epochs that occurred following procaine, the average relative gamma measured on the retrosplenial cortex ($15.31 \pm 1.08\%$) was significantly lower than that in the wake epochs following ringer ($19.71 \pm 0.65\%$, $t = 2.82$, $df = 4$, $p < .05$, according to a paired t test).

Representative samples of the EEG taken shortly after the procaine injection show continuous high amplitude, irregular slow wave activity in the unfiltered EEG traces on all cortical leads (Fig. 10). This activity is evident in the spectra by high amplitude activity in the low frequency range peaking in the delta band (Fig. 10). Relatively low amplitude gamma activity is evident in the high frequency filtered EEG. Some small peaks are present in the gamma range of the spectra across cortical leads (Fig. 10). These EEG and corresponding spectral characteristics are similar to those documented across cortical leads for SWS (Maloney *et al.*, 1997).

In the quantitative analysis of spectra from samples (taken at one minute intervals) from 5 – 13 minutes post-injection, when the EEG was relatively stable, there were significant differences in both the high and low peak frequencies and in the absolute amplitude of gamma and delta bands as well as theta/delta ratio across cortical areas relative to the ringer condition (Table 1). There was a very small decrease in the average frequency of the highest amplitude gamma peak that was statistically significant (Table 1). There was also a small decrease in average absolute amplitude of gamma relative to ringer (Table 1). Across cortical areas, the biggest changes were evident in the low frequency range of the spectra and were characterized by a significant decrease in peak frequency to an average frequency that was slower than that during the ringer condition (during which multiple states occur, as described above). This shift to a lower peak frequency was also reflected in large increases in average absolute delta amplitude and decreases in the theta/delta ratio.

AMPA and NMDA

Microinjections of the glutamate agonists resulted in the immediate elicitation of a waking state, marked by a distinct diminishment of delta activity and characterized by moderately high levels of gamma and theta/delta ratio measured on the retrosplenial cortex (Figs. 6 and 7) and also evident in the EEG traces from all cortical leads. Animals were behaviorally awake, posturally erect and often moving. They also remained immobile for certain periods with back rounded, body tense and ears erect, appearing highly aroused and in a posture similar to that of an attentive animal, yet particularly with NMDA, different from any position and behavior seen in baseline. In 1/5 animals receiving AMPA and in 3/5 animals receiving NMDA, seizure activity was evident intermittently on the EEG during the post-injection period. During seizure activity, the animals remained immobile except for chewing movements which could be observed. EEG epochs with seizure activity (as indicated in Fig. 7) were removed from the spectral analysis data files. The sleep cycle was virtually eliminated by both AMPA (4/5) and NMDA (5/5 rats), although in one rat with AMPA, *t*PS and PS occurred despite an absence of SWS. The incidence of occurrence of PS in the AMPA group, as well as in the NMDA group, was significantly different from that in the ringer group (according to chi square = 6.644, df = 1, $p < .05$ for AMPA and chi square = 10.370, df = 1, $p < .05$ for NMDA).

Across animals, both AMPA and NMDA injections produced significant increases in waking and decreases in SWS and PS during the 30 min post-injection period (Fig. 8). These state changes were associated with a significant increase in relative gamma EEG activity and decrease in relative delta activity measured on retrosplenial cortex (Fig. 9). In addition with NMDA, the theta/delta ratio, was

significantly increased (Fig. 9). Both agonists produced a significant increase in EMG activity. The average theta/delta ratio on the retrosplenial cortex during wake following NMDA (1.80 ± 0.11) was significantly higher than that during wake following ringer (1.54 ± .05; $t = 2.81$, $df = 4$, $p < .05$).

The EEG samples taken shortly after the microinjection of AMPA and NMDA are characterized by the absence of high amplitude delta activity and the presence of faster activity in the unfiltered traces from all cortical leads (Figs. 11 and 12). With NMDA, theta activity is also prominent on the retrosplenial cortex. In the spectral analysis, a peak appears in the low frequency range within the theta band, where it is also particularly prominent with NMDA in the retrosplenial cortex (Fig. 12). In the high frequency filtered EEG traces, gamma activity appears relatively high on all cortical leads following both AMPA and NMDA. In the corresponding spectra, multiple peaks are present in the gamma band, and the overall amplitude in the gamma band appears relatively high across cortical leads (Figs. 11 and 12). Across leads and samples from different animals, no single peak emerged as prominent in the gamma frequency band following AMPA or NMDA. The EEG and their spectra for both AMPA and NMDA are similar to those of the wake state and for NMDA, most particularly to those of active waking behaviors when theta is prominent during that state (Maloney *et al.*, 1997).

In the quantitative analysis of spectra from samples (taken at one minute intervals) from 5 – 13 minutes post-injection, when the EEG was relatively stable following AMPA and NMDA, there were significant differences in both the high and low peak frequencies and in the absolute amplitude of gamma and delta bands as well as theta/delta ratio across cortical areas relative to the ringer condition and more notably relative to the procaine condition (Table 1). Relative to procaine,

there was a significant, though very small, increase in the average high peak frequency (in the gamma range) following NMDA. Although median peak frequency values similarly only reflected a very slight increase in the high peak frequency, there were a greater number of epochs with peaks in the 37 - 43 Hz range and above (44 – the maximum, 51 Hz) than with peaks in the 30-36 Hz range with NMDA as compared to procaine(according to chi square, 17.546, df = 3, n = 216, $p < .001$). There was a significant increase in absolute gamma amplitude compared to ringer following both AMPA and NMDA on average across cortical areas, but which was most robust compared to procaine both on average and in each cortical area (Table 1). There was also a significant interaction of the drug effect with area in gamma amplitude that appeared to be associated particularly with different responses in the frontal cortex to AMPA as compared to NMDA. These differences, however, could be due to the differences in absolute amplitude that occurred between areas and animals. The regional difference in EEG amplitude was a function of the distance from the reference electrode located in the frontal bone, such that the frontal lead, which had the smallest distance, had the lowest amplitude and a significantly lower amplitude than all other leads (see Figs. 10 - 12, Table 1). The interaction was thus further examined by analysis of relative gamma amplitude measures (being percent of total, as in Fig. 9), in which the differences in amplitude between areas and animals were normalized. Despite confirmation of the main effect of drug, the interaction of drug with area and thus the regional differences in response were not present for relative gamma activity ($F = 37.78$, df = 3, $p = 0.000$ for drug; $F = .971$, df = 3 for area; $F = 0.525$, df = 9 for drug*area with $df_{error} = 558$). In the low frequency range of the spectra, the differences following AMPA and NMDA relative to ringer and procaine were large

and also present across cortical areas (Table 1). There was a shift in peak frequency into the theta range following both AMPA and NMDA that was evident on all leads, despite a significant difference across leads in the peak frequency . The median frequency across different cortical areas was 4 to 6.5 Hz following these drugs compared to 2.5 Hz following procaine. The theta/delta ratio was significantly higher following both AMPA and NMDA than ringer and procaine, but also significantly higher following NMDA than AMPA.

Injection site and c-Fos expression in basal forebrain neurons

In all brains, it was confirmed in ChAT-immunostained sections that the tracks of the injection cannulae were located in the vicinity of the cholinergic neurons (Fig. 13). They passed through the caudate-putamen and globus pallidus to extend into the dorsal substantia innominata. Surrounding the tracks, a certain amount of gliosis was evident. ChAT-immunoreactive neurons were distributed below and around the ventral-most part of the track and area of gliosis. In NMDA injected animals, c-Fos expression was evident in a large number of neurons in the area surrounding and beneath the tracks (Figs. 13 and 14). Among these, numerous ChAT-immunoreactive (ChAT+) neurons were immunostained for c-Fos (ChAT+/c-Fos+) in the substantia innominata and magnocellular preoptic nucleus (Figs. 13 and 14) and some in the postero-lateral horizontal limb of the nucleus of the diagonal band. In addition, numerous GAD-immunoreactive neurons were also immunostained for c-Fos (GAD+/c-Fos+) in the same region (Figs. 13 and 14).

DISCUSSION

The present study showed that activation of basal forebrain neurons in the cholinergic cell area with glutamate agonists elicits long-lasting cortical activation, whereas their inactivation with procaine diminishes cortical activation. AMPA and NMDA, increased high frequency gamma activity, and NMDA also enhanced theta activity in association with a waking state, whereas procaine decreased both gamma and theta, while also decreasing PS despite the occurrence of SWS. Together with the c-Fos immunohistochemistry suggesting activation of cholinergic and non-cholinergic, including GABAergic, neurons following NMDA, these data substantiate the important role of the basal forebrain cholinergic and other neurons in eliciting cortical activation, marked by gamma and theta activity, and generating the associated states of wake and PS.

Activation of the basal forebrain with glutamate agonists

Microinjections of AMPA and NMDA produced marked increases in cortical activation accompanied by an increase in the state of wake. Both agonists produced a significant increase in high frequency gamma activity (30 - 60 Hz) that has been shown to reflect behavioral and cortical arousal in the rat (Maloney *et al.*, 1997). These effects could well be due to excitation of cholinergic basal forebrain neurons, which have been shown to be driven to discharge by both AMPA and NMDA *in vitro* (Khateb *et al.*, 1995). Like electrical stimulation, glutamate infusion into the basal forebrain was previously shown to elicit, albeit very transiently, high frequency cortical activity (20 - 40 Hz) in anesthetized rats, that was presumed to depend upon ACh release in the cortex since the effects of electrical stimulation could be blocked by the muscarinic antagonist, atropine (Metherate *et al.*, 1992). In this same study, electrical stimulation of the basal forebrain produced

depolarization and small amplitude fast fluctuations in cortical pyramidal cells recorded intracellularly *in vivo*, similar to the muscarinic effects of ACh documented on the pyramidal cells *in vitro* (Metherate *et al.*, 1992). These fast oscillations depended upon intrinsic mechanisms that were modulated by the slow depolarization induced by ACh. The cholinergic input would thus stimulate but not pace the gamma oscillations in the cortex. Moreover, from *in vitro* studies, it would appear that the cholinergic neurons discharge only at relatively low frequencies (<15 Hz) (Khateb *et al.*, 1992) and could thus only indirectly modulate high frequency activity in the cortex by the postsynaptic action of ACh. Activation of the cholinergic neurons by the glutamate agonists, AMPA and NMDA, in the present study could thus similarly elicit high frequency gamma oscillations in the cortex through the postsynaptic muscarinic modulation of cortical neurons and networks.

In addition to increased gamma activity, NMDA also elicited increased theta activity (4 - 8 Hz) as particularly prominent on the retrosplenial cortex. Retrosplenial, or posterior cingulate, cortex is part of the limbic cortex, where theta bursting cells have been recorded (Holsheimer, 1982; Leung and Borst, 1987). In the natural transition from SWS to PS or active waking, as here following NMDA as compared to procaine, a shift from a delta to a theta low-frequency oscillation is also evident in other cortical regions and could thus represent a rhythmic, phasic influence from the basal forebrain in multiple cortical areas (Maloney *et al.*, 1997). NMDA was previously shown *in vitro* to induce slow rhythmic bursting in the cholinergic basalis neurons (Khateb *et al.*, 1995; Khateb *et al.*, 1997). The theta EEG activity produced by NMDA microinjections into the basal forebrain here may accordingly be caused by slow rhythmic burst discharge of the cholinergic neurons potentially induced by NMDA *in vivo*. Most recently, identified cholinergic cells have

been shown to fire in a rhythmic burst discharge in association with theta-like activity recorded from the retrosplenial and also prefrontal cortex *in vivo* in the anesthetized rat (Manns *et al.*, 1999 and 2000). The theta modulation by such a burst discharge could be mediated by slow muscarinic actions of ACh upon pyramidal cells or more likely by faster muscarinic actions upon interneurons or nicotinic actions upon either or both of these cell populations (McCormick and Prince, 1986; McCormick, 1992; Roerig *et al.*, 1997; Xiang *et al.*, 1998). Accordingly, cholinergic basalis neurons could potentially stimulate rhythmic slow oscillations with a theta frequency in the cortex. In fact, theta activity in cingulate and retrosplenial limbic cortex has been shown to depend upon input from basal forebrain cholinergic cells (Borst *et al.*, 1987; Leung and Borst, 1987), just as that in the hippocampus depends importantly upon input from septal cholinergic cells (Lee *et al.*, 1994). Stimulation of burst discharge by the cholinergic neurons with NMDA in the present study could thus elicit theta-like activity through direct modulation of cortical neurons.

It was previously shown that local injections into the basal forebrain of AMPA and NMDA in the doses employed in the present study stimulate expression therein of c-Fos, the immediate early gene (Page *et al.*, 1993), which has been used for many years as an indicator of neural activity (Dragunow and Faull, 1989). In those studies, c-Fos was found in both cholinergic and non-cholinergic neurons in the basal forebrain following both drugs (Page *et al.*, 1993). In the present study, we examined by dual-immunostaining for c-Fos protein with ChAT or GAD, the presence of c-Fos+ cholinergic, GABAergic or other non-cholinergic cells in the basal forebrain to confirm their presence and plot their distribution therein following NMDA.. Similar to the previously published results, we found numerous cholinergic

and non-cholinergic, including GABAergic, neurons that expressed c-Fos in the basal forebrain and were distributed through the substantia innominata and magnocellular preoptic nucleus near the microinjection cannulae. It would appear from these results together with the previously published ones (Page *et al.*, 1993), that NMDA stimulates GABAergic and other non-cholinergic, in addition to the cholinergic cells in the basal forebrain, some of which would likely be cortically projecting cells (Gritti *et al.*, 1997). The effect of NMDA thus likely also depends upon its action on the non-cholinergic in addition to cholinergic, cortically projecting neurons.

Non-cholinergic, possibly cortically projecting, basal forebrain neurons also display intrinsic properties of rhythmic discharge *in vitro* (Alonso *et al.*, 1996). Although it has not been shown that they can be directly stimulated to discharge rhythmically by NMDA in these *in vitro* studies, it is in any event likely that they may fire in a coordinated manner with cholinergic neurons during rhythmic activity *in vivo*. The non-cholinergic cells discharge in clusters of spikes that recur rhythmically at a slow frequency in the slice (Alonso *et al.*, 1996). As most likely cortically projecting and possibly GABAergic, they could thus modulate rhythmic slow activity and serve together with the cholinergic neurons, as is the case in the septo-hippocampal system (Lee *et al.*, 1994), to modulate theta frequency oscillations in the cerebral cortex. In addition, the non-cholinergic cells fire within each cluster of spikes at a relatively high frequency (20 - 80 Hz) (Alonso *et al.*, 1996) and could thus also possibly elicit high frequency gamma activity. Accordingly, non-cholinergic together with cholinergic basal forebrain cells could stimulate theta and gamma activities in the cerebral cortex as may be manifest in the present study following NMDA microinjections into the basal forebrain.

Serving as the ventral extra-thalamic relay from the brainstem reticular activating system to the cerebral cortex, the basal forebrain neurons would accordingly transmit and possibly transform the activating influence from the reticular formation to modulate the cortex in a rhythmic manner. This rhythmic modulation could be important in providing a template for coherent discharge of functionally related but widely distributed cortical neurons, which may underlie conscious awareness and perception (Singer, 1993; Singer, 1998). Indeed, the documented facilitation of stimulus-specific synchronization in the cortex by stimulation of the reticular formation (Munk *et al.*, 1996; Herculano-Houzel *et al.*, 1999) could importantly involve the relay through the basal forebrain to the cortex in this process. Thus, as may also be the case of the non-specific thalamo-cortical projection system, which serves as the dorsal relay to the cerebral cortex (Steriade *et al.*, 1991; Ribary *et al.*, 1992), the basalo-cortical projection system may in addition to transmitting the activating influence from brainstem, modulate the cortex in a rhythmic manner in order to facilitate coherent cortical activity during active and attentive behavioral and cortical states.

Inactivation of basal forebrain neurons with procaine

Procaine decreased high frequency gamma activity and theta, while increasing delta activity during the day when the rats normally sleep the majority of the time. The waking state that did nonetheless occur in addition to SWS after procaine was characterized by a behaviorally quiet state and an EEG with low gamma and theta activity. Although these results are the first reported concerning decreased gamma EEG activity after inactivation of the basal forebrain, they parallel previous results reporting relative decreases in beta activity (12 - 30 Hz) or increases in delta activity following neurotoxic lesions of the basal forebrain

(Stewart *et al.*, 1984; Buzsaki *et al.*, 1988; Ray and Jackson, 1991; Riekkinen *et al.*, 1992). Such EEG changes were also shown to be associated with behavioral deficits and in particularly discerning studies, the behavioral deficits were consistently shown to involve an attentional dysfunction (Muir *et al.*, 1994). Collectively, these results would support the role of the basalo-cortical system in cortical activation subtending attentive and active waking behaviors.

After procaine microinjections, the sleep cycle was also altered, since PS was absent in most animals despite the occurrence of SWS. It is possible that this absence is due to the deficits in cortical activation, including high frequency gamma and theta activities, which normally occur at levels during PS that are equivalent to the highest levels occurring during waking with active and attentive behaviors (Maloney *et al.*, 1997). The activation during PS must depend like that during waking upon basal forebrain input. Indeed, single units have been recorded in the basal forebrain, some of which were antidromically activated from the cortex, that are active during both waking and PS and some that increase their discharge in advance of PS (Szymusiak and McGinty, 1986b; Detari *et al.*, 1987; Szymusiak and McGinty, 1989). The loss of PS in the present study may also be due to inactivation of descending influences from basal forebrain to the brainstem that are likely important in the sleep cycle (Szymusiak and McGinty, 1986a; Nishino *et al.*, 1995).

The effects of the procaine microinjections on EEG and state are similar to those of serotonin microinjections into the basal forebrain (Cape and Jones, 1998), which has been shown *in vitro* to hyperpolarize and inhibit both cholinergic and non-cholinergic neurons therein (Khateb *et al.*, 1993; Fort *et al.*, 1998). Collectively, these results suggest that decreased gamma and theta that characterizes quiet

waking and SWS normally involves inhibition of cortically projecting basal forebrain neurons. On the other hand, generation of PS would appear from our results to necessitate the activity of the basal forebrain cell populations, including the cortically projecting cholinergic and non-cholinergic neurons, that would stimulate the high gamma and theta activities which characterize PS, as they do active and attentive waking states (Maloney *et al.*, 1997).

ACKNOWLEDGEMENTS

We would like to thank Lynda Mainville for her technical assistance and Angel Alonso, Jean Gotman for their helpful consultation. The research was supported by a grant to Barbara E. Jones from the Canadian Medical Research Council. Edmund G. Cape was supported as a graduate student by the Fonds de Recherche en Sante du Quebec, Reseau de Sante Mentale, Axe Sommeil et Vigilance.

ABBREVIATIONS

AMPA alpha-amino-3-hydroxy-5-methyl-4-isoxazole propionic acid

ACh acetylcholine

β beta

ChAT choline acetyltransferase

δ delta

EEG electroencephalogram

EMG electromyogram

γ gamma

GAD glutamic acid decarboxylase

NMDA N-methyl-D-aspartate

PS paradoxical sleep

SWS slow wave sleep

σ sigma

θ theta

*t*PS transition into paradoxical sleep

*t*SWS transition into slow wave sleep

W wake

LITERATURE CITED

Alonso, A., Khateb, A., Fort, P., Jones, B. E., and Muhlethaler, M. (1996) Differential oscillatory properties of cholinergic and non-cholinergic nucleus Basalis neurons in guinea pig brain slice. *Eur. J. Neurosci.*, **8**, 169-182.

Borst, J. G. G., Leung, L.-W. S., and MacFabe, D. F. (1987) Electrical activity of the cingulate cortex. II. Cholinergic modulation. *Brain Res.*, **407**, 81-93.

Buzsaki, G., Bickford, R. G., Ponomareff, G., Thal, L. J., Mandel, R., and Gage, F. H. (1988) Nucleus basalis and thalamic control of neocortical activity in the freely moving rat. *J. Neurosci.*, **8**, 4007-4026.

Cape, E., and Jones, B. E. (1994) Modulation of sleep-wake state and cortical activity following injection of agonists into the region of cholinergic basal forebrain neurons. *Soc. Neurosci. Abst.*, **20**, 156.

Cape, E. G., and Jones, B. E. (1998) Differential modulation of high frequency gamma electroencephalogram activity and sleep-wake state by noradrenaline and serotonin microinjections into the region of cholinergic basalis neurons. *J. Neurosci.*, **18**, 2653-2666.

Casamenti, F., Deffenu, G., Abbamondi, A. L., and Pepeu, G. (1986) Changes in cortical acetylcholine output induced by modulation of the nucleus basalis. *Brain Res. Bull.*, **16**, 689-695.

Celesia, G. G., and Jasper, H. H. (1966) Acetylcholine released from cerebral cortex in relation to state of activation. *Neurology*, **16**, 1053-1064.

Detari, L., Juhasz, G., and Kukorelli, T. (1987) Neuronal firing in the pallidal region: firing patterns during sleep-wakefulness cycle in cats. *Electroenceph. clin. Neurophysiol.*, **67**, 159-166.

Dragunow, M., and Faull, R. (1989) The use of c-fos as a metabolic marker in neuronal pathway tracing. *J. Neurosci. Meth.*, **29**, 261-265.

Fort, P., Khateb, A., Serafin, M., Muhlethaler, M., and Jones, B. E. (1998) Pharmacological characterization and differentiation of non-cholinergic nucleus basalis neurons *in vitro*. *NeuroReport*, **9**, 1-5.

Gritti, I., Mainville, L., and Jones, B. E. (1993) Codistribution of GABA- with acetylcholine-synthesizing neurons in the basal forebrain of the rat. *J. Comp. Neurol.*, **329**, 438-457.

Gritti, I., Mainville, L., Mancia, M., and Jones, B. E. (1997) GABAergic and other non-cholinergic basal forebrain neurons project together with cholinergic neurons to meso- and iso-cortex in the rat. *J. Comp. Neurol.*, **383**, 163-177.

Herculano-Houzel, S., Munk, M. H. J., Neuenschwander, S., and Singer, W. (1999) Precisely synchronized oscillatory firing patterns require electroencephalographic activation. *J. Neurosci.*, **19**, 3992-4010.

Holsheimer, J. (1982) Generation of theta activity (RSA) in the cingulate cortex of the rat. *Exp. Brain Res.*, **47**, 309-312.

Jasper, H. H., and Tessier, J. (1971) Acetylcholine liberation from cerebral cortex during paradoxical (REM) sleep. *Science*, **172**, 601-602.

Jones, B. E. (1995) Reticular formation. Cytoarchitecture, transmitters and projections. In Paxinos, G. (eds), *The Rat Nervous System.* Academic Press Australia, New South Wales, pp. 155-171.

Jones, B. E., and Beaudet, A. (1987) Retrograde labeling of neurons in the brain stem following injections of [^{3}H]choline into the forebrain of the rat. *Exp. Brain Res.*, **65**, 437-448.

Jones, B. E., and Cuello, A. C. (1989) Afferents to the basal forebrain cholinergic cell area from pontomesencephalic--catecholamine, serotonin, and acetylcholine--neurons. *Neuroscience*, **31**, 37-61.

Jones, B. E., and Yang, T.-Z. (1985) The efferent projections from the reticular formation and the locus coeruleus studied by anterograde and retrograde axonal transport in the rat. *J. Comp. Neurol.*, **242**, 56-92.

Khateb, A., Fort, P., Alonso, A., Jones, B. E., and Muhlethaler, M. (1993) Pharmacological and immunohistochemical evidence for a serotonergic input to cholinergic nucleus basalis neurons. *Eur. J. Neurosci.*, **5**, 541-547.

Khateb, A., Fort, P., Serafin, M., Jones, B. E., and Muhlethaler, M. (1995) Rhythmical bursts induced by NMDA in cholinergic nucleus basalis neurones *in vitro*. *J. Physiol. (Lond.)*, **487.3**, 623-638.

Khateb, A., Fort, P., Williams, S., Serafin, M., Jones, B. E., and Muhlethaler, M. (1997) Modulation of cholinergic nucleus basalis neurons by acetylcholine and N-methyl-D-aspartate. *Neuroscience*, **81**, 47-55.

Khateb, A., Muhlethaler, M., Alonso, A., Serafin, M., Mainville, L., and Jones, B. E. (1992) Cholinergic nucleus basalis neurons display the capacity for rhythmic bursting activity mediated by low threshold calcium spikes. *Neuroscience*, **51**, 489-494.

Lawson, V. H., and Bland, B. H. (1993) The role of the septohippocampal pathway in the regulation of hippocampal field activity and behavior: analysis by the intraseptal microinfusion of carbachol, atropine and procaine. *Exp. Neurol.*, **120**, 132-144.

Lee, M. G., Chrobak, J. J., Sik, A., Wiley, R. G., and Buzsaki, G. (1994) Hippocampal theta activity following selective lesion of the septal cholinergic system. *Neuroscience*, **62**, 1033-1047.

Lehmann, J., Nagy, J. I., Atmadja, S., and Fibiger, H. C. (1980) The nucleus basalis magnocellularis: the origin of a cholinergic projection to the neocortex of the rat. *Neuroscience*, **5**, 1161-1174.

Leung, L.-W. S., and Borst, J. G. G. (1987) Electrical activity of the cingulate cortex. I. Generating mechanisms and relations to behavior. *Brain Res.*, **407**, 68-80.

Lo Conte, G., Casamenti, F., Bigi, V., Milaneschi, E., and Pepeu, G. (1982) Effect of magnocellular forebrain nuclei lesions on acetylcholine output from the cerebral cortex, electrocorticogram and behaviour. *Arch. ital Biol.*, **120**, 176-188.

Maloney, K. J., Cape, E. G., Gotman, J., and Jones, B. E. (1997) High frequency gamma electroencephalogram activity in association with sleep-wake states and spontaneous behaviors in the rat. *Neuroscience*, **76**, 541-555.

Maloney, K. J., Mainville, L., and Jones, B. E. (1999) Differential c-Fos expression in cholinergic, monoaminergic and GABAergic cell groups of the

pontomesencephalic tegmentum after paradoxical sleep deprivation and recovery. *J. Neurosci.* **19**, 3057-3072.

Manns, I., Alonso, A., and Jones, B. E. (1999) Discharge properties of juxtacellularly labeled and immunohistochemically identified cholinergic basal forebrain neurons in relation to cortical EEG activity in anesthetized rats. *Soc. Neurosci. Abst.* **25**, 241.

Manns, I.D., Alonso A., Jones B.E. (2000) Discharge properties of juxtacellularly labeled and immunohistochemically identified cholinergic basal forebrain neurons recorded in association with the electroencephalogram in anesthetized rats. J Neurosci.,20,1505-1518.

Marrosu, F., Portas, C., Mascia, S., Casu, M. A., Fa, M., Giagheddu, M., Imperato, A., and Gessa, G. L. (1995) Microdialysis measurement of cortical and hippocampal acetylcholine release during sleep-wake cycle in freely moving cats. *Brain Res.*, **671**, 329-332.

McCormick, D. A. (1992) Neurotransmitter actions in the thalamus and cerebral cortex and their role in neuromodulation of thalamocortical activity. *Progr. Neurobiol.*, **39**, 337-388.

McCormick, D. A., and Prince, D. A. (1986) Mechanisms of action of acetylcholine in the guinea-pig cerebral cortex in vitro. *J. Physiol.*, **375**, 169-194.

Metherate, R., Cox, C. L., and Ashe, J. H. (1992) Cellular bases of neocortical activation: modulation of neural oscillations by the nucleus basalis and endogenous acetylcholine. *J. Neurosci.*, **12**, 4701-4711.

Moruzzi, G., and Magoun, H. W. (1949) Brain stem reticular formation and activation of the EEG. *Electroenceph. clin. Neurophysiol.*, **1**, 455-473.

Muir, J. L., Everitt, B. J., and Robbins, T. W. (1994) AMPA-induced excitotoxic lesions of the basal forebrain: a significant role for the cortical cholinergic system in attentional function. *J. Neurosci.*, **4**, 2313-2326.

Munk, M. H. J., Roelfsema, P. R., Konig, P., Engel, A. K., and Singer, W. (1996) Role of reticular activation in the modulation of intracortical synchronization. *Science*, **272**, 271-274.

Nishino, S., Tafti, M., Reid, M. S., Shelton, J., Siegel, J. M., Dement, W. C., and Mignot, E. (1995) Muscle atonia is triggered by cholinergic stimulation of the basal forebrain: implication for the pathophysiology of canine narcolepsy. *J. Neurosci.*, **15**, 4806-4814.

Page, K. J., Saha, A., and Everitt, B. J. (1993) Differential activation and survival of basal forebrain neurons following infusions of excitatory amino acids: studies with the immediate early gene c-*fos*. *Exp. Brain Res.*, **93**, 412-422.

Rasmusson, D. D., Clow, K., and Szerb, J. C. (1994) Modification of neocortical acetylcholine release and electroencephalogram desynchronization due to brainstem stimulation by drugs applied to the basal forebrain. *Neuroscience*, **60**, 665-677.

Ray, P. G., and Jackson, W. J. (1991) Lesions of nucleus basalis alter ChAT activity and EEG in rat frontal neocortex. *Electroenceph. clin. Neurophysiol.*, **79**, 62-68.

Ribary, U., Ioannides, A. A., Singh, K. D., Hasson, R., Bolton, J. P. R., Lado, F., Mogilner, A., and Llinas, R. (1992) Magnetic field tomography of coherent thalamocortical 40-Hz oscillations in humans. *Proc. Natl. Acad. Sci. USA*, **89**, 11037-11041.

Riekkinen, P., Riekkinen, M., Sirvio, J., Miettinen, R., and Riekkinen, P. (1992) Loss of cholinergic neurons in the nucleus basalis induces neocortical electroencephalographic and passive avoidance deficits. *Neuroscience*, **47**, 823-831.

Roerig, B., Nelson, D. A., and Katz, L. C. (1997) Fast synaptic signaling by nicotinic acetylcholine and serotonin 5-HT_3 receptors in developing visual cortex. *J. Neurosci.*, **21**, 8353-8362.

Shute, C. C. D., and Lewis, P. R. (1967) The ascending cholinergic reticular system: neocortical, olfactory and subcortical projections. *Brain*, **90**, 497-520.

Singer, W. (1993) Synchronization of cortical activity and its putative role in information processing and learning. *Ann. Rev. Physiol.*, **55**, 349-374.

Singer, W. (1998) Consciousness and the structure of neuronal representations. *Phil. Trans. R. Soc. Lond.*, **353**, 1829-1840.

Starzl, T. E., Taylor, C. W., and Magoun, H. W. (1951) Ascending conduction in reticular activating system, with special reference to the diencephalon. *J. Neurophysiol.*, **14**, 461-477.

Steriade, M., Curro Dossi, R., Pare, D., and Oakson, G. (1991) Fast oscillations (20-40Hz) in thalamocortical systems and their potentiation by mesopontine cholinergic nuclei in the cat. *Proc. Natl. Acad. Sci. USA*, **88**, 4396-4400.

Stewart, D. J., Macfabe, D. F., and Vanderwolf, C. H. (1984) Cholinergic activation of the electrocorticogram: Role of the substantia innominata and effects of atropine and quinuclidinyl benzilate. *Brain Res.*, **322**, 219-232.

Stewart M, Fox SE (1990) Do septal neurons pace the hippocampal theta rhythm? *Trends Neurosci.*, **13**, 163-168.

Szymusiak, R., and McGinty, D. (1986a) Sleep suppression following kainic acid-induced lesions of the basal forebrain. *Exp. Neurol.*, **94**, 598-614.

Szymusiak, R., and McGinty, D. (1986b) Sleep-related neuronal discharge in the basal forebrain of cats. *Brain Res.*, **370**, 82-92.

Szymusiak, R., and McGinty, D. (1989) Sleep-waking discharge of basal forebrain projection neurons in cats. *Brain Res. Bull.*, **22**, 423-430.

Vergnes, M., Marescaux, C., Micheletti, G., Reis, J., Depaulis, A., Rumbach, L., and Warter, J. M. (1982) Spontaneous paroxysmal electroclinical patterns in rat: a model of generalized non-convulsive epilepsy. *Neurosci. Lett.*, **33**, 97-101.

Xiang, Z., Huguenard, J. R., and Prince, D. A. (1998) Cholinergic switching within neocortical inhibitory networks. *Science*, **5379**, 985-988.

Figure 1. Sagittal illustration of rat brain showing the location of the microinjections into the region of the basal forebrain cholinergic cell area, which lies in the ventral path of the ascending reticular activating system (adapted from (Jones, 1995)). Drug loaded cannulae were inserted (bilaterally) and held in the guide cannulae to avoid premature leakage of the drug into the tissue. Once the animal relaxed following the handling procedure and resumed sleeping, the inner cannulae were lowered by a remote mechanism into the region of the cholinergic cells, and the microinjections begun soon thereafter. Abbreviations: ac, anterior commissure; AV, anteroventral thalamic nucleus; CL, centrolateral thalamic nucleus; CPu, caudate putamen; DpMe, deep mesencephalic reticular field; DR, dorsal raphe; FF, fields of Forel; Gi, gigantocellular reticular field; GiA, gigantocellular reticular field, α part; GiV, gigantocellular reticular field, ventral part; GP, globus pallidus; ic, internal capsule; LC, locus coeruleus; LD, laterodorsal thalamic nucleus; LH, lateral hypothalamic area; LP, lateral posterior thalamic nucleus; MCPO, magnocellular preoptic nucleus; opt, optic tract; OtuD, olfactory tubercle, deep layer; PC, paracentral thalamic nucleus; PF, parafascicular thalamic nucleus; PnC, pontine reticular field, caudal part; PnO, pontine reticular field, oral part; PnV, pontine reticular field, ventral part; PPTg, pedunculopontine tegmental nucleus; RRF, retrorubral field; Rt, reticular thalamic nucleus; SIa, substantia innominata, anterior part; Sip, substantia innominata, posterior part; SN, substantia nigra; VL, ventrolateral thalamic nucleus; VM, ventromedial thalamic nucleus; VTA, ventral tegmental area; ZI, zona incerta.

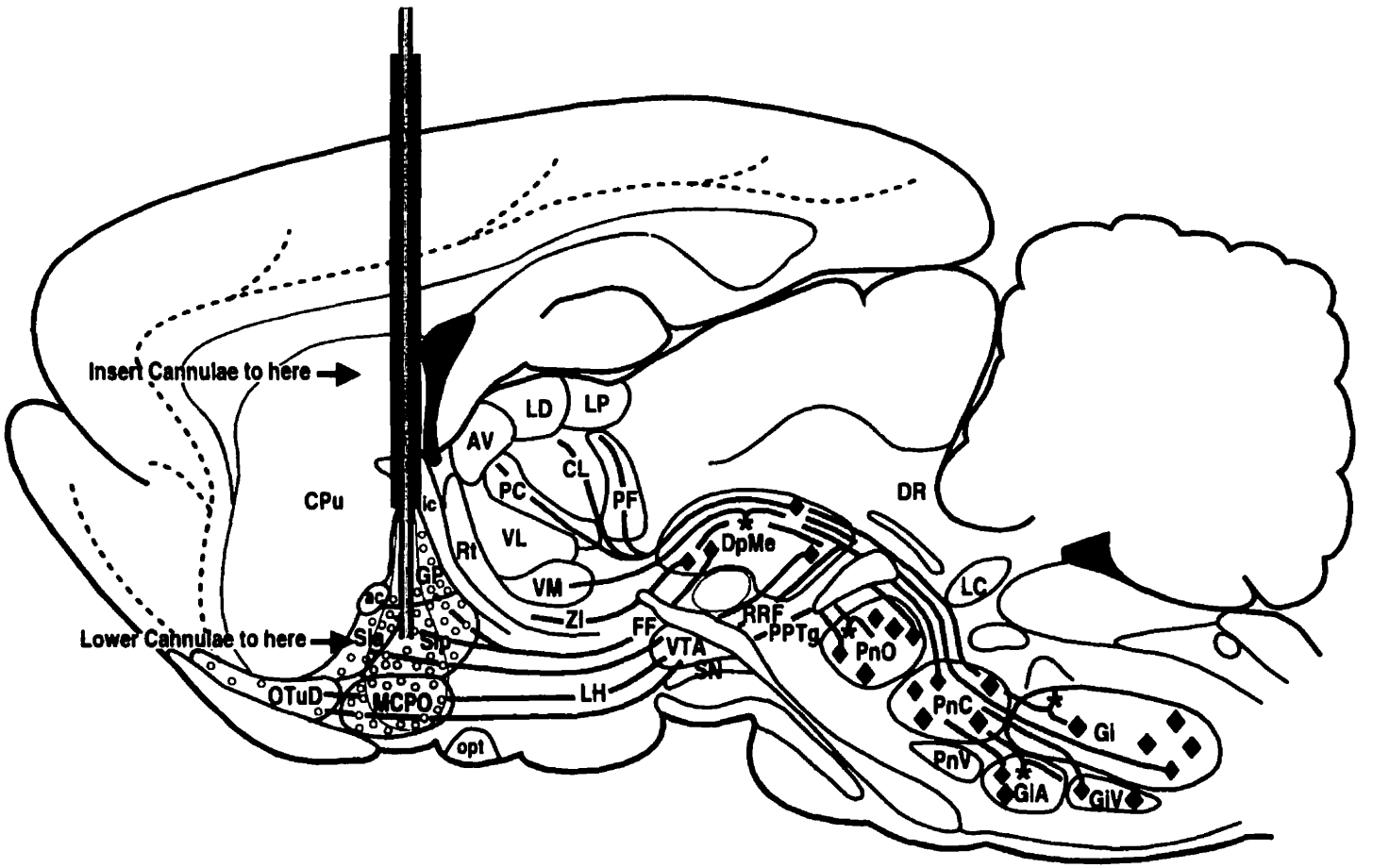
Insert Cannulae to here
Lower Cannulae to here
CPu
ic
LD
LP
AV
CL
PC
PF
VL
Rt
VM
ZI
FF
VTA
SN
LH
GP
ec
Sla
Slp
OTuD
MCPO
opt
DpMe
RRF
PPTg
PnO
DR
LC
PnC
PnV
Gi
GiA
GiV

1 mm

Figure 2. Hypnogram (top) and EEG and EMG frequency band activities (bottom) per 20 sec epoch during morning (left) and afternoon (right) recording periods (rat B19). Recording began in the morning (~1100 = 0) and continued for ~30 min before the animal was handled for mock insertion of injection cannulae (during the break marked by the dividing line). After resumption of sleep (usually in ~30-40 min), recording was begun again for the afternoon, corresponding approximately to the post-injection recording period. Gamma (γ, 30.5 - 58.0 Hz), delta (δ, 1.5 - 4 Hz), and theta/delta ratio (θ, 4.5 - 8.5 Hz /δ, 1 - 4 Hz) from the right retrosplenial cortex and EMG frequency band activities are displayed as amplitude units or ratio (θ/δ) scaled to maximum (with maximum value indicated for each on the left). 100 μV $\cong$ 125 AD units. PS, Paradoxical sleep; SWS slow wave sleep; *t*PS, transition into paradoxical sleep; *t*SWS, transition into slow wave sleep.

Baseline

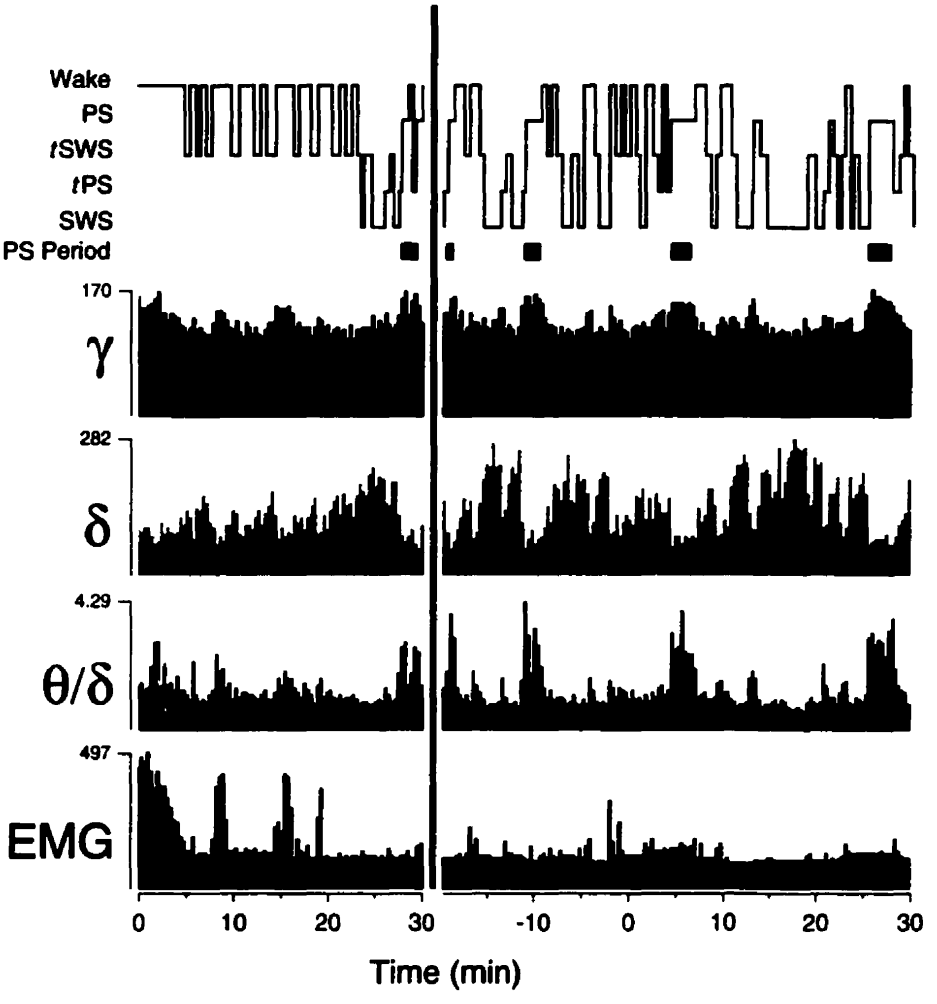
Wake
PS
tSWS
tPS
SWS
PS Period
170
γ
282
δ
4.29
θ/δ
497
EMG
0
10
20
30
-10
0
10
20
30
Time (min)

Figure 3. Average % State, relative EEG and EMG activities during the 30 min afternoon baseline recording period. The % State reflects the amount of time spent in each state over the course of 30 minutes and %γ and δ the relative amplitude (as percent total amplitude) of these amplitude bands. EEG activities are from the right retrosplenial cortex. Data presented as mean + S.E.M for 9 rats. %γ, %δ, θ/δ and EMG all varied significantly as a function of state (ANCOVA with rat as covariate, df = 4, $p < .05$).

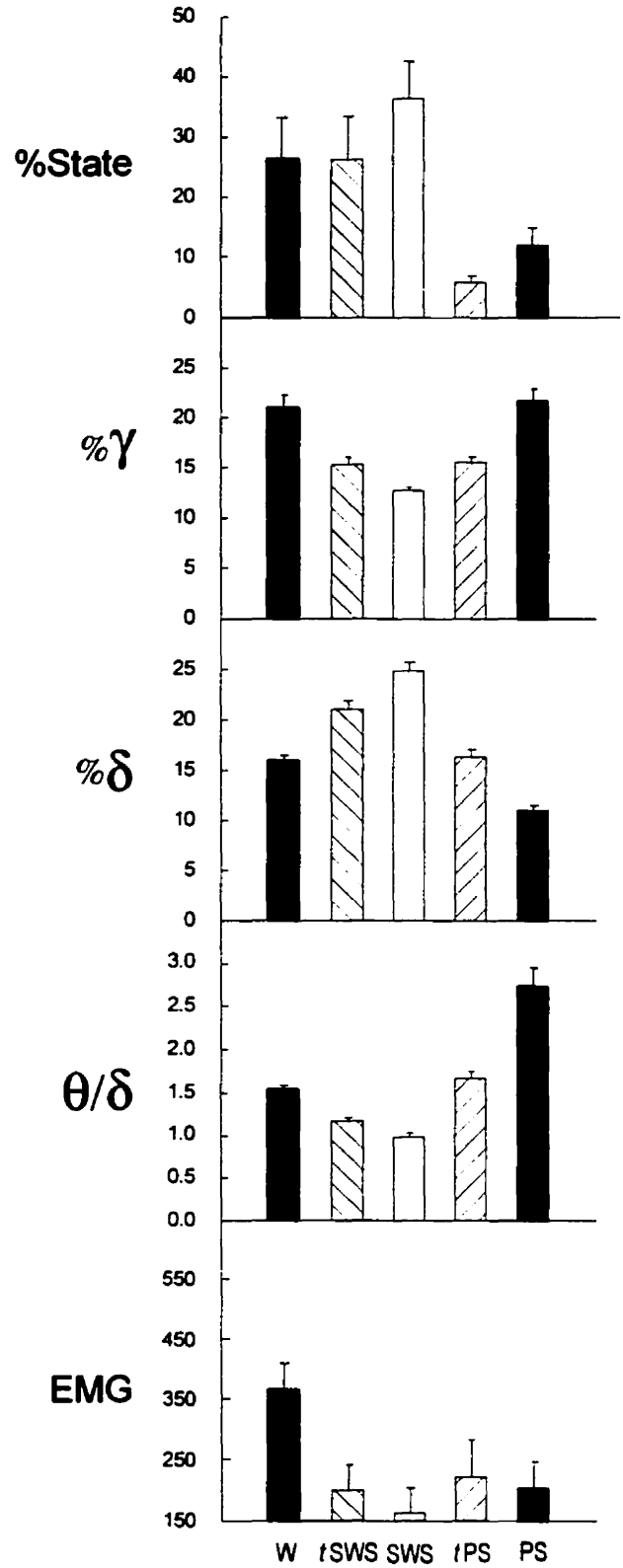
%State
50
40
30
20
10
0
%γ
25
20
15
10
5
0
%δ
25
20
15
10
5
0
θ/δ
3.0
2.5
2.0
1.5
1.0
0.5
0.0
EMG
550
450
350
250
150
W
tSWS
SWS
tPS
PS

Figure 4. Hypnogram and EEG and EMG activities (per 20 sec epoch) during ringer pre- and post-injection recording periods (B19). After the pre-injection recording period, the filled inner cannulae were inserted into the guide cannulae (see Fig. 1), and the animal allowed to resume sleeping before recording was reinitiated. With the appearance of a normal sleep cycle, marked by SWS and PS or *f*PS, the cannulae were lowered via remote control into the basal forebrain (see Fig. 1); the bilateral injection was started ~2 min later and was performed over ~5 min. The post-injection recording period was defined as the 30 min period after the injection was stopped (Time 0 - 30 min at right). Note the minimal disturbance to the sleep-wake cycle caused by the injection procedure and the injection of ringer. γ, δ and θ/δ activities are from the right retrosplenial lead and, together with EMG, are displayed as amplitude units or ratio (θ/δ) scaled to maximum. 100 μV $\cong$ 125 AD units.

Ringer

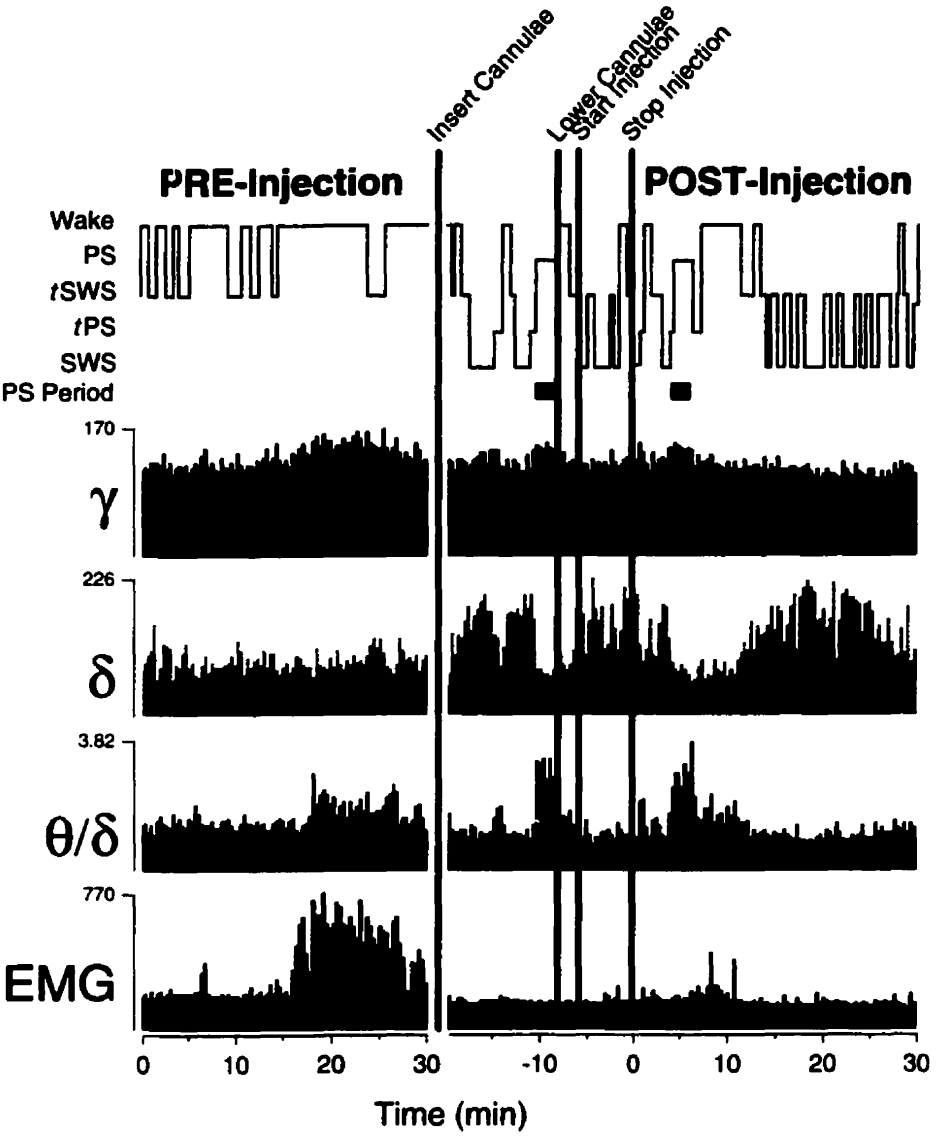
Insert Cannulae
Lower Cannulae
Start Injection
Stop Injection
PRE-Injection
POST-Injection
Wake
PS
tSWS
tPS
SWS
PS Period
170
γ
226
δ
3.82
θ/δ
770
EMG
0
10
20
30
-10
0
10
20
30
Time (min)

Figure 5. Hypnogram and EEG and EMG activities (per 20 sec epoch) during procaine pre- and post-injection recording periods (B17). Note the continuation of SWS following the lowering of the cannulae and the marked increase in delta and decrease in gamma that occurred during and after the injection. γ, δ, θ/δ activities are from the right retrosplenial lead and, together with EMG, are displayed as amplitude units or ratio (θ/δ) scaled to maximum. 100 μV $\cong$ 125 AD units.

Procaine

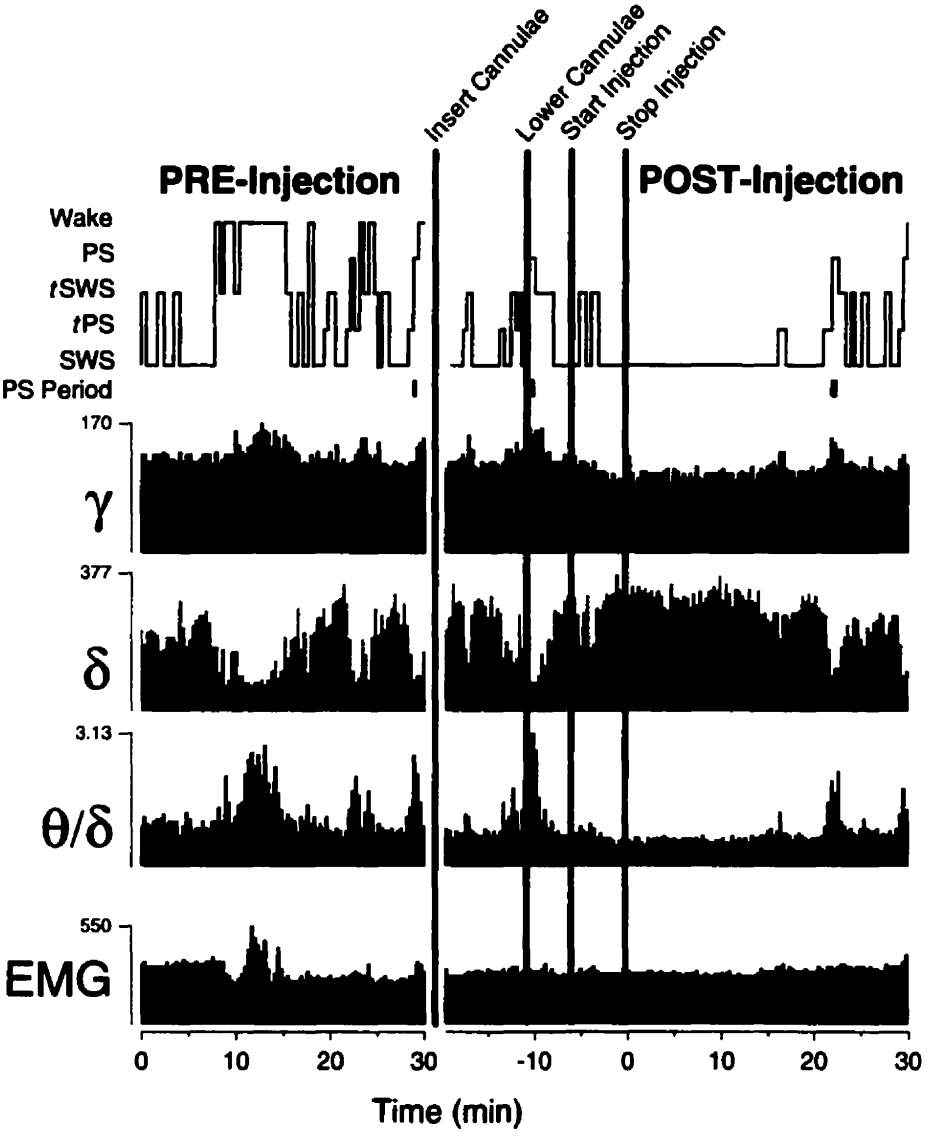
Insert Cannulae
Lower Cannulae
Start Injection
Stop Injection
PRE-Injection
POST-Injection
Wake
PS
tSWS
tPS
SWS
PS Period
170
γ
377
δ
3.13
θ/δ
550
EMG
0
10
20
30
-10
0
10
20
30
Time (min)

Figure 6. Hypnogram and EEG and EMG activities (per 20 sec epoch) during AMPA pre- and post-injection recording periods (B10). Note the occurrence and persistence of the wake state and associated changes in EEG activity from the moment the cannulae were lowered into the basal forebrain. γ, δ, θ/δ activities are from the right retrosplenial lead and, together with EMG, are displayed as amplitude units or ratio (θ/δ) scaled to maximum. 100 μV $\cong$ 125 AD units.

AMPA

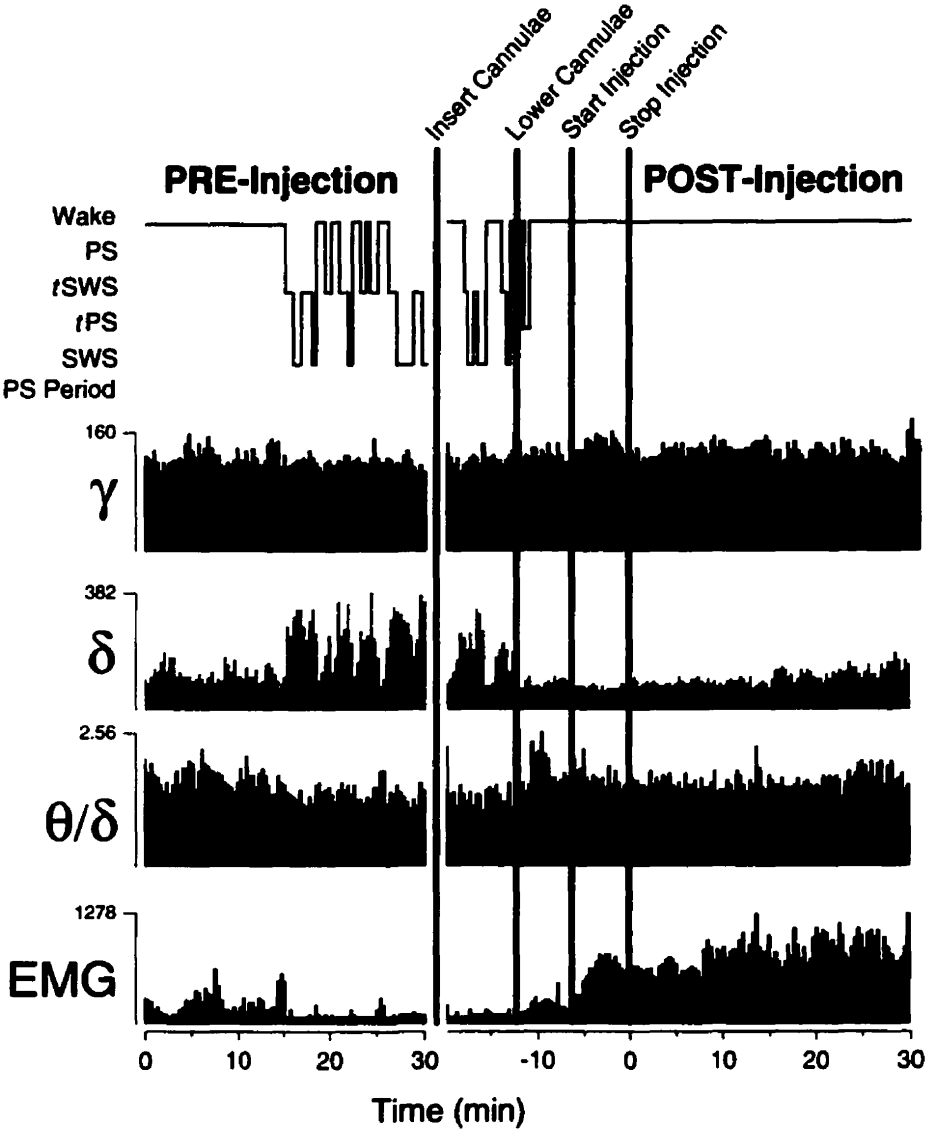
Insert Cannulae
Lower Cannulae
Start Injection
Stop Injection
PRE-Injection
POST-Injection
Wake
PS
tSWS
tPS
SWS
PS Period
160
γ
382
δ
2.56
θ/δ
1278
EMG
0
10
20
30
-10
0
10
20
30
Time (min)

Figure 7. Hypnogram and EEG and EMG activities (per 20 sec epoch) during NMDA pre- and post-injection recording periods (B19). Note the occurrence and persistence of the wake state and associated changes in EEG activity from the moment the cannulae were lowered into the basal forebrain. Seizure-like activity (dashed line showing epochs removed from the quantitative analysis) occurred intermittently during the post-injection period. γ, δ, θ/δ activities are from the right retrosplenial lead and, together with EMG, are displayed as amplitude units or ratio (θ/δ) scaled to maximum. 100 μV $\cong$ 125 AD units.

NMDA

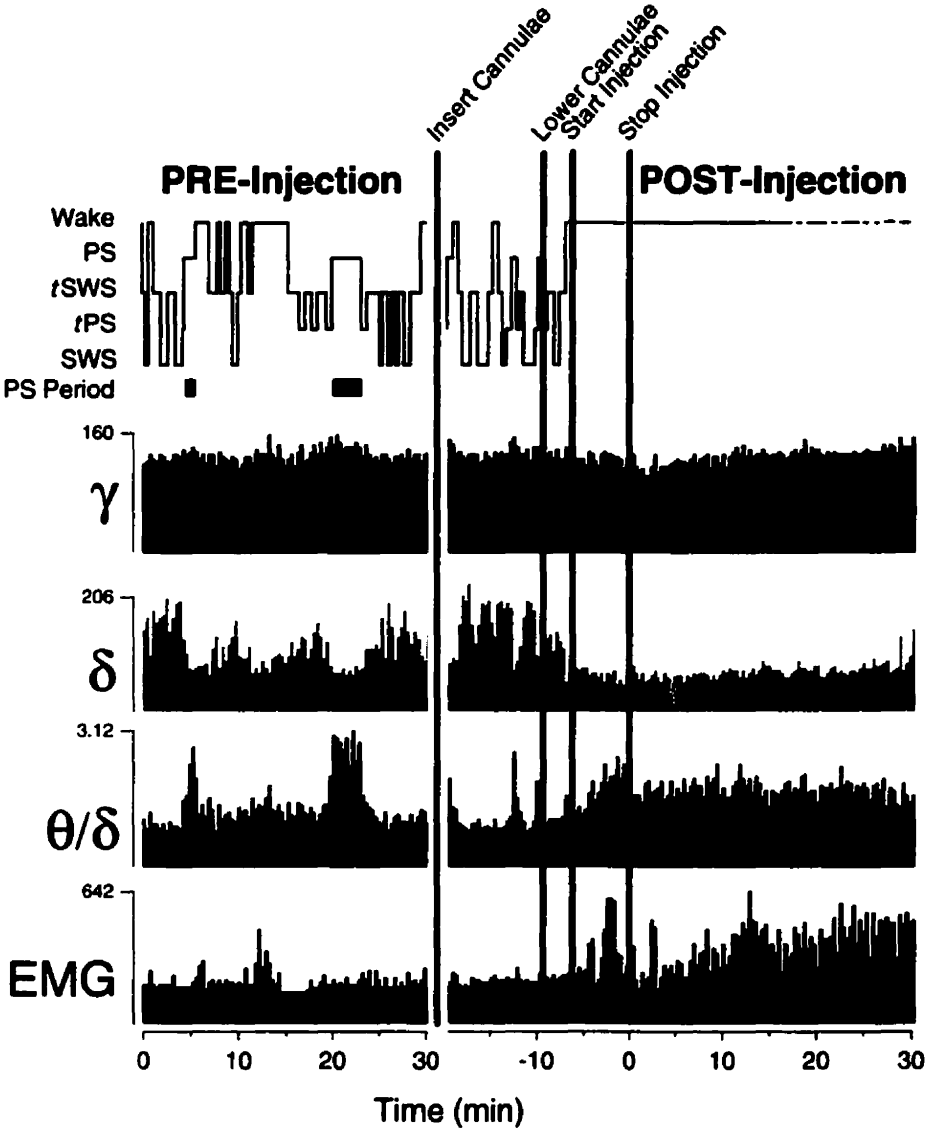
Insert Cannulae
Lower Cannulae
Start Injection
Stop Injection
PRE-Injection
POST-Injection
Wake
PS
tSWS
tPS
SWS
PS Period
160
γ
206
δ
3.12
θ/δ
642
EMG
0
10
20
30
-10
0
10
20
30
Time (min)

Figure 8. Percentage of time spent in sleep-wake states during ringer (R), procaine (Pro), AMPA and NMDA post-injection periods. Values are mean ∀ SEM for R, n = 9; for Pro, AMPA and NMDA, n = 5.. Significantly different from ringer, according to paired comparison t tests: *, $p < .05$; **, $p \leq .01$; ***, $p \leq .001$.

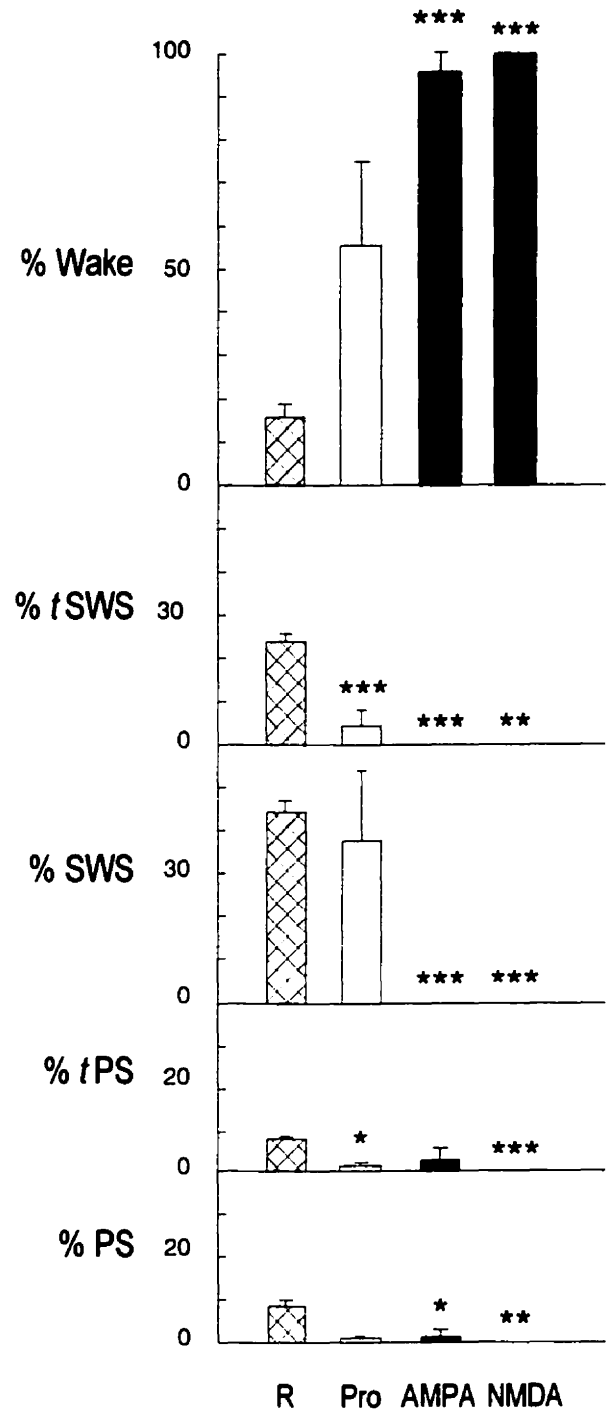
% Wake
100
50
0
% tSWS
30
0
% SWS
30
0
% tPS
20
0
% PS
20
0
***
***
***
***
***
**
***
***
*
***
*
**
R
Pro
AMPA
NMDA

Figure 9. Average EEG and EMG activities during post-injection recording periods after ringer (R), procaine (Pro), AMPA and NMDA microinjections. For EEG (from right retrosplenial lead), γ and δ are expressed as relative activity (% total amplitude), θ/δ as the ratio of absolute activities, and EMG as absolute activity. Data are presented as mean $\forall$ SEM for R, n = 9; for Pro, AMPA and NMDA, n = 5. Significantly different from ringer, according to paired comparison t tests: *, $p < .05$; ** $p \leq .01$; ***, $p \leq .001$.

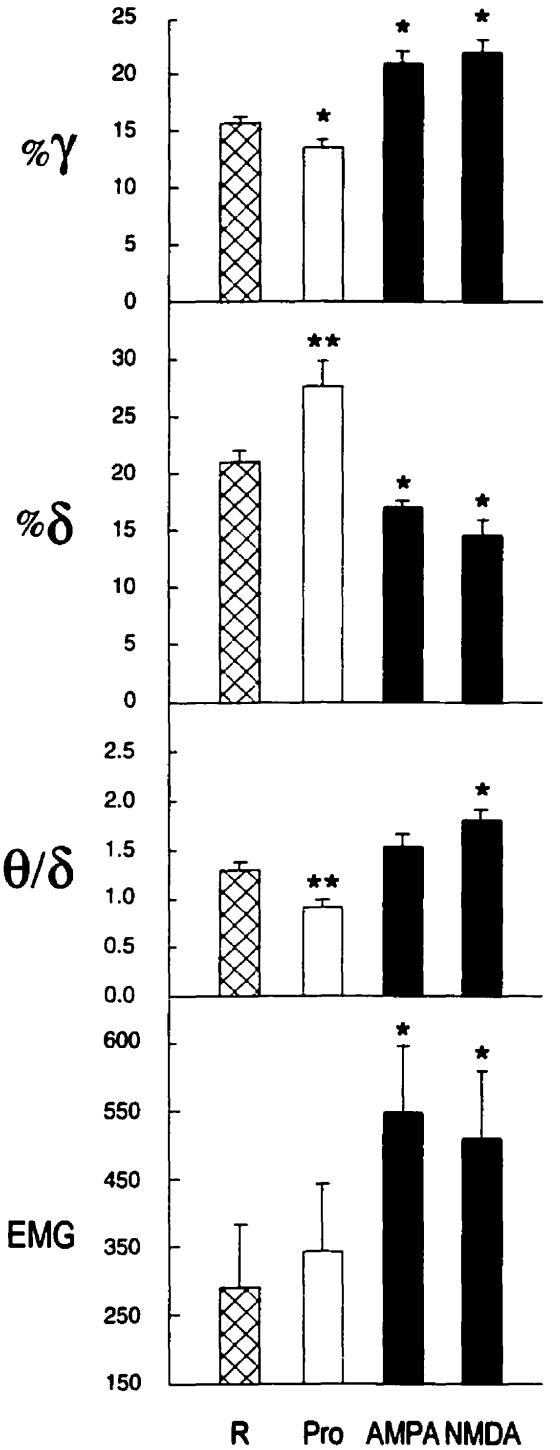
%γ
25
20
15
10
5
0
%δ
30
25
20
15
10
5
0
θ/δ
2.5
2.0
1.5
1.0
0.5
0.0
EMG
600
550
450
350
250
150
R
Pro
AMPA
NMDA

Figure 10. EEG and corresponding amplitude spectra (of a 4 sec epoch) showing the predominant EEG pattern during the post-injection recording period following procaine (rat B17). The sample was taken ~5 min after the injection was stopped when the rat was in a semi-curled sleeping posture with eyes closed. The high voltage, slow EEG pattern (evident in the unfiltered traces) in association with relatively low gamma activity (in high frequency filtered traces), is similar to that of SWS. (Note the low EMG activity in this case, which along with the EKG signal that is often apparent when the EMG activity is low, is also similar to that of normal SWS.) For each region, the unfiltered trace (above) and high frequency gamma (30.5 - 58.0 Hz) filtered trace (below) are presented (on the left) together with the amplitude spectrum for the full range of frequencies (on the right) of the same trace. The EEG was recorded by reference to an electrode in the rostral frontal bone from the frontal, retrosplenial, parietal and occipital cortical regions (shown here for the right side and also recorded from the left side where activity was similar to that of the corresponding contralateral leads). Voltage scales are the same for all cortical leads. Note that the amplitude of the frontal lead is the lowest due to its proximity to the reference electrode. Spectra are displayed in amplitude (AD) units (per 0.5 Hz) shown at different scales for the low frequency range (1.5 - 18.5 Hz) and the high frequency range (19.0 - 58.0 Hz) in order to maximize the appearance of potential peaks in each range. 100 μV $\cong$ 125 AD units. Delta (δ), theta (θ), and gamma (γ) frequency bands are differentially shaded (as in the hypnograms); sigma (σ) and beta (β) bands are shown in white.

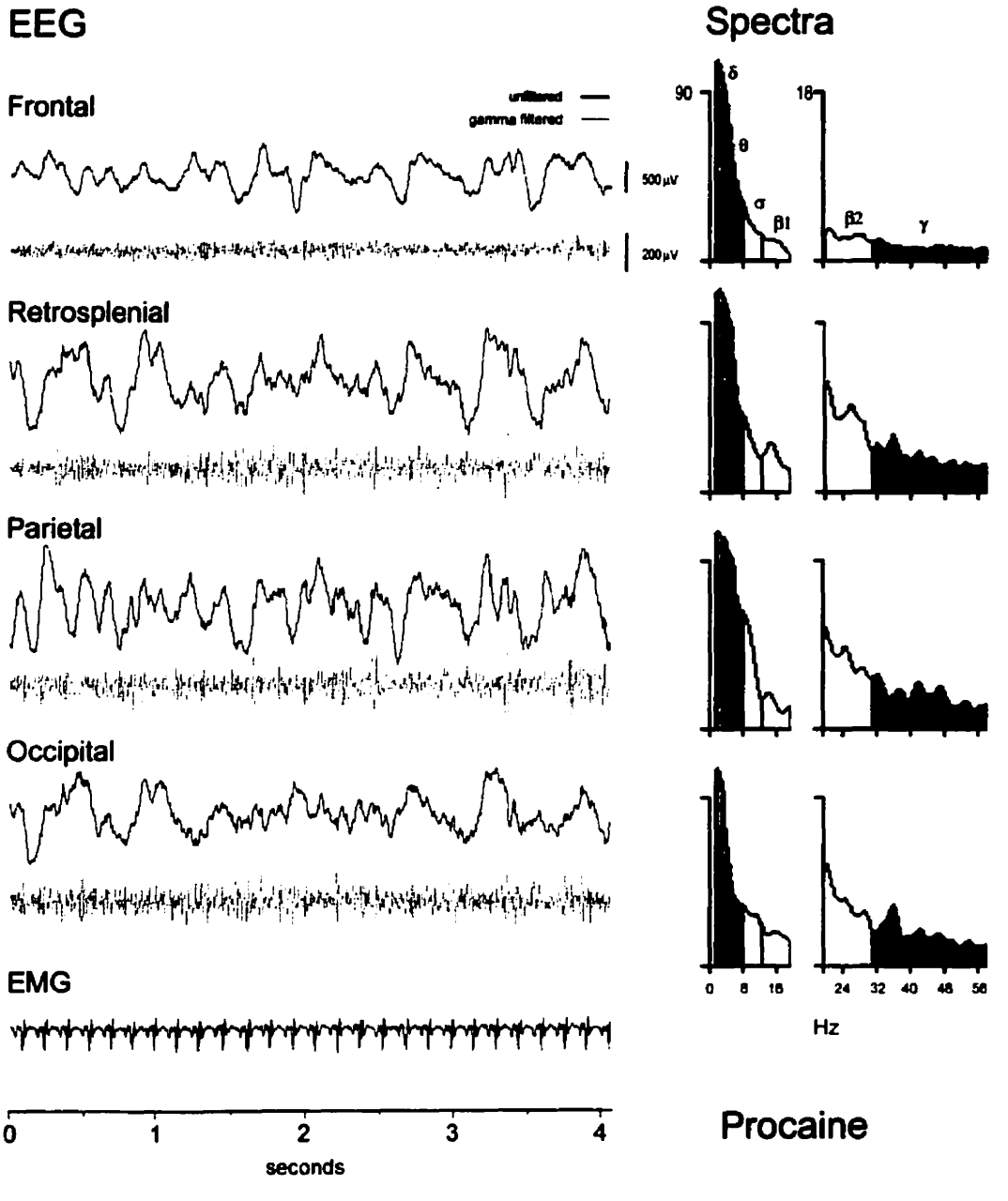
EEG
Spectra
Frontal
unfiltered
gamma filtered
500 µV
200 µV
90
δ
θ
σ
β1
18
β2
γ
Retrosplenial
Parietal
Occipital
EMG
0
8
16
24
32
40
48
56
Hz
0
1
2
3
4
seconds
Procaine

Figure 11. EEG and corresponding amplitude spectra (of a 4 sec epoch) showing the predominant EEG pattern during the post-injection recording period following AMPA (rat B10). The sample was taken ~5 min after the injection was stopped when the rat was behaviorally awake and moving. The EEG is characterized by a relatively low voltage, fast EEG pattern similar to that of an active wake state. In the spectra, gamma activity is relatively high on all leads (taking into consideration the baseline low amplitude of the EEG signal from the frontal cortex). See Fig. 10 for further details.

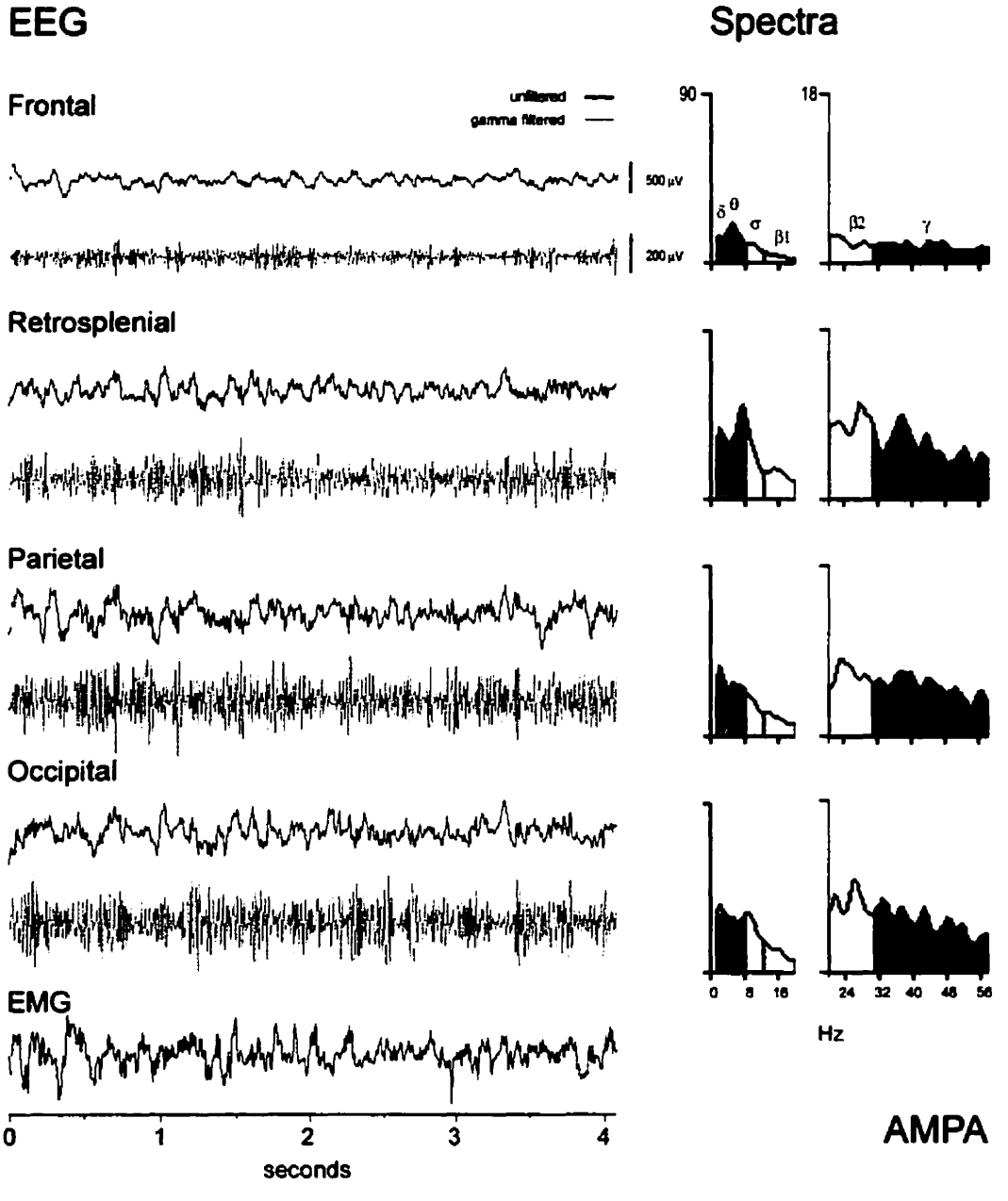
EEG
Spectra
Frontal
unfiltered
gamma filtered
500 µV
200 µV
90
18
δ θ
σ
β1
β2
γ
Retrosplenial
Parietal
Occipital
EMG
0 8 16
24 32 40 48 56
Hz
0 1 2 3 4
seconds
AMPA

FIG. 12. EEG and corresponding amplitude spectra (of a 4 sec epoch) showing the predominant EEG pattern during the post-injection recording period following NMDA (rat B19). The sample was taken ~5 min after the injection was stopped when the rat was behaviorally awake and moving about the cage. The EEG is characterized by a relatively low voltage, fast EEG pattern similar to that of an active wake state. In addition, a slower pattern in a theta frequency is evident on the retrosplenial cortex. In the spectra, a prominent peak is evident in the theta band (at 6.5 Hz) on this lead, and a small peak is evident in this band on the other cortical leads. Gamma activity is relatively high on all cortical leads (taking into consideration the lower baseline amplitude on the frontal lead). See Fig. 10 for further details.

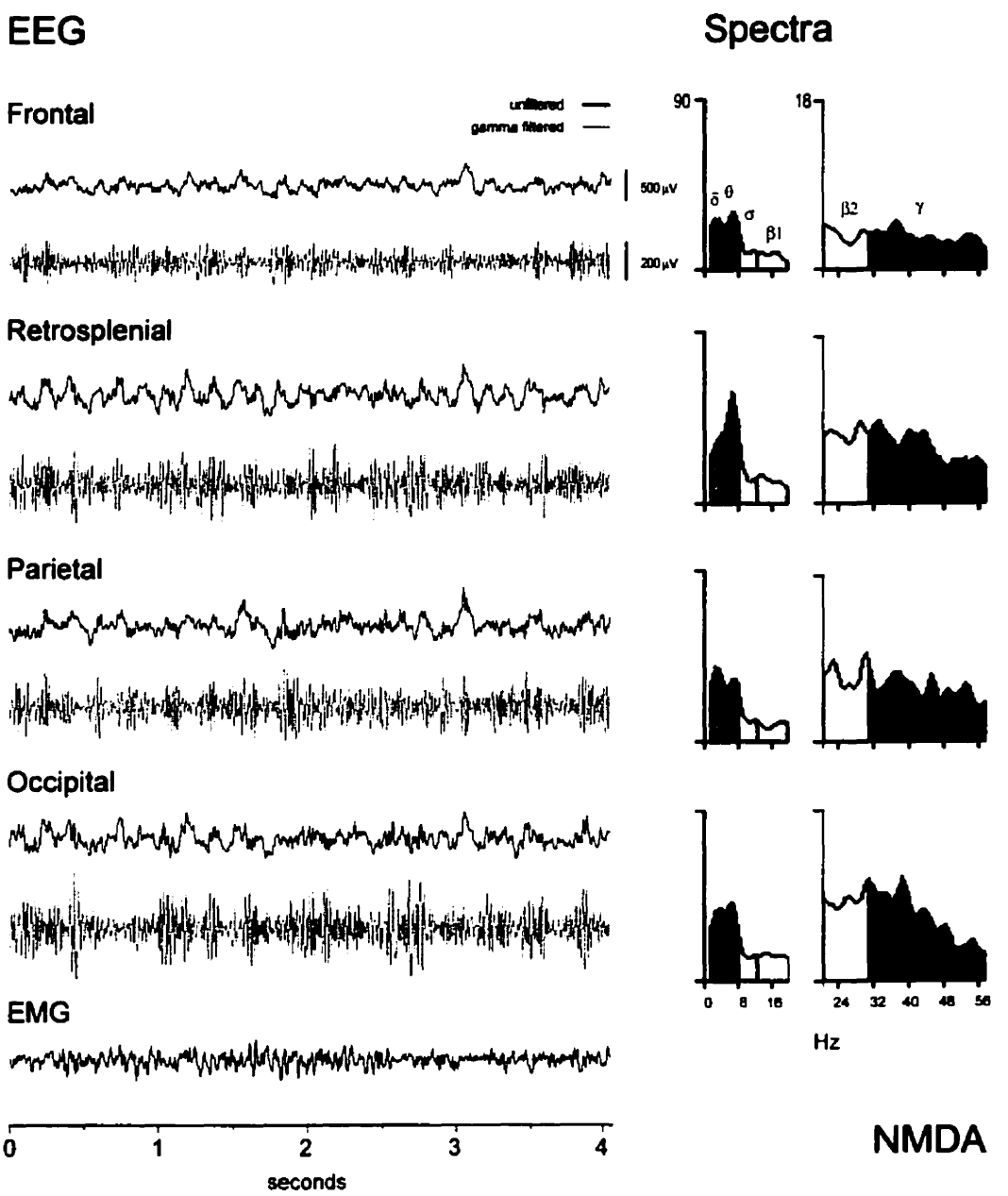
EEG
Spectra
Frontal
unfiltered
gamma filtered
500 µV
200 µV
90
18
δ θ
σ
β1
β2
γ
Retrosplenial
Parietal
Occipital
EMG
0 8 16
24 32 40 48 56
Hz
0 1 2 3 4
seconds
NMDA

Figure 13. Drawing of the injection site in relation to cholinergic and GABAergic neurons in the basal forebrain of the rat. In the top panel, the cannulae were drawn according to the location of their tracks through the brain and in relation to ChAT-immunostained cells. The diffusion of the chemical solution was depicted according to estimates based upon previous injections of the same volume (0.5 μl) of neuroanatomical tracers into the basal forebrain (Jones and Yang, 1985; Jones and Beaudet, 1987; Jones and Cuello, 1989). The lower panel illustrates the location of cells which were dual-immunostained for ChAT (ChAT+/c-Fos+, circles) or GAD (GAD+/c-Fos+, triangles) and c-Fos. The ChAT+/c-Fos+ cells in the lower panel represent a subset of the single labeled ChAT+ cells in the upper panel. The cells were mapped using an image analysis system. Abbreviations: ac, anterior commissure; CPu, caudate putamen; GP, globus pallidus; ic, internal capsule; LPO, lateral preoptic area; MCPO, magnocellular preoptic nucleus; MPA, medial preoptic area; oc, optic chiasm; SI, substantia innominata; st, stria terminalis.

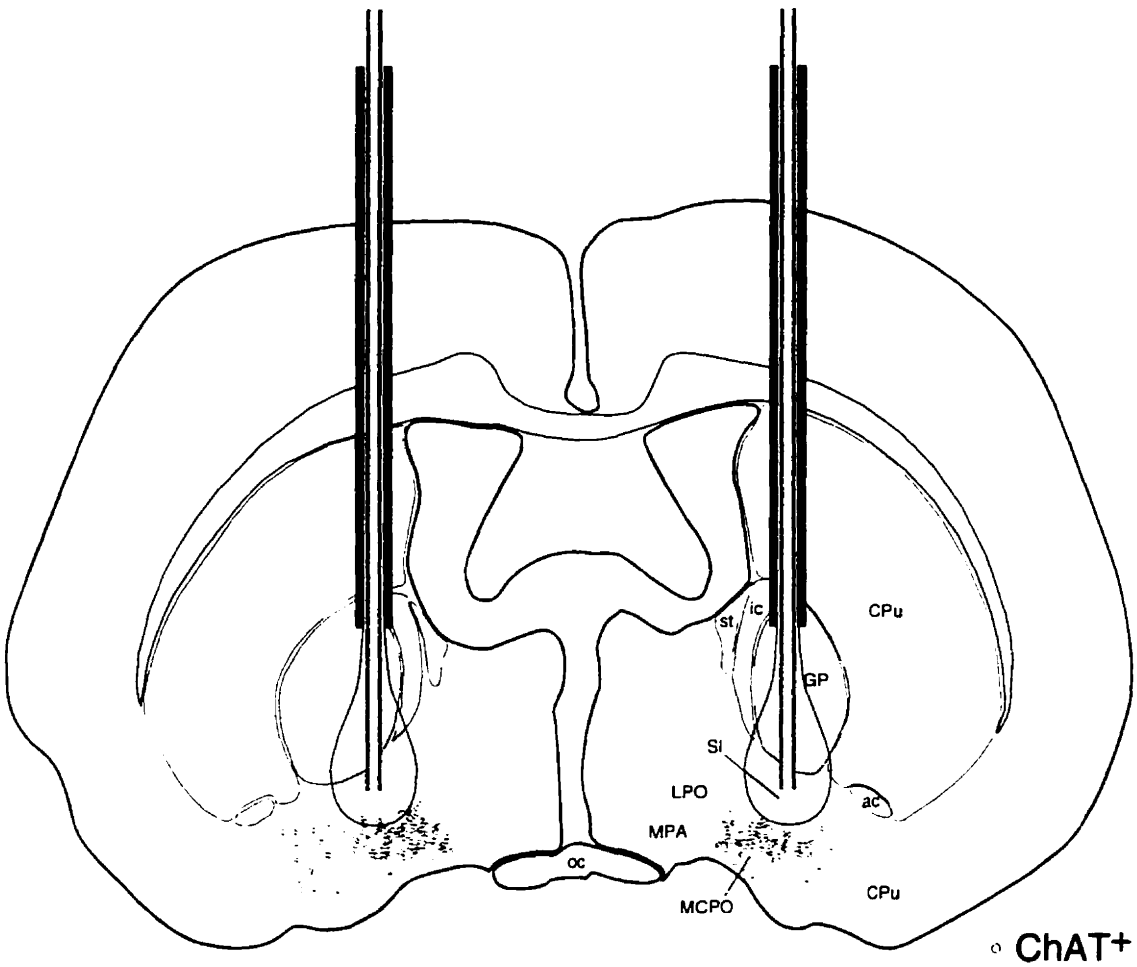
st
ic
CPu
GP
SI
LPO
ac
MPA
oc
MCPO
CPu
○ ChAT+

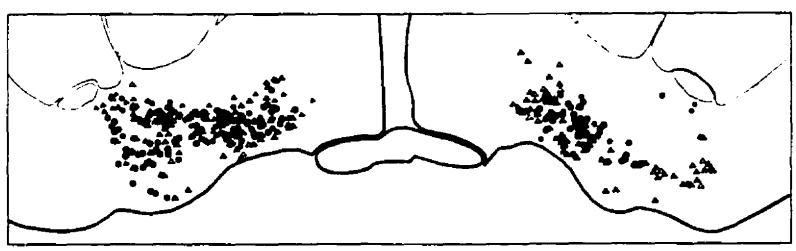
• ChAT+/c-Fos+
△ GAD+ /c-Fos+
1 mm

Figure 14. Photomicrographs of cholinergic and GABAergic cells in the basal forebrain of the rat. Sections are dual-immunostained for ChAT on the left or GAD on the right (floccular staining, DAB) and c-Fos (granular staining, BDHC). Black arrowheads indicate examples of double-labeled cholinergic (ChAT+/c-Fos+) or GABAergic (GAD+/c-Fos+) cells and white arrowheads indicate examples of adjacent single-labeled c-Fos+ cells. Magnification bar = 20 μm.

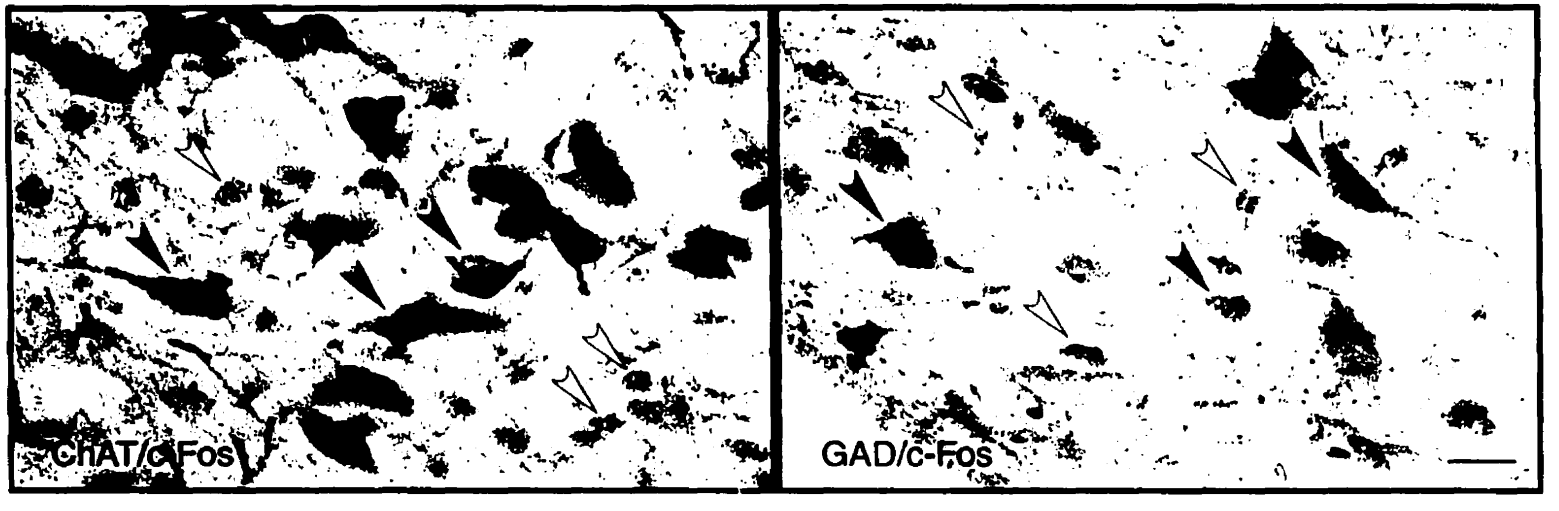
ChAT/c-Fos
GAD/c-Fos

Table 1. EEG frequency peaks and band amplitudes obtained from spectral analysis of 4 sec epochs from four cortical areas across ringer, procaine, AMPA and NMDA drug conditions. [1]

Measure	Area	Drug: Ringer Mean	SEM	Procaine Mean	SEM	AMPA Mean	SEM	NMDA Mean	SEM	ANCOVA: Drug (F)	df	p	Area (F)	df	p	Drug* Area(F)	df	p
Peak Freq (Hz)																		
High	**Avg**	**36.07**	**± 0.25**	**35.00**	**± 0.26^{R}**	**35.51**	**± 0.36**	**36.81**	**± 0.41^{PPP,A}**	**4.87**	**3**	******	**3.77**	**3**	*****	**1.46**	**9**	
(30-60 Hz)	F	35.60	± 0.50	34.26	± 0.24	34.37	± 0.67	37.63	± 1.01									
	RS	36.21	± 0.53	34.52	± 0.35	34.85	± 0.61	36.30	± 0.66									
	P	35.13	± 0.36	35.41	± 0.63	35.37	± 0.65	36.78	± 0.88									
	O	37.33	± 0.53	35.82	± 0.69	37.44	± 0.83	36.52	± 0.71									
Low	**Avg**	**4.07**	**± 0.12**	**2.55**	**± 0.09^{RRR}**	**4.93**	**± 0.24^{RR,PPP}**	**5.09**	**± 0.17^{RRR,PPP}**	**38.46**	**3**	*******	**3.12**	**3**	*****	**0.50**	**9**	
(1-10 Hz)	F	3.73	± 0.23	2.33	± 0.08	4.36	± 0.47	4.57	± 0.36									
	RS	4.00	± 0.24	2.43	± 0.17	5.58	± 0.47	5.48	± 0.34									
	P	4.51	± 0.26	2.80	± 0.23	4.94	± 0.45	5.41	± 0.33									
	O	4.03	± 0.25	2.65	± 0.23	4.82	± 0.53	4.91	± 0.35									
Band Amp (AD)																		
Gamma	**Avg**	**154.82**	**± 5.12**	**122.86**	**± 3.67^{RR}**	**186.56**	**± 8.39^{RRR,PPP}**	**195.15**	**± 11.95^{RRR,PPP}**	**17.92**	**3**	*******	**145.50**	**3**	*******	**2.69**	**9**	******
	F	79.94	± 4.66	72.52	± 5.67	87.52	± 7.85	139.04	± 20.79^{RRR,PPP}	6.70	3	***						
	RS	187.76	± 4.55	152.33	± 3.87^{R}	213.89	± 12.23^{PP}	209.59	± 20.88^{P}	3.04	3	*						
	P	162.76	± 7.31	130.22	± 4.83	195.33	± 8.81^{RR,PPP}	205.41	± 22.33^{RR,PPP}	7.10	3	***						
	O	188.83	± 14.18	136.37	± 3.36	249.48	± 17.55^{RR,PPP}	226.56	± 28.47^{PP}	5.50	3	***						
Delta	**Avg**	**164.14**	**± 6.61**	**270.75**	**± 9.09^{RRR}**	**123.71**	**± 5.73^{RRR,PPP}**	**109.91**	**± 4.46^{RRR,PPP}**	**85.07**	**3**	*******	**32.00**	**3**	*******	**1.58**	**9**	
	F	99.35	± 7.17	188.52	± 10.98	86.82	± 7.25	91.00	± 7.31									
	RS	225.73	± 16.14	326.00	± 17.85	134.15	± 8.36	118.41	± 7.74									
	P	144.14	± 9.66	257.37	± 11.62	121.70	± 10.02	105.96	± 9.40									
	O	187.35	± 12.57	311.11	± 18.40	152.19	± 15.17	124.26	± 10.02									
Theta/Delta	**Avg**	**1.31**	**± 0.04**	**0.81**	**± 0.02^{RRR}**	**1.36**	**± 0.04^{RR,PP}**	**1.54**	**± 0.05^{RRR,PPP,A}**	**75.959**	**3**	*******	**4.806**	**3**	******	**1.557**	**9**	
	F	1.11	± 0.06	0.75	± 0.03	1.32	± 0.06	1.37	± 0.09									
	RS	1.41	± 0.10	0.78	± 0.04	1.47	± 0.07	1.78	± 0.10									
	P	1.35	± 0.06	0.86	± 0.05	1.38	± 0.07	1.54	± 0.09									
	O	1.36	± 0.07	0.84	± 0.05	1.28	± 0.08	1.47	± 0.09									
EMG		**286.03**	**± 42.77**	**286.48**	**± 41.13^{R}**	**634.11**	**± 57.98^{RRR,PP}**	**488.82**	**± 46.66^{RRR,PP}**	**19.979**	**3**	*******	.			.		

[1] Measures were taken from 9, 4 sec samples (at one minute intervals from 5 to 13 minutes post-injection) from the 4 cortical areas (F, frontal; RS, retrosplenial; P, parietal; O, occipital) following each drug condition (Ringer, n=7; Procaine, n=3; AMPA, n=3; NMDA, n=3 rats). Statistics were performed on natural log (Ln) transformed values that were normally distributed. The average (Avg) values per Drug and the individual values for each Area per Drug (mean and SEM) were calculated and reported from the raw values in Hz for frequency, in AD units for amplitude bands (100 μV ≡ 125 AD units) for EEG and EMG, or as the ratio of theta/delta. An analysis of covariance (ANCOVA) was performed with each EEG measure as the dependent variable, Drug (4) and Area (4) as the independent variables and Sample (9) and Rat (n=9) as covariates (with df_{error} = 558). In the case of a significant main effect of Drug (*, p<.05; **, p≤ .01; ***, p≤.001) , post-hoc paired comparisons were performed using Fisher's least significant difference with symbols R, P and A (for ringer, procaine and AMPA) indicating differences relative to that drug condition (and one to three symbols indicating probabilities as per *). In the case of a significant interaction between Drug and Area that occurred for Gamma amplitude, individual ANCOVAs were performed for each cortical area across Drugs (with df_{error} =

NEUROTENSIN-INDUCED BURSTING OF CHOLINERGIC BASAL FOREBRAIN NEURONS PROMOTES THETA AND GAMMA ACTIVITY TOGETHER WITH WAKING AND PARADOXICAL SLEEP

Edmund G. Cape, Ian D. Manns, Angel Alonso,

Alain Beaudet and Barbara E. Jones

A version of this manuscript is in press with the Journal of Neuroscience 2000.

PREFACE

Basal forebrain cholinergic cells are endowed with receptors for NT as shown by binding and internalization of NT *in vitro*. NT elicits a depolarization and excitation and induces rhythmic bursting in the cholinergic neurons in brain slices, where it was also not found to affect non-cholinergic cells. Thus the present study was undertaken *in vivo* to determine the effects of direct, selective modulation of cholinergic basalis neurons and of eliciting rhythmic burst discharge in the cholinergic cells upon EEG activity and sleep-wake state.

To observe the selectivity and character of the modulation in an *in vivo* preparation, local microinjections of a fluorescent NT derivative (Fluo-NT) were examined first to assess whether following microinjection, NT is bound and internalized by cholinergic neurons. Confocal microscopic analysis was employed to determine if Fluo-NT labeling occurred in ChAT-immunoreactive and thus cholinergic basal forebrain neurons. To monitor the modulation in basal forebrain unit activity in response to microinjection of NT, NT was administered by similar microinjection in urethane-anaesthetized rats while recording single unit activity prior to, during, and following injection of NT. The cells were subsequently juxtacellularly labeled and processed for ChAT immunostaining. In the main series of experiments, NT microinjections were performed in freely moving, naturally sleeping-waking rats to measure the effects upon EEG activity, including importantly theta and gamma activity, and upon sleep-wake states.

ABSTRACT

It is known that the basal forebrain cholinergic neurons are important for the modulation of cortical activity across the sleep-waking cycle. These cells are endowed with receptors for NT as shown *in vitro* by selective binding and internalization of NT. NT elicits a depolarization and excitation and notably, induces a rhythmic burst discharge selectively in the cholinergic cells in basal forebrain slices. Given this selective and potent modulation of cholinergic neurons documented *in vitro*, we sought to examine the effects of NT administered into the basal forebrain *in vivo*. The *in vivo* effects of local microinjections of either NT or a fluorescent NT derivative (Fluo-NT) into the basal forebrain were examined on behavior, EEG activity and sleep-wake states in freely moving, naturally sleeping-waking rats. NT microinjections (0.1 to 3.0 mM concentration) produced a dose-dependent decrease in delta activity and an increase in both theta and high frequency gamma activity, measured during a 30 min post-injection period. This EEG pattern was associated with a behaviorally quiet waking state that alternated with paradoxical sleep (PS) and transitional (*t*) PS with no intervening SWS. There were dose-dependent increases in Wake, *t*PS and PS and reciprocal decreases in *t*SWS and SWS. The effects of NT were largely antagonized with systemic injection of the muscarinic antagonist, atropine. To assess binding and internalization of NT in basal forebrain cells, animals were injected with [0.25 mM] Fluo-NT and sacrificed 20 minutes after the injection when the effect upon EEG and state was evident. Confocal microscopic analysis revealed punctate Fluo-NT labeling in the cytoplasm of choline acetyltransferase (ChAT)-immunoreactive, and thus cholinergic, basal forebrain neurons. To monitor the effect upon basal forebrain neurons, single units were recorded in association with EEG prior to, during, and following unilateral microinjection of [1.0 mM] NT in urethane-anesthetized rats. Following successful recordings, the cells

were subsequently labeled with neurobiotin (Nb) using the juxtacellular labeling technique and processed by dual staining for Nb and ChAT for the immunohistochemical identification of cholinergic cells. Identified cholinergic cells showed increases in discharge and a shift to a bursting discharge that became rhythmic with the appearance of theta-like activity on the EEG following NT. The rhythmic unit discharge was correlated with the rhythmic EEG activity. These results suggest that NT, while being internalized, has the capacity to induce rhythmic bursting in cholinergic basal forebrain neurons, which in turn modulates cortical activity in a rhythmic manner evident as theta and associated with gamma EEG activity. These EEG changes occur together with enhanced waking and PS states.

INTRODUCTION

As the primary source of cholinergic innervation to the cerebral cortex (Shute and Lewis, 1967), basal forebrain (BF) cholinergic neurons have been shown to play a major role in the modulation of cortical activity in association with behavioral state. Lesions of basal forebrain cholinergic cells decrease cortical acetylcholine (ACh) release with a parallel decrease in cortical activation (Buzsaki *et al.*, 1988; Lo Conte *et al.*, 1982; Stewart *et al.*, 1984), while electrical stimulation of the cholinergic basalis neurons leads to an increase in cortical ACh release and cortical activation (Casamenti *et al.*, 1986). Accordingly, they are believed to play an important role in the generation and transmission of activating input from the brainstem to the cortex during waking and paradoxical sleep (PS). Despite the clear significance of the cholinergic BF system in cortical activation, over the last decade, numerous immunohistochemical studies have demonstrated that the BF is in fact comprised of a heterogeneous population of neurons. The cholinergic neurons appear to be outnumbered by GABAergic neurons, many of which also project to the cortical mantle (Gritti *et al.*, 1993, 1994). Such non-cholinergic neurons have also been shown to have the capacity, like cholinergic neurons, to discharge rhythmically, albeit in very different patterns and subtended by different mechanisms than the cholinergic cells (Alonso *et al.*, 1996). These results would suggest that cholinergic and non-cholinergic basalo-cortical neurons may modulate the cortex in a rhythmic manner in association with cortical activation that occurs during waking and paradoxical sleep. Indeed, we have recently provided evidence *in vivo* that NMDA, which has been shown to induce rhythmic bursting by cholinergic neurons *in vitro* (Khateb *et al.*, 1994) elicits theta together with enhanced gamma EEG activity in association with an active waking state when microinjected into the basal forebrain in freely moving naturally waking-sleeping rats (Cape and Jones,

2000). As evidenced by c-Fos activation in that study, however, NMDA is, of course, not selective in stimulating cholinergic neurons and its effect was attributed to its action upon GABAergic and other non-cholinergic in addition to the cholinergic neurons in the basal forebrain.

Neurotensin (NT), a tridecapeptide, seems to occupy a strategic position in its capacity to modulate basal forebrain cholinergic neurons in a selective manner. While NT is found throughout the CNS (Uhl *et al.*, 1977; Jennes *et al.*, 1982; Woulfe and Beaudet. 1989), the NT high affinity receptor within the BF seems to be selectively present on cholinergic neurons (Szigethy *et al.*, 1989, 1990; Alonso *et al.*, 1994). Moreover, the fact that the ligand complex is internalized (Faure *et al.*, 1995a) allows the convenient tracking of cells being modulated by NT and thus provides an efficient, reliable means of identifying neurons that bind NT. Light and electron microscopic studies (Szigethy *et al.*, 1989, 1990) have confirmed that NT and its fluorescent analog (Fluo-NT) is internalized selectively in ChAT-immunoreactive neurons in the basal forebrain (Faure *et al.*, 1995a). Moreover, *in vitro* electrophysiological studies found that NT selectively excited cholinergic neurons and stimulated them to discharge in rhythmic bursts (Alonso *et al.*, 1994). NT thus appeared to be an ideal substance capable of selective modulation of cholinergic basal forebrain neurons and induction of rhythmic burst discharge in these cells.

Although it has been well established that septal neurons play a crucial role in hippocampal theta rhythm generation (Vanderwolf 1975; Bland, 1986; Buzsaki *et al.*, 1988; Stewart and Fox, 1990), it has only recently been shown that BF cholinergic neurons are capable of generating rhythmic burst patterns of discharge in association with cortical activation and rhythmic slow activity in neocortex (Manns *et al.*, 2000). With this knowledge, it would appear likely that rhythmic burst discharge by cholinergic

neurons could modulate cortical activity at a theta-like frequency, while also stimulating gamma activity, and potentially eliciting waking and/or paradoxical sleep states during which these activities normally occur. In the present study, we sought to test this hypothesis by administering NT by local microinjection into the basal forebrain of freely moving, naturally sleeping-waking rats. In the same study, we examined whether NT, by using the fluorescent analog Fluo-NT appeared to bind and be internalized by cholinergic neurons, and whether it induced burst discharge in identified cholinergic neurons. Preliminary results of this study have been reported (Cape *et al.*, 1996, 1998, 1999).

METHODS

Animals and surgery

Microinjection experiments in freely moving, naturally sleeping-waking rats employed twenty-two (22) male Wistars (200 – 215 g, Charles River, Canada). The rats were operated on for implantation of chronically indwelling guide cannulae and EEG electrodes under barbiturate anesthesia (Somnotol, 67 mg/Kg). Surface EEG electrodes were placed bilaterally on the dura over the frontal, retrosplenial and parietal cortices in addition to the right occipital cortex as previously described (Cape and Jones, 1998). Field potential recordings were also performed in some animals within the hippocampus (-4.0 mm AP, 2.2 mm L, -3.5 mm V relative to bregma) and entorhinal cortex (-7.6 mm AP, 5.2 mm L, -7.2 mm V relative to bregma) using tripolar tungsten wire electrodes. EMG was recorded using 2 stainless steel wires inserted in the neck musculature. Guide cannulae were placed using a stereotaxic apparatus 2 mm above the basal forebrain target such that the tips of cannulae (extending 2 mm beyond the guides) were placed in the region of the basal forebrain (7.6 mm AP, 2.5 mm L, and 1.5 V relative to ear bar zero). Animals recovered for a minimum of two days in the animal facilities before being individually housed in a plexiglas box inside a large electrically shielded recording chamber. Rats were maintained on a 12:12 light-dark cycle with food and water available *ad lib*.

For combined unit recording and microinjection experiments acute experiments were performed on 6 adult Long Evans rats (200-250 g, Charles River, Canada) anesthetized with urethane (ethyl carbamate; Sigma, St.-Louis, Mo; initial i.p. dose 1.4 g/Kg). Adequate anesthesia was confirmed by the lack of withdrawal in response to pinching of the hind limb. Additional anesthetic (0.1 – 0.15 g/Kg, i.p.) was administered

if a response appeared. Body temperature was maintained at 37°C with a heating pad attached to a thermostatic control instrument (Yellow Springs Instruments, Yellow Springs, OH). The animals were placed in a stereotaxic frame (David Kopf Instruments, Tujunga, CA) and held there for the duration of the experiment. Trephine windows were made in the cranium over the left and right basal forebrain for descent of microelectrodes. For recording of EEG, stainless steel screws were threaded into the skull to come into contact with the dura over the retrosplenial cortex (–4 mm AP, ± 0.5 mm L relative to bregma). For the purpose of antidromic activation of basal forebrain units, a bipolar stimulating electrode (with a separation of 0.5 mm between the tips) was placed in the prefrontal cortex on each side (2.0 mm AP, ± 1.0 mm L, and -2.0 mm V). This electrode was also used to record the field potential in the prefrontal cortex.

EEG recording and behavioral observations

Signals were recorded using a Grass model 78D polygraph and sent to an IBM compatible computer for digitization, storage and subsequent analysis using Stellate Systems software (Montreal, Quebec). Behavioral observations were made using a video camera and monitor. Nine categories of behavior were recorded on the on-line EEG record: attentive, moving, eating, grooming, and quiet waking behaviors were noted in addition to uncurled, curled, moving (postural shifts), and twitch sleeping behaviors (Maloney *et al.*, 1997).

Experiments were performed beginning in the late morning and usually ending by 1500h. The EEG computer file consisted of a morning recording period (~1100-1130) taken prior to handling and an afternoon recording period (~1230-1500) taken following placement of the inner injection cannulae. The afternoon recording began once the rat had resumed sleeping. Baseline recordings were the first recordings to be

performed and occurred at least two days following introduction to the new environment. During the baseline experiment, animals were picked up and handled as would occur during an experiment with insertion of the cannulae.

Microinjections

The ringer and NT microinjections proceeded in several stages as previously described (Cape and Jones, 1998) (Figs. 3, 4). The pre-injection period was defined as the 30 minute morning recording, at the end of which point the injection apparatus was installed. The injection began once the animal recovered from the handling procedure, at which point the cannulae were lowered by remote control before waiting 2 minutes before initiating the microinjection. The microinjection took place over the course of 5 minutes. The post-injection period was defined as the 30 minute period immediately following the complete delivery of the injection.

Bilateral microinjections were delivered using 1 μl Hamilton syringes (Reno, Nevada) simultaneously driven by a syringe pump (Sage Instruments, Cambridge, Mass). The solutions were injected in a volume of 0.5 μl over the course of 5 min. Initial doses and or concentrations of drugs were based in part on published studies (Faure *et al.*, 1995a; Lambert *et al.*, 1996) and the dose that produced a consistent robust effect. In pilot experiments in three (3) rats, 0.500, 1.00 and 1.50 nmol (240 ng, 480 ng and 720 ng) doses were tested. A 0.500 nmol dose was selected and administered to 5 rats as 240 ng NT in 0.5μl per side corresponding to 1 mM concentration for the main series of experiments. Dose response analysis was subsequently performed by repeated trials on 7 animals. Five doses were tested including ringer and representing in concentration 0, 0.10, 0.25, 1.00 and 3.00 mM. Drug administrations were separated by a minimum 48 hr interval and doses as well as ringer were randomized in the order in which they

were administered across animals. The complete series of five doses was successfully obtained from 4 of the 7 rats.

The NT effect on EEG activity was tested in the presence of the muscarinic antagonist, atropine in 3 animals. In these experiments, atropine (30 mg/Kg, i.p.) was administered once the microinjection inner cannulae were inserted, which was usually approximately thirty minutes prior to the microinjection of NT, depending upon the time taken by each animal to relax after placement of the cannulae. NT was subsequently microinjected at a dose of 0.125 nmole corresponding to 0.25 mM concentration, following the established microinjection protocol.

Microinjection of Fluo-NT

Fluo-NT was administered at a dose of 0.125 nmole or 0.25 mM concentration in a manner similar to that for NT (above) in 4 rats following pilot studies with 3 rats that received one of 0.500 nmole, 0.250 nmole and 0.050 nmole doses. Recording was performed for 15 minutes following the Fluo-NT microinjection before the animal was sacrificed (below). The chosen dose represented the second dose within the dose response analysis yielding sufficient fluorescent labeling together with a significant pharmacological effect. Fluo-NT was dissolved in ringer solution and 15 mg/ml relatorphan (a peptidase inhibitor). Nα-Bodipy-NT, generically referred to as Fluo-NT, was synthesized and purified as described by Faure *et al.*, 1995b. The pharmacological properties of this ligand have been characterized extensively elsewhere (Faure *et al.*, 1995b). Three (3) acute preparations under pentobarbital anesthesia (Somnotol, 67 mg/Kg) were used to verify the specificity of the Fluo-NT internalization process by administering equal amounts of Fluo-NT per side (60 ng, ≈ 0.110 nmol) with one side co-injected with excess amounts of NT (360 ng, ≈ 0.650 nmol).

EEG and sleep-wake state data analysis

The polygraph record was scored off-line by visual assessment of 20 sec epochs and labeled as either Wake (W), transition into Slow Wave Sleep (*t*SWS), Slow Wave Sleep (SWS), transition into Paradoxical Sleep (*t*PS) or Paradoxical Sleep (PS) (Maloney *et al.*, 1997). Behavioral annotations were considered together with the EEG and EMG activities for state scoring, particularly during the post-injection condition. Consequently, the annotations were used in order to identify any dissociation between behavior and the normal associated EEG patterns of the different states (Maloney *et al.*, 1997). Each state was reported for the post-injection recording period as % of total recording time.

Spectra were computed using Stellate Systems software by Fast Fourier Transform (FFT) based on 512 points corresponding to 2 sec epochs (256 samples/sec) with a resolution of 0.5 Hz. A 7-point smoothing window is applied by this program thus allowing a minimum of 1.5 Hz and a maximum 63.5 Hz in the spectral computation. Frequency bands were defined as delta: 1.5 – 4.0 Hz, theta: 4.5 – 8.5 Hz, sigma: 9.0 – 14.0 Hz, beta1: 14.5 – 18.5 Hz, beta2: 19:0 – 30.0 Hz and gamma: 30.5 – 58.0 Hz (eliminating frequencies around 60.0 Hz to avoid any possible contamination from AC noise) (Maloney *et al.*, 1997). Based upon scored records, sleep-wake hypnograms were displayed in association with EEG frequency band activities for 20 sec epochs over the recording sessions using Eclipse software (Stellate Systems). Spectral analysis was also performed on a subset of rats (below) across all the right cortical leads using Rhythm software (Stellate Systems). Spectrum and frequency band activities were displayed and reported in AD amplitude units for which the average gain was calibrated as (1500 AD units per mV on the EEG channels). The ratio of theta/delta was calculated and reported as a reflection of regular theta activity in the EEG (Maloney *et*

al., 1997). EMG amplitude was computed for the total spectrum up to 58.0 Hz. Plotting the EEG and EMG data for the figures was accomplished with Origin (v5.0) (Microcal Software, Northampton, MA).

EEG records and hypnograms displaying sleep-wake state and frequency band activity were examined following recording to establish a normal EEG and an effective microinjection. Of 22 rats, 2 were eliminated from the single dose experiments due to abnormal seizure activity common to rodents (Vergnes *et al.*, 1982).

Statistical analysis

The data were analyzed in several different ways according to the specific experiment. First, the effects of [1mM] NT were examined across all animals (n=9) upon retrosplenial EEG activity and sleep-wake state by employing simple paired t tests per variable. In this case, relative EEG activity (% total activity) was examined for gamma and delta and each of the sleep-wake states. Second, the effects of different concentrations of NT were analyzed for the repeated trials (n=4) and thus using a repeated measures ANOVA. In this case, absolute amplitude of gamma and delta retrosplenial EEG activity was examined, for which reason the EEG data were entered as the natural log values (Ln) in order to normalize the data. For each variable, (gamma, delta, theta/delta and EMG), repeated measures analysis of variance (ANOVA) was performed with dose entered as the metric 0, 0.10, 0.25, 1.0, 3.0 corresponding to the mM concentrations of the NT solution. Dose-dependent changes in sleep-wake states were similarly analyzed, but the transitional states were grouped with their respective states for simplification (*t*SWS with SWS and *t*PS with PS). In a third series aimed at examining changes in peak frequency together with absolute amplitude of EEG activity from all cortical leads, spectra were sampled in 5 rats having

received [1 mM] NT. Nine (9), 4 sec epoch samples were taken at exactly one minute intervals in the period between approximately 4 – 12 minutes following the end of the microinjection of NT and ringer, when the effect was maximal and most uniform for NT. In order to compare these measures across regions, the data were first normalized by taking the natural log (Ln) values of each measure. An analysis of covariance was subsequently employed with the EEG measurement as the dependent variable, drug (ringer and NT) and area (frontal, retrosplenial, parietal and occipital) as independent or grouping variables, and spectral sample (9) as covariates. The antagonism experiments with atropine (n=3) were analyzed with a repeated measures ANOVA across drug trials: ringer, NT and atropine & NT for each EEG dependent variable: %gamma, %delta, and theta/delta. A similar model was created to examine changes in the sleep-wake states, in this case examining the totals of *t*SWS +SWS and *t*PS + PS. With significant main effects, post-hoc paired comparisons were performed using the appropriate orthogonal c-matrices to examine the hypothesis that atropine reversed the effect of NT upon EEG activity and state. Lastly, in the Fluo-NT studies (n=3), the EEG activity and sleep-wake states were analyzed for the 15 min post-injection period prior to sacrifice and accordingly compared to a 15 min post-injection period following unlabelled NT injected in the same concentration of 25 mM. All statistics were performed using Systat (v9.0) software (Evanston, Illinois).

Unit recording and labeling

Unit recordings were performed with glass microelectrodes, which were pulled to a fine tip, broken to an external diameter of ~0.5 -1.5 μm, and filled with 0.5 M sodium acetate containing 2.5 - 5.0% Neurobiotin (Nb) (Vector Laboratories, Burlingame, CA). Using a hydrostatic micromanipulator (MX510, Newport Corp., Irvine, CA), the electrode was moved into the region of the basal forebrain to a position just below the anterior

commissure. At this juncture, single units were isolated as the electrode was descended through the basal forebrain. Upon isolation, the units were characterized in association with spontaneous irregular slow wave activity and stimulation-induced rhythmic slow activity on the EEG. The stimulation consisted of a continuous pinch of the tail. Neurons were also tested for their response to antidromic stimulation from the prefrontal cortex. Antidromic criteria included the ability to follow single pulses (0.3 ms, 100 - 600 μA) with a constant latency and to follow high frequency stimulus trains of two or three pulses at 100 - 200 Hz. NT microinjection was then performed to assess its effect upon unit activity. After the injection neurons were labeled using the 'juxtacellular' method (Pinault 1996; Manns *et al.*, 2000).

Unit discharge was examined prior to the adminstration of NT, immediately following and during the maximal effect of NT. Using one minute epochs of stationary data, the average discharge rate was calculated from the peri-stimulus histogram (PSH), the predominant instantaneous firing frequency determined from the first-order interspike interval histogram (ISIH) and the presence of rhythmic unit and unit-to-EEG cross-correlated discharge was assessed by auto-correlation histogram (ACH) and spike triggered averaging (STA), as described previously (Manns *et al.*, 2000).

Immunohistochemistry & Immunofluorescence

Animals were sacrificed under barbiturate anesthesia (Somnotol, ~120 mg/kg) and perfused through the heart with a fixative solution (3.0% paraformaldehyde, as published previously; Gritti *et al.*, 1993). The brains were frozen and subsequently processed for histochemistry.

In animals having received microinjections of NT, the brains were collected for immunohistochemical processing for ChAT to allow assessment of the injection sites in

relation to the cholinergic basal forebrain cell population. Coronal sections were cut at 25 μm thickness on a freezing microtome. Series of adjacent sections were collected every 200 μm for immunohistochemical processing. Immunohistochemistry was performed using the peroxidase-antiperoxidase (PAP) technique, according to previously published procedures (Gritti et al., 1993; Maloney et al., 1999). Sections were incubated overnight with rabbit anti-ChAT antiserum (1:3000, Chemicon International, Temecula, CA) at room temperature using a Tris saline solution (0.1M) containing 1% normal donkey serum (NDS), following a pre-incubation with Tris saline containing 6% NDS and Triton (0.1%). They were subsequently placed in donkey anti-rabbit secondary antisera and then in rabbit PAP antibodies (Jackson ImmunoResearch Laboratories, West Grove, PA). The peroxidase was revealed with diamino benzidine (DAB).

In animals having received microinjections of Fluo-NT, coronal sections were cut 20 μm thick on a freezing microtome. Series of adjacent sections were collected every 200 μm for processing. Half of the series was cold mounted for simple visualization of the Fluo-NT fluorescence and the other half was free-floated for immunofluorescent staining of ChAT and dual visualization of Fluo-NT and ChAT.

For immunofluorescent staining of ChAT, sections were initially floated in NaPB, rinsed twice (10 min per rinse) in Tris saline before incubated at 4°C overnight in rabbit anti-ChAT antiserum (1:200, Chemicon International Temecula, CA). Following rinsing, they were incubated for 2 hours at room temperature with Goat anti-Rabbit Texas Red (1:50, Jackson ImmunoResearch Laboratories, West Grove, PA). The slides were coverslipped using aqua polymount (Polyscience, Warrington, PA).

For dual labeling of Neurobiotin and ChAT to determine if the labeled neurons were cholinergic, coronal frozen sections were cut at 30 μm, washed thoroughly in

phosphate buffer and incubated overnight in a primary antibody for ChAT (rabbit anti-ChAT antiserum, 1:3500, Chemicon, Temecula, CA). The following day, the sections were washed and incubated with secondary antibodies for 2.5 hours. A Cy2-conjugated streptavidin (1:800, Jackson ImmunoResearch Laboratories, Inc., West Grove, PA), was used to reveal Nb. A Cy3-conjugated donkey anti-rabbit antiserum (1:1000, Jackson ImmunoResearch Laboratories), was used to reveal ChAT-immunostaining. Sections were then mounted and viewed by fluorescent microscopy using a Leitz Dialux microscope equipped with a Ploemopak 2 reflected light fluorescence illuminator with Leica filter cubes for fluorescein (I3) and rhodamine (N2.1).

Confocal Microscopy

Sections were examined using a Zeiss confocal laser scanning microscope (CLSM 410) equipped with an Axiovert 100 inverted microscope and an argon/krypton laser. FITC signals for Fluo-NT were imaged by exciting samples with 488 nm light, and Texas red for ChAT in the same sections by 568 nm light. Images were acquired sequentially as single transcellular optical sections and averaged over 32 scans/frame. Images, processed using the Carl Zeiss CLSM software (v3.1), were mounted and prepared for publication using Adobe Photoshop (v5.0) (Adobe Systems, San Jose, CA).

RESULTS

The sites of microinjection were confirmed as being symmetrically placed above the major population of basal forebrain cholinergic neurons by viewing the tracks of the cannulae in relation to ChAT-immunostained cells in peroxidase immunostained material (Fig. 1). The tracks were evident passing through the caudate putamen and medial part of the globus pallidus and extending ventrally into the substantia innominata (SI) above the magnocellular preoptic nucleus (MCPO), where large numbers of ChAT-immunoreactive cells are located (Fig. 1).

In brains of animals having received microinjections of Fluo-NT (n=4, see below), evidence of fluorescent labeling was visible by light microscopy immediately surrounding the tracks of the inner injection cannulae. A light diffuse fluorescent staining of the cytoplasm of a small number of cells was evident in the immediate vicinity of these tracks. Beyond this region, very light and fine labeling was detectable in the SI and MCPO. When examined by confocal laser scanning microscopy, this fluorescent staining was seen to correspond to punctate labeling within the cytoplasm of neuronal perikarya (Fig. 2, left). The Fluo-NT punctate fluorescent staining was evident predominantly in medium-to-large cells, which varied in shape from fusiform to polygonal. Such Fluo-NT+ cells were found within the SI and MCPO extending in a radius of up to 1 mm from the injection tracks and thus beyond the region which was estimated by volume of the solution as the immediate injection site. In sections immunostained for ChAT, it appeared that although diffuse fluorescent labeling was present in some ChAT-negative cells in the immediate vicinity of the tracks, the Fluo-NT punctate labeling was found within ChAT-immunostained neurons in the SI and MCPO (Fig. 2, right).

The specificity of the labeling with Fluo-NT was tested in acute experiments in anesthetized rats by simultaneous injections of excess unlabelled NT (360 ng, ~ 1.5 mM) on one side in animals receiving bilateral microinjections of Fluo-NT (60 ng, ~ 0.25 mM). In these experiments, although some diffuse fluorescent labeling remained in neurons around the track, the punctate Fluo-NT perikaryal labeling was not visible on the side of the co-injected unlabelled NT (n=3, not shown), as analyzed by confocal laser scanning microscopy.

Effects of Neurotensin on EEG and Sleep-Wake States

Microinjections of NT into the basal forebrain altered the EEG and natural sleep-wake cycle of the rat (Figs. 3 and 4). Once the NT-filled cannulae were lowered into the tissue and for the duration of the injection and post-injection periods (Fig. 4), delta activity was diminished and associated with a loss of SWS during the day, when the rat is normally in SWS the majority of the time (Fig. 3). In the absence of delta activity and SWS, theta activity was relatively high and associated with moderate gamma activity, and a state of PS alternated directly with a state of Wake. In association with the theta and gamma activity on the EEG, at one moment the rat would be lying quietly with eyes open, epochs thus scored as Wake, and the next moment, without changing position, manifesting twitches with eyes closed, epochs scored as PS or *t*PS depending upon the theta activity in the EEG (see below). All rats receiving [1.0 mM] NT (9/9) showed transitions from Wake directly into PS or *t*PS with no intervening SWS or *t*SWS. As recorded in the behavioral annotations, the Wake state following NT was predominantly a quiet Wake state, characterized by a reclining, outstretched posture, and the passage into *t*PS or PS was usually marked only by closing of the eyes with no other postural change. A direct passage from an attentive or active (moving, eating, grooming) waking behavior, to a PS-like state was never seen.

Across animals receiving [1.0 mM] NT, there was a significant increase in relative gamma band activity, decrease in relative delta band activity and increase in theta/delta ratio on the retrosplenial lead, as compared to ringer (Table 1). There were no significant changes in EMG. There were significant changes in sleep-wake states, marked by a significant increase in Wake and in *t*PS and PS and a significant decrease in SWS. In one animal (B29), PS reached 23% and tPS 36%, representing together ~60%, of total recording time. Within these states, the EEG activity did not differ significantly from that during the same states with ringer, except for higher relative gamma in epochs of SWS with NT (not shown).

Whereas the predominant EEG activity was composed of slow, irregular delta activity in association with SWS following Ringer (Fig. 5), the predominant EEG activity was composed of relatively rhythmic theta-like activity in association with Wake, *t*PS and PS following NT on all cortical leads (Fig. 6). In comparison to the Ringer SWS, the gamma activity was consistently higher in association with the theta-like activity following NT (Figs. 6,7, and 8). These different activity profiles were evident in the corresponding spectra for the epochs following Ringer and NT. Whereas the peak frequency was in the delta band (~1-4 Hz) during SWS following Ringer (Fig. 5), it was in the theta band (4.5-8.5 Hz) during the Wake, *t*PS or PS scored epochs following NT (Figs. 6,7,8). This shift in peak frequency was evident on all cortical leads, even though the precise activity and peak of activity appeared to differ across leads. In animals with electrodes in the hippocampus and entorhinal cortex, theta activity was also present on these leads during periods when it was seen on cortical leads (not shown). The cortical theta was most often different in frequency and phase to that on the hippocampal and entorhinal leads, although it did appear to occur in phase occasionally for very brief periods when theta was most robust. In relation to the spectra associated with Ringer SWS, the

overall amplitude in the gamma band of the spectra appeared higher with NT, though no particular peak in that band was prominent on any lead.

Systematic analysis of the changes in peak frequency based on spectral samples of 4 sec epochs, which were taken at exactly one minute intervals during the maximal and most stable post-injection period (~ 4 –12 minutes post-injection), revealed significant increases in the average low peak frequency following NT as compared to ringer microinjections (n=5, Table 2). Although there was a significant difference in the average low peak frequency across cortical leads, there was not a significant interaction between drug condition and area, indicating that there was a parallel shift to higher peak frequencies across areas following NT as compared to ringer. This shift in peak frequencies was also reflected in the average significant decrease in delta band absolute amplitude and increase in theta/delta ratio across leads. Despite these parallel changes across leads, there were significant differences in peak frequency and theta/delta ratio across cortical leads, according to which they were highest on the retrosplenial cortex and lowest on the frontal cortex (Table 1). There was no comparable shift in average peak frequency in the gamma range on any lead, although there was a significantly higher average absolute amplitude in the gamma band following NT as compared to ringer on all leads. In these sampled epochs, there was also a significantly higher average EMG following NT as compared to Ringer (Table 2).

The dose dependency of the EEG and sleep-wake state changes produced by NT over the 30 min post-injection period was examined by repeated trials (n=4). Increasing doses of NT were associated with increasing absolute amplitude of gamma, decreasing amplitude of delta and increasing theta-delta ratio (Fig. 9). The changes in EMG across doses were not significant. Paralleling these EEG changes were dose-dependent increases in Wake and in *t*PS and PS and decreases in *t*SWS and SWS

(Fig. 10). PS and *t*PS increased in a dose-dependent manner to reach a maximum with [1.0 mM] NT and represent together ~40% of recording time on average with that dose. At 3.0 mM NT, PS and tPS were similar in amount to ringer (<20%), whereas Wake increased to a maximum, representing of ~75% of recording time.

Microinjections of [0.25 mM] Fluo-NT resulted in changes in EEG activity and sleep-wake states that did not differ from those following [0.25 mM] unlabelled NT. There were similar increases in %gamma (21.1 ± 1.9%) and theta/delta (1.75 ± 0.18), and decrease in %delta (12.2 ± 1.4%) during the 15 min post-injection period studied with the fluorescent as compared to those with the non-fluorescent NT (%gamma: 19.56 ± 1.41%; theta/delta: 1.78 ± 0.19; delta: 12.11 ± 1.59%). All rats receiving Fluo-NT also experienced epochs of PS during the15 min post-injection period. The average amounts of Wake (41.67 ± 13.44%) and *t*PS+PS (28.89 ± 9.59) occurring post Fluo-NT, did not differ from those following [0.25 mM] unlabelled NT (Wake: 37.22 ± 11.45%; *t*PS+PS: 28.89 ± 11.33%).

The changes in EEG induced by [0.25 mM] NT were largely antagonized with the systemic administration of (30 mg/kg, i.p.) atropine (Table 3). Atropine by itself produced a continuous Wake state characterized behaviorally often as an active, moving state, despite the frequent appearance of slow wave activity on the EEG, as has been described in many studies. Microinjection of NT following atropine no longer produced an increase in gamma or decrease in delta as it did prior to atropine as compared to ringer (Table 3). As an index of theta, the theta/delta ratio was not increased by NT following atropine, although the comparison to ringer did not reach significance in the statistical test of the hypothesis that atropine antagonized the effect of NT (Table 3). It was however noted that during the wake state produced by atropine alone, the animal was often active and during such behavior, theta activity was present

in the EEG and spectra accompanying a slower baseline activity. This dissociated wake state and atropine-resistant theta may have partially obscured an antagonistic effect of atropine upon NT-induced theta activity. However, atropine clearly prevented the enhancement of *t*PS and PS during which theta was most prominent following NT.

Effects of NT microinjections upon unit discharge

of identified cholinergic neurons

The effect of NT microinjection upon discharge rate and pattern in basal forebrain units was examined in urethane-anesthetized animals (n=6). Each unit was labelled by juxtacellular application of Neurobiotin (Nb) for subsequent immunohistochemical processing for ChAT. Three units displayed discharge properties typical of cholinergic neurons according to previously established characteristics, notably the presence of high frequency burst discharge with stimulation-induced cortical activation (Manns *et al.*, 2000). Of these, two were successfully labeled with Nb and found to be immunoreactive for ChAT (Fig. 11). These Nb+/ChAT+ neurons, as well as the cholinergic-like cell, all showed changes in their rate and pattern of discharge that were associated with changes in EEG activity following NT microinjections as compared to the pre-injection recording baseline (Fig. 12). All increased their average rate of discharge (according to peri-stimulus histogram, PSH, measures) and instantaneous firing frequency (according to interspike interval histogram, ISIH, measures) shortly after if not before the end of the microinjection (middle panel, Fig. 12). Most distinctly, they all showed high frequency bursts (>80 Hz) in their activity following NT, which were infrequent preceding NT (arrows, Fig. 12). In two cells, this bursting discharge became rhythmic spontaneously (Fig. 12, SI and not shown) and in the other cell it did so with somatosensory stimulation (Fig. 12, MCPO, as evaluated by autocorrelation histogram, ACH, measures). The rhythmic discharge of all three was temporally cross-correlated

with the retrosplenial and prefrontal EEG signals during the rhythmic bursting (as evaluated by spike triggered average, STA, measures, Manns *et al.*, 2000). The rhythmic discharge of the MCPO unit matched the predominant activity in the retrosplenial cortex (at 2.7 Hz), whereas that of the SI unit matched the slower activity in the prefrontal cortex (at 1.1 Hz).

DISCUSSION

The results of the present study demonstrate that NT, which is selectively internalized by and induces bursting in cholinergic neurons, promotes theta and gamma EEG activity and Wake and PS states following its microinjection into the basal forebrain. These results moreover document a potent capacity of cholinergic BF neurons to stimulate theta and gamma EEG activity and to elicit the states of Wake and PS.

The changes in cortical activity observed following NT are most likely due to the excitation of BF cholinergic neurons which would result in an increased release of ACh from cholinergic terminals in the cortex. An increase in ACh release could thus underlie the decrease in delta activity and increase in high frequency gamma activity, marking cortical activation. Previous studies have shown NT's capacity to enhance cholinergic transmission by increasing ACh turnover in the diencephalon following intracerebroventricular administration (Malthe-Sorenssen *et al.*, 1978) and by increasing evoked ACh release in the parietal cortex following bath application in brain slices (Lapchak *et al.*, 1990). In the present study, evidence that NT may act by increasing cortical ACh release is demonstrated by the ability of atropine, a muscarinic antagonist to antagonize the changes in gamma and delta following NT. An increase in ACh release in the cortex would depolarize the membrane potential of cortical neurons by blocking potassium channels (McCormick and Prince, 1986), and thus potentiate an increase in high-frequency tonic firing by cortical neurons (Krnjevic, 1967; McCormick, 1992; Metherate *et al.*, 1992). These changes in activity would be reflected in the EEG as a change from a high voltage, slow EEG, to a low voltage, fast EEG reflected here in the increase in high frequency gamma activity during a period of the day when the animals are normally in SWS the majority of the time. Finally, this increase in cortical activation is consistent

with our previous findings that show an increase in gamma activity following BF microinjection of AMPA, NMDA (Cape and Jones, 2000) or noradrenaline (Cape and Jones, 1998), agonists that are known to depolarize and excite cholinergic neurons (Khateb *et al.*, 1995, 1997; Fort *et al.*, 1995). On similar lines, these effects are opposite to those found with BF microinjections of serotonin (Cape and Jones, 1998) known to hyperpolarize and inhibit cholinergic BF neurons (Khateb *et al.*, 1993), or procaine, a general anesthetic (Cape and Jones, 2000), which produce decreases in gamma activity.

In addition to an increase in gamma activity, there was a marked increase in the amount of theta EEG activity following NT. This effect elicited here by microinjection into the basal forebrain parallels the increase in EEG theta elicited by intracerebroventricular administration of NT (Castel *et al.*, 1989). The increase was measured here as an increase in the ratio of theta to delta which is an appropriate measure of theta, since it reflects the amplitude of activity associated with a peak in the theta band and not that associated with a peak in the delta band which overlaps into the theta band (Maloney *et al.*, 1997). It was also measured as a higher average peak frequency in sampled epochs during the stable maximal effect following NT as compared to the same period following ringer. In these measures, the increase in both ratio and low peak frequency were apparent on all cortical leads, including the occipital, parietal and frontal leads, in addition to the retrosplenial lead. Although theta activity from the former non-limbic regions has been attributed to volume conduction from the hippocampus, the fact that the peak frequencies differ significantly across the cortical regions here following NT and in previous studies during natural Wake and PS states (Maloney *et al.*, 1997) render this interpretation inadequate. It was also found that theta recorded on hippocampal and entorhinal leads here only occasionally and transiently

appeared to be of similar frequency and phase as that on the cortical leads. Both the theta/delta ratio and low peak frequency were highest on the retrosplenial cortex and lowest on the frontal lead, which is over the anterior medial frontal cortex. In other studies, it was clearly shown that theta in the retrosplenial cortex is generated by cortical theta bursting cells and persists following lesions of the medial septum, indicating that it is dependent upon input from the basal forebrain for its modulation (Borst *et al.*, 1987; Leung *et al.*, 1987). Most recently it has been shown that identified cholinergic basal forebrain neurons do discharge in rhythmic bursts in association with theta-like activity on the retrosplenial cortex in urethane-anesthetized rats (Manns *et al.*, 2000). The juxtacellular unit recordings and identification of cholinergic neurons performed here similarly found a burst discharge by cholinergic neurons, while confirming NT's capacity *in vivo* to stimulate rhythmic bursting in the BF cholinergic neurons previously shown *in vitro* (Alonso *et al.*, 1994). It was also found in our previous study, that different cholinergic neurons discharged in rhythmic bursts at different frequencies, including some that discharged in a slower frequency that matched a slower theta-like EEG activity on the prefrontal cortex as compared to the retrosplenial cortex. Similarly here, one unit (SI) discharged in slow rhythmic bursts that cross-correlated with the EEG activity on the prefrontal cortex, whereas the other (MCPO) did so in bursts that cross-correlated with the faster rhythmic slow activity on the retrosplenial cortex. Accordingly, the theta activity on different cortical leads observed following NT microinjections in the freely moving, naturally sleeping-waking rats may be stimulated by bursting cholinergic neurons projecting to different regions of the cerebral cortex and stimulating slightly different frequencies of theta-like, slow rhythmic activity. This interpretation is consistent with our previous experiments in freely moving rats that show an increase in theta activity across cortical leads, though of different frequencies, following BF

administration of NMDA (Cape and Jones, 2000), a glutamate agonist also known to induce bursting in BF cholinergic neurons (Khateb *et al.*, 1995, 1997). Finally, this increase in theta activity was not evident following BF microinjections of AMPA (Cape and Jones, 2000) or noradrenaline (Cape and Jones, 1998) that excite cholinergic neurons, but stimulate tonic discharge, not bursting activity in the slice (Khateb *et al.*, 1995, 1997; Fort *et al.*, 1995).

In contrast to the increase in gamma and decrease in delta, the increase in the theta/delta ratio following NT microinjections though apparently attenuated was not conclusively antagonized by atropine, since the results were not statistically significant. As noted here, however, atropine produces a dissociated state of behavioral waking in the presence of slow, often delta frequency EEG yet sometimes accompanied by theta, thus called atropine-resistant theta, during movement (Vanderwolf, 1975). Theta seen on the EEG after NT microinjections following atropine could represent such atropine-resistant theta occurring during active waking. Such theta could also be stimulated by cholinergic neurons by being mediated in the cortex through actions on cortical neurons having nicotinic receptors. It is possible that nicotinic receptors would be important in the temporally punctate modulation of the cortex that must occur within a theta-like frequency (Mann *et al.*, 2000). Atropine-resistant theta could also be due to rhythmic activity in non-cholinergic cortically projecting neurons (Alonso *et al.*, 1996; Gritti *et al.*, 1997), as would appear to be activated according to c-Fos immunohistochemistry in association with theta activity during waking following NMDA (Cape and Jones, 2000). Here, non-cholinergic neurons could become enlisted in rhythmic discharge through local interconnections following NT-induced burst discharge in the cholinergic neurons. Yet, the most prominent theta which occurred with enhanced *t*PS and PS following NT

was fully antagonized by atropine, indicating the importance of both the cholinergic neurons and muscarinic receptors in this response to NT.

Within the context of these possibilities, several findings in the present study suggest that NT elicits the changes in EEG due to relatively selective activation of cholinergic BF neurons. In addition to the partial antagonism by atropine, the fact that NT induced an increase in gamma and theta in a dose-dependent manner clearly provides evidence of an NT receptor-dependent excitation of the cholinergic cells. The selective nature of the NT high affinity binding on cholinergic neurons within the BF was previously reported (Szigethy *et al.*, 1987, 1989, 1990). The vast majority (95%) of BF cholinergic neurons (identified as acetylcholine esterase (AchE)-reactive) were found to bind neurotensin, whereas non-cholinergic neurons were not (Szigethy *et al.*, 1990). In brain slices, electrophysiological studies showed the selective excitation and burst-elicitation by NT on electrophysiologically identified cholinergic neurons (Alonso *et al.*, 1994). In that study, effects of NT were not found on the non-cholinergic units examined. In the same studies, Fluo-NT labelled receptor-ligand complex was found to be selectively internalized in ChAT-immunoreactive neurons (Faure *et al.*, 1995a). Using Fluo-NT here, it was found that during the period that a pharmacological enhancement of gamma and theta activity occurred, the Fluo-NT labelled receptor-ligand complex was being internalized in ChAT-immunoreactive neurons, as evident by bright puncta in their perikarya and proximal dendrites. This, punctate Fluo-NT perikaryal labeling was markedly diminished when administered with the unlabelled NT, indicating that it depended upon the high affinity binding of the NT to the receptor on the cholinergic cells.

In addition, to provide direct electrophysiological confirmation of the NT-induced modulation within the BF, unit recordings were performed here together with

juxtacellular labeling of cells with neurobiotin (Nb) in an anesthetized preparation. The injection of Nb permitted the subsequent immunohistochemical identification of the recorded cells as cholinergic. The Nb+/ChAT+ units increased their rate of discharge and also showed high frequency burst discharge that was cross-correlated with the cortical theta-like activity. As had been documented in a previous study (Manns *et al.*, 2000), the burst discharge matched frequencies of either retrosplenial or prefrontal cortical EEG. Together with the observation that theta was evident following NT microinjections at different frequencies across all cortical, as well as hippocampal and entorhinal, leads, these results suggest that the basal forebrain cholinergic system may act in a coordinated, though regionally particularized, manner to modulate cortical activity in a rhythmic manner. The cholinergic neurons would in turn stimulate high frequency gamma activity by release of ACh and stimulation of muscarinic receptors in the cortex and moreover promote theta activity therein by rhythmic modulation of cortical neurons perhaps additionally involving nicotinic receptors.

The cholinergically mediated changes induced by NT in cortical activity were also associated with changes in sleep-wake states. First, SWS was diminished in a dose-dependent manner by the NT microinjections during the time of day when the rats are normally in SWS the majority of the time. Wake was reciprocally increased. Yet, it was a quiet wake state, often marked by a reclining, outstretched normally sleeping posture, but with eyes open. Despite this quiet waking behavioral state, theta activity was present on the EEG, an association rarely if ever seen in the normal rat (Maloney *et al.*, 1997), in which as is the case well known and characterized for hippocampal theta (Vanderwolf, 1969), it accompanies moving or attentive states. NMDA stimulated theta by microinjection into the BF was as in normal rats associated with an active moving waking state (Cape and Jones, 2000). But NMDA would, as evidenced by c-Fos

activation, also be associated with stimulation of multiple cell types in the basal forebrain, stimulating high EMG activity along with cortical activation. Here, NT microinjections were not associated with a dose-dependent increase in EMG activity, perhaps because of the relatively selective stimulation of the cholinergic neurons. With this process, NT also lead to dose-dependent increases in PS and the transitional phase normally preceding PS (*t*PS) and following upon SWS, yet here in the absence of SWS. This extraordinary induction of theta EEG activity associated with the occurrence and enhancement of narcoleptic-like PS is perhaps the consequence of rhythmic burst discharge in cholinergic neurons, in absence of activation of other basal forebrain neurons which would otherwise be active along with cholinergic neurons during active and attentive waking.

Our results have revealed a potent capacity and mechanism by which BF cholinergic neurons can induce the state of PS. Enhancement of the intrinsic capacity of rhythmic discharge from the cholinergic BF cells may thus occur in the sleep-wake cycle by afferent projections that in isolation, or in combination with other afferents induce cholinergic neurons to burst, which in turn, stimulate the appropriate downstream events associated with the state of PS. The present results indicate that NT which is contained in afferents from both forebrain and brainstem (Morin *et al.*, 1996) is capable of selectively exciting and stimulating rhythmic discharge in cholinergic neurons that may underlie theta together with gamma activity and the state of paradoxical sleep.

CONCLUSION

Selectively bound and internalized, NT excites and induces a rhythmic bursting discharge in cholinergic basal forebrain neurons. This rhythmic discharge modulates cortical activity in a rhythmic manner eliciting theta with gamma activity across the cerebral cortex. Depending upon the discharge of other basal forebrain neurons, the burst discharge by cholinergic neurons is associated with a waking or paradoxical sleep state. Accordingly we conclude that NT promotes theta and gamma EEG activity together with waking and PS states by stimulating rhythmic burst discharge in cholinergic basal forebrain neurons.

ACKNOWLEDGEMENTS

We would like to thank Advanced Bioconcept for donation of the Fluoro-neurotensin (Fluo-NT). We thank Dominique Nouel and Thomas Stroh for their consultation for the Fluo-NT experiments and Lynda Mainville for her participation in preparing the histological material. The research was supported by a grant to Barbara E. Jones from the Canadian Medical Research Council. Edmund G. Cape was supported as a graduate student by the Fonds de Recherche en Santé du Québec (FRSQ), Réseau de Santé, Axe Sommeil et Vigilance and Ian Manns as a graduate student by the National Science and Engineering Council of Canada (NSERC).

LITERATURE CITED

Alonso A, Faure M-P, Beaudet A (1994) Neurotensin promotes oscillatory bursting behavior and is internalized in basal forebrain cholinergic neurons. *J. Neurosci.*, **14,** 5778-5792.

Alonso A, Khateb A, Fort P, Jones BE, Muhlethaler M (1996) Differential oscillatory properties of cholinergic and non-cholinergic nucleus Basalis neurons in guinea pig brain slice. *Eur. J. Neurosci.*, **8,** 169-182.

Bland BH (1986) The physiology and pharmacology of hippocampal formation theta rhythms. *Prog. Neurobiol.* **26**(1),1-54.

Borst JGG, Leung L-WS, MacFabe DF (1987) Electical activity of cingulate corte. XII. Cholinergic modulation. *Brain Res.* **407**, 81-93.

Buzsaki G, Bickford RG, Ponomareff G, Thal LJ, Mandel R, Gage FH (1988) Nucleus basalis and thalamic control of neocortical activity in the freely moving rat. *J. Neurosci.*, **8**, 4007-4026.

Cape EG, Alonso A, Beaudet A, Jones BE (1996) Neurotensin micro-injections into the basal forebrain promote cortical activation associated with the states of Wake and PS in the rat. *Soc. Neurosci. Abst.*, **22**, (64.17).

Cape EG, Beaudet A, Jones BE (1998) Binding and internalization of fluorescent neurotensin in basal forebrain neurons is associated with cortical activation, waking and paradoxical sleep. *Soc. Neurosci. Abst.*, **24**, (664.8).

Cape EG, Jones BE (1998) Differential modulation of high frequency gamma electroencephalogram activity and sleep-wake state by noradrenaline and serotonin microinjections into the region of cholinergic basalis neurons. *J. Neurosci.*, **18,** 2653-2666.

Cape EG, Manns I, Alonso A, Jones BE (1999) Local microinjections of neurotensin in basal forebrain induces rhythmic discharge of identified cholinergic neurons in association with rhythmic EEG activity. *Soc. Neurosci. Abst.* **25** (243.15).

Cape EG, Jones BE (2000) Effects of glutamate agonist versus procaine microinjections into the basal forebrain cholinergic cell area upon gamma and theta EEG activity and sleep-wake state. *Euro. J. Neurosci.*, **12**, 2166-2184.

Casamenti F, Deffenu G, Abbamondi AL, Pepeu G (1986) Changes in cortical acetylcholine output induced by modulation of the nucleus basalis. *Brain Res. Bull.*, **16**, 689-695.

Castel M-N, Stutzmann J-M, Lucas M, Lafforgue J, Blanchard J-C (1989) Effects of ICV administration of neurotensin and analogs on EEG in rats. *Peptides* **10**, 95-101.

Faure M-P, Alonso A, Nouel D, Gaudriault G, Dennis M, Vincent J-P *et al.* (1995a) Somatodendritic internalization and perinuclear targeting of neurotensin in the mammalian brain. *J. Neurosci.*, **15,** 4140-4147.

Faure M-P, Nouel D, Beaudet A (1995b) Axonal and dendritic transport of internalized neurotensin in rat mesostriatal dopaminergic neurons. *Neuroscience*, **68**(2), 519-529.

Fort P, Khateb A, Pegna A, Muhlethaler M, Jones BE (1995) Noradrenergic modulation of cholinergic nucleus basalis neurons demonstrated by *in vitro* pharmacological and immunohistochemical evidence in the guinea pig brain. *Eur. J. Neurosci.*, **7,** 1502-1511.

Gritti I, Mainville L, Jones BE (1993) Codistribution of GABA- with acetylcholine-synthesizing neurons in the basal forebrain of the rat. *J. Comp. Neurol.*, **329,** 438-457.

Gritti I, Mainville L, Mancia M, Jones BE (1997) GABAergic and other non-cholinergic basal forebrain neurons project together with cholinergic neurons to meso- and iso-cortex in the rat. *J. Comp. Neurol.*, **383,** 163-177.

Jennes L, Stumpf WE, Kalivas PW (1982) Neurotensin: topographical distribution in rat brain by immunohistochemistry. *J. comp. Neurol.*, **210**, 211-224.

Khateb A, Fort P, Alonso A, Jones BE, Muhlethaler M (1993) Pharmacological and immunohistochemical evidence for a serotonergic input to cholinergic nucleus basalis neurons. *Eur. J. Neurosci.*, **5,** 541-547.

Khateb, A., Fort, P., Serafin, M., Jones, B. E., and Muhlethaler, M. (1995) Rhythmical bursts induced by NMDA in cholinergic nucleus basalis neurones *in vitro*. *J. Physiol. (Lond.)*, **487.3**, 623-638.

Khateb A, Fort P, Williams S, Serafin M, Jones BE, Muhlethaler M (1997) Modulation of cholinergic nucleus basalis neurons by acetylcholine and N-methyl-D-aspartate. *Neuroscience*, **81,** 47-55.

Krnjevic K (1967) Chemical transmission and cortical arousal. *Anesthesiology*, **28,** 100-104.

Lambert PD, Ely TD, Gross RE, Kilts CD (1996) Neurotensin induces FOS and ZIF268 expression in limbic nuclei of the rat brain. *Neuroscience*, **75**(4), 1141-1151.

Lapchak PA, Araujo DM, Quirion R, Beaudet A (1990) Neurotensin regulation of endogenous acetylcholine release from rat cerebral cortex: effect of quinolinic acid lesions of the basal forebrain. *J. Neurochem.*, **55**(4), 1397-1403.

Leung L-WS, Borst JGG (1987) Electrical activity of ingulate corte. XI. Generating mechanisms and relations to behavior. *Brain Res.*, **407**, 68-80.

Lo Conte G, Casamenti F, Bigi V, Milaneschi E, Pepeu G (1982) Effect of magnocellular forebrain nuclei lesions on acetylcholine output from the cerebral cortex, electrocorticogram and behaviour. *Arch. ital Biol.*, **120**, 176-188.

Maloney KJ, Cape EG, Gotman J, Jones BE (1997) High frequency gamma electroencephalogram activity in association with sleep-wake states and spontaneous behaviors in the rat. *Neuroscience*, **76,** 541-555.

Malthe-Sorenssen D. Wood PL. Cheney DL. Costa E. (1978) Modulation of the turnover rate of acetylcholine in rat brain by intraventricular injections of thyrotropin-releasing hormone, somatostatin, neurotensin and angiotensin II. *J. Neurochem.* **31**(3), 685-91.

Manns ID, Alonso A, Jones BE (2000) Discharge properties of juxtacellularly labeled and immunohistochemically identified cholinergic basal forebrain neurons recorded in association with the electroencephalogram in anesthetized rats. *J. Neurosci.* **20**(4),1505-18.

McCormick DA (1992) Cellular mechanisms underlying cholinergic and noradrenergic modulation of neuronal firing mode in the cat and guinea pig dorsal lateral geniculate nucleus. *J. Neurosci.*, **12,** 278-289.

McCormick DA, Prince DA (1986) Mechanisms of action of acetylcholine in the guinea-pig cerebral cortex *in vitro*. *J. Physiol.*, **375,** 169-194.

Metherate R, Cox CL, Ashe JH (1992) Cellular bases of neocortical activation: modulation of neural oscillations by the nucleus basalis and endogenous acetylcholine. *J. Neurosci.*, **12,** 4701-4711.

Morin AJ, Tajani M, Jones BE, Beaudet A (1996) Neurotensinergic innervation of cholinergic neurons in the rat basal forebrain: a light microscopic study with three-dimensional reconstruction. *J. Chem. Neuroanat.*, **10,** 147-156.

Pinault D. (1996) A novel single-cell staining procedure performed *in vivo* under ectrophysiological control: morpho-functional features of juxtacellularly labeled thalamic cells and other central neurons with biocytin or Neurobiotin. *J. Neurosci. Methods.* **65**(2):113-36.

Shute CCD, Lewis PR (1967) The ascending cholinergic reticular system: neocortical, olfactory and subcortical projections. *Brain*, **90**, 497-520.

Stewart DJ, Macfabe DF, Vanderwolf CH (1984) Cholinergic activation of the electrocorticogram: Role of the substantia innominata and effects of atropine and quinuclidinyl benzilate. *Brain Res.*, **322**, 219-232.

Szigethy E, Beaudet A (1987) Selective association of neurotensin receptors with cholinergic neurons in the rat basal forebrain. *Neurosci. Lett.*, **83,** 47-52.

Szigethy E, Wenk GL, Beaudet A (1989) Anatomical substrate for neurotensin-acetylcholine interaction in the rat basal forebrain. *Peptides* **9**, 1227-1234.

Szigethy E, Leonard K, Beaudet A (1990) Ultrastructural localization of [^{125}I]Neurotensin binding sites to cholinergic neurons of the rat nucleus basalis magnocellularis. *Neuroscience* **36**(2), 377-391.

Uhl GR, Snyder SH (1977) Regional and subcellular distribution of brain neurotensin. *Life Sci.* **19**, 1827-1832.

Vanderwolf CH (1969) Hippocampal electrical activity and voluntary movement in the rat. *Electroencephalogr. Clin. Neurophysiol.*, **26**, 407-418

Vanderwolf CH (1975) Neocortical and hippocampal activation relation to behavior: effects of atropine, eserine, phenothiazines, and amphetamine. *J. Comp. Physiol. Psyc.*, **88,** 300-323.

Vergnes M, Marescaux C, Micheletti G, Reis J, Depaulis A, Rumbach L, Warter JM (1982) Spontaneous paroxysmal electroclinical patterns in rat: a model of generalized non-convulsive epilepsy. *Neurosci. Lett.*, **33**, 97-101.

Woulfe J, Beaudet A (1989) Immunocytochemical evidence for direct connections between NT-containing axons and dopaminergic neurons in the rat ventral midbrain tegmentum. *Brain Res.* **479**, 402-406.

Figure 1. Schematic atlas section through the basal forebrain showing the location of the microinjection cannulae in relationship to ChAT-immunoreactive neurons and "juxtacellular" recorded $Nb^{+}/ChAT^{+}$ neurons (stars). Bilateral microinjections of ringer or neurotensin were performed by insertion of inner injection cannulae into chronically indwelling guide cannulae. The cannulae are drawn according to the coordinates used for implantation and the histological verification of their position. At the time of the experiment, inner cannulae, which were filled with the chemical for injection, were first inserted within the guide cannulae (to within ~2 mm of tip, marked by arrow), where they were held until the time of injection. Immediately prior to injection, the inner cannulae on both sides were lowered by a remote driving mechanism (~4 mm) to pass out of the guide cannulae, through the globus pallidus (GP) into the substantia innominata (SI, to ~2 mm below guide cannulae, marked by lower arrow) and above the magnocellular preoptic nucleus (MCPO). The representation of the injected fluid is based upon estimates previously established with neuroanatomical tracers. In this area and beyond extending through the entire SI and MCPO, Fluo-NT was visible within ChAT-immunoreactive cells viewed by confocal microscopy. Stars on the left show approximate location of units which were recorded during NT microinjections in urethane-anesthetized rats (see Fig. 11). Abbreviations: ac: Anterior commissure; CPu, caudate putamen; GP, globus pallidus; LPO, lateral preoptic area; MCPO, magnocellular preoptic nucleus; oc, optic chiasm; SI, substantia innominata.

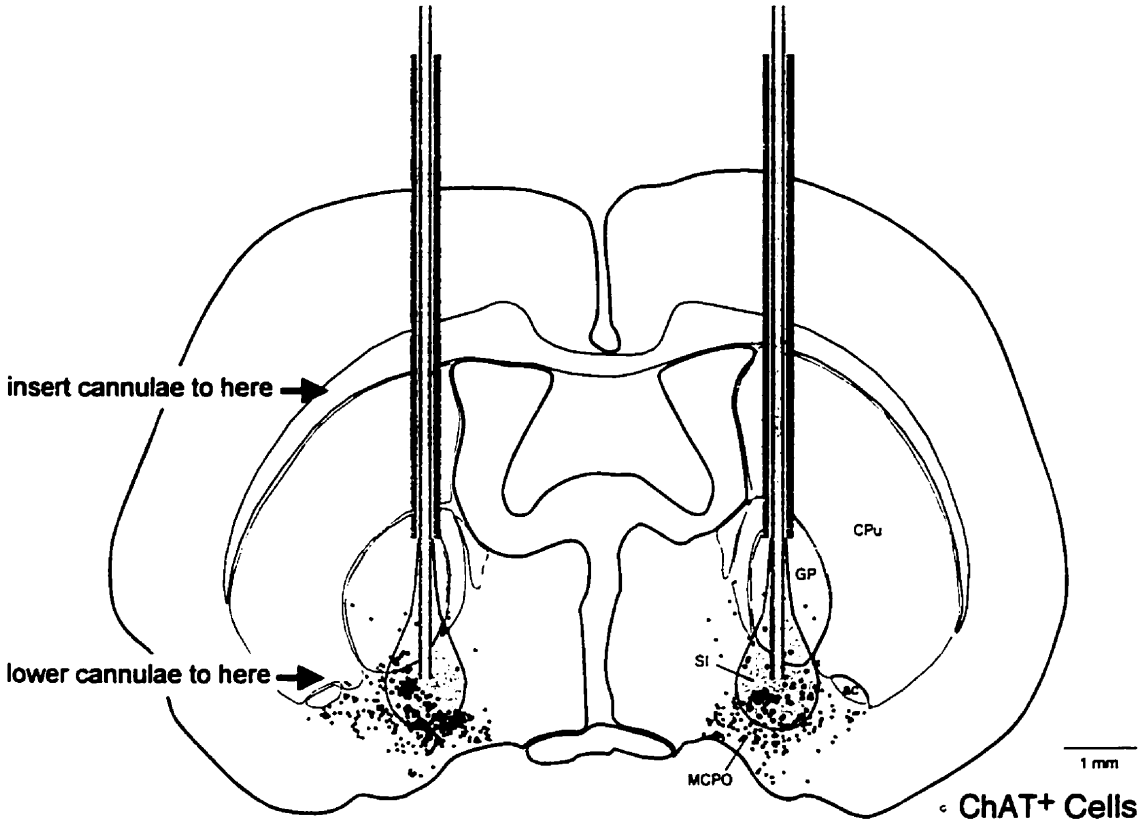
insert cannulae to here
lower cannulae to here
CPu
GP
SI
MCPO
1 mm
ChAT+ Cells

Figure 2. Photomicrographs showing evidence of binding and internalization of Fluo-NT in ChAT-immunostained neurons. Punctate fluorescent granules (arrowheads, Fluo-NT) were present in the cytoplasm of perikarya and proximal dendrites of relatively large neurons, when viewed under illumination for fluorescein, in the substantia innominata and magnocellular preoptic nucleus. Viewed under illumination for rhodamine, the fluorescent granules were found to be located within ChAT-immuno-reactive cells.
Magnification bar=20 μm.

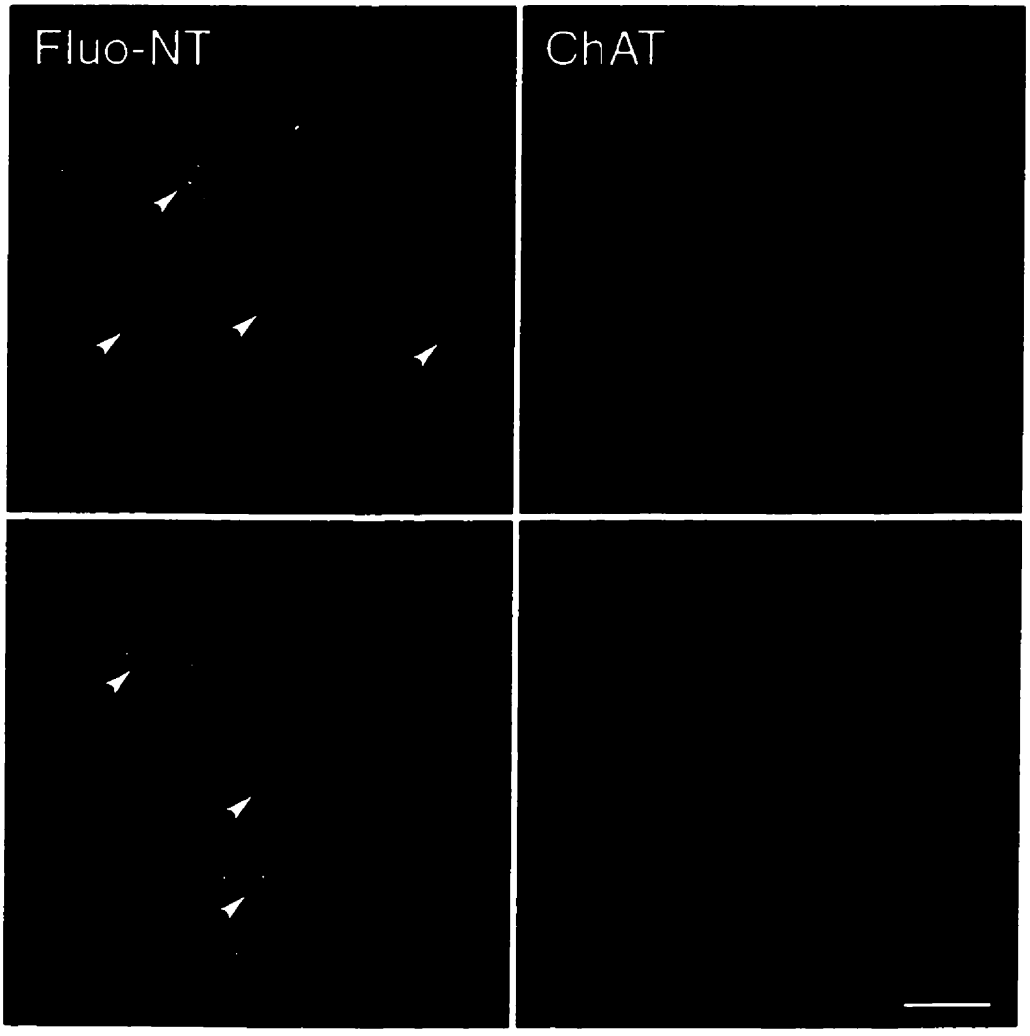
Fluo-NT
ChAT

Figure 3. Hypnogram showing sleep-wake state changes in conjunction with EEG and EMG activity changes pre and post- microinjection of ringer (Rat B11). Microinjections were performed in several stages. Following insertion of the inner cannulae into the indwelling cannulae (Fig. 1), the animals were allowed to relax before recording was resumed, after which the drug-filled cannulae were lowered into the tissue (see Cape and Jones, 1998). Two minutes later, the injection was begun and performed over 5 min (at a rate of 0.1 μl/ min). Note that during and following microinjection of ringer, the sleep-wake cycle appears undisturbed and is associated with the usual reciprocal changes in delta, gamma and theta across the states of SWS, Wake and PS. The EEG is from the right retrosplenial lead and shows band activities for gamma (γ: 30-58 Hz), delta (δ: 1-3 Hz), and theta (θ/δ: 4-8 Hz/1-3 Hz); EMG is from the neck muscles (1-58 Hz). Each activity is scaled to maximum and reported in AD units, where 100 μV ≅ 125 AD units) for 20 sec epochs.

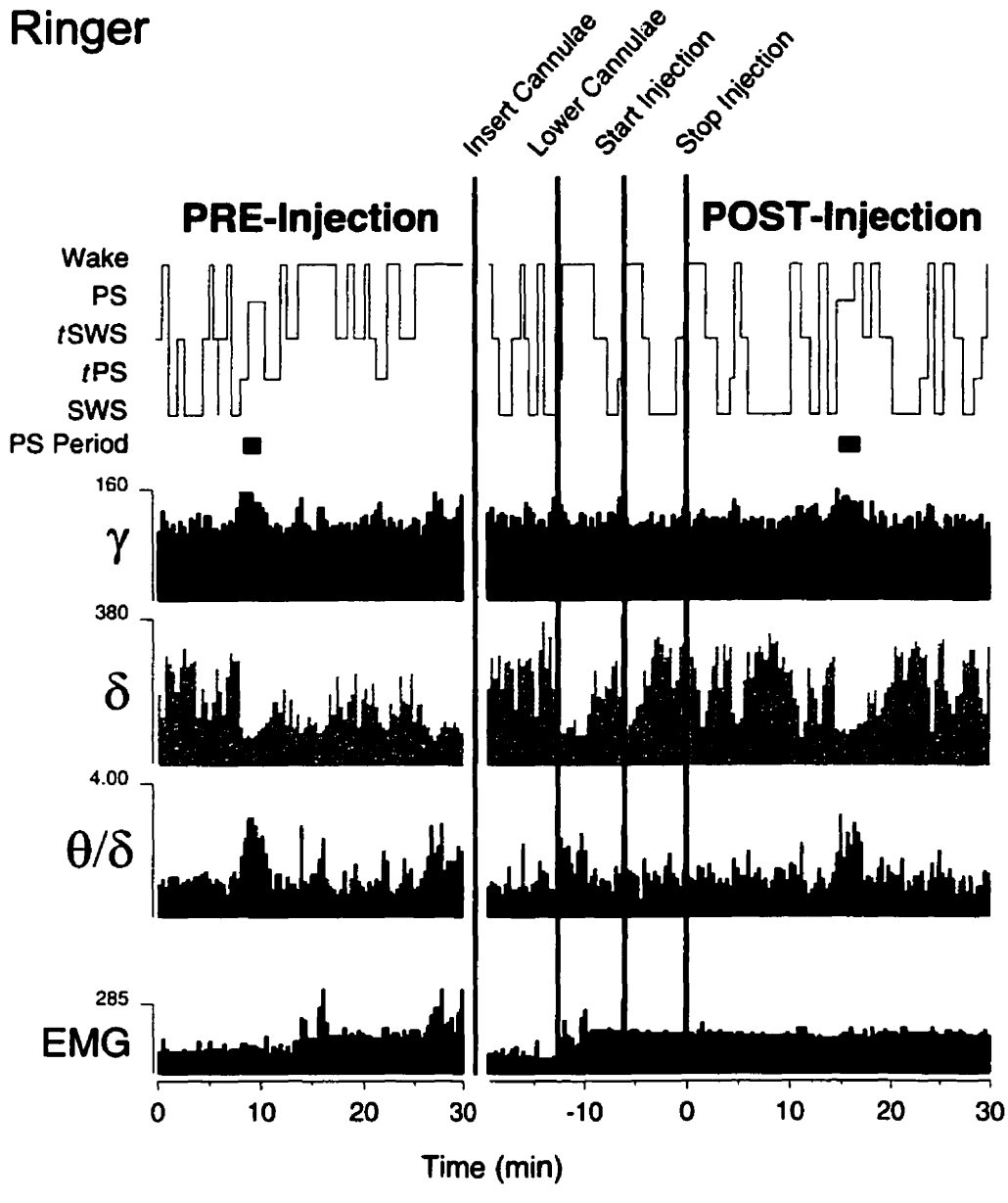
Ringer
Insert Cannulae
Lower Cannulae
Start Injection
Stop Injection
PRE-Injection
POST-Injection
Wake
PS
tSWS
tPS
SWS
PS Period
160
γ
380
δ
4.00
θ/δ
285
EMG
0
10
20
30
-10
0
10
20
30
Time (min)

Figure 4. Hypnogram showing changes (pre- and) post-microinjection of [1mM] Neurotensin (NT in rat B11). Following the lowering of the drug-filled cannulae into the tissue, delta is diminished in association with an absence of SWS. Theta becomes relatively high and together with gamma increases in association with the occurrence of PS soon after the injection is stopped. The sleep cycle of the animal is clearly altered, as evident from the direct transitions from Wake to PS in the absence of SWS.

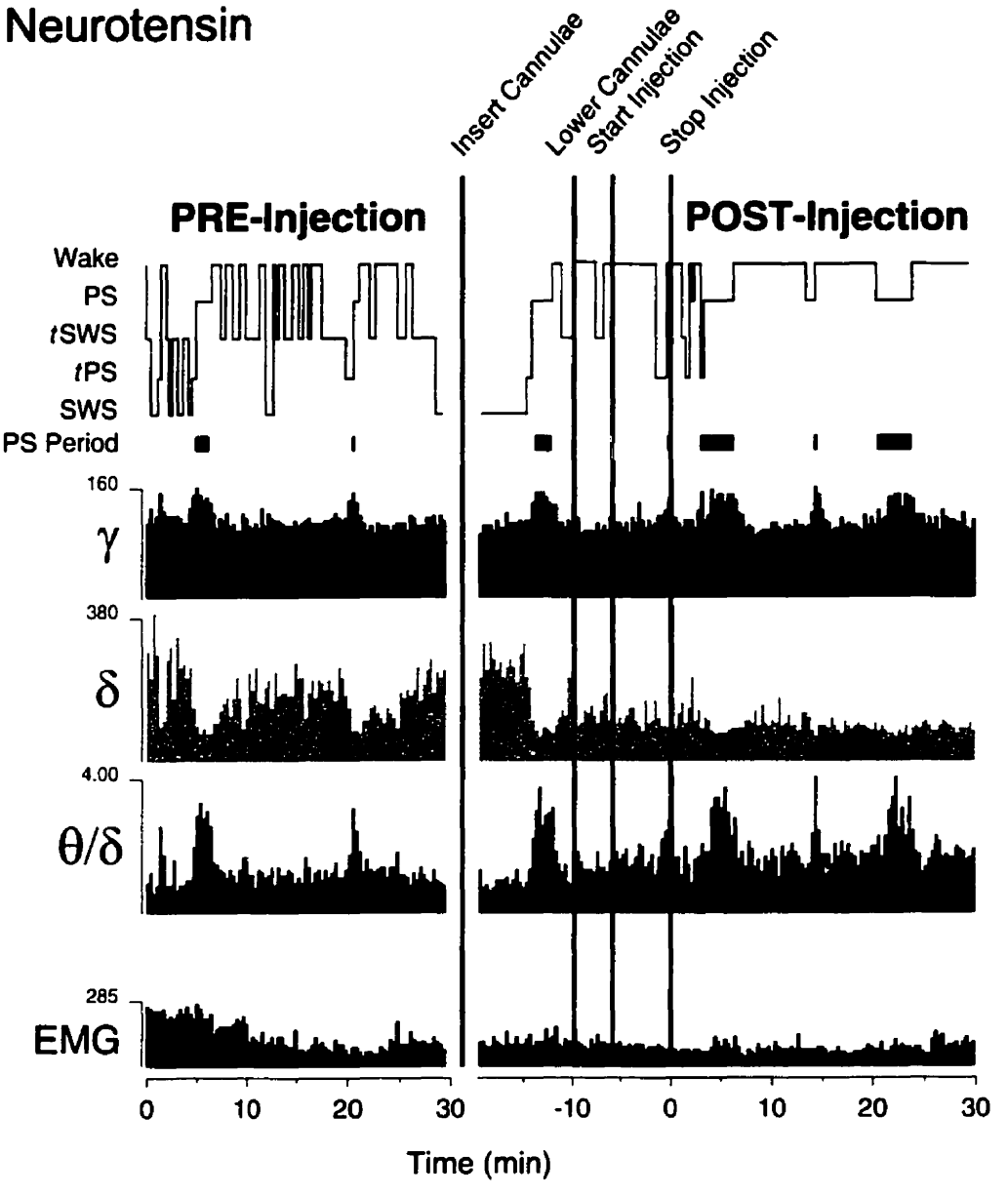
Neurotensin
Insert Cannulae
Lower Cannulae
Start Injection
Stop Injection
PRE-Injection
POST-Injection
Wake
PS
tSWS
tPS
SWS
PS Period
160
γ
380
δ
4.00
θ/δ
285
EMG
0
10
20
30
-10
0
10
20
30
Time (min)

Figure 5. EEG record and spectral analysis following ringer microinjection (in rat B11). Following ringer, SWS was the predominant state and, like normal SWS, was characterized behaviorally by a curled sleeping posture and on the EEG by high amplitude, irregular slow activity, as evident in the unfiltered trace (upper, shown in black), and relatively low amplitude high frequency gamma activity, as evident in the gamma filtered EEG trace (lower, shown in gray). These characteristics are further evident in the spectra from the same 4 sec epochs (to the right), in which the predominant peak on all leads is in the delta band (2.0 Hz), and accompanied by a relatively low amplitude in the gamma band. The EEG was recorded by reference to an electrode in the rostral frontal bone from the frontal, retrosplenial, parietal and occipital cortical regions (shown here for the right side and also recorded from the left side where activity was similar to that of the corresponding contralateral leads). Voltage scales are the same for all cortical leads. Note that the amplitude of the frontal lead is the lowest due to its proximity to the reference electrode. Spectra are displayed in amplitude (AD) units (per 0.5 Hz). 100 μV $\cong$ 125 AD units. Delta (δ), theta (θ), and gamma (γ) frequency bands are differentially shaded (as in the hypnograms); sigma (σ) and beta (β) bands are shown in white.

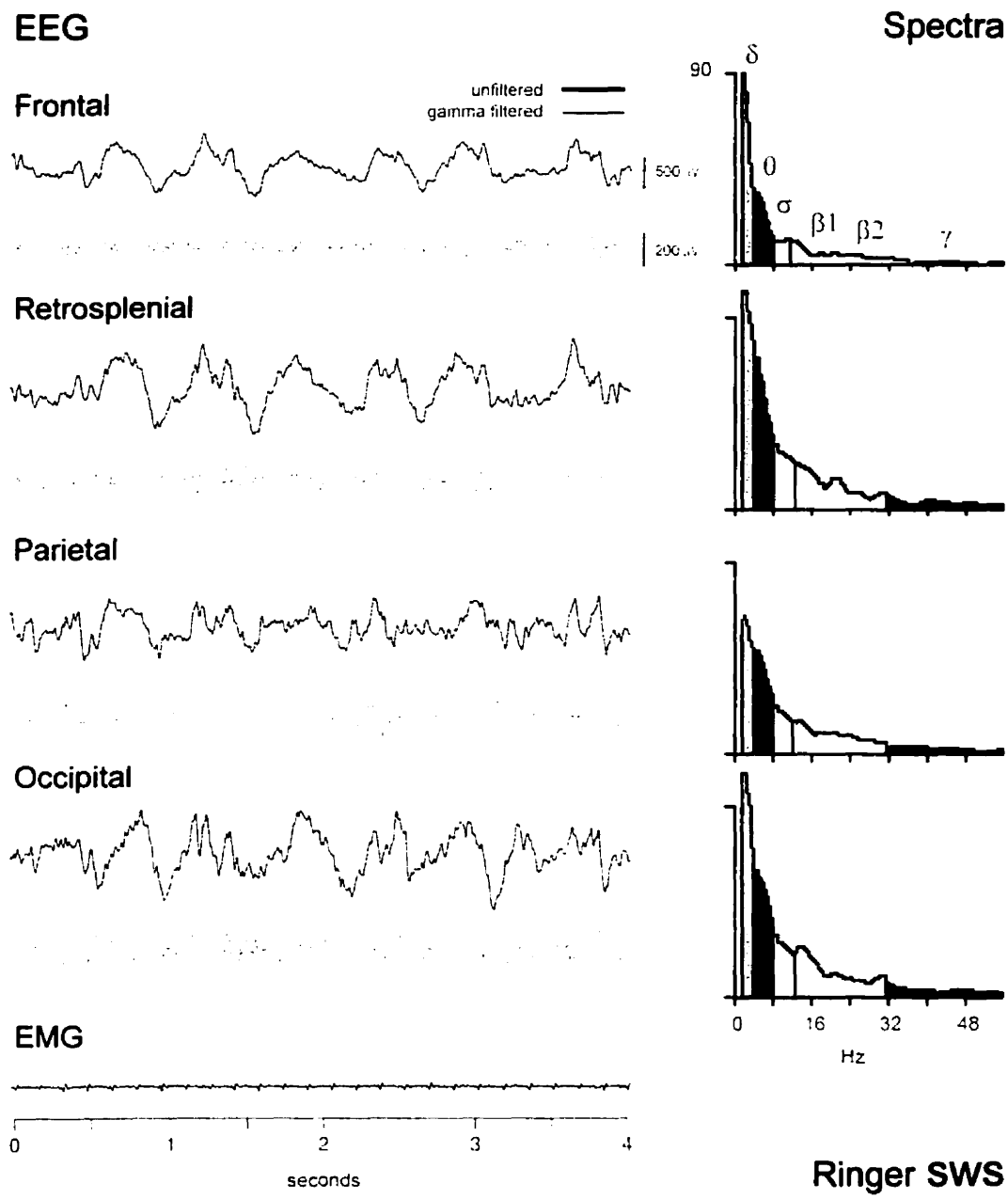
EEG
Spectra
Frontal
unfiltered
gamma filtered
Retrosplenial
Parietal
Occipital
EMG
0
1
2
3
4
seconds
90
δ
θ
σ
β1
β2
γ
0
16
32
48
Hz
Ringer SWS

Figure 6. EEG record and spectral analysis following neurotensin (in rat B11). The predominant state was Wake and often characterized behaviorally (as during this epoch) by a quiet state and a reclining, uncurled posture. The unfiltered EEG (black trace) is dominated by the occurrence of slow rhythmic activity on all leads that appears concurrently with moderately high amplitude fast gamma activity. The spectra from the same 4 sec epoch reveal a peak in the theta band (~7.5 Hz). Relative to SWS (Fig. 5), the overall amplitude in the gamma band appears higher. See Fig. 5 for details.

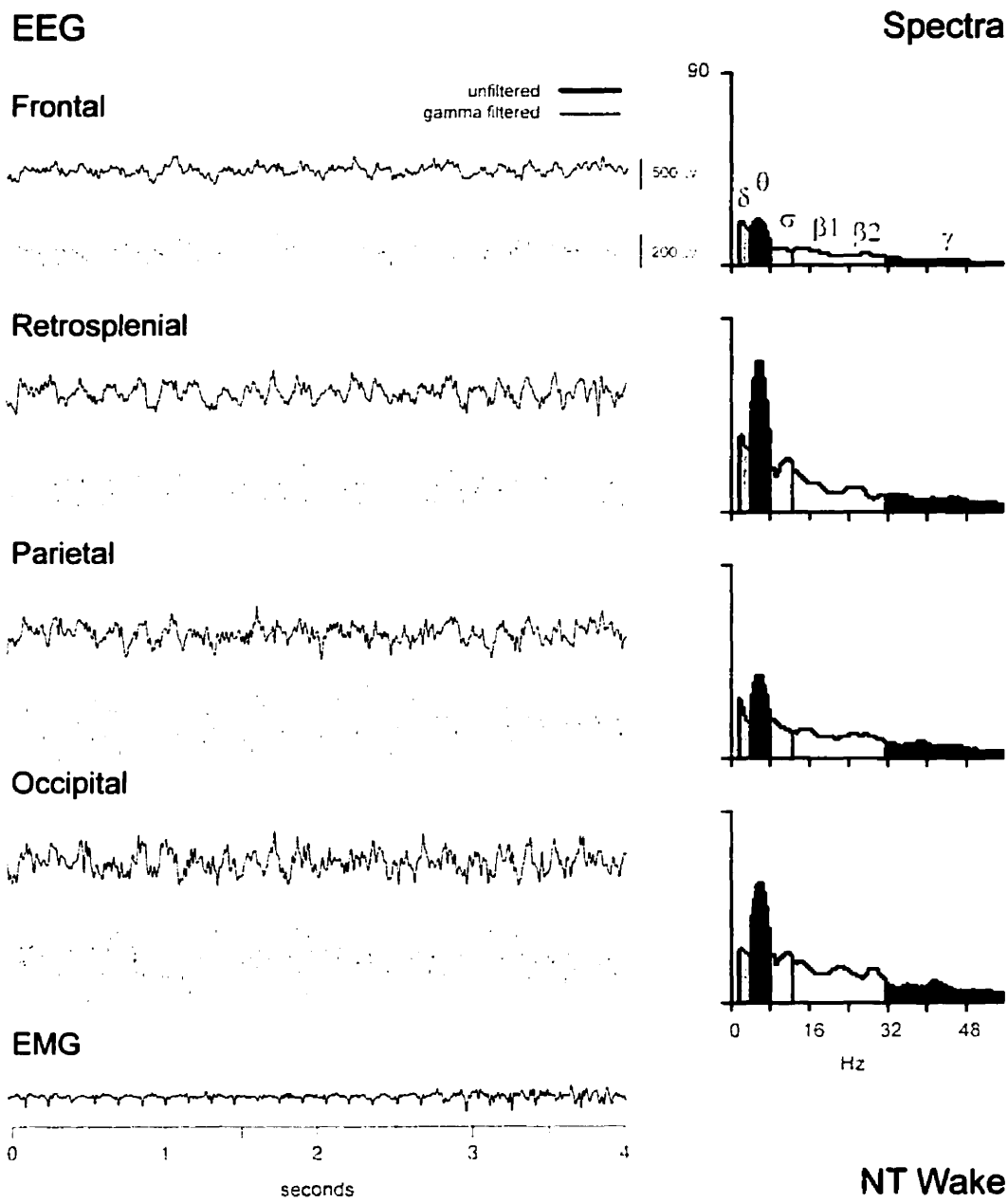
EEG
Spectra
Frontal
unfiltered
gamma filtered
500
200
90
δ
θ
σ
β1
β2
γ
Retrosplenial
Parietal
Occipital
EMG
0
16
32
48
Hz
0
1
2
3
4
seconds
NT Wake

Figure 7. EEG and spectral analysis during a transition (*t*PS) into PS directly from Wake following neurotensin (NT in rat B11). A large percentage of time was represented by the transitional state, *t*PS, that occurred directly following wake, as evident behaviorally when the animal closed its eyes, yet did not change from a reclining uncurled posture, (as noted here for this epoch following directly upon a wake epoch). In these cases (as shown here), the EEG was characterized by the presence of very rhythmic theta-like activity on all leads, as evident in the unfiltered trace (black). This activity nonetheless varied in time and across leads in frequency, in some cases containing delta waves and in others spindle-like activity, as is typical of *t*PS. Gamma activity appears to be moderately high, as evident in the gamma filtered trace (gray). The spectral analysis reveals a peak at the low end of the theta band (~4.5 Hz) on the frontal, and retrosplenial leads, and in the middle of the theta band (6.0 Hz) on the parietal lead. Marking this epoch as transitional, albeit normally between SWS and PS, activity is high in delta and theta bands with a peak at the border between the two bands on the occipital lead (3.0 Hz), and spindle activity is evident as a secondary peak (10 Hz) in the sigma band on the retrosplenial lead. Gamma band activity is high relative to SWS (Fig. 5). See Fig. 5 for other details.

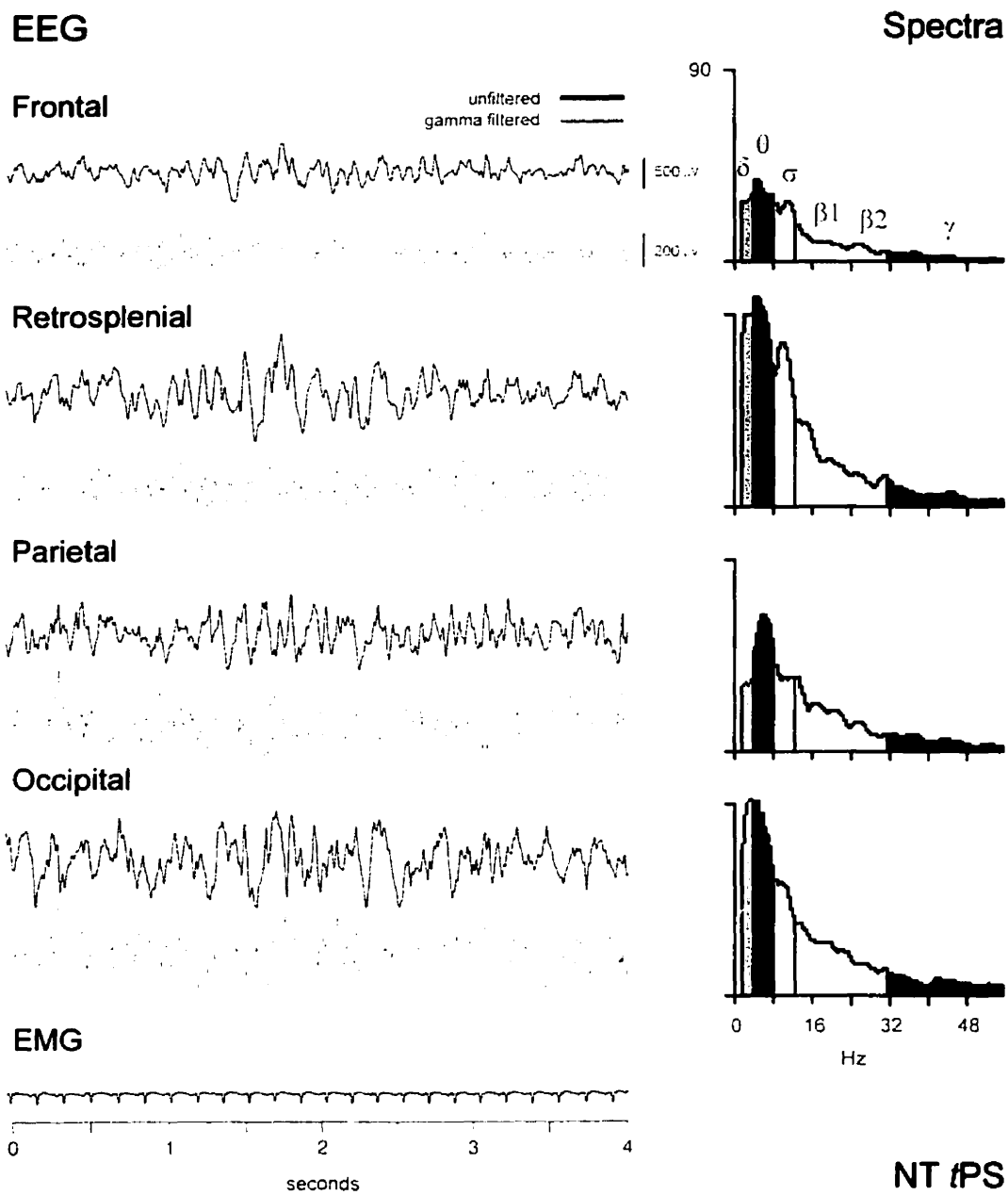
EEG
Spectra
Frontal
unfiltered
gamma filtered
200 uV
90
0
δ
σ
β1
β2
γ
Retrosplenial
Parietal
Occipital
EMG
0
16
32
48
Hz
0
1
2
3
4
seconds
NT fPS

Figure 8. EEG record and spectral analysis during PS following neurotensin (NT, in rat B11). Typical PS, that was behaviorally and electroencephalographically indistinguishable from normal PS occurred a large percent of the time following NT. In these cases (as observed for this epoch), muscle twitches were evident, while the animal was in a reclining, curled or here, uncurled posture with eyes closed. The unfiltered EEG (black trace) is dominated by theta-like activity on all leads, which occurs in association with relatively high amplitude gamma activity (gray trace). The spectra from the same epoch reveal a peak at the high end of the theta band (8.0 Hz) on all leads. Relative to SWS (Fig. 5), amplitude in the high frequency gamma band is high. See Fig. 5 for details.

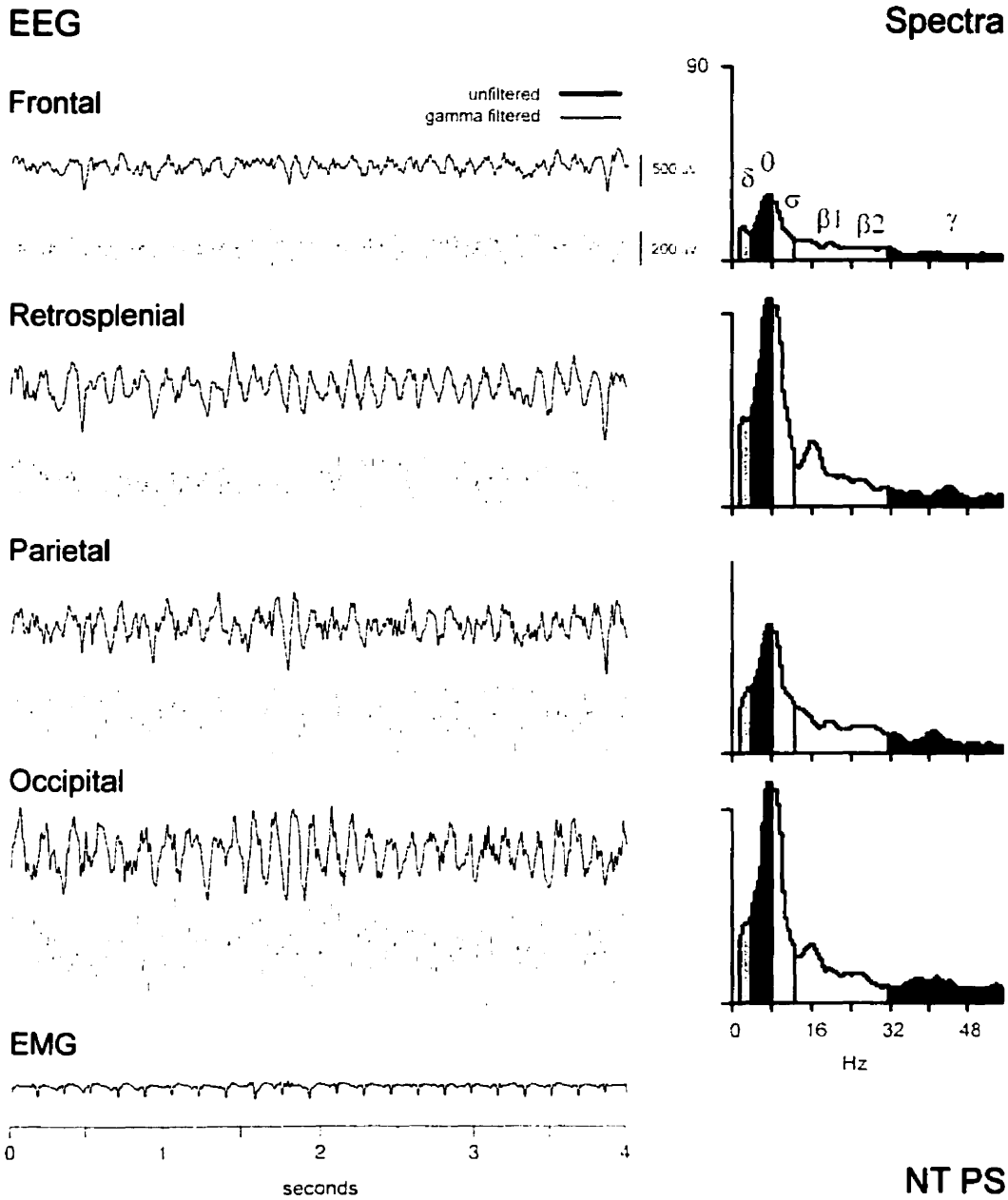
EEG
Spectra
Frontal
unfiltered
gamma filtered
500 μ
200 μ
90
δ 0
σ
β1
β2
γ
Retrosplenial
Parietal
Occipital
EMG
0
1
2
3
4
seconds
0
16
32
48
Hz
NT PS

Figure 9. Changes in EEG activities as a function of the dose of neurotensin. With increasing doses of neurotensin, delta activity decreased, whereas gamma and theta increased. Gamma and delta activities are presented as average amplitude in AD units (100 $\mu V \cong 125$ AD units), theta as the ratio of theta/delta amplitude and EMG as amplitude in AD units during the 30 min post injection period (mean ± SEM from 4 rats). Statistics were performed on natural log (Ln) transformed values that were normally distributed. The data were examined by ANOVA with dose (5) as a repeated measure (performed with the metric 0, 0.1, 0.25, 1.0, 3.0 mM) and polynomial contrasts for linear trend analysis (showing a significant trend for gamma, according to the third order, cubic polynomial: $F = 10.45$, $df=1,3$, $p=.048$; for delta, according to the first order, linear: $F = 47.25$, $df=1,3$, $p= 0.006$; and theta/delta, according to the second order, quadratic:, $F = 38.76$, $df=1,3$, $p = 0.008$; *, $p<.05$; **, $p\leq .01$).

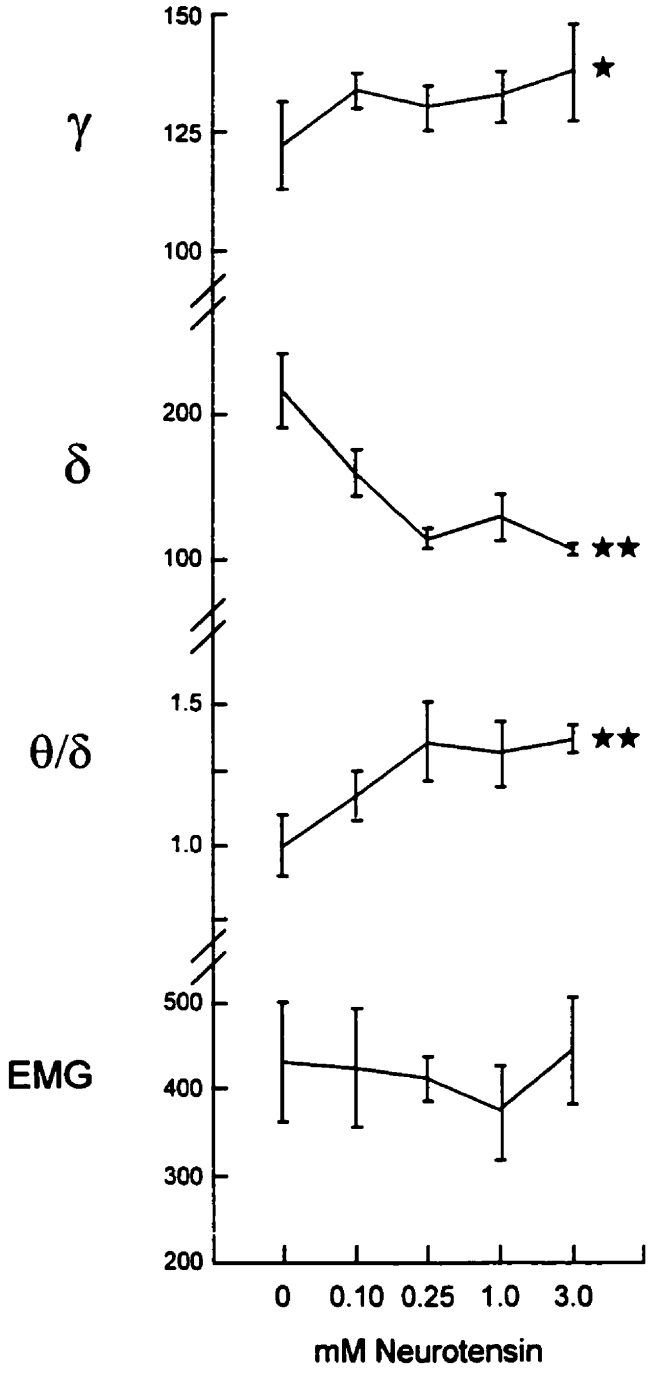
γ
150
125
100
★
δ
200
100
★★
θ/δ
1.5
1.0
★★
EMG
500
400
300
200
0
0.10
0.25
1.0
3.0
mM Neurotensin

Figure 10. Changes in sleep-wake states as a function of the dose of neurotensin. Whereas Wake and PS together with *t*PS, increased as a function of dose, SWS, together with *t*SWS decreased as a function of dose of NT. State data (mean ± SEM from 4 rats) are presented as the % of the 30 min post-injection recording period. The data were analyzed by repeated measures ANOVA for dose (performed with the metric: 0, 0.10, 0.25, 1.0, and 3.0 mM). In an overall test, in which dose was examined across states (5 levels entered as a grouping factor), % state varied significantly as a function of dose ($F= 3.842$, df 4,60, $p= 0.008$) with a significant interaction of state and dose ($F=4.121$, df=16,60, $p=.000$). Given the parallel changes in transitional states, subsequent ANOVAs were performed for W, for *t*SWS together with SWS and for *t*PS together with PS (maintaining state as a grouping factor in the latter two cases). In each case, there was a significant main effect of dose, although the linear trend, examined by polynomial contrasts differed per state (Wake with a first order, linear polynomial, $F=54.666$, df=1,3, $p=.005$; *t*SWS, SWS with a first order, linear, $F=29.057$, df=1,6, $p=.002$; and *t*PS, PS with a 2nd order, quadratic $F= 24.073$, df=1,6, 0.003; **, $p\leq .01$).

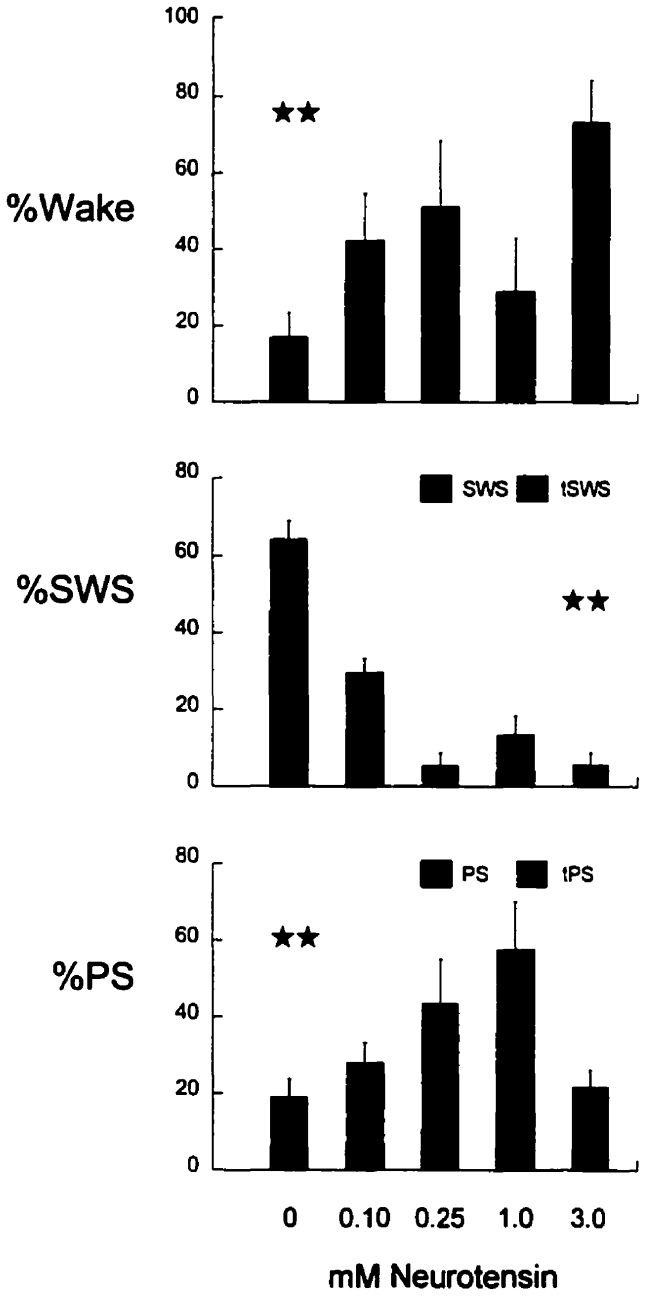
%Wake
%SWS
%PS
100
80
60
40
20
0
★★
SWS
tSWS
PS
tPS
0
0.10
0.25
1.0
3.0
mM Neurotensin

Figure 11. Photomicrographs of recorded and juxtacellularly labeled Nb+/ChAT+ neurons located in the basal forebrain cholinergic cell area (see Fig. 1). Neurobiotin (Nb) was revealed with green fluorescent Cy2-conjugated streptavidin (left) and ChAT-immunostaining with red fluorescent Cy3-conjugated secondary antibodies (right). *Top*, Nb+/ChAT+ neuron (NT5) in MCPO lying among other ChAT+ cells (see star in Fig. 1). *Bottom* Nb+/ChAT+ neuron (NT10) in SI (see star in Fig. 1). Scale bar 20μm.

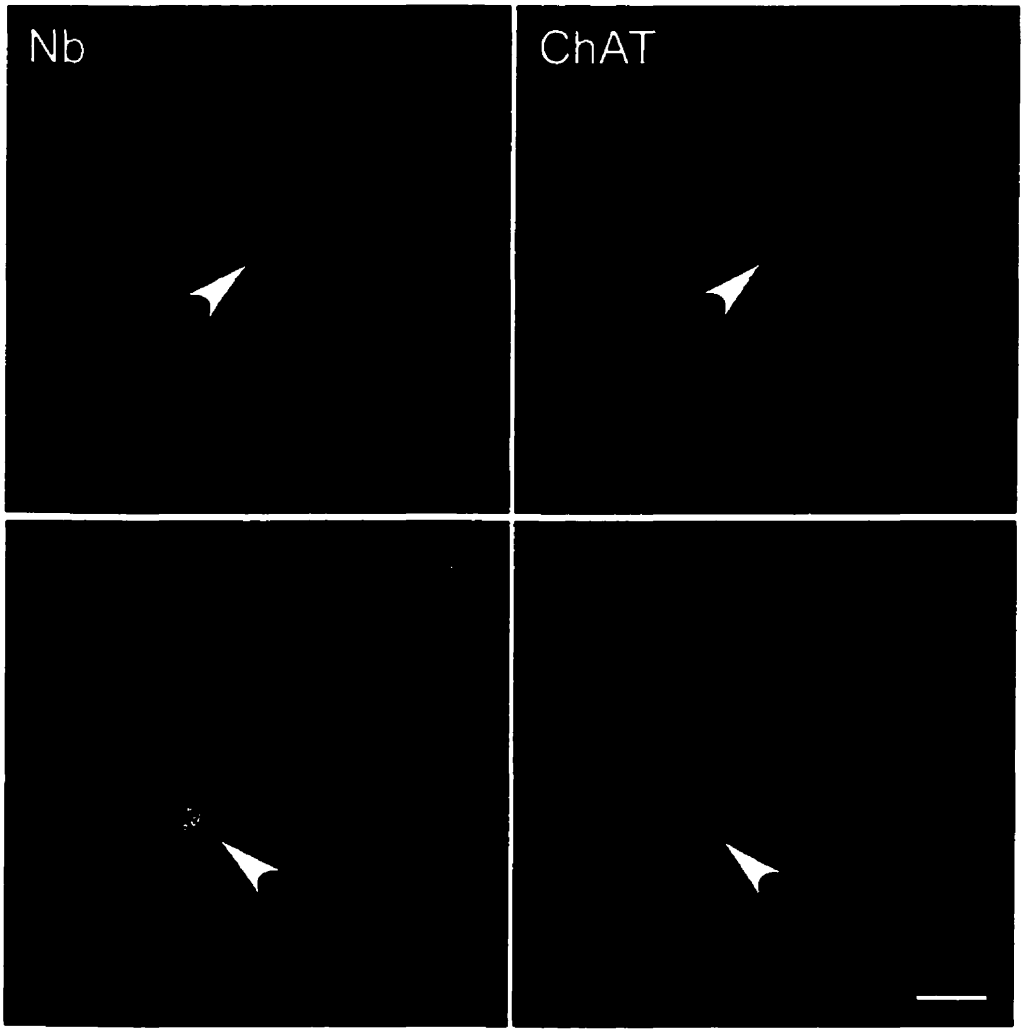
Nb
ChAT

Figure 12. Discharge patterns of Nb+/ChAT+ neurons of MCPO and SI nuclei in association with NT microinjection (NT5, top, and NT10, bottom, as in Fig. 11, top and bottom, respectively) in urethane-anesthetized animals. Presented are EEG activity from prefrontal (PFCx) and retrosplenial cortex (RSCx) and associated unit activity prior to, one minute following, and several minutes after the NT microinjection (*left to right*). Note the change from an irregular discharge pattern to a burst-like discharge pattern, in addition to an increased rate of firing, following NT microinjection. This burst-like discharge takes on a rhythmic character in association with EEG activation (spontaneously in NT10, *bottom*, and with somatosensory stimulation in NT5, *top*).

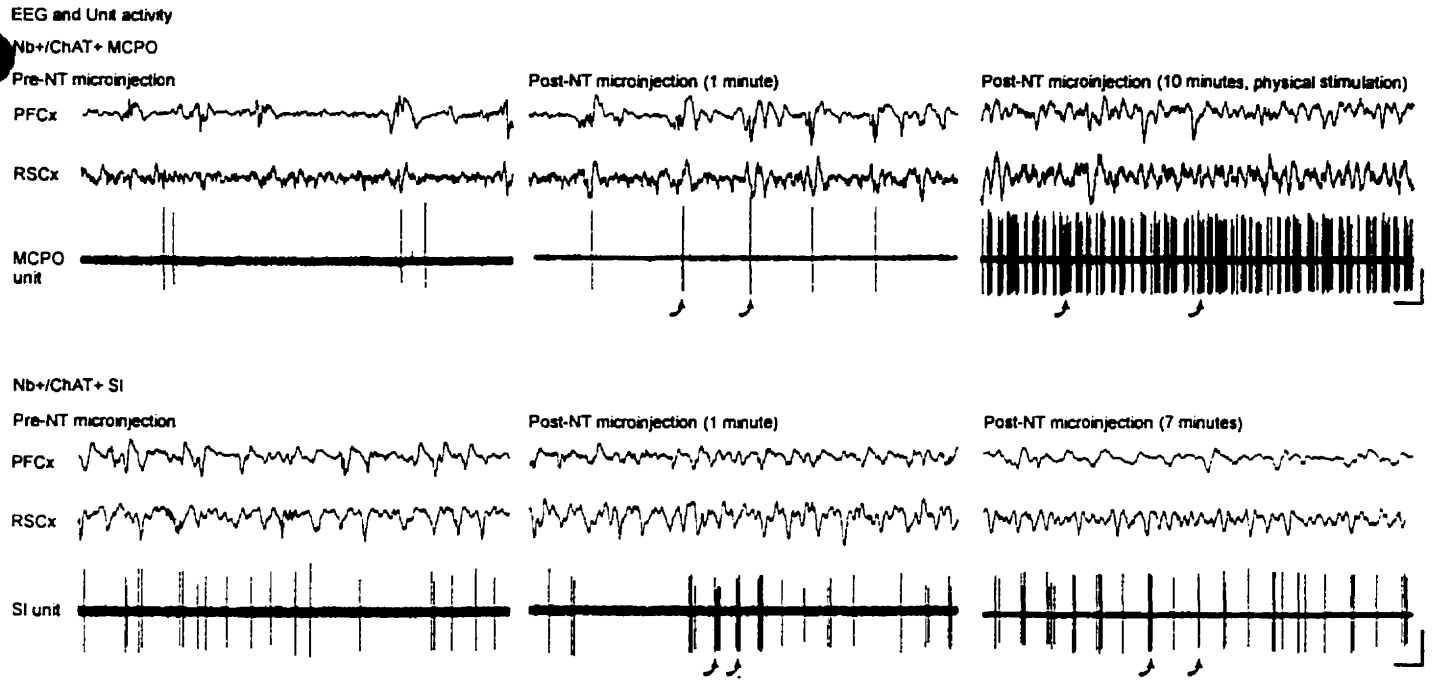
EEG and Unit activity
Nb+/ChAT+ MCPO
Pre-NT microinjection
Post-NT microinjection (1 minute)
Post-NT microinjection (10 minutes, physical stimulation)
PFCx
RSCx
MCPO unit
Nb+/ChAT+ SI
Pre-NT microinjection
Post-NT microinjection (1 minute)
Post-NT microinjection (7 minutes)
PFCx
RSCx
SI unit

Table 1. Relative EEG activity and time spent in sleep-wake states in the 30 min post-injection period following ringer and NT.[a]

	Drug trials		
	Ringer	[1.0 mM] NT	Statistic[a] (p)
Activity (Total)			
Gamma	15.4 ± 0.9	18.7 ± 0.7	***
Delta	21.8 ± 1.3	17.0 ± 0.8	***
Theta/Delta	1.10 ± 0.07	1.40 ± 0.07	***
EMG	308.5 ± 63.0	295.7 ± 51.5	
State			
Wake	26.5 ± 7.1	45.3 ± 8.4	*
*t*SWS	19.5 ± 2.9	11.9 ± 3.7	
SWS	39.8 ± 4.8	3.1 ± 1.8	***
*t*PS	9.9 ± 2.6	25.5 ± 7.0	*
PS	4.2 ± 1.0	14.2 ± 2.4	*

[a] Data are presented as mean ± SEM in repeated trials with 9 rats comparing ringer and NT conditions in the 30 minute post-injection period. For EEG activity, gamma and delta are presented as relative amplitude (% total amplitude), together with theta/delta ratio and EMG absolute amplitude (AD units) . Statistics based on Student paired t-test (* $p \leq 0.05$, *** $p \leq 0.001$). For % state, a repeated ANOVA was also performed to establish a significant overall effect of drug (as repeated measure) by state (as grouping factor) revealing a significant interaction between drug and state ($F = 18.2$, $df = 1,40$, $p=0.000$), prior to testing paired comparisons per state.

Table 2. EEG frequency peaks and band amplitudes obtained from spectral analysis of 4 sec epochs from four cortical areas following ringer and [1.0 mM] neurotensin. [a]

		DRUG TRIALS		ANCOVA					
		Ringer	NT	Drug (F)	df	Area (F)	df	Drug*Area (F)	df
High Peak Frequency (30-60 Hz)			**Mean ± SEM**						
	AVG	**36.1 ± 0.3**	**36.3 ± 0.2**	**0.7**	**1**	**1.2**	**3**	**0.6**	**3**
Area	F	36.2 ± 0.7	35.8 ± 0.6						
	RS	36.7 ± 0.5	36.4 ± 0.5						
	P	36.0 ± 0.6	36.7 ± 0.5						
	O	35.4 ± 0.9	35.9 ± 0.4						
Low Peak Frequency (1-10 Hz)									
	AVG	**3.1 ± 0.1**	**4.1 ± 0.2**	**19.51**	**1*****	**9.9**	**3*****	**1.0**	**3**
	F	2.4 ± 0.1	3.0 ± 0.3						
	RS	3.2 ± 0.3	4.6 ± 0.3						
	P	3.4 ± 0.2	4.2 ± 0.3						
	O	3.3 ± 0.2	4.3 ± 0.3						
Band Amplitude (AD)									
Gamma	**AVG**	**139.2 ± 3.5**	**145.911 ± 3.8**	**4.129**	**1***	**325.0**	**3*****	**0.6**	**3**
	F	74.3 ± 1.8	81.000 ± 3.1						
	RS	168.1 ± 3.6	170.667 ± 4.7						
	P	143.0 ± 4.5	157.600 ± 7.1						
	O	170.3 ± 4.8	174.378 ± 4.4						
Delta	**AVG**	**224.7 ± 8.8**	**123.278 ± 4.6**	**117.8**	**1*****	**32.9**	**3*****	**0.2**	**3**
	F	149.3 ± 11.6	82.778 ± 6.5						
	RS	281.1 ± 19.9	147.600 ± 9.7						
	P	205.4 ± 8.7	121.044 ± 8.7						
	O	263.0 ± 15.1	141.689 ± 8.2						
Theta/Delta	**AVG**	**1.02 ± 0.03**	**1.27 ± 0.03**	**39.04**	**1*****	**8.24**	**3*****	**1.01**	**3**
	F	0.89 ± 0.04	1.03 ± 0.04						
	RS	1.06 ± 0.08	1.40 ± 0.08						
	P	1.06 ± 0.05	1.25 ± 0.05						
	O	1.08 ± 0.07	1.37 ± 0.08						
EMG	**AVG**	**326.7 ± 23.0**	**385.0 ± 26.5**	**4.41**	**1***		**3**		**3**

[a] Measures were taken from 9, 4 sec samples (at one minute intervals from 4 to 12 minutes post-injection) from the 4 cortical areas (F, frontal; RS, retrosplenial; P, parietal; O, occipital) following Ringer and NT in 5 rats. Statistics were performed on natural log (Ln) transformed values that were normally distributed. The average (Avg) values per Drug condition and the individual values for each Area per Drug (mean and SEM) were calculated and reported from the raw values in Hz for frequency, in AD units for amplitude bands (100 $\mu V \equiv 125$ AD units) for EEG and EMG, or as the ratio of theta/delta. An analysis of covariance (ANCOVA) was performed with each EEG measure as the dependent variable, Drug (2) and Area (4) as the independent variables and Sample (9) and Rat (n=5) as covariates (with $df_{error} = 349$). Significant main effects of Drug (*, $p<.05$; **, $p \leq .01$; ***, $p \leq .001$) were not associated with any significant interactions of Drug with Area, thus not calling for post-hoc tests per Area.

Table 3. EEG and state effects of NT microinjection following prior systemic administration of atropine.[a]

	Drug trials			
	Ringer	[0.25 mM] NT	Atropine & [0.25 mM]NT	Statistic[a] (F)
Activity (Total)				
Gamma	14.3 ± 1.2	19.0 ± 0.3	14.1 ± 1.0	45.3 *
Delta	19.6 ± 2.2	14.4 ± 2.2	22.9 ± 0.9	37.3 *
Theta/Delta	1.18 ± 0.09	1.42 ± 0.18	1.08 ± 0.02	4.90
EMG	269.8 ± 93.1	313.9 ± 67.0	323.2 ± 72.1	
State				
Wake	22.8 ± 6.5	41.8 ± 15.8	75.6 ± 24.4	
tSWS+SWS	62.2 ± 1.8	5.7 ± 4.6	14.8 ± 14.8	7.9 *
tPS+PS	15.0 ± 5.0	52.5 ± 17.4	9.6 ± 9.6	11.9 *

[a] Data are presented as mean ± SEM for ringer, NT and NT following prior systemic administration of atropine (30 mg/kg, i.p) in repeated trials with 3 rats. For activity, gamma and delta are presented as relative amplitude (% total amplitude), together with theta/delta ratio and EMG absolute amplitude for the total 30 minute post-injection period. For each variable, a repeated measures ANOVA was performed to test the post-hoc hypothesis with orthogonal c-matrices that the effect of NT was reversed by atropine. Results are shown in those cases where ringer did not differ significantly from atropine & NT (with coefficients for ringer: -.707, NT: 0, and atropine & NT: +.707), and show the F-ratio for the c-matrix comparing NT on the one hand to ringer and atropine & NT on the other (with coefficients for ringer: -.408, NT: +.816, and atropine & NT: -.408, where * indicates $p < 0.05$, df =1, 6). For gamma and delta, the hypothesis was confirmed. Despite a lack of significant difference between ringer and atropine & NT, the difference in theta/delta between NT and ringer on the one hand, and NT and atropine & NT on the other did not reach significance. For % state, a repeated measures multivariate ANOVA was first performed across drug conditions (ringer, NT or atropine & NT) with state (3) as a grouping factor. In this case, there was a significant interaction of drug with state ($F = 7.69$, df = 4, 12, $p = 0.003$). Across states, it was known that atropine in itself produced a behaviorally wake state with dissociated EEG activity. Thus, in post-hoc tests using the previously mentioned orthogonal c-matrices for each state, it was confirmed that wake following atropine & NT differed significantly from ringer ($F = 7.22$, $p = 0.036$, df = 1, 6), and not (together with ringer) from NT ($F = 0.40$, df = 1,6). For *t*SWS+SWS and for *t*PS+PS, however, the difference between ringer and atropine&NT was not significant, whereas that between NT on the one hand and ringer and atropine&NT on the other was, as indicated.

SUMMARY AND CONCLUSION

Several lines of evidence indicate that cholinergic basalis neurons play an important role in cortical activation. The basal forebrain lies in the path of the ventral, extrathalamic relay from the ascending reticular activating system and therein may play a significant role in transmitting activation of the cerebral cortex. Thus the aim of the experiments was to reveal to what extent the basal forebrain neurons possess the capacity to modulate the cortical EEG and state of a naturally sleeping-waking animal. The results of these studies clearly point to a fundamental role of cholinergic basal forebrain neurons in the modulation of cortical activation, which underlies consciousness and cognitive processes of the states of wakefulness and paradoxical sleep.

To quantify changes in cortical activation, an initial study was performed to study the specific trends in electroencephalogram (EEG) activity in freely moving rats during the normal sleep-wake cycle. Gamma was highest during active waking behaviors and lowest during sleep onset and slow wave sleep (SWS). Gamma thus proved to be a reliable indicator of behavioral and cortical arousal. Gamma can be high during aroused behavior when the muscle tone of the animal was high, such as during locomotion, but not during grooming. Gamma was also high during periods of cortical arousal when the muscle tone was low as occurs during paradoxical sleep (PS), but not during quiet wake. Thus a means of measuring changes in cortical activation independent of changes in muscle tone was also identified by monitoring gamma activity within the EEG of the rat. Furthermore, it was also found that gamma and delta varied in a reciprocal manner. This work also showed how gamma activity varied in a parallel manner to theta activity, well known to occur during periods of active waking and PS. Lastly, the fact that theta activity appeared across the cortex with different peak frequencies provided fodder for a basalo-cortical driven theta rhythm.

The next series of experiments explored the role of the basal forebrain in the modulation of cortical activativity and sleep-wake state through a pharmacological study

based upon the previous *in vitro* characterization of the cholinergic and non-cholinergic neurons and their modulation by specific neurotransmitters. Given the fact that the basal forebrain lies in the path of the ventral, extrathalamic relay from the ascending activating system which include monoaminergic fibers from the locus coeruleus and dorsal raphe, studies were first undertaken to determine the effect of noradrenergic and serotonergic modulation of the cholinergic neurons on cortical EEG activity and sleep-wake states. The neurotransmitters were injected into the region of the basalis neurons by remote control in freely moving, naturally sleeping-waking rats during the day when the rats are normally asleep the majority of the time. Effects were observed on behavior and EEG activity, including high-frequency gamma activity. Noradrenaline (NA), which has been shown in previous *in vitro* studies to depolarize and excite the cholinergic cells, eliciting a tonic discharge, produced a dose-dependent increase in gamma-EEG activity, a decrease in delta, and an increase in waking. Serotonin, which has been found in previous *in vitro* studies to hyperpolarize the cholinergic neurons, produced a dose-dependent decrease in gamma-EEG activity with no significant changes in amounts of wake or SWS. Both chemicals resulted in a dose-dependent decrease in PS.

Glutamate is believed to be the primary neurotransmitter of neurons in the brainstem reticular activating system which project to the basal forebrain. The next set of experiments were undertaken to examine the effects upon EEG activity and sleep-wake state of activation of basal forebrain neurons with glutamate agonists and conversely inactivating them with procaine. Activation of the region was accomplished by microinjections of AMPA and NMDA. Inactivation was produced with procaine injections into the basal forebrain. Inactivation of the basal forebrain region with procaine produced an increase in slow EEG activity, marked by an increase in delta and a reciprocal decrease in gamma activity. In contrast, activation with the glutamate agonists produced a decrease in slow EEG activity and sleep and elicited high frequency

EEG, marked by a decrease in delta and reciprocal increase in gamma, changes which were associated with a behaviorally awake state. In addition, NMDA, which has been documented *in vitro* to induce rhythmic bursting activity in the cholinergic neurons, produced an increase in theta EEG activity, marked by an increase in the theta/delta ratio. Activation of neurons by NMDA was confirmed by revelation of c-Fos in cholinergic, as well as GABAergic and other neurons, in the substantia innominata and magnocellular preoptic nucleus.

Lastly, afferents to the basal forebrain also arise from neurons which contain neurotensin (NT). Basal forebrain cholinergic cells are endowed with receptors for NT as shown by binding and internalization of NT *in vitro*. Also, as evidenced *in vitro*, NT elicits a depolarization and excitation of the cholinergic cells and induces a rhythmic burst discharge. The present study was undertaken *in vivo* to determine the effects of local microinjections of NT and a fluorescent NT derivative (Fluo-NT) upon EEG activity and sleep-wake state. Furthermore, this series of experiments represented an opportunity to test whether a selective activation of cholinergic neurons would be sufficient to induce a cortically activated state. Thus, the effects of local microinjections of either NT or Fluo-NT into the basal forebrain were examined on both behavior and EEG in freely moving, naturally sleeping-waking rats. NT microinjections produced a decrease in delta activity and an increase in both high frequency gamma activity and rhythmic theta activity. This EEG pattern was associated with a behaviorally quiet, waking state that alternated with PS. The effects of NT were antagonized with systemic injection of atropine, a muscarinic cholinergic antagonist. To assess internalization of NT in basalis neurons, animals were injected with Fluo-NT and sacrificed 20 minutes after the injection when an effect on EEG and state was observed. Confocal microscopic analysis revealed that Fluo-NT was internalized within ChAT-immunoreactive, and thus cholinergic basal forebrain neurons. Fluo-NT was visualized

as small punctate fluorescent granules in the cytoplasm of ChAT+ perikarya and proximal dendrites. To monitor the modulation in basal forebrain unit activity in response to microinjection of NT, experiments were performed in urethane-anaesthetized rats while recording single unit activity prior to, during, and following injection of NT. The cells were subsequently juxtacellularly labeled with Neurobiotin (Nb) and processed for ChAT immunostaining. Nb labeled and ChAT immunoreactive cells showed rhythmic discharge correlated with theta-like activity following NT microinjections in the basal forebrain. The results suggest that NT may be a crucial neuropeptide in the regulation of behavioral state by promoting rhythmic discharge in cholinergic neurons and thereby enhancing gamma and theta cortical activity associated with the states of wake and PS.

In summary, the modulation of cortical activity in these experiments occurred in a manner consistent with the differential participation of the cholinergic cells, and serves to emphasize the potent capacity of this subgroup of neurons in the regulation of EEG activity and sleep-wake state. Thus while the discharge of cholinergic neurons associated with increased cortical acetylcholine release may dampen slow, delta activity and stimulate high frequency, gamma activity, these data also suggest that bursting activity seems centrally important in the capacity of the cholinergic neurons to drive cortical theta activity. For instance, the basal forebrain's capacity to potentiate the state of wake in association with gamma activity when exposed to NA, AMPA, NMDA or NT is congruent with the fact that they are known to excite and activate the cholinergic neurons. Further, the basal forebrain's capacity to induce theta activity when exposed to NMDA or NT is consistent with the fact that these same chemicals induce bursting activity in the cholinergic cells.

On the other hand, within the fundamental change in cortical activation, the role of the non-cholinergic neurons seems important in shaping the type of response. For instance, while both NMDA and NT increased the propensity for wake in association with

an increase in cortical activation (evident with an increase in gamma and theta EEG activity), NMDA elicited a more active state of wake in contrast to the quiet wake behavior viewed with NT. These differences may be explained by the differential activation of the non-cholinergic neurons, since as evidenced by c-Fos activation, cholinergic, GABAergic and many other neurons were activated with NMDA as would be expected. From *in vitro* evidence, confirmed here, NT would act more selectively through high affinity receptors on cholinergic neurons. Similar comparisons could be made with NA and AMPA which both depolarize cholinergic neurons but would appear to have differential affects on the non-cholinergic neurons, as suggested by the *in vitro* results that NA can in fact inhibit a group of non-cholinergic basal forebrain neurons, whereas glutamate agonists are known to depolarize most neurons in the brain. While both agonists induced a state of wake, the effect with NA seemed by far the most physiological/natural as evidenced in the behavioral observations, and the lack of seizure activity that occurred occasionally with the glutamate agonists. NA produced a significant increase in gamma not only across the total recording period but also during waking epochs, being associated with enhanced gamma (as evidenced by an increase in relative gamma) and often a behaviorally attentive state.

These experiments have also demonstrated the potent capacity of the basal forebrain to induce either the state of wake or PS while playing a more permissive role in SWS. While all the agonists known to activate the cholinergic cell population increase the occurrence of wake, the fact that an increase in PS occurred only with the more selective activation of cholinergic neurons makes this finding of particular relevance in first revealing the selective nature of the neuronal populations involved in PS and second linking the burst mode of discharge of the cholinergic neurons with the state of PS. This link, in turn associated with increased amounts of theta activity is further supported by both experiments with those chemicals known to either hyperpolarize and

inhibit the cholinergic cells (serotonin), or shut-down neuronal activity (procaine), both of which prevented the occurrence of PS, evident by the virtual elimination of the state and a decrease in theta and gamma EEG activities following these microinjections. This evidence for the active participation of the basal forebrain neurons in the generation of PS is unlike the permissive role of these neurons in the production of SWS as suggested particularly the procaine experiments that would be associated with silencing of all basal forebrain neurons without preventing the normal occurrence of SWS. Taken together, these data demonstrate the potent capacity of the basal forebrain neurons to modulate EEG activity across the sleep-waking cycle and to play a differential role in the generation of different sleep-wake states by differential participation of neuronal cohorts, including importantly the cholinergic neurons that promote theta and gamma together with waking and paradoxical sleep.

LETTERS OF PERMISSIONS TO REPRINT JOURNAL ARTICLES